2014

PREDICTION OF HUMAN SYSTEMIC, BIOLOGICALLY RELEVANT PHARMACOKINETIC (PK) PROPERTIES USING QUANTITATIVE STRUCTURE PHARMACOKINETIC RELATIONSHIPS (QSPKR) AND INTERSPECIES PHARMACOKINETIC ALLOMETRIC SCALING (PK-AS) APPROACHES FOR FOUR DIFFERENT PHARMACOLOGICAL CLASSES OF COMPOUNDS

Gopichand Gottipati
Virginia Commonwealth University

PREDICTION OF HUMAN SYSTEMIC, BIOLOGICALLY RELEVANT PHARMACOKINETIC (PK) PROPERTIES USING QUANTITATIVE STRUCTURE PHARMACOKINETIC RELATIONSHIPS (QSPKR) AND INTERSPECIES PHARMACOKINETIC ALLOMETRIC SCALING (PK-AS) APPROACHES FOR FOUR DIFFERENT PHARMACOLOGICAL CLASSES OF COMPOUNDS

A dissertation submitted in partial fulfillment of the requirements for the degree of
Doctor of Philosophy at Virginia Commonwealth University
by

Gopichand Gottipati, B.Pharm.,
Ph.D. Candidate, Department of Pharmaceutics,
School of Pharmacy

Under the supervision of

JÜRGEN VENITZ, M.D., Ph.D.,
Professor and Director, PK/PD Laboratory
Department of Pharmaceutics, School of Pharmacy

Virginia Commonwealth University
Richmond, Virginia
July 28, 2014

Acknowledgement

I would like to take this opportunity to express my heartfelt gratitude to Dr. K. P. R. Chowdary, and one of my close friends, Vamsi Krishna Karuturi, who inspired and guided me to pursue Ph.D. graduate studies.

I thank my Ph.D. major advisor, Dr. Jürgen Venitz, for providing me the opportunity to pursue my graduate research project under his tutelage. His breadth of knowledge, passion and motivation has set high standards for me in teaching, research. His excellent training and mentorship have constantly (positively) challenged me to do better and improve as an individual. I am grateful for all of his efforts and time in doing so, and I will always be indebted to him for creating a world of opportunities.

My graduate advisory committee members, Dr. Peter Byron, Dr. Phillip Gerk, Dr. Glen Kellogg and Dr. Lemont Kier for their valuable thoughts and comments on my dissertation project.

A special note of appreciation to Dr. Larry Lesko, Dr. An Guohua for providing me opportunity to intern at the Center for Pharmacometrics and Systems Pharmacology, University of Florida at Lake Nona. Other faculty, post-docs and graduate students at the center for making the internship experience very memorable.

Dr. Wu Pong, Dr. Nikhil Parekh and Dr. Angela Men for their mentoring during Personal and Professional Development Program (PPDP).

VCU Departmental and PK/PD research group alumni, Satjit, Lokesh, Pankaj, Pravin and Prajakta, who played a significant role in guiding me professionally and their invaluable inputs during my tenure as a graduate student and beyond.

Keyetta and Laura (Department of Pharmaceutics) for their tireless assistance with anything and everything I needed. Gai, Chris, Larvell and Romano with all the technology related issues.

My friends, Morse, Apoorva, Megha, Poonam, Renish, Juni, Stuti, Sadashiv, Gandhi, Rajesh, Vamsi, Ajay, Raju, Anusha and Suresh for their support and encouragement all through. Badri and Aravind for being amazing roommates and making sure that I didn't stay hungry, especially during the dissertation writing phase. Other colleagues, Heta, Mengyao, Bishoy and each and every one of who made my experience at VCU memorable.

Last, but not least, Rakesh, my elder brother, my parents and my grandmother for their unconditional support, understanding, inspiration and love.

Table of Contents

List of Tables

List of Figures

List of Abbreviations

AAG	-	Alpha-acid glycoprotein
AAR	-	Antiarrhythmic
ACh	-	Acetylcholine
AChE	-	Acetylcholine esterase
ADMET	-	Absorption, distribution, metabolism, elimination and toxicology
AS	-	Allometric scaling
ASN	-	Aminosteroid nucleus
B:P Ratio	-	Blood-to-plasma ratio
BIQ	-	Benzylisoquinolonium
BW	-	Body weight
BZD	-	Benzodiazepines
CCB	-	Calcium channel blockers
$logD_{7.4}$	-	Calculated logarithm of the distribution coefficient at pH of 7.4
clogP	-	Calculated logarithm of the partition coefficient
CL_{hep}	-	Hepatic clearance
CL_{int}	-	Intrinsic hepatic clearance
CL_{nonren}	-	Nonrenal plasma clearance
CL_{nonren}^{u}	-	Nonrenal plasma clearance of the unbound drug
CL_{nonren}^{blood}	-	Nonrenal blood clearance
CL_{ren}	-	Renal clearance
CL_{ren}^{u}	-	Renal clearance of the unbound drug
CL_{tot}	-	(Apparent) Total (systemic) body clearance
CL_{tot}^{u}	-	(Apparent) Total (systemic) body clearance of the unbound drug
CNS	-	Central nervous system
CV	-	Cross validation
CYP2C19	-	Cytochrome P450 2 C19

CYP3A	-	Cytochrome P450 3A
DME	-	Drug metabolizing enzymes
DT	-	Drug transporters
ER_{hep}	-	Hepatic extraction ratio
EW	-	Extracellular water
f_e	-	Fraction of the dose excreted unchanged in the urine
f_u	-	Fraction of the drug unbound in plasma
$GABA_A$	-	Gamma amino butyric acid
GFR	-	Glomerular filtration rate
GI	-	Gastrointestinal tract
HBA	-	Number of hydrogen bond acceptors
HBD	-	Number of hydrogen bond donors
HT	-	Hydroxytryptamine
I.V.	-	Intravenous
IVIVE	-	*In-vitro-in-vivo* extrapolation
IW	-	Intracellular water
K_i	-	Receptor binding affinity
LBF	-	Liver blood flow
LOO	-	Leave-out-one method
LR	-	Linear regression
MLLR	-	Multiple log linear regression
MPE	-	Mean prediction error
MV	-	Molar volume
MW	-	Molecular weight
nAChR	-	Nicotinic acetylcholine receptors
nRot	-	Number of rotatable bonds
PBPK	-	Physiological based pharmacokinetics

PC	-	Molecular and physiochemical properties
PD	-	Pharmacodynamics
PK	-	Pharmacokinetics
PKV	-	Pharmacokinetic variable
PPB	-	Plasma protein binding
PSA	-	Polar surface area
QSPKR	-	Quantitative structure pharmacokinetic relationship
RBC	-	Red blood cells
RMSE	-	Root mean square error
RPF	-	Renal plasma flow
RRA	-	Relative receptor affinity
S	-	Sensitivity of the change in y-variable relative to x-variable (Slope)
TRP	-	Triptans
TBW	-	Total body water
UGT	-	Uridinediphosphate-glucuronosyltransferase
Vd_{pss}	-	Volume of the distribution at pseudo steady-state
Vd_{ss}	-	Volume of the distribution at steady-state
Vd_{ss}^{u}	-	Volume of distribution at steady state of the unbound drug
Vd_{β}	-	Volume of distribution during terminal phase
β-ARLs	-	Beta (β) adrenergic receptor ligands
β-LAs	-	Beta (β) lactam antibiotics

Abstract

PREDICTION OF HUMAN SYSTEMIC, BIOLOGICALLY RELEVANT PHARMACOKINETIC (PK) PROPERTIES USING QUANTITATIVE STRUCTURE PHARMACOKINETIC RELATIONSHIPS (QSPKR) AND INTERSPECIES PHARMACOKINETIC ALLOMETRIC SCALING (PK-AS) APPROACHES FOR FOUR DIFFERENT PHARMACOLOGICAL CLASSES OF COMPOUNDS

Gopichand Gottipati, B.Pharm.,
Ph.D. Candidate, Department of Pharmaceutics,
School of Pharmacy

A dissertation submitted in partial fulfillment of the requirements for the degree of
Doctor of Philosophy at Virginia Commonwealth University

Virginia Commonwealth University, 2014

Under the supervision of

JÜRGEN VENITZ, M.D., Ph.D.,
Professor and Director, PK/PD Laboratory
Department of Pharmaceutics, School of Pharmacy

This research developed and validated QSPKR models for predicting *in-vivo* human, systemic biologically relevant PK properties (i.e., reflecting the disposition of the unbound drug) of four, preselected, pharmacological classes of drugs, namely, benzodiazepines (BZD), neuromuscular blocking agents (NMB), triptans (TRP) and class III antiarrhythmic agents

(AAR), as well as PK allometric scaling (PK-AS) models for BZD and NMB, using pertinent human and animal systemic PK information (f_u, CL_{tot}, Vd_{ss} and f_e) from published literature.

Overall, lipophilicity ($logD_{7.4}$) and molecular weight (MW) were found to be the most important and statistically significant molecular properties, affecting biologically relevant systemic PK properties, and the observed relationships were mechanistically plausible:

For relatively small MW and lipophilic molecules, (e.g., BZD), an increase in $logD_{7.4}$ was associated with a decrease in f_u, an increase in Vd_{ss}^u and CL_{nonren}^u, suggesting the prevalence of nonspecific hydrophobic interactions with biological membranes/plasma proteins as well as hepatic partitioning/DME binding. Similar trends were observed in f_u and Vd_{ss}^u for intermediate to large MW, hydrophilic molecules (e.g., NMB).

However, although similar trends were observed in f_u and Vd_{ss}^u for relatively hydrophilic, intermediate MW molecules (e.g., TRP), and a heterogeneous class (e.g., Class III AAR), $logD_{7.4}$ and MW were found to be highly correlated, i.e., the indepdendent effects of logD7,4 and MW cannot be assessed NMB, TRP and Class III AAR show mechanistically diverse clearance pathways, e.g., hepatobiliary, extrahepatic, enzymatic/chemical degradation and renal excretion; therefore, effects of the $logD_{7.4}$ and/or MW are note generalizable for any of the clearances across classes.

PK-AS analyses showed that Vd_{ss}^u and Vd_{ss} scaled well with body weight across animal species (including humans) for BZD. Overall, within the limitations of the methods (and the sample size), 'acceptable' predictions (i.e., within 0.5- to 2.0-fold error range) were obtained for Vd_{ss}^u and Vd_{ss} for BZD (and f_u correction resulted in improvement of the prediction); however, none of the CL_{tot} predictions were acceptable, suggesting major, qualitative interspecies differences in drug metabolism, even after correcting for body weight (BW).

NMB undergo little extravascular distribution owing to their relatively large MW and charged nature, and, as a result, a high percentage of acceptable predictions was obtained for Vd_{ss} (based on BW). Similarly, the prediction of CL_{ren} (based on BW and glomerular filtration rate, GFR) was acceptable, suggesting that NMB are cleared by GFR across species, and there are no interspecies differences in their tubular handling. On the other hand, CL_{tot} (and/or CL_{nonren}) could not be acceptably predicted by PK-AS, suggesting major differences in their clearance mechanisms across animal species.

CHAPTER 1. Introduction

1.1 Background and Significance

The discovery and development of new candidate drug molecules is a cost-[1], resource- and time-consuming[1] process. This is in part due to the high attrition rates of drug candidates that enter clinical development, such that, approximately, only 1 in every 10 ultimately become marketed as therapeutically safe and effective drugs[2,3]. When the reasons for such high attrition rates were investigated, the lack of favorable human pharmacokinetic (PK) properties ("druggability") of the candidates[3, 4] has been reported to be one of the most prominent causes. This suggests that the process by which new drugs are discovered and developed could benefit greatly if (a) there were better preclinical characterization of absorption, distribution, metabolism, elimination and toxicological properties (ADMET)[5] of each candidate, and (b) the predicted human PK characteristics were deemed 'acceptable' (e.g., oral bioavailability and duration of exposure are projected to be appropriate for conducting pivotal efficacy studies) early in the development. Therefore, the development and application of reliable quantitative methods to predict human drug disposition may decrease the overall attrition of drug candidates during clinical development by reducing the number of candidates with unacceptable PK characteristics. Furthermore, selecting only compounds with likely acceptable PK properties for their intended therapeutic use could maximize the ultimate clinical utility and market success. Consequently, several studies have investigated the use of (a) approaches, such as, quantitative structure PK

property relationships (QSPKR), which can be used for prospective *in-silico* screening of potentially important lead candidates with favorable 'drug-like' properties[6,7], and/or (b) experimental methods such as, interspecies PK-allometric scaling (AS)[8–13] approaches, based on disposition in the preclinical species, physiologically-based-PK (PBPK) modeling[14] and *in-vitro-to-in-vivo* extrapolation (IVIVE)[3] etc.

The aim of this research project is to develop and validate mathematical/statistical *in-silico* models for predicting biologically relevant human PK properties of select pharmacological classes of compounds, namely, benzodiazepines (BZD), neuromuscular blocking agents (NMB), triptans (TRP) and class III antiarrhythmic agents (AAR) using two approaches, QSPKR modeling and interspecies PK-AS.

The anticipated findings will help in supporting the rational application of quantitative methods in drug discovery and development and screening of new drug candidates with more favorable 'druggable' properties and better integration of physicochemical/molecular properties with PK/ADME properties of already existing drugs.

1.2. Quantitative Structure Pharmacokinetic Relationships

The introduction of quantitative structure-activity relationships (QSAR) in the 1960s was pioneered by Hansch and co-workers[15], who investigated quantitative relationships between physicochemical properties and *in-vitro* potency at the target for homologous series of compounds. A lot of work has been carried out over the past few decades in developing analogous relationships between structural/molecular properties of compounds (homologous series of compounds sharing a common structural scaffold or structurally diverse compounds),

determined either by computational or experimental means and relating them to experimental *in-vitro* and/or *in-vivo* PK properties in preclinical animal species and humans[5,16–29].

One of the overarching goals in the development of new drugs is to identify early an acceptable therapeutic dosing regimen (both in terms of how much and how often the drug needs to be dosed, see Figure - 1.1 below) that results in adequate patient compliance and effective therapy. In order to achieve this objective, *in-silico* approaches such as QSPKR models can be useful to adequately predict the disposition of drug candidates. For instance, (a) the dosing interval is usually affected by systemic PK properties, such as volume of distribution at steady-state (Vd_{ss}) and total (systemic) body clearance (CL_{tot}), while; (b) the dose amount is affected by oral bioavailability (for drugs administered by the oral route) and CL_{tot}. The QSPKR paradigm[17,30] is shown in Figure 1.1 below.

Molecular/PC Properties

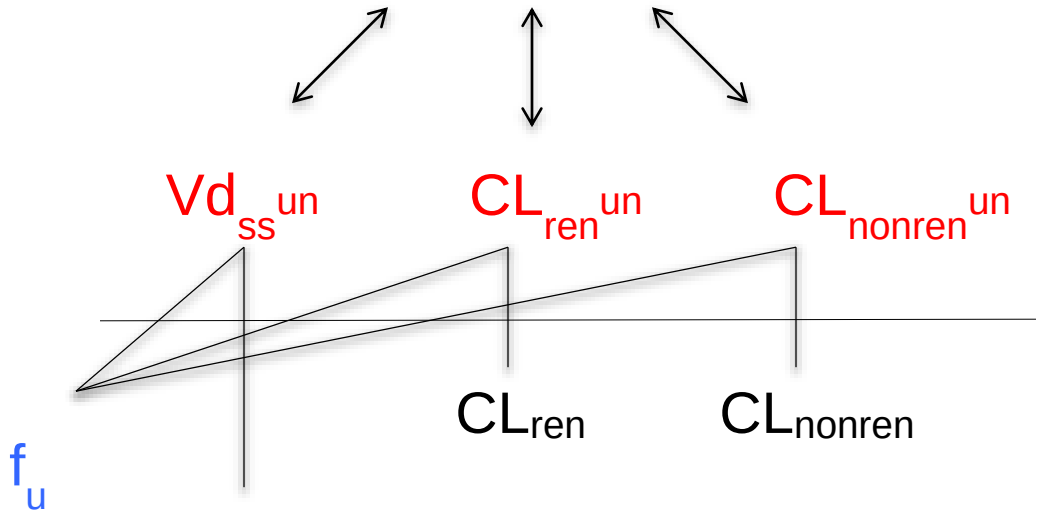

Vd_{ss} f_e

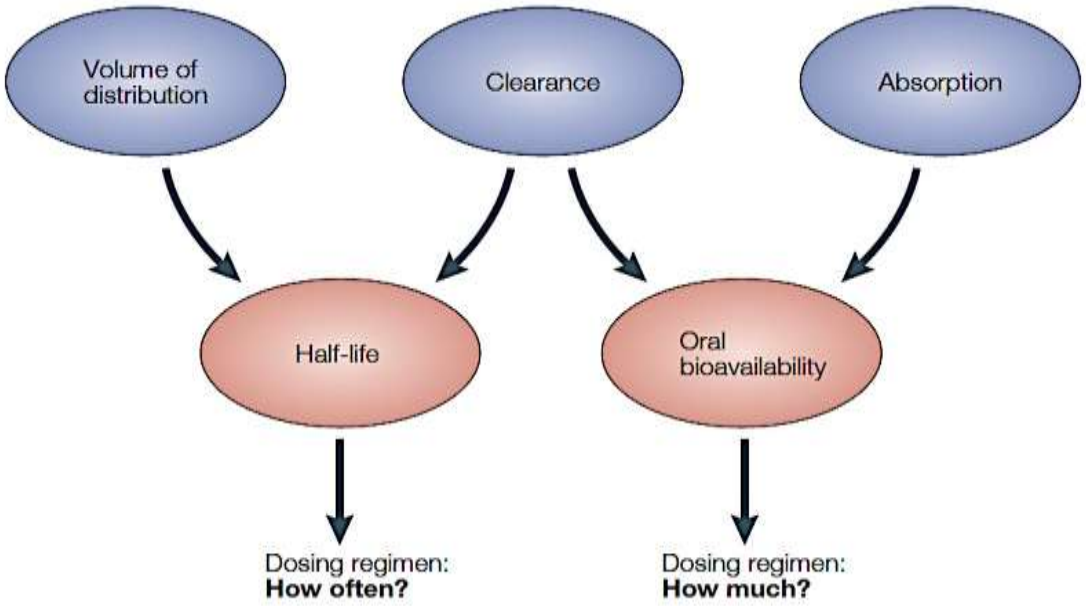

(Dosing interval) **(Dose Amount)**

The present work is unique relative to published in the literature in the following respects:

1. A few QSPKR studies in the literature attempted to predict the apparent CL_{tot} (i.e., CL_{tot}/F_{oral}) and apparent Vd_{ss} (i.e., Vd_{ss}/F_{oral}) after oral administration to humans (from the results of preclinical species)[8,31,32]. Any observed trends are difficult to mechanistically interpret because these relationships cannot be unambiguously attributed to the systemic component (i.e., systemic CL_{tot} and Vd_{ss}) versus the presystemic component (i.e., F_{oral}). Furthermore, in order to avoid the confounding effects of system-dependent factors, such as gastrointestinal (GI) absorption (possible incomplete solubility and/or permeability in GI tract); and also system-independent factors such as, formulation properties etc., only the systemic PK, i.e., exclusively after I.V. administration, were considered in the present work.
2. Each relevant PK property value reported in the literature was carefully scrutinized and included only after critical evaluation of study design, type of subjects, dosing regimen, PK sampling schedule, PK analysis and bioanalytical assay procedures etc. Specific importance was given to PK sampling schedule - i.e., only studies in which (a) adequate blood sampling was performed for at least 2-3 terminal half-lives ($t_{1/2}$); and (b) the analytical technique used to quantitate plasma and urinary concentrations was sensitive over the adequate sampling period, were included in the database.
3. In order to differentiate mechanistically between renal and nonrenal elimination pathways, the fraction of the drug excreted unchanged in the urine (f_e) was compiled from the urinary excretion studies following I.V. administration, after ensuring that the urine samples were collected completely for at least 2 - 3 terminal $t_{1/2}$. Additionally, renal clearance (CL_{ren}) estimates were compiled from studies following oral administration, provided they were estimated from the ratio of amount of drug ultimately excreted in the urine unchanged (A_∞)

relative to systemic exposure (AUC_{∞}). After differentiating the systemic CL_{tot} into CL_{ren} and nonrenal (CL_{nonren}) pathways, separate QSPKR relationships for each of them were investigated, in order to better understand and mechanistically interpret the molecular/structural properties, potentially affecting the respective clearance pathways.

4. A fundamental assumption in PK/pharmacodynamics (PD) is that only the unbound drug is available for absorption, distribution, metabolism, excretion and interaction with the PD targets. Therefore, QSPKR (and AS-PK) models were built for the biologically relevant, i.e., unbound PK properties (after correcting the reported *in-vivo* systemic PK variables for PPB). Such relationships with the unbound systemic human PK properties have rarely been explored in the literature.
5. The QSPKR model building and validation process followed strict statistical rules using univariate and multivariate log-linear regression, collinearity amongst molecular/PC variables was considered, based on the criteria of $r > 0.80$, in order to address the possibility of statistical interactions between the molecular properties. Next, potentially important molecular/PC covariates were screened by univariate regression based on the criteria - $r^2 > 0.3$, $p < 0.05$ (i.e., the molecular/PC variable accounts for greater than 30% variability in the PK variable, and a finding that the slope of the relationship is significant at $p < 0.05$). Finally, multivariate log-linear regression (MLLR) was carried out in forward inclusion followed by backward elimination manner and validated using leave-out-one method by cross-validation.

However, the following limitations of the information in the database need to be considered carefully before interpreting the findings.

1. The majority of the compounds in the final human PK(/PD) database are (tested and/or) approved for clinical use, i.e., it is implied that these compounds possess acceptable 'druggable' molecular/PC properties. However, unfortunately, it does not contain compounds, which were tested in humans, but failed to reach the marketplace, at least in part due to their poor druggability. This suggests that there is an inherent, systematic (publication) bias in the selection of compounds.
2. Furthermore, even for the compounds that have been included in the database, there were several missing values in their molecular/PC and/or PK properties (in human and preclinical species), especially, plasma protein binding (PPB) and urinary excretion data, and, therefore, the results should be carefully interpreted, especially for the unbound clearance pathways.
3. Primary PK variables reported in the literature were collected from multiple clinical pharmacology studies (e.g., diazepam[33–38]). Each of the reported values may be subject to bias and imprecision, depending on the study characteristics such as study design, characteristics of the study subjects, PK sampling times, PK analysis and bioanalytical procedures etc. In cases, where drugs were administered at more than one dose level (or dosing regimen), dose-proportionality in the systemic PK was evaluated, subject to availability of pertinent information; if not, it was assumed. In case of any obvious PK non-linearities, systemic PK at the lowest dose level was used for analysis. Similarly, concentration-independent PPB and/or red blood cell (RBC) binding was assumed in cases where there was inadequate evidence in the literature.

4. The final values of PK variables in the database were estimated as mean values from multiple studies and did not account for intersubject/interstudy variability.
5. For relatively lipophilic compounds, e.g., BZD (and few NMB), that are subject to extensive metabolism (both hepatic as well as extrahepatic), f_e (and thus CL_{ren}) values were poorly estimated due to very low values for f_e less than 1%. For certain drugs, e.g., TRP and Class III AAR, extrahepatic clearance was assumed based on the fact that CL_{nonren}^{Blood} (or CL_{nonren}) exceeds hepatic blood flow (LBF) (or in a few instances, exceeding the cardiac output) with the absence of adequate mechanistic evidence in the literature.
6. The molecular/PC properties may sometimes be collinear, i.e., highly correlated with one another, which makes it difficult to separate the effects of one over the other.
7. There are several algorithms available for computing the molecular/structural PC properties, but they may differ in the estimation method(s). Thus, selection of the appropriate PC variables becomes very important. Certain PC properties, although showing significant trends, may be difficult to interpret mechanistically compared to others.

The choice of the two-dimensional molecular/structural PC properties was based on their biological plausibility and their widespread use in the literature[6,29,39,40]. They are considered as "bulk" properties, because they do not contain information that may confer specificity towards the interaction with the PK - relevant biological entities (such as membranes, intra/extracellular proteins etc.) unlike those with PD targets. These molecular/PC properties include molecular weight (MW), polar surface area (PSA), logarithm of the partition coefficient (logP), pKa, number of rotatable bonds (nRot), number of hydrogen bond acceptors (HBA) and number of hydrogen bond donors (HBD). Additionally, the logarithm of the distribution coefficient (logD) was estimated based on logP and pKa using equations (shown in Chapter 3).

For the purpose of *in-silico* screening and identification of "druggable" lead candidate(s) for further development, experimental determination of the molecular/PC properties is a tedious and time consuming process. Therefore, for QSPKR studies, they are estimated computationally and were estimated in a similar manner.

1.3. Interspecies PK - Allometric Scaling (PK-AS)

Allometry assumes anatomical, physiological and biochemical similarity (other than body size) across animal species and is used to study relationships of different physiological variables as a function of body size, usually, BW[41,42]. It is based on the relationship between physical compartment, organ size, perfusion rate and BW, characterized by the power model:

$$Y = a*(BW)^b \qquad \text{..... Eq 1.1}$$

Where Y is the parameter of interest (e.g., PK property like CL_{tot}, Vd_{ss}, etc.) and a and b are the intercept and exponent (coefficient) of the allometric equation, respectively. Various physiological volumes and organ perfusion rates have been allometrically scaled; the obtained

AS exponents are shown in Table 2.1 (in Chapter 2). In general, physiological volumes scale with AS exponent close to 1.0, while the organ perfusion rates scale with a factor of between 0.7 to 0.8.

PK-AS approaches have been widely used in literature for predicting human PK from preclinical *in-vivo* animal PK studies[10,11]. However, there is a lot of variability in this approach, such as, choice of the animal species for predicting human PK, choice of the PK endpoints, scaling and validation methods, etc. For example, Ward et al. studied the systemic PK properties (after I.V administration), namely CL_{tot}[11] and Vd_{ss}[10] for 103 compounds in rats, dogs, monkeys and humans. They found that (BW-based) AS scaling approaches using two animal species was less successful in predicting human CL_{tot} than LBF-based methods using a single species. In particular, with the compounds in the dataset, human CL_{tot} and Vd_{ss} predictions from monkey seemed to be the most accurate and least biased compared to predictions from other animal species. They also concluded that r^2 is not a good measure for characterizing the predictive ability of the allometric relationship, but rather propose to assess bias (% mean prediction error) and imprecision (% root mean square error).

Mahmood et al[8,12,13,43,44] proposed several correction factors that may improve the AS predictability from preclinical species, e.g., including maximum lifespan potential or brain weight correction, rule of exponents, and *in-vitro* correction. Additionally, other quantitative approaches explored the use of mechanistic correction factors based on LBF and glomerular filtration rate (GFR) (especially for drugs which are primarily renally excreted), etc.

Assumptions

Overall, AS is based on the assumption that there are anatomical, physiological and biochemical similarities among animals, and physiological parameters scale based on BW across species. Following are the assumptions that underpin each of the individual prediction methods

CL_{tot}-prediction methods:

1. Single species-BW based scaling without f_u correction - there are no qualitative/quantitative interspecies differences in PPB, metabolic pathways, intrinsic clearance and excretory functioning.
2. Single species-BW based scaling with f_u correction - there are no qualitative/quantitative interspecies differences in metabolic pathways, intrinsic clearance and excretory functioning; and PPB differences are accounted for by f_u correction.
3. Single species - LBF-based scaling without f_u correction - there are no qualitative/quantitative interspecies differences in PPB and B:P ratio; clearance occurs primarily via hepatic route.
4. Single species - LBF-based scaling with f_u correction - there are no qualitative/quantitative interspecies differences in B:P ratio; Clearance occurs primarily via hepatic route; and PPB differences are accounted for by f_u correction.
5. Single species - GFR-based scaling without f_u correction - there are no qualitative/quantitative interspecies differences in PPB; Clearance occurs primarily via renal routes by net glomerular filtration and that there are species differences in tubular pathways.

6. Single species - GFR-based scaling with f_u correction - Clearance occurs primarily via renal routes by net glomerular filtration and that there are species differences tubular pathways; and PPB differences are accounted for by f_u correction.

Vd_{ss}-prediction methods:

1. Single species-BW based scaling without f_u correction - there are no qualitative/quantitative interspecies differences in PPB and tissue binding
2. Single species-BW based scaling with f_u correction - there are no qualitative/quantitative interspecies differences in tissue binding; and PPB differences are accounted for by f_u correction.

Qualitative differences across species, in terms of the existence of different drug metabolizing enzymes (DME), differences in the enzyme expression, activity and affinity has been extensively documented in literature[45,46]. Similarly, quantitative differences across the animal species in the amount of CYP content per mg protein[47]. Differences in the Phase II metabolism via glucuronidation have been reported, e.g., rhesus monkey and dog liver microsomes have shown 7- to 5-fold higher UGT1 activity than human liver microsomes respectively[48, 49].

Concentrations of plasma proteins, e.g., α-acid glycoprotein (AAG), are known to be different across the animal species, i.e., smaller animal species have higher concentrations than larger animals (See Table 2.2 in Chapter 2). Furthermore, since basic drugs commonly bind to AAG, this could be a possible explanation for quantitative interspecies differences in PPB. There are several genetic polymorphisms reported for several isoforms in humans that may or may not be relevant in the preclinical species. Similarly, the influence of covariates such as age, gender etc.,

on the systemic PK both in humans as well as in preclinical species may also contribute to quantitative/qualitative species differences, which may further contribute to species differences, complicating PK-AS approaches.

Limitations of PK-AS

The PK-AS approach is empiric, based on the assumption that PK properties can be scaled by body size only and there are little/no intrinsic, i.e., size-independent, qualitative species differences with respect to PPB, tissue distribution, DME etc. Furthermore, for compounds that are metabolized by extrahepatic routes, biliary excretion pathways involving (active) transport by drug transporters, species differences in these mechanisms, differences in expression and affinity towards transporters, etc., may cause significant prediction errors. Lastly, in order for better predictions, a large range in BW is desired, i.e., when predicting human systemic PK properties, corresponding data from species that have BW both smaller as well as larger than human BW are ideally sought, which is typically not available.

1.4. Overview - Selection of Drug Classes

Most of the QSPKR studies in the literature are either based on (a) congeneric series of compounds, which share a similar structural scaffold (but only differ in the functional groups or substituents) and typically act at a common biological target (e.g., receptor, enzyme, etc.)[39,40,50–52]; or (b) heterogeneous datasets, which include compounds from different structural scaffolds and/or belong to different pharmacological classes, i.e., have different mechanism of action[9,10,28]. While the use of a homologous series primarily aims at identifying the contribution of particular

substituent/functional groups at specific positions of the molecular scaffold, the range in the molecular/PC and/or PK property space is, in general, narrow and overlaps, and the identification of important (bulk) molecular/PC descriptors becomes difficult. Furthermore, the use of MLLR methods on heterogeneous datasets may neglect interaction(s) amongst the molecular descriptors (i.e., highly correlated molecular/PC variables).

In the present work, defined pharmacological classes of compounds, namely, benzodiazepines (BZD), neuromuscular blockers (NMB), triptans (TRP) and class III AAR, were selected because the underlying assumption is that the drug-target interactions are driven by (specific) molecular properties while the drug-biomolecule interactions during systemic disposition (PK) depend predominantly on (bulk) PC properties. Compounds belonging to each of the pharmacological class are known to hit a (respective) specific molecular target, e.g., gamma amino butyric acid ($GABA_A$) receptors in the CNS for BZD, post-ganglionic nicotinic acetylcholine receptors (nAChR) at the neuromuscular endplate for NMB, post-synaptic serotoninergic ($5\text{-}HT_{1B/1D}$) receptors in the CNS for TRP and cardiac K^+ channels for class III AAR. Additionally, (in general), compounds to respective classes share a similar structural scaffold (within each class). Lastly, there was adequate literature on I.V. human PK for a sufficient number of compounds (in each class) enabling the QSPKR analysis.

The ultimate utility of these QSPKR models in the drug discovery/development relies on the property space[5] both in terms of molecular/PC as well as PK, i.e., the larger is the property space(s), the more general is the applicability of the models, and the more likely they are to successfully predict the PK of a new compound.

.

CHAPTER 2. Research Hypotheses

Using the publicly available PK/PD information on the drugs/compounds belonging to these four pharmacological classes, namely, BZD, NMB, TRP and Class III AAR:

Research Hypothesis I:

Molecular/PC properties affect the *in-vivo* human systemic disposition of drugs, and the effect of these (bulk) molecular/PC properties on the biologically relevant human systemic PK properties is similar across pharmacological classes, while the drug-target (i.e., PD) interactions are driven by more specific molecular properties. In order to test this hypothesis:

a. Pertinent human systemic PK/PD properties of these select pharmacological classes of compounds were collected from the biomedical literature, and FDA website (for drug label, biopharmaceutic drug reviews, new drug application approval documents), and, subsequently, their biologically relevant PK properties were estimated.

b. Molecular/PC properties were derived computationally.

c. The effect of these different molecular/PC variables on PK/PD properties was explored statistically, and, as appropriate, relationships were compared across the different pharmacological classes.

d. QSPKR models were developed for predicting biologically relevant human systemic PK properties and validated for their predictive performance.

Research Hypothesis II: Human systemic PK properties can be predicted by scaling from available *in-vivo* animal systemic PK properties using inter-species PK-AS approaches. In order to test this hypothesis:

a. Pertinent animal *in-vivo* systemic PK properties of the BZD and NMB were collected from the biomedical literature, and, subsequently, their biologically relevant animal PK properties were estimated.

b. PK properties of BZD were compared across the different species

c. Allometric relationships were explored statistically using systemic and biologically relevant animal PK for BZD and NMB.

d. Different allometric-based prediction methods were assessed and validated for their predictive performance.

CHAPTER 3. Quantitative Structure Pharmacokinetic Relationships (QSPKR)

3.1. Introduction

Good predictability of any QSPKR model depends on the property space, both in terms of the underlying molecular/PC properties as well as systemic PK properties of the compounds that are included in the dataset to develop and validate the model. The larger the property space (i.e., large dispersion of the individual properties), the better the predictability and thus the applicability of the model, in terms of the prediction of PK properties for new molecules within the property space.

BZD, NMB, TRP and Class III AAR were chosen for developing QSPKR models because the compounds/drugs belonging to each class (a) hit a common biological target, e.g., BZD at $GABA_A$ receptors, TRP at $5\text{-}HT_{1B/D}$ receptors etc., (b) share a common molecular scaffold (at least the majority of them) and (c) show considerable diversity in molecular/PC as well as systemic PK variables, and the property spaces that these classes encompass have not been explored. Furthermore, there was substantial publicly available information in the biomedical literature on the systemic PK after intravenous (I.V.) administration for a sufficient number of compounds of each class. Lastly, there were no obvious PK nonlinearities reported for any of these pharmacological classes. Thus, the objective of the current study was to develop and validate QSPKR models to predict the biologically relevant human PK.

3.2. Specific Aims

- Collect and compile valid human systemic PK/PD properties from the literature.
- Estimate biologically relevant PK variables in humans.
- Assess the effect of different molecular/PC descriptors on various PK/PD variables.
- Develop and validate QSPKR models for biologically relevant PK properties.

3.3. Methods I

3.3.1. Computation of Molecular/PC Properties

Molecular/PC descriptors, namely MW, (most acidic or basic) pKa, logP, and two-dimensional molecular descriptors, namely PSA, MV, nRot, HBA, HBD were obtained using SciFinder Scholar (version 2014; Chemical Abstracts Service: Columbus, OH) for BZD, TRP and class III AAR, while ACD/Labs (version 12.01, Advanced Chemistry Development, Inc., Toronto, ON, Canada, 2014) was used for NMB (due to the lack of availability of that information in SciFinder).

The name of the compound was entered into the "substance identifier" column in SciFinder or ACD/Labs and the molecular structure was reviewed to confirm the selected compound, and the values for the respective properties were compiled. Furthermore, lipophilicity, characterized by $logD_{7.4}$ (calculated logD at a physiologically relevant pH of 7.4) was estimated based on the (most acidic/basic) pKa and pH using the following equations[6]:

$$logD_{7.4} = logP - \log (1+ 10^{7.4 - pKa}) \quad \text{…. for acids … Eq 3.1}$$

$$logD_{7.4} = logP - \log (1+ 10^{pKa - 7.4}) \quad \text{…. for bases … Eq 3.2}$$

Rationale: The PC descriptors used in the current project were chosen because they are reported to likely affect the human systemic PK properties[29]. Additionally, $logD_{7.4}$ is considered preferable over logP because it is believed to be a more reliable (and physiologically relevant) marker for lipophilicity for compounds with ionizable functional groups[6].

3.3.2. Compilation of Systemic PK Properties

The biomedical literature was searched exhaustively for original research and/or review articles on human (and animal) systemic PK/PD properties of 20 BZD (including a $GABA_A$ receptor antagonist), 16 NMB (15 non-depolarizing blockers and 1 depolarizing blocker), 7 TRP and 7 Class III AAR.

PK studies (including the ones that had urinary excretion data) in which the selected compounds are administered exclusively by the I.V route to healthy humans were considered. In case of clinical studies aimed to investigate, e.g., (1) effect of a certain compromised physiological condition such as renal or hepatic disease/dysfunction, or (2) effect of drug-drug interactions, or (3) absolute oral bioavailability; only the treatment arm with healthy subjects, drug of interest alone after I.V were considered. In studies where the pertinent PK properties were not reported, but the (mean) plasma concentration - time plots were available, the respective concentration-time plots were digitized using GraphClick (version 3.0.2, Arizona, AZ), and non-compartmental PK analysis[54] was performed to estimate systemic PK variables. Lastly, oral administration studies were considered if both plasma and urinary concentrations were collected over time to estimate renal clearance (see Table 3.2)

Values for f_u were obtained from *in-vitro* PPB studies, at concentrations in the therapeutic range (and ascertaining the absence of any nonlinearities). Blood-to-plasma (B:P) ratios were

obtained from *ex-vivo* or *in-vitro* studies with whole blood and plasma from healthy humans. RBC partitioning (γ) values were estimated from f_u and B:P ratio using pertinent equations (see Table 3.2)

In-vivo systemic PK properties, namely total body clearance, CL_{tot}, volume of distribution at steady-state, Vd_{ss} (or volume of distribution at pseudo steady-state, Vd_{pss}) and fraction of the dose excreted ultimately unchanged into urine, f_e, were compiled after critical evaluation of study design, type of subjects, dosing regimen, PK sampling schedule, PK analysis and bioanalytical assay procedures etc. Particular importance was given to plasma and urine sampling schedule - i.e., adequate sampling should have been done for at least 2-3 terminal half-lives ($t_{1/2}$); and if the analytical technique used to quantitate plasma and urine concentrations was sensitive over the adequate sampling period. In the majority of studies, Vd_{ss} values were reported; however, in studies where volume of the drug in the central compartment (Vd_{cc}) and micro-rate constants (k_{12}, k_{21}) were available for a two compartmental model, Vd_{ss} was estimated[54].

In case the systemic PK properties were collected from multiple studies, the arithmetic mean was calculated across studies. BW-correction of the systemic PK properties was performed based on widely reported values reported in literature for AS-PK, a body weight for animals (see Table - 3.2) and 70 kg for humans[55]. Each individual study compiled and included respective PK property value is presented in a comprehensive manner in Appendices I through IV.

3.3.3. Compilation of PD Properties

In order to evaluate if the drug molecule-PD target interactions are driven by and can be explained by the (bulk) molecular/PC properties for the different pharmacological classes of compounds, their (pertinent) respective *in-vitro/ex-vivo/in-vivo* PD properties, were compiled.

In-vivo, the main molecular target of BZD is the postsynaptic inhibitory, gamma amino butyric acid ($GABA_A$) receptor. Binding affinities (K_i) of BZD to $GABA_A$ receptors were compiled from *in-vitro* studies investigating the displacement of (pre-incubated) radiolabeled ligands, e.g., [^{3}H]-diazepam or [^{3}H]-flunitrazepam, in the presence of increasing concentrations in homogenized rat/human brain.

The underlying assumption in these studies is that BZD (competitively) inhibit the radiolabeled ligand, which can be assayed by liquid scintillation counting of the unbound radiolabeled ligand (which is usually separated, accounting for non-specific binding).

TRP, on the other hand show high selectivity and potent agonist activity at the serotoninergic receptors, namely 5-$HT_{1B/1D}$ subtypes[56] (which are presumed to be the molecular targets for alleviating migraine pain[57,58]). Thus, binding affinities (K_i) of TRP to 5-$HT_{1B/1D}$ were compiled from *in-vitro* studies investigating the displacement of (pre-incubated) radiolabeled ligands, e.g., [^{3}H]-eletriptan or [^{3}H]-sumitriptan, in stably transfected cell lines (HeLa) expressing human 5-$HT_{1B/1D}$ receptors.

In the case of NMB, *in-vivo* PD properties namely, equilibration rate constant between plasma and biophase, (k_{eo}), plasma concentration producing half-maximal effect (cp_{ss}^{50}) and steepness of the concentration - effect relationship (γ) were compiled from *in-vivo* human PD

studies after ensuring that the same PD endpoint, i.e., 95% depression in the muscle twitch following ‘train-of-four’ stimulus was considered.

Table 3.1: List of Physiological Variables in Humans and Various Animal Species

Species	BW	TBW	IW	EW	Plasma Volume	Blood Volume	LBF	RPF	GFR
	(kg)	(l/kg)					(ml/min/kg)		
Mouse	0.02	0.73			0.05	0.09	90	40	15
Rat	0.25	0.67	0.37	0.30	0.03	0.05	55	21	5.2
Rabbit	2.5	0.72	0.47	0.25	0.04	0.07	71	21	3.1
Rhesus Monkey	5	0.69	0.49	0.21	0.04	0.07	44	17	2.1
Dog	10	0.60	0.33	0.28	0.05	0.09	31	12	6.1
Human	70	0.60	0.34	0.26	0.04	0.07	21	10	1.8
AS Exponent		**0.98**	**0.97**	**0.98**	**1.01**	**1.01**	**0.83**	**0.84**	**0.79**

BW - Body weight; TBW - Total body water space; IW - Intracellular water space; EW - Extracellular water space; LBF - Liver blood flow; RPF - Renal plasma flow and GFR - Glomerular filtration rate
AS - Allometric Scaling Exponent
Values compiled from reference[55]

3.3.4. Estimation of Biologically Relevant PK Variables

A fundamental assumption in PK/PD is that only the unbound drug is available for disposition, i.e., distribution, metabolism and elimination. Therefore, the compiled PK variables, Vd_{ss}, CL_{tot}, CL_{ren}, CL_{nonren} were corrected for PPB, to obtain their biologically relevant variables, i.e., only for the unbound drug, namely, Vd_{ss}^{u}, CL_{tot}^{u}, CL_{ren}^{u}, CL_{nonren}^{u} and $CL_{int}^{In\text{-}vivo}$; the equations used are shown in Table 3.2 below.

Table 3.2: Estimation of *In-vitro*/*In-Vivo* Systemic PK Variables

***In-vivo/In-vitro* PK Variable**	**Equation**
Red blood cell (RBC) Partition Coefficient (γ)	$\gamma = \left(\frac{B:P-(1-H)}{H*f_u}\right)$; H=hematocrit (0.46)[59] for humans
Vd_{ss}	$Vd_{ss} = Vd_{cc} * \left(1 + \frac{k_{12}}{k_{21}}\right)$ $Vd_{ss} = CL_{tot} * \left(\frac{\frac{A}{\alpha^2} + \frac{B}{\beta^2}}{\frac{A}{\alpha} + \frac{B}{\beta}}\right)$ For a 2-compartmental model, after I.V. bolus administration
Vd_{ss}^{u}	$Vd_{ss}^{u} = Vd_{ss}/f_u$
CL_{tot}	$CL_{tot} = CL_{ren} + CL_{nonren}$
CL_{ren}	$CL_{ren} = f_e * CL_{tot}$ (f_e = fraction of the dose excreted ultimately unchanged in urine after I.V. administration) $CL_{ren} = U_\infty/AUC_\infty$ (After P.O. or I.V. administration: U_∞ = Amount ultimately excreted unchanged in urine, AUC_∞ = Area under the plasma concentration-time curve from 0 - ∞)
CL_{nonren}	$CL_{tot} - CL_{ren}$
CL_{tot}^{u}	$CL_{tot}^{u} = CL_{tot}/f_u$
CL_{ren}^{u}	$CL_{ren}^{u} = CL_{ren}/f_u$
CL_{nonren}^{u}	$CL_{nonren}^{u} = CL_{tot}^{u} - CL_{ren}^{u}$
CL_{nonren}^{blood} (assuming absence of extra-hepatic metabolism)	$CL_{nonren}^{blood} = CL_{nonren}/(B:P)$
Hepatic extraction ratio (ER_{hep})	$ER_{hep} = CL_{nonren}^{blood}/Q_{hep}$ (Q_{hep} = hepatic blood flow, 21 ml/min/kg for humans)
$CL_{int}^{In\text{-}vivo}$	$CL_{int}^{In\text{-}vivo} = (Q_{hep}*CL_{hep})/((f_u/B:P)*(Q_{hep} - CL_{hep}))$

3.3.5. PK Classification of Drugs

For mechanistic interpretation of the observed/reported as well as of the biologically relevant PK data, the classifications shown in Table 3.3 were followed for all the drugs.

Table 3.3 - Categorization By PK Properties

PK Property Categorization	Cut-off
Based on PPB	
High PPB	$f_u < 10\%$
Intermediate PPB	$10\% < f_u < 90\%$
Low PPB	$f_u > 90\%$
Based on route of metabolism	
Highly metabolized, and hepatic metabolism is the major elimination pathway (assuming there is no extrahepatic metabolism and no biliary excretion)	$f_e < 20\%$
Based on hepatic extraction ratio (ER_{hep})	
Low ER_{hep}	$ER_{hep} < 0.3$
Intermediate ER_{hep}	$0.3 < ER_{hep} < 0.7$
High ER_{hep}	$ER_{hep} > 0.7$
Based on extra-hepatic metabolism	
Evidence of extrahepatic metabolism	$CL_{nonren}^{Blood} > Q_{hep}$
Based on renal handling	
Compounds renally cleared by net glomerular filtration	$CL_{ren}^{u} = GFR$
Compounds renally cleared by net tubular reabsorption	$CL_{ren}^{u} < GFR$
Compounds renally cleared by net tubular secretion	$CL_{ren}^{u} > GFR$

3.3.6. Physiological Interpretation

Fraction of the drug unbound in plasma (f_u): It is one of the important biologically relevant PK properties, since only the drug that is not bound to plasma proteins (e.g., albumin, alpha-acid glycoprotein, etc.) is available for tissue distribution, metabolism, elimination and drug-target receptor binding. High PPB (low f_u) may prevent the drug from being widely distributed (i.e., low Vd_{ss}) and/or cleared (e.g., low ER_{hep} or low CL_{ren}), although unbound drug may show wide distribution (high Vd_{ss}^{u}), and/or have high clearance (e.g., high hepatic intrinsic clearance, CL_{int} or high unbound renal clearance CL_{ren}^{u}).

B:P ratio: It is the reported ratio of whole blood to plasma concentrations and (a) depends on f_u and RBC partition coefficient *(*γ), i.e., low B:P ratio may result from high PPB (low f_u); and/or high affinity of drug to RBC may result in a high B:P. Furthermore, B:P ratio allows the estimation of γ (from f_u, see Table - 3.2) and determines the blood clearance, CL_{nonren}^{Blood}, to compare with the LBF.

RBC partition coefficient (γ): Apart from plasma proteins, drugs may also bind to RBC in the blood, which in turn may limit their distribution and/or elimination. Therefore, it is another important biologically relevant PK property, and denotes the ratio of concentration of the drug in the RBC to that unbound in plasma (i.e., after correcting for PPB). Physiologically, higher γ indicates higher affinity of the drug to RBC relative to plasma water, potentially due to binding to RBC membranes and/or intraerythrocytic proteins.

Volume of distribution at steady-state (Vd_{ss}): It is the apparent volume that the drug occupies at steady state, i.e., when the unbound concentrations throughout the body are equal. Since only the unbound drug in plasma will be available for tissue distribution, Vd_{ss} has to be corrected for f_u (Vd_{ss}^{u}), so as to be interpreted mechanistically by comparing it to various

physiological body compartments/spaces[55] (e.g., plasma volume, blood volume, intracellular and/or extracellular water, total body water etc., listed in Table - 3.1).

Total clearance (CL_{tot}): It is the volume of plasma that is completely cleared of the drug per unit time. Further separation of the elimination pathways of CL_{tot} can be accomplished based on f_e data into CL_{ren} and CL_{nonren}.

Renal clearance (CL_{ren}): Since only the unbound drug in plasma can undergo glomerular filtration (GFR) and/or tubular secretion, CL_{ren} has to be corrected for f_u to obtain biologically relevant CL_{ren}^{u} in order to evaluate the net tubular secretion/reabsorption (See Table 3.3)

Nonrenal clearance (CL_{nonren}): It indicates clearance by all the pathways other than renal, namely, hepatic (i.e., metabolism and/or biliary excretion) and/or extrahepatic, which may include metabolism in the RBC, hydrolysis in the plasma and/or tissue, etc. CL_{nonren}^{blood} is physiologically more meaningful than plasma clearance, since the organs are perfused by blood (not just plasma). Also, mechanistically, the blood clearances can be compared to organ blood flow(s), e.g., LBF; and if $CL_{nonrenal}^{blood}$ exceeds LBF, it suggests extrahepatic clearance. (See Table 3.3)

Hepatic extraction ratio (ER_{hep}): It reflects the intrinsic ability of the liver to extract drug (as reflected in the difference in the hepatic artery (and portal vein) - hepatic vein concentrations). Based on a widely used hepatic venous equilibration/"well-stirred" model[60], ER_{hep} is affected by CL_{int} (intrinsic ability of the liver to clear the drug in the absence of flow and binding restrictions), f_u and Q_{hep} (hepatic blood flow).

$$ER_{hep} = f_u*CL_{int}/ (Q_{hep} + f_u*CL_{int}) \ldots. \text{Eq } 3.3$$

Receptor binding affinity (K_i): It indicates intrinsic binding affinity of the drug molecule to the target receptor.

k_{e0}: It characterizes the equilibration rate constant between plasma and biophase (i.e., where the drug-targets are present). It is inversely related to the time it takes for this equilibration to occur.

Cp_{ss}^{50}: It is the concentration in plasma at steady-state producing half-maximal effect (cp_{ss}^{50}), when the unbound plasma and biophase concentrations are equal.

γ (PD): It characterizes the steepness/slope of the concentration - effect relationship.

3.4. Methods II - Statistical Analyses

3.4.1. Descriptive Statistics

Statistical distributions for molecular/PC, *in-vivo* human systemic and *in-vitro* PK/PD properties were investigated, and mean, median, quartiles and fold-range (maximum/minimum) for each variable was reported. Most PK(/PD) variables exhibited skewed distribution(s) and/or wide dispersion and, therefore were log-transformed for regression analyses.

All the statistical analyses were performed using JMP 11.0 (SAS, Cary, NC).

3.4.1.1. Collinearity Analyses

Correlation analyses for both PC and PK/PD variables were assessed using correlation matrices, based on the criterion set *a-priori*, i.e., (absolute value of) correlation coefficient (r) > 0.8. If PC covariates were found to collinear, only one of them was used (based on mechanistic plausibility) for further regression analyses.

3.4.1.2. Univariate Screening of Molecular/PC Covariates

All (potentially important) molecular/PC descriptors that may affect the biologically relevant PK/PD properties were screened. For this, the univariate linear relationships of (log-transformed) PK/PD variables as a function of PC variables were studied. Goodness of fit statistics was evaluated using r^2 (which characterizes the variability in the PK/PD (dependent) variable that can be accounted for by the PC (independent) variable). Relationships with $r^2 \geq 0.3$ (i.e., 30% explained variability) and a p-value <0.05 were used as cut-offs for choosing a PC covariate. Furthermore, the slopes of the univariate relationships were used to evaluate the sensitivity (S) of changes in the PK variable changes in the relative to PC variable.

3.4.2. Final QSPKR Model Building and Evaluation

Final QSPKR model building for the biologically relevant systemic PK variables was performed by stepwise, multiple log linear regression (MLLR) - an initial forward inclusion step, followed by a backward elimination step. Goodness of fit statistic, r^2 and $p < 0.05$, and the sensitivity (S) (and its precision) for the final QSPKR model were reported.

3.4.3. Cross - Validation

The predictive performance of the final QSPKR model was evaluated by cross-validation (CV) by leave-out-one (LOO) method[61] using RStudio v0.96.330[62].

This method leaves out one observation from the entire dataset and uses it for validation, while the rest of the dataset is used as the training set. This is then repeated until each observation is left out once (serving as the validation 'set'). For each model, the excluded observation is predicted and the cross-validated explained variance (q^2) is calculated[61] using the equation below.

$$q^2 = 1 - \frac{\sum(Predicted - Observed)^2}{\sum(Observed - Mean)^2} \quad \text{.... Eq 3.4}$$

A model with $q^2 \geq 0.40$ is considered acceptable[61].

CHAPTER 4. QSPKR of BZD

4.1. Background

BZD are used therapeutically as sedatives, hypnotics, anticonvulsants, and these effects arise from their action in the CNS. Within the CNS, the main molecular target of BZD is the postsynaptic inhibitory neurotransmitter, namely, gamma-amino butyric acid ($GABA_A$) receptor. BZD act as allosteric modulators of the $GABA_A$ receptor, increasing the affinity of GABA at its receptor, resulting in higher chloride conductance, and overall potentiating the (inhibitory) effects of GABA in the CNS[63]. The therapeutic effects, by large, are dependent on the half-live of the drug (and active metabolites), e.g., short acting (0 - 6 h) for pre-anesthesia prior to surgery, intermediate (6 - 24 h) acting for insomnia, long acting (> 24 h) for treating anxiety, convulsions[64]. In general, BZD are small MW and lipophilic compounds, mostly unionized so as to facilitate the permeation through blood-brain barrier in order to reach the CNS target. Most of the BZD are structural analogues and share a common scaffold (1, 4, benzo-diazepin ring, shown in Figure 4.1). A brief account of structure - activity relationship (SAR)[65,66] of BZD is given below.

Figure 4.1 - Common Structural Scaffold - 1, 4 - Benzodiazepine

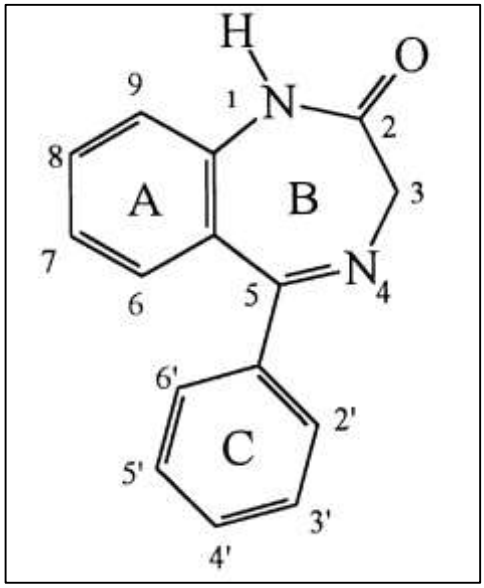

The known SAR is as follows**:**

Rings A & B:

1. Methylation of N at position 1 increased the therapeutic potency (anxiolytic activity)
2. Substitutions of 1 - 2 with either imidazo- or triazo- ring (e.g., alprazolam, midazolam) resulted in significant increase in receptor binding affinity.
3. A hydrogen-bond-accepting group substituent at position 2 is important for interactions with hydrogen bonding donating site in the $GABA_A$ receptor.
4. Substituents at position 3 and 8 are involved in ionic interactions with the $GABA_A$ receptor.
5. A strong electronegative (electron withdrawing group) group at position 7 increased therapeutic potency by several-fold.

Ring C:

4-1. It is involved in hydrophobic interactions with the $GABA_A$ receptor

4-2. Substitution at position 2' increased therapeutic potency

4.2. Results

4.2.1. PC/Molecular Property Space of BZD

The final PC/molecular and human systemic PK/PD database consists of twenty BZD, including three metabolites, N-desmethyl diazepam (N-DMD), chlor-desmethyl diazepam (Chor-DMD), N-desmethyl adinazolam (N-DMAD) as well as flumazenil, a GABA antagonist. Structurally, most of the BZD in the final dataset share the 5-aryl, 1, 4-BZD scaffold (see Figure 4.1), thus exhibiting fairly similar values for nRot, HBA, HBD, which is also evident from low diversity (2- to 3-fold, n = 20) in these properties (as shown in Table - 4.1) except for Ro 48-6791 and Ro 48-8684, with higher nRot and HBA. BZD are relatively low MW (ranging from 271 to 412 Da, n = 20) compounds.

For all the BZD in the final dataset that have two pK_as, only pK_{a1}, i.e., due to weakly acidic group (e.g., -OH group) (n = 7) is relevant at physiological pH of 7.4, while the rest of the BZD are all bases (n = 13), and only pK_{a2} (i.e., due to weakly basic group e.g., $-NH_2$) is relevant. All BZD are lipophilic, i.e., $logD_{7.4} > 1$ (ranging from 1.10 to 3.78, except N-DMAD with a $logD_{7.4}$ of 0.75). The majority of BZD in the current dataset are unionized at pH 7.4, and, therefore, the estimated $logD_{7.4}$ values are identical to the SciFinder predicted logP. N-DMAD (the least lipophilic BZD in the dataset) is present in the form of cationic species (55% ionized) at physiological pH of 7.4, consequently, its $logD_{7.4}$ value is lower than its respective SciFinder-predicted logP. On the other hand, although Ro 48-8684 is present predominantly in the form of cationic species (66% ionized), the impact of ionization is less pronounced, i.e., its estimated $logD_{7.4}$ (2.97) is comparable to SciFinder-predicted logP (3.38), possibly owing to the presence of large aromatic functional groups (as evident from its high MW relative to the rest of BZD in the database).

Descriptive statistics (as shown in Table 4.2) show that mean and median values are comparable for most of the molecular/PC properties. The low dispersion (relatively low standard deviations and range) is indicative of their low diversity of the molecular/PC property space. Based on the acceptance criteria set *a-priori* for collinearity i.e., $r \geq 0.80$, MW is highly correlated with MV ($r = 0.81$, $n = 20$), MV with nRot ($r = 0.84$, $n = 20$) and nRot with HBA ($r = 0.83$, $n = 20$) (shown in Table 4.3). Thus, $logD_{7.4}$, MW, PSA, HBA and HBD were used for subsequent analysis (i.e., MV and nRot were excluded).

Table 4.1 - Molecular/PC Property Space of BZD

Label	Drug	MW (Da)	logP	pK_{a1}	pK_{a2}	LogD at pH 7.4	% Ionized at pH 7.4	Charge at pH 7.4	PSA (A^2)	MV (cm^3/mol)	nRot	HBD	HBA
1	Chlordiazepoxide	300	2.49		2.38	2.49	0%		53	231	1	4	1
2	Clonazepam	316	2.52	11.21	1.55	2.52	0%		87	210	2	6	1
3	Clorazepate	315	2.54		3.43	2.54	0%		79	215	2	5	2
4	Diazepam	285	2.80		3.40	2.80	0%		37	226	1	3	0
5	N-DMD	271	2.78	11.72	3.22	2.78	0%		42	205	1	3	1
6	Chlor-DMD	305	2.94	11.58	2.22	2.94	0%		42	214	1	3	1
7	Lorazepam	321	2.38	10.80	0.17	2.38	0%		62	211	2	4	2
8	Nitrazepam	281	2.36	11.35	2.55	2.36	0%		87	201	2	6	1
9	Flunitrazepam	313	2.13		1.68	2.13	0%		79	225	2	6	0
10	Oxazepam	287	2.22	10.94	1.17	2.22	0%		62	202	2	4	2
11	Temazepam	301	2.20	11.70	1.58	2.20	0%		53	223	2	4	1
12	Adinazolam	352	1.27		7.09	1.10	33%	*Cation*	46	268	3	5	0
13	N-DMAD	338	1.09		7.48	0.75	55%	*Cation*	55	246	3	5	1
14	Alprazolam	309	1.92		2.37	1.92	0%		43	226	1	4	0
15	Midazolam	326	3.80		6.03	3.78	4%	*Cation*	30	240	1	3	0
16	Triazolam	343	2.08		2.29	2.08	0%		43	235	1	4	0
17	Ro 48-6791	412	3.05		6.36	3.01	8%	*Cation*	80	307	7	8	0
18	Ro 48-8684	411	3.38		7.59	2.97	61%	*Cation*	67	318	7	7	0
19	Brotizolam	394	2.46		2.01	2.46	0%		71	220	1	4	0
20	Flumazenil	303	2.15		0.86	2.15	0%		64	217	3	6	0
	N	20	20			20			20	20	20	20	20
	Mean	271	2.43			2.38			59	232	2	5	1
	Maximum	412	3.80			3.78			87	318	7	8	2
	Minimum	324	1.09			0.75			30	201	1	3	0
	-fold range	2	5			5			3	2	7	3	2

Table 4.2 - Descriptive Statistics of PC/Molecular Properties of BZD

	N	Mean	SD	95% CI	Minimum	10%	25%	Median	75%	90%	Maximum
MW (Da)	20	**324**	40.7	305, 343	271	281	300	**314**	342	409	412
$LogD_{7.4}$	20	**2.4**	0.66	2.1, 2.7	0.8	1.2	2.1	**2.4**	2.8	3.0	3.8
PSA (A^2)	20	**59**	17.4	51, 67	30	37.5	43	**59**	77	86.3	87
MV (cm^3/mol)	20	**232**	31.9	217, 247	201	202	212	**224**	239	303	318
nRot	20	**2.3**	1.77	1.4, 3.1	1	1	1	**2**	2.8	6.6	7
HBA	20	**4.7**	1.42	4.0, 5.4	3	3	4	**4**	6	7	8
HBD	20	**0.7**	0.74	0.3, 1.0	0	0	0	**0.5**	1	2	2

Table 4.4 - Correlation Matrix of PC/Molecular Variables of BZD

	MW (Da)	$LogD_{7.4}$	PSA (A^2)	MV (cm^3/mol)	nRot	HBA	HBD
MW (Da)	1.00						
$LogD_{7.4}$	0.05	1.00					
PSA (A^2)	0.24	-0.05	1.00				
MV (cm^3/mol)	**0.81**	0.06	0.02	1.00			
nRot	0.70	0.03	0.42	**0.84**	1.00		
HBA	0.53	-0.11	0.76	0.56	**0.83**	1.00	
HBD	-0.44	-0.07	0.23	-0.51	-0.21	-0.20	1.00

4.2.2. Humans Systemic PK/PD Property Space of BZD

The final mean *in-vitro*/*in-vivo* human systemic PK and *ex-vivo/in-vitro* PD properties compiled from various studies in the literature are shown in Table - 4.4 and 4.6, respectively and the estimated biologically relevant PK properties in Table 4.5. Appendix 1 contains all the supplemental information with respect to the *in-vitro*/*in-vivo* human systemic PK and *ex-vivo/in-vitro* PD data compiled for each of the compound from the literature.

There is considerable to large diversity in the *in-vitro/in-vivo* systemic PK/PD properties of BZD in the current dataset ranging from 20- to 1950-fold (n = 5 - 17). The descriptive statistics for these PK/PD variables (shown in Table 4.7) indicate that the mean values for most of them (except f_u, and B:P ratio) are greater than their respective median values. Owing to this skewed distribution and high diversity, all the systemic PK/PD variables (except f_u, B:P ratio and γ) were log transformed for further analysis. Several correlations are observed between the *in-vitro*/*in-vivo* human systemic and biologically relevant PK variables (shown in Table 4.8). Most of these correlations are mechanistically plausible, e.g., CL_{nonren}^{u} is highly correlated (r = 0.99, n = 8) with CL_{tot}^{u}, and f_e values for most of the BZD ranges between 0.02 - 11% (except for N-DMAD, whose f_e = 72%), suggesting the contribution of renal pathways towards total clearance is low for BZD.

PPB of BZD in the final dataset varies 33-fold (n = 17). With the exception of N-DMAD (the least lipophilic BZD in the dataset with $logD_{7.4}$ of 0.75, and f_u of 65%) and flumazenil, the majority of the BZD show a high degree of PPB, probably owing to their high degree of lipophilicity. There is larger diversity in the Vd_{ss}^{u} values (118-fold, n = 16) than Vd_{ss} values (20-fold, n = 19). Furthermore, it is observed that the mean Vd_{ss}^{u} value (21.5 l/kg) is higher than Vd_{ss} value (1.5 l/kg). Therefore, it seems that the high Vd_{ss}^{u} values (for most of the BZD) are offset

by high PPB (i.e., low f_u), resulting in low Vd_{ss} values, suggesting that BZD tissue distribution is restricted by PPB. Vd_{ss}^u values for all the BZD in the dataset exceed BW (70 kg) (except for the most hydrophilic N-DMAD and flumazenil, whose estimates are close to 1 L/kg), indicating they undergo moderate to extensive extravascular distribution into tissues, and, also potential binding to plasma membranes etc. CL_{tot}^u varies 74-fold (n = 17) while CL_{tot} varied 1550-fold (n = 20, Ro 48-6791 with Ro 48-8684 showing a relatively high CL_{tot} but lacking f_u and f_e data). The high CL_{tot}^u values seem to be offset by high PPB (i.e., low f_u), resulting in low CL_{tot} values for the majority of BZD with available information.

The contribution of renal pathway towards CL_{tot} is low ($f_e \leq 10\%$) for all the BZD in the dataset with available information (n = 9), except for N-DMAD (f_e = 71%), suggesting they are all subject to extensive hepatic metabolism (with no obvious evidence of extrahepatic clearance pathway(s) for any of the BZD). CL_{ren}^u estimates for all the BZD in the dataset with available information (n=9) are higher than GFR (1.7 ml/min/kg), suggesting they undergo net renal tubular reabsorption, except for N-DMAD, which shows CL_{ren}^u value greater than GFR, suggesting it undergoes net renal tubular secretion (potentially involving drug transporters as it is positively charged at pH 7.4).

Based on the CL_{nonren} estimates (n=9), relative to LBF of 21 ml/min/kg, midazolam and flumazenil show intermediate (to high) ER_{hep}, while the rest of BZD with available information show low ER_{hep}, either because of low hepatic CL_{int} (e.g., chlordiazepoxide, lorazepam, nitrazepam etc.) and/or high PPB (e.g., diazepam, oxazepam etc.). The B:P ratio for most BZD in the current dataset with available information (n = 9) show values of less than 1.0; the plausible explanation is the high degree of PPB (e.g., diazepam, chlordiazepoxide) and/or low RBC partitioning, γ (e.g., midazolam). However, the B:P ratios for Ro 48-6791 and Ro 48-8684 are

higher than 1.0, which is possibly be due to high RBC binding and/or low PPB. CL_{nonren}^{Blood} values for BZD in the dataset with available information (n=5) are lower than LBF (21 ml/min/kg), confirming that these BZD are low ER_{hep} compounds. In general, CL_{nonren}^{blood} values are much lower than respective CL_{nonren}^{plasma}, except for midazolam, for which CL_{nonren}^{blood} is greater than CL_{nonren}^{plasma} possibly owing to low B:P ratio and/or high PPB. The contribution of a specific metabolic pathway ($f_{pathway}$) e.g., CYP3A, CYP2C19 etc., towards the total clearance estimated from *in-vivo* drug - drug interaction studies using specific inhibitors (e.g., ketoconazole, itraconazole etc.) and pharmacogenetic studies (e.g., poor vs. extensive metabolizers of diazepam) is indicated in Appendix - 1.

For compounds with available information (n = 6), $f_{pathway}$ via CYP3A is the primary elimination route for alprazolam (75%), midazolam (80%), triazolam (95%) and brotizolam (80%), while for chlordiazepoxide (35%) it is found to be relatively low. CYP2C19 is the major elimination pathway for diazepam (83%).

BZD binding affinity (K_i) to $GABA_A$ relative to [^{3}H] Diazepam varies 245-fold (n = 11); and K_i relative to [^{3}H] Flunitrazepam varies 1950-fold (n = 11). Early BZD discovery was based on the synthesis of the metabolites (e.g., flunitrazepam, oxazepam etc.) of the already existing BZD (nitrazepam and diazepam, respectively) and were evaluated for improved potencies, and therefore, there is such a large diversity in the binding affinities.

Table 4.4 - *In-vitro* and *In-vivo* Human PK Systemic Properties of BZD

	***In-vitro* PK Variables**		***In-vivo PK Variables***				
Drug	**f_u [%]**	**B:P Ratio**	**Vd_{ss}/Vd_{pss} [l/kg]**	**CL_{tot} [ml/min/kg]**	**f_e [%]**	**CL_{ren} [ml/min/kg]**	**CL_{nonren} [ml/min/kg]**
Chlordiazepoxide	5.1%	0.66	0.39	0.44	1.0%	0.0044	0.44
Clonazepam	14%	.	3.0	0.91	.	.	.
Clorazepate	.	.	*0.22*	0.020	11%	0.0022	0.018
Diazepam	2.0%	0.58	1.1	0.39	0.30 %	0.0012	0.39
N-DMD	3.2%	.	*1.2*	0.17	.	.	.
Chlor-DMD	3.2%	.	*3.9*	0.26	.	.	.
Lorazepam	9.6%	.	1.3	1.2	0.50 %	0.0062	1.2
Nitrazepam	13%	.	*1.9*	0.83	1.0%	0.0083	0.82
Flunitrazepam	22%	0.75	2.4	1.7	.	.	.
Oxazepam	5.2%	1.0	0.60	1.1	1.0%	0.011	1.1
Temazepam	3.1%	.	.	1.4	.	.	.
Adinazolam	30%	0.70	1.0	5.8	.	.	.
N-DMAD	65%	.	0.68	2.9	71%	2.1	0.85
Alprazolam	32%	0.78	0.91	0.81	.	.	.
Midazolam	3.7%	0.55	0.87	7.0	0.15 %	0.010	6.9
Triazolam	11%	0.76	0.60	2.7	.	.	.
Ro 48-6791	.	1.3	2.4	31	.	.	.
Ro 48-8684	.	1.4	4.3	31	.	.	.
Brotizolam	9.8%	.	*0.66*	1.6	.	.	.
Flumazenil	58%	0.94	0.87	15	0.10 %	0.015	15
N	17	9	19	20	9	9	9
Mean	17%	0.86	1.5	5.3	9.6%	0.24	3.0
Maximum	65%	1.4	4.3	31	71%	2.1	14.8
Minimum	2.0%	0.58	0.22	0.020	0.10 %	0.0012	0.018
-fold range	33	11	20	1550	710	1778	834

Table 4.5 - Biologically Relevant *In-vivo* Human PK Properties of BZD

Drug	Vd_{ss}^{u}/Vd_{pss}^{u} [l/kg]	CL_{tot}^{u} [ml/min/kg]	CL_{ren}^{u} [ml/min/kg]	CL_{nonren}^{u} [ml/min/kg]	CL_{nonren}^{BL} [ml/min/kg]	γ
Chlordiazepoxide	7.7	8.7	0.087	8.6	0.084	5.2
Clonazepam	21	6.3	.	.	.	.
Clorazepate	.	.	.	.	.	.
Diazepam	57	20	0.060	20	0.087	4.5
N-DMD	*39*	5.4	.	.	.	.
Chlor-DMD	124	8.3	.	.	.	.
Lorazepam	13	13	0.064	13	.	.
Nitrazepam	*15*	6.6	0.066	6.5	.	.
Flunitrazepam	11	7.6	.	.	.	2.0
Oxazepam	12	21	0.21	20	0.050	21
Temazepam	.	44	.	.	.	.
Adinazolam	3.4	19	.	.	.	1.1
N-DMAD	1.0	4.5	3.2	1.3	.	.
Alprazolam	2.9	2.6	.	.	.	0.78
Midazolam	24	189	0.026	189	12	0.60
Triazolam	5.5	25	.	.	.	4.3
Ro 48-6791	.	.	.	.	.	.
Ro 48-8684	.	.	.	.	.	.
Brotizolam	*6.8*	16	.	.	.	.
Flumazenil	1.5	26	0.03	26	9.9	1.5
N	16	17	8	8	5	9
Mean	22	25	0.50	36	4.4	4.6
Maximum	124	189	3.2	189	12	21
Minimum	1.0	2.6	0.026	1.3	0.050	0.60
-fold range	118	74	125	145	233	36

Table 4.6 - *In-vitro/Ex-vivo* (Relative) BZD-GABA$_A$ Binding Affinities (K_i)

	Mean Relative Receptor Affinity (K_i) (in nM)	
Drug	**[^{3}H] Diazepam**	**[^{3}H] Flunitrazepam**
Chlordiazepoxide	567	780
Clonazepam	2.3	1.1
Clorazepate	44	.
Diazepam	14	19
N-DMD	8.8	5.6
Lorazepam	2.8	1.4
Nitrazepam	16	11
Flunitrazepam	3.2	2.2
Oxazepam	40	21
Temazepam	38	.
Alprazolam	.	4.2
Midazolam	.	0.40
Triazolam	2.6	0.50
N	11	11
Mean	67	77
Maximum	567	780
Minimum	2.3	0.40
-fold range	245	1950

Table 4.7 - Descriptive Statistics of Human Systemic PK/PD Variables of BZD

	N	Mean	SD	95% CI	Minimum	10%	25%	Median	75%	90%	Maximum
Vd_{ss} (L/kg)	19	**1.5**	1.2	0.92, 2.1	0.22	0.39	0.66	**1.0**	2.4	3.9	4.3
CL_{tot} (ml/min/kg)	20	**5.3**	9.4	0.88, 9.7	0.020	0.18	0.53	**1.3**	5.1	29	31
CL_{ren} (ml/min/kg)	9	**0.24**	0.69	-0.29, 0.78	0.0010	0.0010	0.0030	**0.0080**	0.013	2.1	2.1
CL_{nonren} (ml/min/kg)	9	**2.9**	4.9	-0.84, 6.7	0.020	0.020	0.40	**0.80**	4.1	15	15
f_u (%)	17	**17**	19	7.2, 27	1.9	1.9	3.4	**9.8**	30	59	65
Vd_{ss}^{u} (L/kg)	16	**22**	31	4.9, 38	1.0	1.3	3.9	**11**	23	77	124
CL_{tot}^{u} (ml/min/kg)	17	**25**	43	2.4, 47	2.6	4.1	6.4	**13**	23	73	189
CL_{ren}^{u} (ml/min/kg)	8	**0.52**	1.1	-0.39, 1.4	0.030	0.030	0.10	**0.10**	0.28	3.2	3.2
CL_{nonren}^{u} (ml/min/kg)	8	**36**	62	-17, 88	1.3	1.3	7.0	**16**	24	189	189
CL_{nonren}^{Blood} (ml/min/kg)	5	**4.4**	5.9	-3.0, 12	0.050	0.050	0.065	**0.090**	11	12	12
B:P Ratio	11	**0.86**	0.28	0.67, 1.1	0.55	0.55	0.66	**0.76**	1.0	1.4	1.4
RBC Partitioning	9	**4.7**	6.3	-0.22, 9.5	0.60	0.60	1.3	**2.0**	4.9	21	21
[^{3}H] Diazepam RRA (nM)	11	**67**	166	-44, 179	2.0	2.2	3.0	**14**	40	462	567
[^{3}H] Flunitrazepam RRA (nM)	11	**77**	233	-80, 234	0.40	0.50	1.0	**4.0**	19	628	780

Table 4.8 - Correlation Analysis of Human Systemic PK Variables of BZD

	Vd_{ss} (L/kg)	**CL_{tot} (ml/min/kg)**	**CL_{ren} (ml/min/kg)**	**CL_{nonren} (ml/min/kg)**	**f_u**	**Vd_{ss}^u (L/kg)**	**CL_{tot}^u (ml/min/kg)**	**CL_{ren}^u (ml/min/kg)**	**CL_{nonren}^u (ml/min/kg)**
Vd_{ss} (L/kg)	1.00								
CL_{tot} (ml/min/kg)	0.34	1.00							
CL_{ren} (ml/min/kg)	-0.66	-0.33	1.00						
CL_{nonren} (ml/min/kg)	0.38	**0.99**	-0.39	1.00					
f_u	-0.02	**0.80**	0.24	0.76	1.00				
Vd_{ss}^u (L/kg)	**0.81**	0.05	-0.62	0.09	-0.38	1.00			
CL_{tot}^u (ml/min/kg)	0.41	-0.03	-0.43	-0.01	-0.51	0.63	1.00		
CL_{ren}^u (ml/min/kg)	-0.74	-0.42	**0.99**	-0.48	0.13	-0.67	-0.40	1.00	
CL_{nonren}^u (ml/min/kg)	0.48	0.01	-0.48	0.04	-0.49	0.69	**0.99**	-0.46	1.00

4.3. QSPKR Analysis, Model Building and Evaluation

The results of the univariate regression of the *in-vitro/(*log-transformed) *in-vivo* biologically relevant and reported PK/PD variables as a function of the molecular/PC descriptors are summarized in Tables 4.9 and 4.10 respectively. MW shows significant univariate relationships ($r^2 \geq 0.30$ and $p < 0.05$) with log (CL_{tot}); $logD_{7.4}$ with f_u, log (Vd_{ss}^u), log (CL_{nonren}^u), and log (CL_{ren}); HBA shows a significant relationship with f_u; and HBD with Log (CL_{tot}) and γ (RBC partitioning). These relationships are shown in Figures 4.2 - 4.8 (please refer Table 4.1 in page 34 for the individual compounds representing the numbers shown in all the plots in this chapter). There are only a few other relationships in which PC/molecular variable(s) explained more than 30% of the variability in the PK/PD variable, but the slope was not statistically significant from zero. During the final (multivariate) model building process (using MLLR with forward inclusion followed by backward elimination), $logD_{7.4}$ was found to be the single most important determinant affecting biologically relevant systemic PK of BZD (discussed below), and the final models are summarized in Table 4.11. Overall, the final QSPKR models developed for BZD gave acceptable predictions ($q^2 \geq 0.40$) for Vd_{ss}^u and CL_{nonren}^u only.

4.3.1. Effect of $LogD_{7.4}$ on Systemic and Biologically Relevant PK Variables for BZD

There is a significant negative association between $logD_{7.4}$ and f_u, i.e., an increase in $logD_{7.4}$ is associated with decrease in f_u (increase in PPB) for BZD (Slope = -0.20, $r^2 = 0.51$, n = 17) as shown in in Figure 4.2. A significant positive association is observed with each of (log-transformed) Vd_{ss}^u (Slope = 0.57, $r^2 = 0.61$, n = 16), CL_{nonren}^u (Slope = 0.66, $r^2 = 0.81$, n = 16) and CL_{ren} (Slope = -0.88, $r^2 = 0.56$, n = 9). Overall, due to the offsetting effects of $logD_{7.4}$ on f_u and Vd_{ss}^u; and f_u and CL_{nonren}^u, their uncorrected counterparts, i.e., Vd_{ss} and CL_{nonren},

respectively, did not depend on $logD_{7.4}$. Although there is a positive association of CL_{tot}^{u} with $logD_{7.4}$, the slope is insignificant, and a plausible explanation for such a finding may be because of the limited diversity in $logD_{7.4}$ for BZD (range: 0.75 to 3.8). The contribution of renal pathways for majority of the BZD (except N-DMAD) within the dataset with available information is negligible (f_e < 1%), and as a result CL_{ren} values are very low, which limits the confidence in these estimates.

Table 4.9 - Univariate Regression Between PC/Molecular Descriptors and Biologically Relevant PK Variables of BZD

	f_u	**Log (Vd_{ss}^u) [l/kg]**	**Log (CL_{tot}^u) [ml/min/kg]**	**Log (CL_{ren}^u) [ml/min/kg]**	**Log (CL_{nonren}^u) [ml/min/kg]**	**Log (CL_{nonren}^{Blood}) [ml/min/kg]**	**γ**
MW (Da)	N.S.	N.S.	N.S.	*n =8* *r^2 = 0.40* *Slope = 0.019* *N.S*	N.S.	*n = 5* *r^2 = 0.66* *Slope = 0.059* *N.S*	N.S
$LogD_{7.4}$	n = 17 r^2 = 0.51 Slope = -0.20 -0.31, -0.092	n = 16 r^2 = 0.57 Slope = 0.61 0.31, 0.90	N.S.	N.S	n = 8 r^2 = 0.81 Slope = 0.66 0.35, 0.98	N.S.	N.S
PSA (A^2)	N.S	N.S	N.S	N.S	N.S	N.S	N.S
HBA	n = 17 r^2 = 0.33 Slope = 0.099 0.022, 0.18	*n = 16* *r^2 = 0.26* *Slope = -0.20* *-0.49, -0.011*	N.S.	N.S.	N.S	N.S	N.S
HBD	N.S	N.S	N.S	N.S	N.S	*n = 5* *r^2 = 0.44* *Slope = -0.89* *N.S.*	n = 9 r^2 = 0.86 Slope = 8.3 5.3, 11.3

In red: $r^2 \geq 0.30$ and $p<0.05$;
In italic and red: *$r^2 \geq 0.30$ but $p>0.05$ or $r^2 < 0.30$ but $p<0.05$;*
N.S = Not Significant ($r^2 < 0.30$ and $p>0.05$);

Table 4.10 - Univariate Regression Between PC/Molecular Descriptors and Reported PK/PD Variables of BZD

	Log (Vd_{ss}) [l/kg]	Log (CL_{tot}) [ml/min/kg]	Log (CL_{ren}) [ml/min/kg]	Log (CL_{nonren}) [ml/min/kg]	Log RRA (K_i in nM)	
					[^{3}H] Diazepam	[^{3}H] Flunitrazepam
MW (Da)	N.S.	n = 20 r^2 = 0.40 Slope = 0.012 0.0050, 0.019	*n = 9* *r^2 = 0.35* *Slope = 0.028* *N.S.*	N.S	N.S	*n = 11* *r^2 = 0.35* *Slope = -0.030* *N.S.*
LogD$_{7.4}$	N.S	N.S	n = 9 r^2 = 0.56 Slope = -0.88 -1.6, -0.18	N.S	N.S	N.S
PSA (A^2)	N.S	N.S	N.S	N.S	N.S.	N.S.
HBA	N.S	*n = 16* *r^2 = 0.29* *Slope = 0.29* *0.065, 0.52*	N.S	N.S	N.S	N.S
HBD	N.S	n = 20 r^2 = 0.36 Slope = -0.62 -1.0, -0.21	N.S	*n = 9* *r^2 = 0.32* *Slope = -0.54* *N.S.*	N.S	N.S

Table 4.11 - Final Multivariate QSPKR Models for BZD

Final QSPKR Model	**N**	**Slope (95% CI)**	**r^2**	**q^2**
$f_u = 0.63 - 0.20 * LogD_{7.4}$	17	- 0.20 (-0.31, -0.09)	0.51	0.33
$Log\ (Vd_{ss}^{u}) = - 0.38 + 0.60 * LogD_{7.4}$	16	0.60 (0.30, 0.90)	0.57	**0.40**
$Log\ (CL_{nonren}^{u}) = - 0.40 + 0.66 * LogD_{7.4}$	8	0.66 (0.35, 0.98)	0.81	**0.66**

$q^2 \geq 0.40$: Acceptable

Figure 4.2: f_u vs. $logD_{7.4}$ for BZD

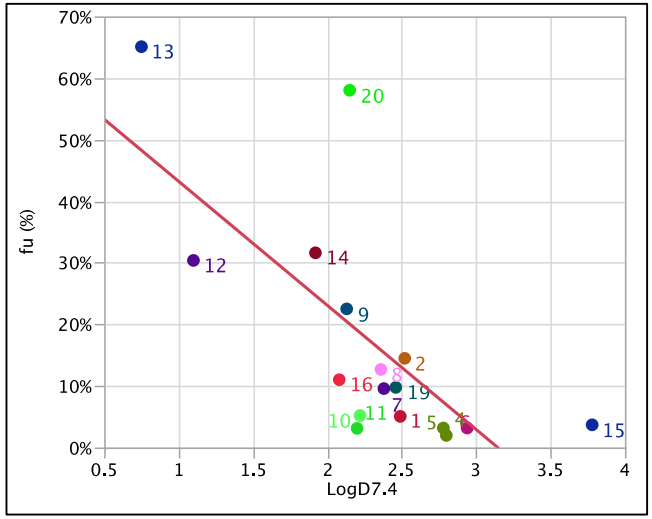

Figure 4.3: Vd_{ss}^{u} vs. $logD_{7.4}$ for BZD

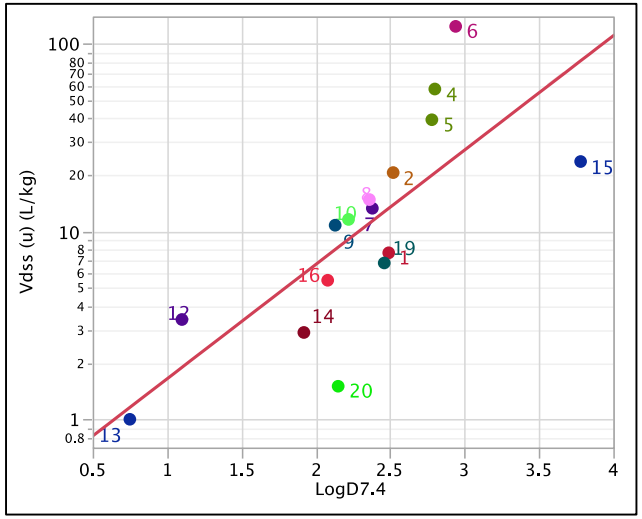

Figure 4.4: CL_{nonren}^{u} vs. $logD_{7.4}$ for BZD

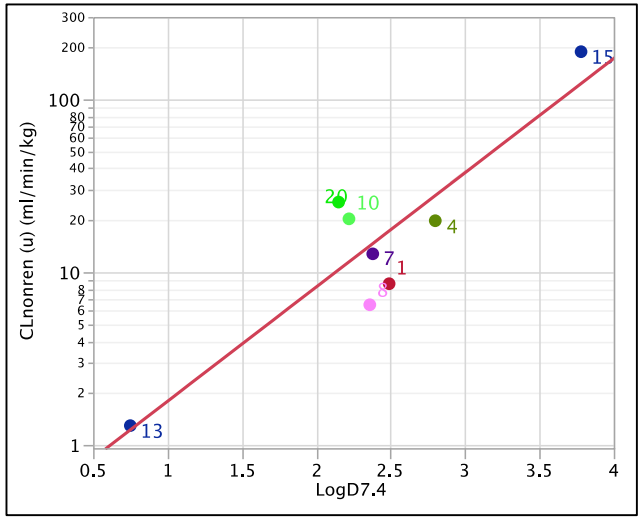

(Please refer Table 4.1 in Page 34, for the list of the individual compounds labeled in the figures 4.2 - 4.4)

Figure 4.5: f_u vs. HBA for BZD

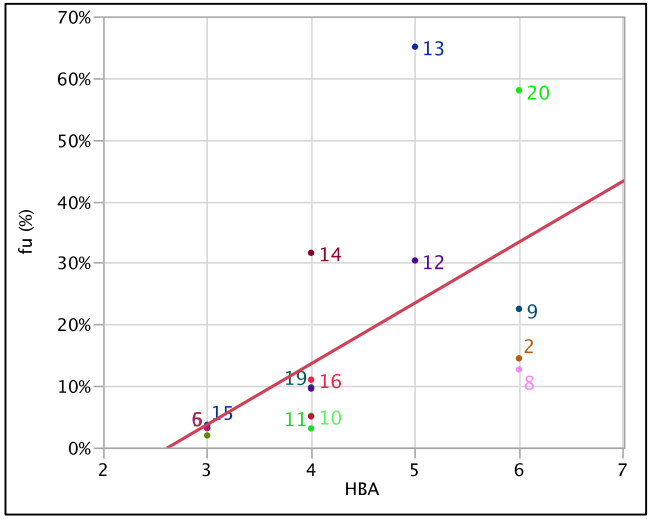

Figure 4.6: γ vs. HBD for BZD

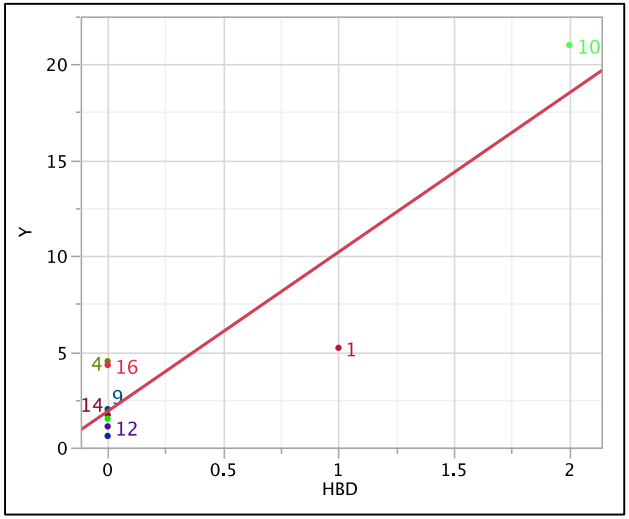

Figure 4.7: CL_{tot} vs MW for BZD

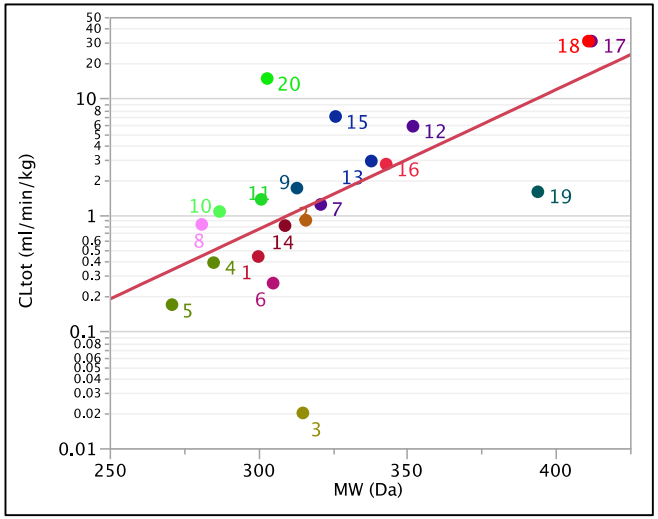

Figure 4.8: CL_{tot} vs HBD for BZD

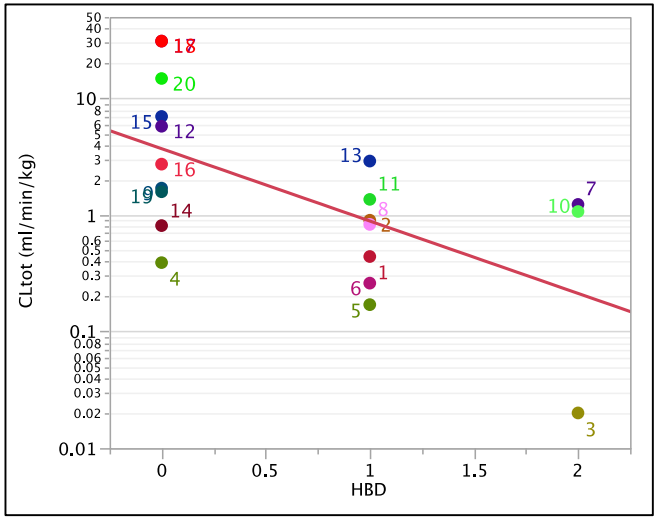

(Please refer Table 4.1 in Page 34, for the list of the individual compounds labeled in the figures 4.5 - 4.8)

4.4. Discussion

Structurally, most of the BZD in the current dataset share the 5-aryl, 1, 4-BZD scaffold and, overall, their PC/molecular property space has low diversity (2- to 3-fold, n = 20). BZD are relatively low MW (ranging from 271 to 412 Da, n = 20) lipophilic, i.e., $logD_{7.4}$ > 1.0 (ranging from 1.10 to 3.78, except for N-DMAD with a $logD_{7.4}$ of 0.75), acids (n = 7) or bases (n = 13), and the majority of them are unionized at pH 7.4 (except N-DMAD and Ro 48-8684).

Most of the BZD are extensively PPB and their Vd_{ss}^{u} values indicate moderate to extensive extravascular distribution into tissues, potential binding to plasma membranes, possibly owing to their high degree of lipophilicity and hydrophobic interactions. It seems that the high Vd_{ss}^{u} values are offset by high PPB, resulting in low Vd_{ss} values, suggesting that their extravascular tissue distribution is restricted by PPB. CL_{tot}^{u} varies 74-fold (n = 17) while CL_{tot} varies 1550-fold (n = 20). Again, high CL_{tot}^{u} values seem to be offset by high PPB, which resulted in low CL_{tot} values. Most of the BZD with available information in the dataset are highly metabolized (i.e., $f_e \leq 10\%$), with no obvious evidence of extrahepatic clearance pathway(s). CL_{ren}^{u} values for all the BZD in the dataset with available information (n=9) suggest that they undergo net renal tubular reabsorption (except for NDMAD).

Based on the CL_{nonren} values (n=9), midazolam and flumazenil show intermediate (to high) ER_{hep}, while the rest of BZD with available information show low ER_{hep}, either because of low hepatic CL_{int} (e.g., chlordiazepoxide, lorazepam, nitrazepam etc.) and/or high PPB (e.g., diazepam, oxazepam etc.). For the compounds with available information (n = 6), metabolism by CYP3A is the primary nonrenal, hepatic elimination route for alprazolam ($f_{pathway}$ = 75%), midazolam (80%), triazolam (95%) and brotizolam (80%), while, for chlordiazepoxide (35%), it is found to be relatively low. CYP2C19 is the major hepatic elimination pathway for diazepam

(83%). Although lipophilicity was found to be the major determinant affecting CL_{nonren}^{u} (CL_{int}) for BZD, the contribution of the specific metabolic pathway reflects the affinity towards DME, wasn't captured using the molecular/PC descriptors.

The B:P ratio for most BZD in the current dataset with available information (n = 9) show values of less than 1.0, and the plausible explanation is either high PPB (e.g., diazepam, chlordiazepoxide) and/or low RBC partitioning (e.g., midazolam). Overall, there is large diversity in the *in-vitro/in-vivo* systemic PK/PD properties of BZD in the current dataset ranging from 20- to 1950-fold (n = 5 - 17).

$LogD_{7.4}$ is found to be the important determinant affecting biologically relevant systemic PK properties, namely, f_u, Vd_{ss}^{u} and CL_{nonren}^{u}:

(a) An increase in $logD_{7.4}$ is associated with a decrease in f_u, suggesting that they bind to plasma proteins primarily by hydrophobic interactions. Similar relationships were observed in other studies reported in the literature with corticosteroids (n = 11) in humans[40], adenosine A_1 receptor agonists[67] (n = 12) and barbiturates (n = 12) in rats[68] as well with a heterogeneous dataset of 554 compounds[29]. Lucek et al[69] reported the role of hydrophobic binding of various derivatives 1, 4-BZD to human plasma proteins by incorporating lipophilic substituents.

(b) A significant positive association is observed between Vd_{ss}^{u} and $logD_{7.4}$ for BZD in the final dataset suggesting that their extravascular distribution with tissue, cellular plasma membranes etc., is also driven by hydrophobic interactions. Similar relationships were observed for Vd_{ss}^{u} in humans and cats as a function of reversed-phase HPLC retention times[70,71], and human Vd_{ss}^{u} as a function of octanol : buffer partition coefficients[71].

(c) Non-specific hydrophobic interactions with the drug metabolizing enzymes or partitioning into the hepatocytes seem to be plausible explanation for positive association and CL_{nonren}^{u} and $logD_{7.4}$.

Due to the offsetting effects of $logD_{7.4}$ on f_u and Vd_{ss}^{u}; and f_u and CL_{nonren}^{u}, their uncorrected counterparts, Vd_{ss} and CL_{nonren}, respectively, did not depend on $clogD_{7.4}$.

A significant positive association was observed between HBD and RBC partitioning (γ), and this trend seems to be driven by oxazepam, which shows the highest RBC partitioning, although it has only two HBD.

Overall, BZD-$GABA_A$ interactions seem to be driven by more specific molecular interactions, while nonspecific hydrophobic interactions with biological membranes and/or body tissues and metabolizing enzymes seem to affect biologically relevant human PK properties such as Vd_{ss}^{u} and CL_{nonren}^{u}. The final QSPKR models of BZD gave acceptable predictions for Vd_{ss}^{u} and CL_{nonren}^{u}.

CHAPTER 5. QSPKR of NMB

5.1. Background

NMB are routinely used during the administration of anesthesia to facilitate surgical access to body cavities, especially the abdomen and thorax without hindrance from the voluntary or reflex muscle movement[72]. The therapeutic selection of NMB is based on achievement of a pharmacokinetic profile consistent with the duration of the interventional procedure, i.e., rapid equilibration between the plasma and effect site, resulting in immediate onset, but the duration dependent on the procedures (lasting from a few minutes to several days/weeks)[63]. Based on their mechanism of action, NMB are classified into

(a) Depolarizing blocking agents, e.g., succinylcholine (SCh): Their initial action is to depolarize the postsynaptic membrane (with nicotinic acetylcholine, nACh receptors) by opening the ion channels, in a similar manner as acetylcholine (ACh). However, SCh persists for longer duration at the neuromuscular junction (primarily due to its resistance to acetylcholinesterase, AChE, hydrolysis) causing prolonged depolarization, resulting in inactivation of nACh, by continuing neuromuscular blockade.

(b) Non-depolarizing blocking agents: They compete with ACh to bind with the nACh (competitive antagonists) and do not possess intrinsic activity, thus preventing depolarization at the NM endplate and causing neuromuscular blockade. Their action can be overcome by increasing ACh concentrations in the synaptic cleft by administering AChE inhibitors like neostigmine etc.

Structurally, NMB possess either a aminosteroid (ASN) (Figure 5.1) or benzylisoquinolinium (BIQ) scaffold (Figure 5.2); a brief account of structure activity relationships (SAR)[63,73–75] for each.

Figure 5.1 - ASN Structural Scaffold

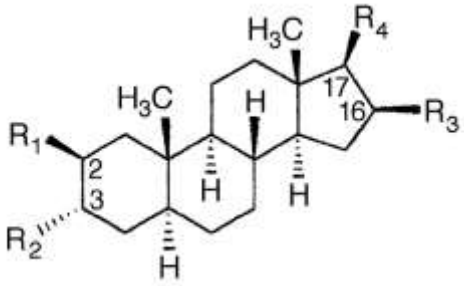

Figure 5.2 - BIQ Structural Scaffold

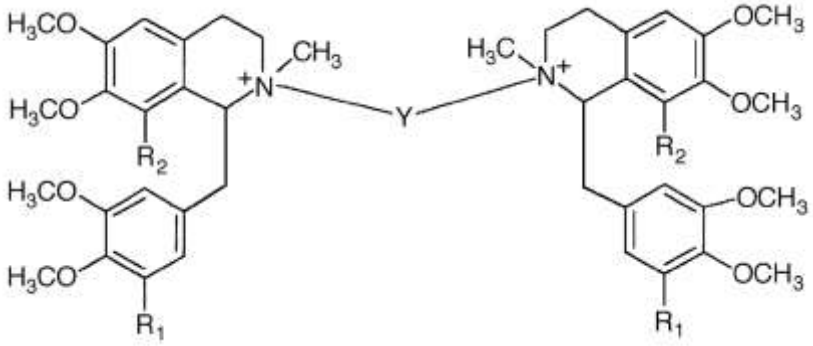

SAR

In general, NMB are large, bulky and rigid molecules. Substituents (e.g., mono or poly substituted benzyl groups and/or larger complex ring systems) on or around quaternary ammonium "cationic head" are considered favorable for high NMB potency. The distance

between the quaternary groups is typically around 1.0 nm. In general, alkyl substituent greater than methyl or ethyl on the quaternary ammonium group(s) reduced potency.

For NMB with ASN scaffold, highest potency was seen if quaternary substituents were present at 2- and 16- positions and additional substitutions at 3- and 17- contributed positively to NMB effects. For NMB with BIQ scaffold, the higher the methoxy substitutions each of BIQ nucleus, the higher is the potency (owing to the hydrophobic interactions with the nicotinic receptor).

In-vivo PD properties namely, equilibration rate constant between plasma and biophase, (k_{eo}), concentration in plasma producing half-maximal effect (cp_{ss}^{50}) and steepness of the concentration - effect relationship (γ) were compiled from *in-vivo* human PD studies after ensuring that the same PD endpoint, i.e., 95% depression in the muscle twitch following 'train-of-four' stimulus was considered.

5.2. Results

The final PC/molecular and human systemic PK/PD database consisted of sixteen NMB, fifteen of which were non-depolarizing blockers, including two metabolites, Org 7268 and Org 9488 of vecuronium and rapacuronium, respectively, and one depolarizing blocker, namely, succinylcholine, SCh.

5.2.1. PC/Molecular Property Space of NMB

The PC/molecular property space exhibited by NMB in the current dataset is presented in Table - 5.1 (median values were presented instead of mean values because of SCh, which skewed the distributions, see below). Structurally, NMB in the current dataset exhibit two common scaffolds - (a) relatively older generation compounds with aminosteroid (ASN) nucleus, (n = 9) and (b) relatively newer generation compounds with benzylisoquinolinium (BIQ) nucleus (n = 5); while fazadinium and SCh are classified under the miscellaneous category. With the exception of SCh (MW = 290 Da), the NMB in the current dataset show fairly large MW (ranging from 444 - 1035 Da, n = 15). At physiological pH (7.4), all NMB are basic (n = 16), with two positive charges (as quaternary nitrogens). Despite the lack of the information on a few NMB in the current database, there is a fairly large diversity (7-fold, n = 12) in the $logD_{7.4}$ values ranging from -5.00 to 2.08, and the majority of them are hydrophilic, i.e., $logD_{7.4} < 1.0$ (n = 10, i.e., excluding rapacuronium and fazadinium).

Overall, the PC/molecular property space shown by a few properties e.g., $logD_{7.4}$, nRot (8-fold, n = 11), etc., is relatively more diverse than the others (2- to 4-fold, n = 11-12), based on the NMB in the current dataset with available information. Although the compounds within each structural class (ASN and BIQ) exhibit fairly similar values for PC/molecular properties and thus low diversity in their respective property spaces, the compounds with a BIQ scaffold show

significantly higher mean values for MW, nRot, PSA and HBA compared to those with an ASN scaffold (shown in Tables 5.3 and 5.2, respectively).

The descriptive statistics of PC/molecular variables are shown in Table 5.4; the mean values are higher than the corresponding median values suggesting that the underlying distributions are skewed. Based on the acceptance criteria set *a-priori* for collinearity (i.e., $r \geq 0.80$), MW is highly correlated with PSA ($r = 0.90$, $n = 11$), MW with nRot ($r = 0.86$, $n = 11$) and MW with HBA ($r = 0.90$, $n = 11$), PSA with nRot ($r = 0.97$, $n = 11$), PSA with HBA ($r = 0.99$, $n = 11$) and nRot with HBA ($r = 0.97$, $n = 11$) (shown in Table 5.5). Thus, $logD_{7.4}$, MW, and HBD were used for subsequent analysis (i.e., PSA, nRot and HBA were excluded).

Table 5.1 - Molecular/PC Property Space of NMB

	Label	Drug	MW (Da)	logP	LogD at pH 7.4	PSA (A^2)	nRot	HBD	HBA
ASN	1	Rocuronium	530	-0.21	-0.40	59	7	1	6
	2	Pipercuronium	603	.	.	.	.	.	.
	3	Pancuronium	572	-1.2	-1.2	53	6	0	6
	4	Vecuronium	558	0.62	-0.26	56	6	0	6
	5	Org 7268	516	0.55	-0.38	50	5	1	5
	6	Rapacuronium	598	2.6	1.7	.	.	.	.
	7	Org 9488	556	.	.	.	.	.	.
	8	Org 9489	572	.	.	.	.	.	.
	9	Org 9453	586	.	.	.	.	.	.
BIQ	10	Alcuronium	667	-3.1	-3.1	47	8	2	6
	11	Doxacurium	1035	-2.1	-2.1	163	29	0	18
	12	Mivacurium	1029	0.37	0.37	145	30	0	16
	13	Atracurium	929	-0.27	-0.27	126	26	0	14
	14	Cisatracurium	933	-0.27	-0.27	126	26	0	14
	15	Fazadinium	444	2.1	2.1	43	4	0	6
	16	Succinylcholine	290	-5.0	-5.0	53	11	0	6
		N	16	12	12	11	11	11	11
		Median	579	-0.23	-0.33	56	8	0	6
		Maximum	1035	-2.6	2.1	163	30	2	18
		Minimum	290	-5.0	-5.0	43	4	0	5
		-fold range	4	8	7	4	8	2	4

Table 5.2 - Molecular/PC Properties of NMB with ASN Scaffold

	Label	Drug	MW (Da)	logP	LogD at pH 7.4	PSA (A^2)	nRot	HBD	HBA
ASN	1.	Rocuronium	530	-0.21	-0.40	59	7	1	6
	2.	Pipercuronium	603	.	.	.	.	.	.
	3.	Pancuronium	572	-1.2	-1.2	53	6	0	6
	4.	Vecuronium	558	0.62	-0.26	56	6	0	6
	5.	Org 7268	516	0.55	-0.38	50	5	1	5
	6.	Rapacuronium	598	2.6	1.7	.	.	.	.
	7.	Org 9488	556	.	.	.	.	.	.
	8.	Org 9489	572	.	.	.	.	.	.
	9.	Org 9453	586	.	.	.	.	.	.
		N	9	5	5	4	4	4	4
		Mean *(95% CI)*	566 *(543, 588)*	0.47 *(-1.2, 2.2)*	-0.10 *(-1.4, 1.2)*	55 *(48, 61)*	6 *(5, 7)*	0.50 *(-0.04, 1.4)*	6 *(5.0, 6.5)*
		Maximum	603	2.59	1.71	59	7	1	6
		Minimum	516	-1.18	-1.18	50	6	0	5
		-fold range	1.2	3.8	2.9	1.2	1.2	1	1.2

Table 5.3 - Molecular/PC Properties of NMB with BIQ Scaffold

	Drug	MW (Da)	logP	LogD at pH 7.4	PSA (A^2)	nRot	HBD	HBA
BIQ	1. Alcuronium	667	-3.1	-3.1	47	8	2	6
	2. Doxacurium	1035	-2.1	-2.1	163	29	0	18
	3. Mivacurium	1029	0.37	0.37	145	30	0	16
	4. Atracurium	929	-0.27	-0.27	126	26	0	14
	5. Cisatracurium	933	-0.27	-0.27	126	26	0	14
	N	5	5	5	5	5	5	5
	Mean ***(95%CI)***	920 *(733, 1104)*	-1.1 *(-2.9, 0.73)*	-1.1 *(-2.9, 0.73)*	121 *(66, 177)*	24 *(13, 35)*	0.40 *(-0.70, 1.5)*	14 *(8, 19)*
	Maximum	1035	0.37	0.37	163	30	2	18
	Minimum	667	-3.07	-3.07	47	8	0	6
	-fold range	1.6	3.4	3.4	3.5	3.8	2.0	3.0

Table 5.4 - Descriptive Statistics of PC/Molecular Properties of NMB

	N	Mean	SD	95% CI	Minimum	10%	25%	Median	75%	90%	Maximum
MW (Da)	16	**651.0**	214.93	536.6, 765.7	290.0	397.8	536.5	**579.0**	863.5	1030.8	1035.0
$LogD_{7.4}$	12	**-0.7**	1.95	-2.0, 0.5	-5.0	-4.4	-1.9	**-0.3**	0.2	2.0	2.1
PSA (A^2)	11	**83.7**	45.85	52.9, 114.5	43.0	43.8	50.0	**56.0**	126.0	159.4	163.0
nRot	11	**14.4**	10.82	7.1, 21.6	4.0	4.2	6.0	**8.0**	26.0	29.8	30.0
HBD	11	**0.4**	0.67	-0.1, 0.8	0.0	0.0	0.0	**0.0**	1.0	1.8	2.0
HBA	11	**9.4**	4.98	6.0, 12.7	5.0	5.2	6.0	**6.0**	14.0	17.6	18.0

Table 5.5 - Correlation Matrix of PC/Molecular Variables of NMB

	MW (Da)	$LogD_{7.4}$	PSA (A^2)	nRot	HBA	HBD
MW (Da)	1.00					
$LogD_{7.4}$	0.14	1.00				
PSA (A^2)	**0.90**	-0.01	1.00			
nRot	**0.86**	-0.11	**0.97**	1.00		
HBA	**0.90**	0.01	**0.99**	**0.97**	1.00	
HBD	-0.17	-0.23	-0.42	-0.39	-0.43	1.00

5.2.2. Human Systemic PK/PD Property Space of NMB

The final median (instead of mean values were presented because of their skewed distribution) *in-vitro* and *in-vivo* human systemic PK/PD properties compiled from various studies in the literature are shown in Table - 5.6 and 5.12, respectively, and the estimated biologically relevant PK properties in Table 5.9. Appendix 2 contains all the supplemental information with respect to the *in-vitro*/*in-vivo* human systemic PK and *in-vivo* PD data compiled for each of the compound from the literature.

There is considerable to large diversity in the *in-vitro/in-vivo* systemic PK/PD properties of NMB in the current dataset with available information, ranging from 4- to 266-fold (n = 8 - 16). Within the NMB with ASN scaffold, the systemic and biologically relevant PK/PD property space is relatively less diverse (Tables 5.7, 5.10 and 5.13) ranging from 1.4- to 26-fold and shows relatively lower mean values, while NMB with the BIQ scaffold show a more diverse space (Tables 5.8, 5.11, 5.14) ranging from 1.3- to 224-fold and in general, higher mean values (which are not statistically different from those with ASN scaffold).

The descriptive statistics for these PK/PD variables are shown in Table 5.15 and for a few of these variables, the mean values are higher than the median values. Furthermore, owing to the skewed distribution and considerable diversity, all the systemic PK/PD variables (except f_u, f_e, k_{eo} and γ) were log transformed for further analysis.

Several correlations are observed between the *in-vitro*/*in-vivo* human systemic and biologically relevant PK variables of NMB (shown in Table 5.16). However, most of these correlations are mechanistically plausible, e.g., (a) CL_{tot}^{u} is highly correlated with CL_{nonren} (r = 0.92, n = 14), while CL_{tot} is highly correlated with CL_{ren}^{u} (r = 0.91, n = 13) and CL_{nonren} (r = 0.84, n = 15), suggesting that few NMB (within the dataset with available information) show significant renal

clearance while the rest have significant nonrenal clearance mechanisms; (b) Vd_{ss} was highly correlated (r = 0.94, n = 14) with Vd_{ss}^{u}, suggesting that, overall, PPB of NMB (in the current dataset) is not significant.

Overall, PPB varies 4-fold (n =14) and the majority of NMB in the dataset are not extensively bound to plasma proteins, i.e., they show relatively high free fraction in plasma, possibly because of their low lipophilicity. On average, NMB belonging to each structural class, i.e., ASN- and BIQ-scaffold, show similar values for f_u, however, NMB with ASN scaffold show more diversity (4-fold, n = 8), while NMB with BIQ scaffold show comparable values. Vd_{ss}^{u} varies 24-fold (n =14) compared to Vd_{ss} (12-fold, n = 16), and their mean values are comparable, suggesting that PPB did not offset the Vd_{ss}^{u} (because NMB are not extensively PPB, see above). The higher diversity in Vd_{ss}^{u} values relative to Vd_{ss} may be due to greater diversity in PPB. The majority of NMB have Vd_{ss}^{u} values much lower than BW (70 kg), suggesting they undergo little extravascular distribution (primarily into the extra and/or intracellular water, 0.2 - 0.3 l/kg), which is true for NMB within each structural class. MW and/or charged nature of the molecule(s) could be plausible explanation(s) for the lack of extravascular/trans-membrane tissue penetration (i.e., low Vd_{ss}^{u} values).

Most of NMB show clearance through renal pathways (f_e ranging from 5% to 72%, n = 14). Overall, there is considerable diversity in the CL_{ren}^{u} values (11-fold, n = 13), and it is comparable between the structural classes. With the exception of mivacurium, the rest of NMB have CL_{ren}^{u} values lower than GFR (1.7 ml/min/kg), suggesting that (a) they are potentially poorly filtered in the glomerulus, due to their large size and/or (b) they undergo net tubular reabsorption possibly involving drug transporters. Mivacurium shows CL_{ren}^{u} value close to RPF, suggesting it undergoes net tubular secretion, possibly involving of drug transporters.

Overall, CL_{nonren} varies 266-fold (n = 15). CL_{nonren} of NMB in the current dataset with BIQ scaffold show large diversity (224-fold, n = 5) and encompasses diverse mechanisms e.g., (a) mivacurium is the newest generation NMB that was designed to have immediate onset of action, and undergoes rapid hydrolysis by plasma cholinesterase[76,77] (see Appendix 2), which is a plausible explanation for having CL_{nonren} value exceeding cardiac output (i.e., blood-flow independent, extrahepatic clearance pathways). (b) atracurium and cisatracurium are known to undergo chemical degradation via Hoffman elimination[78] (see in Appendix 2), occurring both in plasma and tissue compartments (i.e., in an organ-independent manner). (c) alcuronium and doxacurium have CL_{nonren} values lower than LBF (21 ml/min/kg) and are low ER_{hep} drugs (assuming B:P ratio is close to 1 and there are no extrahepatic clearance pathways).

There is relatively low diversity in CL_{nonren} values (13-fold, n = 9) of NMB with ASN structural scaffold and available information in the current dataset; all of them have CL_{nonren} values lower than LBF, suggesting they are low ER_{hep} drugs (assuming B:P ratio is close to 1 and there are no extrahepatic clearance pathways). SCh (in the miscellaneous category) undergoes enzymatic hydrolysis and thus exhibits extrahepatic clearance pathways.

In-vivo PD properties, namely, equilibration rate constant, k_{eo} varies 4-fold (n = 8), Cp_{ss}^{50} (in mM) varies 68-fold (n = 9), and sigmoidicity varies 4-fold (n = 9) (shown in Table 5.12). Overall, the equilibration half-lives ranges from 3 - 14 minutes, which are orders of magnitude smaller than the respective terminal plasma half-lives, suggesting that NMB, in general, equilibrate rapidly with their target compartment. Furthermore, it can be observed that the k_{eo} values are lower (i.e., slower equilibration half-lives) and for NMB with BIQ scaffold (and SCh within miscellaneous category) than for NMB with ASN scaffold. There were considerable differences in the molar potencies (Cp_{ss}^{50}) between the NMB. The sigmoidicity (γ) for all the

NMBs is found to be much greater than 1, suggesting that the PD effects (neuromuscular blockade) changes are very sensitive to the changes in the biophase concentrations. SCh, a depolarizing NMB shows the highest sigmoidicity (2-3 fold higher) relative to all the other nondepolarizing NMB.

Table 5.6 - *In-vitro* and *In-vivo* Human PK Systemic Properties of NMB

		In-vitro PK Variable	***In-vivo PK Variables***				
	Drug	**f_u [%]**	**Vd_{ss} [l/kg]**	**CL_{tot} [ml/min/kg]**	**f_e [%]**	**CL_{ren} [ml/min/kg]**	**CL_{nonren} [ml/min/kg]**
ASN	Rocuronium	65%	0.21	3.5	25%	0.88	2.6
	Pipercuronium	98%	0.32	2.6	*41%*	1.1	1.5
	Pancuronium	75%	0.22	1.6	*58%*	0.93	0.70
	Vecuronium	48%	0.20	5.0	7%	0.35	4.6
	Org 7268	69%	0.26	4.3	18%	0.77	3.5
	Rapacuronium	38%	0.32	8.3	9%	0.75	7.6
	Org 9488	.	0.21	1.2	53%	0.62	0.58
	Org 9489	39%	0.46	5.8	8%	0.46	5.3
	Org 9453	28%	0.18	6.9	5%	0.35	6.6
BIQ	Alcuronium	.	0.31	0.90	72%	0.65	0.25
	Doxacurium	53%	0.20	2.5	26%	0.65	1.8
	Mivacurium	71%	0.19	72	7%	5.1	67
	Atracurium	57%	0.15	6.3	6%	0.38	5.9
	Cisatracurium	62%	0.15	5.0	16%	0.80	4.2
	Fazadinium	49%	0.19	2.1	*50%*	1.1	1.1
	Succinylcholine	80%	0.040	37.0	.	.	.
	N	14	16	16	15	15	15
	Median	59%	0.20	4.7	18%	0.80	3.5
	Maximum	98%	0.46	72	72%	5.1	67
	Minimum	28%	0.040	0.90	5%	0.35	0.25
	-fold range	4	12	80	14	15	266

Table 5.7 - *In-vitro* and *In-vivo* Human PK Systemic Properties of NMB with ASN Scaffold

		In-vitro PK Variable	***In-vivo PK Variables***				
	Drug	**f_u [%]**	**Vd_{ss} [l/kg]**	**CL_{tot} [ml/min/kg]**	**f_e [%]**	**CL_{ren} [ml/min/kg]**	**CL_{nonren} [ml/min/kg]**
ASN	Rocuronium	65%	0.21	3.5	25%	0.88	2.6
	Pipercuronium	98%	0.32	2.6	*41%*	1.1	1.5
	Pancuronium	75%	0.22	1.6	*58%*	0.93	0.70
	Vecuronium	48%	0.20	5.0	7%	0.35	4.6
	Org 7268	69%	0.26	4.3	18%	0.77	3.5
	Rapacuronium	38%	0.32	8.3	9%	0.75	7.6
	Org 9488	.	0.21	1.2	53%	0.62	0.58
	Org 9489	39%	0.46	5.8	8%	0.46	5.3
	Org 9453	28%	0.18	6.9	5%	0.35	6.6
	N	8	9	9	9	9	9
	Mean	58%	0.3	4.4	25%	0.7	3.7
	(95% CI)	*(28%, 77%)*	*(0.2, 0.3)*	*(2.5, 6.2)*	*(9%, 41%)*	*(0.5, 0.9)*	*(1.7, 3.7)*
	Maximum	99%	0.5	8.3	58%	1.1	7.6
	Minimum	28%	0.2	1.2	5%	0.3	0.6
	-fold range	4	3	7	12	4	13

Table 5.8 - *In-vitro* and *In-vivo* Human PK Systemic Properties of NMB with BIQ Scaffold

	Drug	**f_u [%]**	**Vd_{ss} [l/kg]**	**CL_{tot} [ml/min/kg]**	**f_e [%]**	**CL_{ren} [ml/min/kg]**	**CL_{nonren} [ml/min/kg]**
BIQ	Alcuronium	.	0.31	0.90	72%	0.65	0.25
	Doxacurium	53%	0.20	2.5	26%	0.65	1.8
	Mivacurium	71%	0.19	72	7%	5.1	67
	Atracurium	57%	0.15	6.3	6%	0.38	5.9
	Cisatracurium	62%	0.15	5.0	16%	0.80	4.2
	N	4	5	5	5	5	5
	Mean	61%	0.2	17.4	25%	1.5	15.9
	(95% CI)	*(48%, 73%)*	*(0.1, 0.3)*	*(-20.8, 55.5)*	*(-8%, 59%)*	*(-1.0, 4.0)*	*(-19.8, 51.6)*
	Maximum	71%	0.3	72.2	72%	5.1	67.1
	Minimum	53%	0.2	0.9	6%	0.4	0.3
	-fold range	1.3	1.5	80.2	12.0	12.8	223.7

Table 5.9 - Biologically Relevant *In-vivo* Human PK Variables of NMB

	Drug	Vd_{ss}^{u} [l/kg]	CL_{tot}^{u} [ml/min/kg]	CL_{ren}^{u} [ml/min/kg]	CL_{nonren}^{u} [ml/min/kg]
ASN	Rocuronium	0.32	5.4	1.4	4.1
	Pipercuronium	0.33	2.7	1.1	1.6
	Pancuronium	0.29	2.1	1.2	0.90
	Vecuronium	0.42	10.3	0.72	9.6
	Org 7268	0.38	6.2	1.1	5.1
	Rapacuronium	0.84	21.9	2.0	19.9
	Org 9488	.	.	.	.
	Org 9489	1.2	14.9	1.2	13.7
	Org 9453	0.64	24.6	1.2	23.4
BIQ	Alcuronium	.	.	.	.
	Doxacurium	0.38	4.7	1.2	3.5
	Mivacurium	0.27	101.7	7.1	94.6
	Atracurium	0.26	11.1	0.77	10.4
	Cisatracurium	0.24	8.1	1.3	1.5
	Fazadinium	0.39	4.3	2.1	2.1
	Succinylcholine	0.050	46.3	.	.
	N	14	14	13	13
	Median	0.4	9.2	1.2	6.8
	Maximum	1.2	101.7	7.1	94.6
	Minimum	0.050	2.1	0.72	0.90
	-fold range	24	48	11	106

Table 5.10 - Biologically Relevant *In-vivo* Human PK Variables of NMB with ASN Scaffold

	Drug	Vd_{ss}^{u} [l/kg]	CL_{tot}^{u} [ml/min/kg]	CL_{ren}^{u} [ml/min/kg]	CL_{nonren}^{u} [ml/min/kg]
ASN	Rocuronium	0.32	5.4	1.4	4.1
	Pipercuronium	0.33	2.7	1.1	1.6
	Pancuronium	0.29	2.1	1.2	0.90
	Vecuronium	0.42	10.3	0.72	9.6
	Org 7268	0.38	6.2	1.1	5.1
	Rapacuronium	0.84	21.9	2.0	19.9
	Org 9488	.	.	.	.
	Org 9489	1.2	14.9	1.2	13.7
	Org 9453	0.64	24.6	1.2	23.4
	N	8	8	8	8
	Mean	0.6	11.0	1.2	9.8
	(95% CI)	*(0.3, 0.8)*	*(3.8, 18.2)*	*(1.0, 1.5)*	(2.7, 16.9)
	Maximum	1.2	24.6	2.0	23.4
	Minimum	0.3	2.1	0.7	0.9
	-fold range	4	12	3	26

Table 5.11 - Biologically Relevant *In-vivo* Human PK Variables of NMB with BIQ Scaffold

	Drug	Vd_{ss}^{u} [l/kg]	CL_{tot}^{u} [ml/min/kg]	CL_{ren}^{u} [ml/min/kg]	CL_{nonren}^{u} [ml/min/kg]
BIQ	Alcuronium	.	.	.	.
	Doxacurium	0.38	4.7	1.2	3.5
	Mivacurium	0.27	101.7	7.1	94.6
	Atracurium	0.26	11.1	0.77	10.4
	Cisatracurium	0.24	8.1	1.3	1.5
	N	4	4	4	4
	Mean	0.3	31.4	2.6	28.8
	(95% CI)	*(0.2, 0.4)*	*(-43.3, 106.1)*	*(-2.3, 7.4)*	*(-41.1, 98.7)*
	Maximum	0.4	101.7	7.1	94.6
	Minimum	0.2	4.7	0.7	1.5
	-fold range	2	22	10	63

Table 5.12 - *In-vivo* Human PD Properties of NMB

	Drug	k_{eo} (min^{-1})	Cp_{ss}^{50} (mM)	γ
ASN	Rocuronium	0.17	2.13	6.1
	Pipercuronium	.		.
	Pancuronium	0.17	0.17	4.8
	Vecuronium	0.24	0.2	5.8
	Org 7268	0.26	0.25	.
	Rapacuronium	.		.
	Org 9488	0.11	3.29	4.3
	Org 9489	.		.
	Org 9453	.		.
BIQ	Alcuronium	.	0.82	5.0
	Doxacurium	0.05	0.05	5.5
	Mivacurium	.		.
	Atracurium	.		.
	Cisatracurium	0.05	0.16	6.9
	Fazadinium	.	.	.
	Succinylcholine	0.06	2.62	19.3
	N	8	9	9
	Median	0.14	0.25	5.7
	Maximum	0.26	3.29	19.3
	Minimum	0.05	0.05	4.3
	-fold range	5	68	4

Table 5.13 - *In-vivo* Human PD Properties of NMB with ASN Scaffold

	Drug	k_{eo} (min^{-1})	Cp_{ss}^{50} (mM)	γ
ASN	Rocuronium	0.17	1.13	6.1
	Pipercuronium	.	.	.
	Pancuronium	0.17	0.10	4.8
	Vecuronium	0.24	0.11	5.8
	Org 7268	0.26	0.13	.
	Rapacuronium	.	.	.
	Org 9488	0.11	1.83	4.3
	Org 9489	.	.	.
	Org 9453	.	.	.
	N	5	5	4
	Mean	0.19	1.21	5.3
	(95% CI)	*(0.11, 0.27)*	*(-0.57, 2.99)*	*(3.9, 6.6)*
	Maximum	0.26	3.29	6.1
	Minimum	0.11	0.17	4.3
	-fold range	2.4	19.4	1.4

Table 5.14 - *In-vivo* Human PD Properties of NMB with BIQ Scaffold

	Drug	k_{eo} (min^{-1})	Cp_{ss}^{50} (mM)	γ
BIQ	Alcuronium	.	0.82	5.0
	Doxacurium	0.05	0.05	5.5
	Mivacurium	.	.	.
	Atracurium	.	.	.
	Cisatracurium	0.05	0.16	6.9
	N	2	3	2
	Mean	0.05	0.34	5.8
	(95% CI)	*(0.05, 0.05)*	*(-0.69, 1.38)*	*(3.4, 8.2)*
	Maximum	0.05	0.82	6.9
	Minimum	0.05	0.05	5.0
	-fold range		16	1.4

Table 5.15 - Descriptive Statistics of Human Systemic PK/PD Variables of NMB

	N	Mean	SD	95% CI	Minimum	10%	25%	Median	75%	90%	Maximum
Vd_{ss} (L/kg)	16	**0.2**	0.09	0.2, 0.3	0.04	0.1	0.2	**0.2**	0.3	0.4	0.5
CL_{tot} (ml/min/kg)	16	**10.3**	18.6	0.4, 20.2	0.9	1.1	2.2	**4.7**	6.8	47.6	72.2
CL_{ren} (ml/min/kg)	15	**1.0**	1.15	0.4, 1.6	0.4	0.4	0.5	**0.8**	0.9	2.7	5.1
CL_{nonren} (ml/min/kg)	15	**7.6**	16.65	-1.7, 16.7	0.3	0.4	1.1	**3.5**	5.9	31.4	67.2
f_u	14	**0.6**	0.19	0.5, 0.7	0.3	0.3	0.5	**0.6**	0.7	0.9	1.0
Vd_{ss}^{u} (L/kg)	14	**0.4**	0.29	0.3, 0.6	0.1	0.2	0.3	**0.4**	0.5	1.0	1.2
CL_{tot}^{u} (ml/min/kg)	14	**18.9**	26.62	3.5, 34.3	2.1	2.4	4.6	**9.2**	22.5	74.0	101.7
CL_{ren}^{u} (ml/min/kg)	13	**1.7**	1.67	0.7, 2.7	0.7	0.7	1.1	**1.2**	1.7	5.1	7.1
CL_{nonren}^{u} (ml/min/kg)	13	**15.1**	24.90	0.002, 30.095	0.9	1.2	2.8	**6.8**	16.8	66.1	94.6
k_{eo} (min^{-1})	8	**0.1**	0.08	0.07, 0.21	0.1	0.1	0.1	**0.1**	0.2	0.3	0.3
Cp_{ss}^{50} (mM)	9	**1.1**	1.26	0.1, 2.0	0.1	0.1	0.2	**0.3**	2.4	3.3	3.3
γ (Sigmoidicity)	8	**7.2**	4.95	3.1, 11.4	4.3	4.3	4.9	**5.7**	6.7	19.3	19.3

Table 5.16 - Correlation Analysis of Human Systemic PK Variables of NMB

	Vd_{ss} (L/kg)	**CL_{tot} (ml/min/kg)**	**CL_{ren} (ml/min/kg)**	**CL_{nonren} (ml/min/kg)**	**f_u (%)**	**Vd_{ss}^u (L/kg)**	**CL_{tot}^u (ml/min/kg)**	**CL_{ren}^u (ml/min/kg)**	**CL_{nonren}^u (ml/min/kg)**
Vd_{ss} (L/kg)	1.00								
CL_{tot} (ml/min/kg)	-0.51	1.00							
CL_{ren} (ml/min/kg)	-0.67	0.77	1.00						
CL_{nonren} (ml/min/kg)	-0.14	**0.91**	0.59	1.00					
f_u (%)	**-0.83**	0.37	0.79	0.03	1.00				
Vd_{ss}^u (L/kg)	**0.94**	-0.42	-0.77	-0.06	**-0.97**	1.00			
CL_{tot}^u (ml/min/kg)	0.07	0.77	0.26	**0.92**	-0.30	0.24	1.00		
CL_{ren}^u (ml/min/kg)	-0.59	**0.84**	**0.98**	0.70	0.66	-0.66	0.41	1.00	
CL_{nonren}^u (ml/min/kg)	0.64	0.26	-0.18	0.62	-0.72	0.72	0.78	-0.02	1.00

5.2.3. QSPKR Analysis, Model Building and Evaluation

The results of the univariate regression of the *in-vitro/(*log-transformed) *in-vivo* biologically relevant and reported PK/PD variables as a function of the molecular/PC descriptors of NMB, namely, MW, $logD_{7.4}$ and HBD, are shown in Table 5.17 - 5.22. MW shows significant univariate relationships ($r^2 \geq 0.3$, $p < 0.05$) with log (Cp_{ss}^{50}) and $logD_{7.4}$ with f_u and log (Vd_{ss}^{u}) (Figures 5.1 - 5.3). Please refer Table 5.1 in page 60 for the individual compounds representing the numbers shown in all the plots in this chapter. Although there are other relationships in which > 30% of the variability in certain *in-vivo* systemic and/or biologically relevant PK/PD variables could be explained, the slopes of none of them differed statistically from zero.

In general, the model fits (i.e., r^2) with respect to MW and HBD are comparatively better for both systemic and biologically relevant PK variables for NMB with BIQ than for those with ASN scaffold. This is mechanistically plausible because the former is relatively more heterogeneous than the latter in their molecular/PC and PK property space. During the final (multivariate) model building process (using MLLR with forward inclusion followed by backward elimination), $logD_{7.4}$ was found to be the single most important determinant affecting biologically relevant systemic PK of NMB. The final models are summarized in Table 5.23. Overall, none of the final QSPKR models developed across all NMB for f_u and Vd_{ss}^{u} gave acceptable predictions ($q^2 \geq 0.40$).

5.2.3.1. Effect of $LogD_{7.4}$ on Systemic and Biologically Relevant PK Variables of NMB

There is a significant negative association between $logD_{7.4}$ and f_u, i.e., an increase in $logD_{7.4}$ is associated with a decrease in f_u (increase in PPB) of NMB (Slope = -0.04, r^2 = 0.42, n = 11, shown in Figure - 5.1), and a significant positive association is found with (log-transformed) Vd_{ss}^{u} (Slope = 0.13, r^2 = 0.68, n = 11, shown in Figure 5.2). Due to the offsetting effects of

$logD_{7.4}$ on f_u and Vd_{ss}^u, its uncorrected counterpart, Vd_{ss} did not depend on $logD_{7.4}$. None of the other relationships were statistically different. It can be seen from Figures 5.1 and 5.2, SCh (labeled as compound 16, most hydrophilic, highest f_u and lowest Vd_{ss}^u) is pivotal in defining the slopes of these relationships. When stratified by structural class, it can be seen that the relationship shown with f_u is significant for neither class of NMB, possibly because of the reduction in the diversity and/or sample size. Additionally, NMB with the ASN scaffold show a significant positive association between $logD_{7.4}$ and log Vd_{ss}^u (Slope = 0.17, r^2 = 0.99, n = 5, Figure 5.4), log CL_{tot}^u (Slope = 0.34, r^2 = 0.84, n = 5, Figure 5.5) and log CL_{tot} (Slope = 0.22, r^2 = 0.79, n = 5, Figure 5.6), while NMB with BIQ scaffold show a significant positive association with log CL_{nonren} (Slope = 0.55, r^2 = 0.84, n = 4, Figure 5.7)

Table 5.17 - Log-Linear Regression Between MW and Biologically Relevant PK Variables of NMB

	f_u	Log (Vd_{ss}^u) [l/kg]	Log (CL_{tot}^u) [ml/min/kg]	Log (CL_{ren}^u) [ml/min/kg]	Log (CL_{nonren}^u) [ml/min/kg]
NMB (All)	N.S.	N.S.	N.S.	N.S.	N.S.
NMB with ASN Scaffold	N.S.	N.S.	N.S.	N.S.	N.S.
NMB with BIQ Scaffold	N.S.	*n = 4* *r^2 = 0.49* *Slope =0.001* *N.S.*	N.S.	*n = 4* *r^2 = 0.40* *Slope =0.005* *N.S.*	N.S.

Table 5.18 - Log-Linear Regression Between MW and Reported PK/PD Variables of NMB

	Log (Vd_{ss}) [l/kg]	Log (CL_{tot}) [ml/min/kg]	Log (CL_{ren}) [ml/min/kg]	Log (CL_{nonren}) [ml/min/kg]	k_{eo} (min^{-1})	Log (Cp_{ss}^{50}) (mM)	γ
NMB (All)	N.S.	N.S.	N.S.	N.S	N.S.	n = 9 r^2 = 0.50 Slope = -0.002 -0.004, -0.001	N.S.
NMB with ASN Scaffold	N.S.	N.S	N.S.	N.S.	N.S.	N.S.	*n = 4* *r^2 = 0.41* *Slope =-0.031* *N.S.*
NMB with BIQ Scaffold	*n = 5* *r^2 = 0.48* *Slope =-0.001* *N.S.*	*n = 5* *r^2 = 0.44* *Slope =0.003* *N.S.*	N.S.	*n = 5* *r^2 = 0.58* *Slope =0.005* *N.S.*	N.S.	*n = 3* *r^2 = 0.98* *Slope =-0.003* *N.S.*	N.S.

In red: $r^2 \geq 0.30$ and $p<0.05$;
In italic and red: *$r^2 \geq 0.30$ but $p>0.05$ or $r^2 < 0.30$ but $p<0.05$;*
N.S = Not Significant ($r^2 < 0.30$ and $p>0.05$);

Table 5.19 - Log-Linear Regression Between $LogD_{7.4}$ and Biologically Relevant PK Variables of NMB

	f_u	Log (Vd_{ss}^u) [l/kg]	Log (CL_{tot}^u) [ml/min/kg]	Log (CL_{ren}^u) [ml/min/kg]	Log (CL_{nonren}^u) [ml/min/kg]
NMB (All)	n = 11 r^2 = 0.42 Slope = -0.044 -0.083, -0.005	n = 11 r^2 = 0.68 Slope = 0.129 0.062, 0.196	N.S.	N.S.	N.S.
NMB with ASN Scaffold	*n = 5* *r^2 = 0.76* *Slope = -0.125* *N.S.*	n = 5 r^2 = 0.96 Slope = 0.165 0.103, 0.226	n = 5 r^2 = 0.84 Slope = 0.318 0.064, 0.571	*n = 5* *r^2 = 0.36* *Slope = 0.087* *N.S.*	*n = 5* *r^2 = 0.75* *Slope = 0.403* *N.S.*
NMB with BIQ Scaffold	*n = 4* *r^2 = 0.70* *Slope =0.061* *N.S.*	*n = 4* *r^2 = 0.80* *Slope = -0.072* *N.S.*	*n = 4* *r^2 = 0.58* *Slope = 0.420* *N.S.*	N.S.	*n = 4* *r^2 = 0.63* *Slope = 0.461* *N.S.*

Table 5.20 - Log-Linear Regression Between $LogD_{7.4}$ and Reported PK/PD Variables of NMB

	Log (Vd_{ss}) [l/kg]	Log (CL_{tot}) [ml/min/kg]	Log (CL_{ren}) [ml/min/kg]	Log (CL_{nonren}) [ml/min/kg]	k_{eo} (min^{-1})	Log (Cp_{ss}^{50}) (mM)	γ
NMB (All)	*n = 12* *r^2 = 0.33* *Slope = 0.069* *N.S.*	N.S	N.S.	N.S.	*n = 7* *r^2 = 0.31* *Slope = 0.029* *N.S.*	N.S.	*n = 7* *r^2 = 0.55* *Slope =-2.170* *N.S.*
NMB with ASN Scaffold	*n = 5* *r^2 = 0.64* *Slope = 0.062* *N.S.*	n = 5 r^2 = 0.79 Slope = 0.215 0.009, 0.421	N.S.	*n = 5* *r^2 = 0.67* *Slope = 0.301* *N.S.*	*n =4* *r^2 = 0.38* *Slope = 0.068 N.S.*	N.S.	*n = 3* *r^2 = 0.87* *Slope =1.238* *N.S.*
NMB with BIQ Scaffold	*n = 5* *r^2 = 0.67* *Slope =-0.073* *N.S.*	*n = 5* *r^2 = 0.75* *Slope =0.422* *N.S.*	N.S.	n = 5 r^2 = 0.84 Slope = 0.554 0.108, 1.000	N.S.	N.S.	*n = 3* *r^2 = 0.99* *Slope =0.690* *N.S.*

Table 5.21 - Log-Linear Regression Between HBD and Biologically Relevant PK Variables of NMB

	f_u	Log (Vd_{ss}^u) [l/kg]	Log (CL_{tot}^u) [ml/min/kg]	Log (CL_{ren}^u) [ml/min/kg]	Log (CL_{nonren}^u) [ml/min/kg]
NMB (All)	N.S.	N.S.	N.S.	N.S.	N.S.
NMB with ASN Scaffold	N.S.	N.S.	N.S.	*n = 4* $r^2 = 0.30$ *Slope = 0.112 N.S.*	N.S.
NMB with BIQ Scaffold	N.S.	N.S.	N.S.	N.S.	N.S.

Table 5.22 - Log-Linear Regression Between HBD and Reported PK/PD Variables of NMB

	Log (Vd_{ss}) [l/kg]	Log (CL_{tot}) [ml/min/kg]	Log (CL_{ren}) [ml/min/kg]	Log (CL_{nonren}) [ml/min/kg]	k_{eo} (min^{-1})	Log (Cp_{ss}^{50}) (mM)	γ
NMB (All)	N.S.	N.S.	N.S.	N.S.	*n = 7* $r^2 = 0.30$ *Slope = 0.101 N.S.*	N.S.	N.S.
NMB with ASN Scaffold	*n =4* $r^2 = 0.30$ *Slope =0.047 N.S.*	N.S.	N.S.	N.S.	N.S.	*n =4* $r^2 = 0.45$ *Slope =0.597 N.S.*	*n = 3* $r^2 = 0.46$ *Slope =0.800 N.S.*
NMB with BIQ Scaffold	n = 5 r^2 = 0.80 Slope = 0.129 0.011, 0.247	*n =5* $r^2 = 0.39$ *Slope =-0.492 N.S.*	N.S.	*n =4* $r^2 = 0.56$ *Slope =-0.736 N.S.*	N.S.	*n =3* $r^2 = 0.83$ *Slope =0.481 N.S.*	*n =3* $r^2 = 0.50$ *Slope =-0.600 N.S.*

Table 5.23 - Final QSPKR Models for NMB

Final QSPKR Model	N	Slope (95% CI)	r^2	q^2
$f_u = 0.583 - 0.044 * LogD_{7.4}$	11	- 0.044 (-0.083, -0.005)	0.42	0.21
$Log (Vd_{ss}^u) = - 0.461 + 0.129 * LogD_{7.4}$	11	0.129 (0.062, 0.196)	0.68	0.21

$q^2 \geq 0.40$: Acceptable

Figure 5.3 - f_u vs. $logD_{7.4}$ for NMB

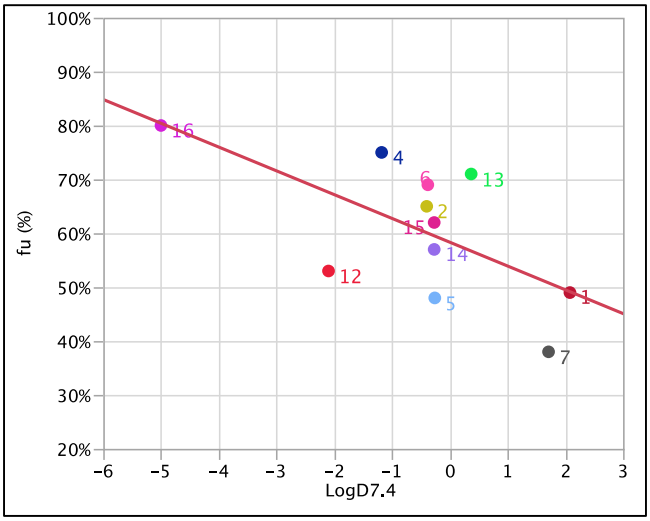

Figure 5.4 - Vd_{ss}^u vs. $logD_{7.4}$ for NMB

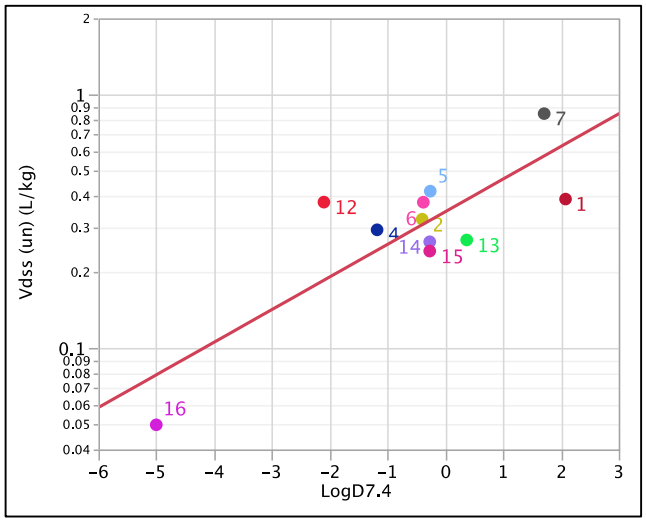

(Please refer Table 5.1 in Page 60, for the list of the individual compounds labeled in the figures 5.3 and 5.4)

Figure 5.5 - Cp_{ss}^{50} vs. MW for NMB

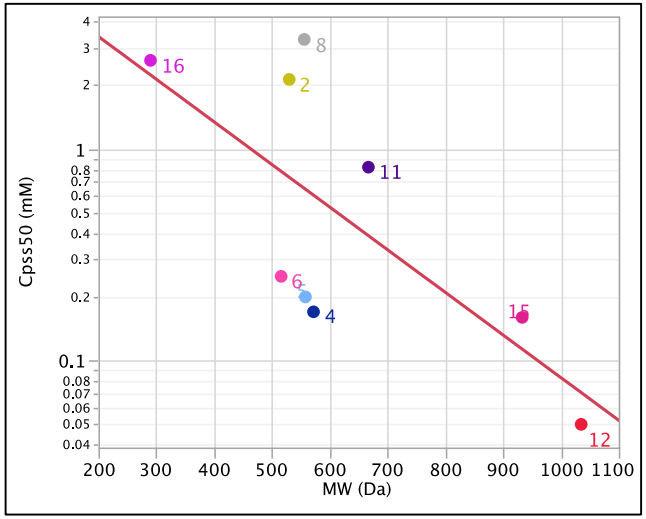

(Please refer Table 5.1 in Page 60, for the list of the individual compounds labeled in figure 5.5)

Figure 5.6 - Vd_{ss}^{u} vs. $logD_{7.4}$ for NMB with ASN Scaffold

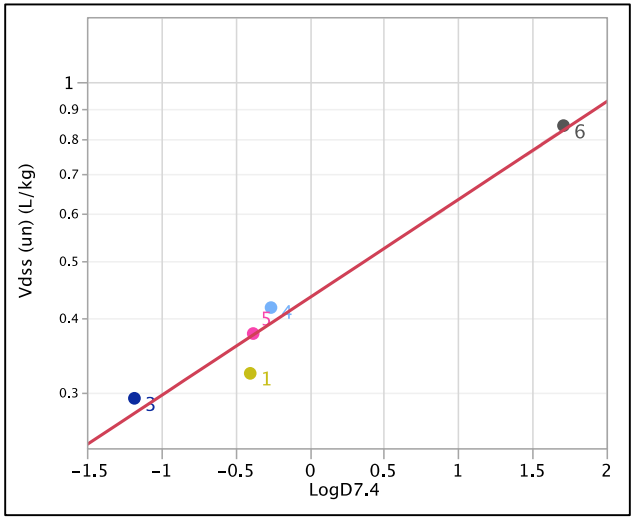

(Please refer Table 5.2 in Page 61, for the list of the individual compounds labeled in figure 5.6)

Figure 5.7 - CL_{tot}^{u} vs. $logD_{7.4}$ for NMB with ASN Scaffold

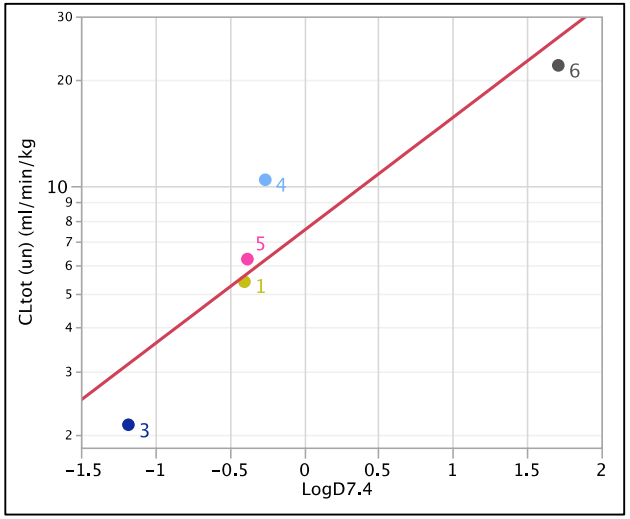

Figure 5.8 - CL_{tot} vs. $logD_{7.4}$ for NMB with ASN Scaffold

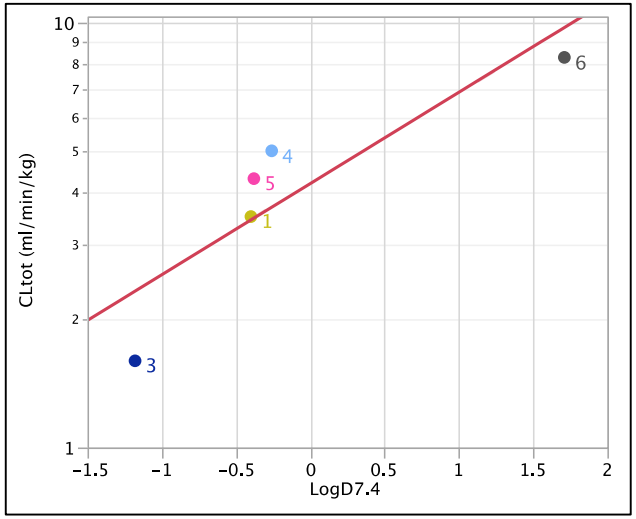

(Please refer Table 5.2 in Page 61, for the list of the individual compounds labeled in the figures 5.7 and 5.8)

Figure 5.9 - CL_{nonren} vs. $logD_{7.4}$ for NMB with BIQ Scaffold

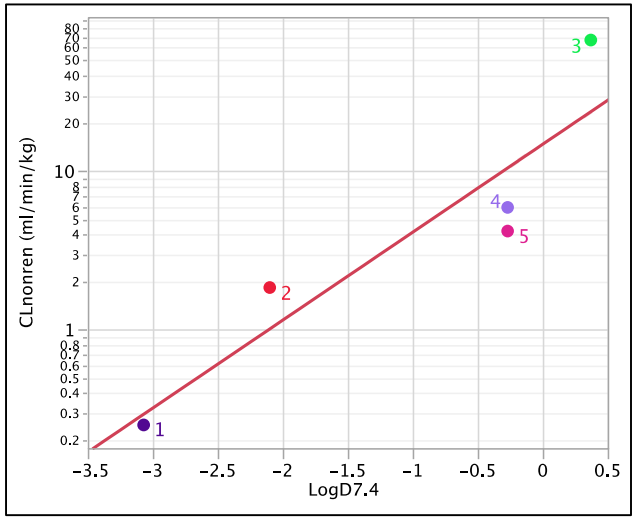

(Please refer Table 5.3 in Page 62, for the list of the individual compounds labeled in the 5.8)

5.3. Discussion

Structurally, NMBs in the current dataset (n = 16) exhibit two common scaffolds - ASN (n = 9) and BIQ (n = 5), while fazadinium and SCh are classified under the miscellaneous category. Overall, the PC/molecular property space has fairly large diversity (2- to 8-fold, n = 11 - 16), and NMB with the BIQ scaffold seem to be relatively more heterogeneous than those with ASN scaffold. NMB have fairly large MW (ranging from 444 - 1035 Da, n = 15, except SCh), mostly hydrophilic, i.e., $logD_{7.4} < 1.0$ (n = 10, i.e., excluding rapacuronium and fazadinium), ranging from -5.00 to 2.08 (n = 12), bases with two positive charges. Roy et al[79] determined the experimental values of (logarithm of) distribution coefficient for seven NMB, including SCh and they found that all of the values were negative, i.e., they are all hydrophilic. The ACD/Labs predicted $logD_{7.4}$ values for mivacurium, atracurium and cisatracurium are lower than their corresponding experimental determined values, while for vecuronium, rocuronium and SCh, the ACD/Labs predicted values are comparable to their corresponding experimentally determined values. This suggests that the accuracy of ACD/Labs predicted $logD_{7.4}$ is less reliable, especially for the relatively more polar compounds.

Most NMB are not extensively plasma protein bound, and their Vd_{ss}^{u} values indicate little extravascular distribution (primarily into extra and/or intracellular water) - possibly due to their hydrophilic nature and/or large MW. Despite low PPB values in general, it seem to still offset the Vd_{ss}^{u} resulting in lower Vd_{ss} values, indicated binding-restricted distribution.

The available CL_{ren}^{u} values suggest net tubular reabsorption, potentially involving transporters. Few compounds, i.e., atracurium, cisatracurium, mivacurium and SCh, show significant extrahepatic clearance pathways by enzymatic/chemical degradation, while the rest of NMB show (non-binding restricted) low to intermediate ER_{hep}.

In-vivo PD properties suggested that NMB, in general, equilibrate with the biophase compartment fairly rapidly (equilibration half-lives ranging between 3 - 14 minutes). Overall, there is considerable to large diversity in the *in-vitro/in-vivo* systemic PK/PD properties of NMB in the current dataset with available information, ranging from 4- to 266-fold (n = 8 - 16), and NMB with BIQ scaffold seem to be relatively more heterogeneous than those with ASN scaffold. $LogD_{7.4}$ is found to be the important determinant affecting biologically relevant systemic PK properties, namely, f_u and $Vd_{ss}{}^u$. An increase in $logD_{7.4}$ is associated with a decrease in f_u (Figure 5.3), suggesting that NMB bind to plasma proteins by hydrophobic interactions. These findings are consistent with binding of quaternary ammonium compounds in rats[80], and a similar relationship was also found between *in-vitro* PPB of NMB in human plasma (fraction bound) and experimentally determined (log of) the partition coefficient (octanol/Krebs buffer) (Slope = 0.18, $r^2 = 0.75$, n = 15)[81].

Obach et al[29] investigated a diverse set of 554 drugs found that (non-specific) hydrophobic interactions with the plasma proteins drive the negative trend between f_u and $logD_{7.4}$. $Vd_{ss}{}^u$ shows a positive association with $logD_{7.4}$ (Figure 5.4), and this relationship is comparable to that obtained for sulfonamides in rats (Slope = 0.20, $r^2 = 0.69$, n = 6)[82], β-adrenergic ligands in humans (Slope = 0.33, $r^2 = 0.71$, n = 13)[39]. Because of the offsetting effect of $logD_{7.4}$ on f_u and $Vd_{ss}{}^u$, Vd_{ss} did not show any relationship with $logD_{7.4}$.

None of the other PC variables show significant relationships with the other biologically relevant systemic PK variables (namely $CL_{tot}{}^u$, $CL_{ren}{}^u$ and $CL_{nonren}{}^u$) across all the NMB and a plausible explanation may be the diverse clearance mechanisms that cannot be explained by (bulk) PC/molecular properties. However, when NMB are stratified based on their structural scaffold, NMB with the ASN scaffold show a significant positive association between $Vd_{ss}{}^u$ and $logD_{7.4}$

(Figure 5.6) but NMB with the BIQ scaffold do not (Table 5.19). Furthermore, significant positive associations are observed with CL_{tot}^{u} (as well as CL_{tot}) as a function of $logD_{7.4}$ only for NMB with the ASN scaffold (Table 5.19 and Figures 5.7 and 5.8). Wierda et al[83] reported a similar trend for NMB in humans (n = 5) both for CL_{tot}^{u} and CL_{tot} as a function of lipophilicity (despite the offsetting effects of lipophilicity on f_u).

None of the PD properties show significant relationships with the PC/molecular variables, except log Cp_{ss}^{50} with MW (Table 5.22 and Figure 5.5). Notably, an increase in MW is associated with a decrease in Cp_{ss}^{50} (or increase in potency, when concentration is expressed in molar terms). A similar relationship was obtained by Roy et al[79] who investigated NMB with ASN-, BIQ-scaffolds and also SCh. Although the exact reason for such a relationship is not fully understood, MW has also been proposed to be an important determinant in the speed of onset of action (despite the presence of permanently positively charged nitrogens)[84].

Overall, nonspecific hydrophobic interactions with plasma proteins (and tissues) appear to be a plausible explanation for the observed significant relationships of $logD_{7.4}$ with f_u and Vd_{ss}^{u} for NMB seen in this study. Within the limitations of the study, none of the PC variables for NMB correlated with elimination clearances and PD (except molar Cp_{ss}^{50} with MW) variables, suggesting high molecular selectivity of the various clearance mechanisms (i.e., chemical/enzymatic degradation, hepatobiliary excretion and/or renal tubular reabsorption) and drug - target interactions. Final QSPKR models did not give acceptable predictions for NMB.

CHAPTER 6. QSPKR of TRP

6.1. Background

TRP are used therapeutically to alleviate migraine pain. Although the underlying etiology of migraine is not fully understood, the role of serotonin (5-hydroxy-tryptamine, 5-HT) has been implicated in its pathogenesis[57,58]. TRP show high selectivity and potent agonist activity at the serotoninergic, G-protein coupled receptors and more specifically at 5-$HT_{1B/1D}$ subtypes[56]. The distribution of these receptors and pharmacological action of TRP at these receptors is shown in Figure - 6.1 below[85].

Figure 6.1 - 5-$HT_{1B/1D}$ Receptors in CNS and Their Pharmacological Actions

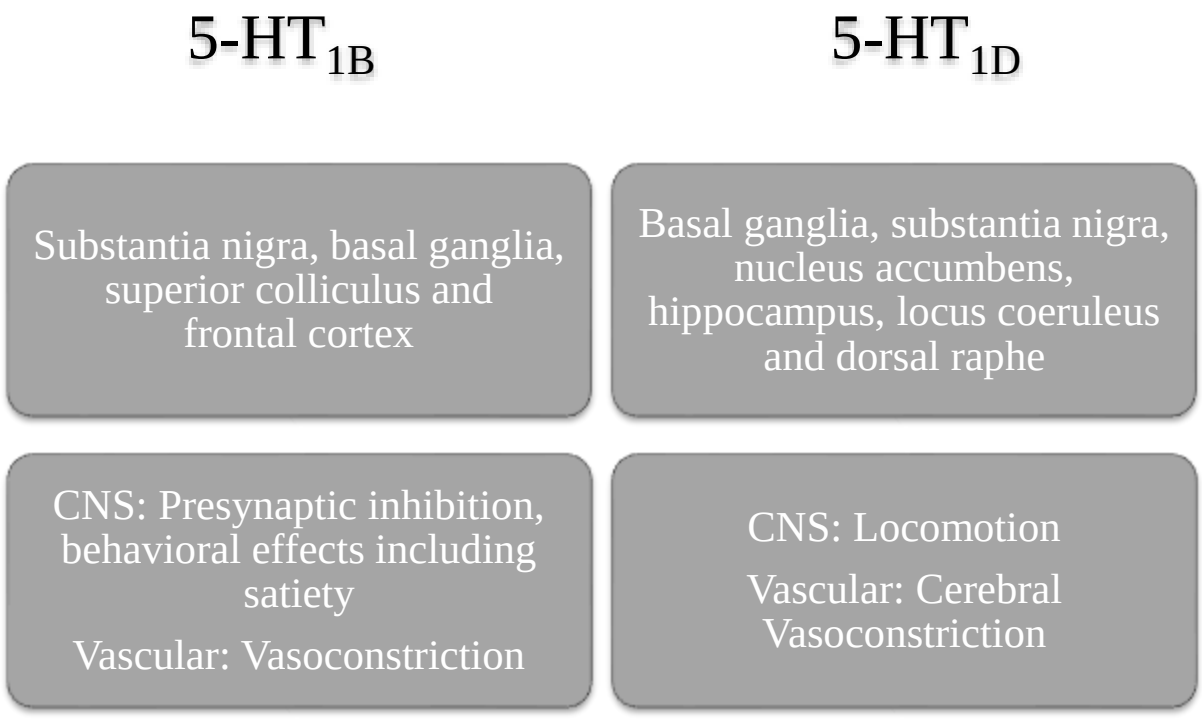

Consistent with their 5-HT target receptors, structurally, TRP show a tryptamine nucleus:

Figure 6.2 - Tryptamine nucleas

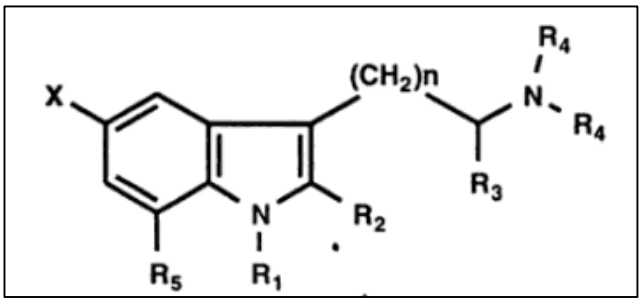

The following structure activity relationships (SAR)[86] were identified:

1. Recognition of the ligand at 5-$HT_{1B/1D}$ requires the presence of an indole ring and linkage of the basic nitrogen to the 3-position (i.e., tryptamine nucleus), which is involved in hydrogen bonding interactions with the receptor.
2. Substitution at R2 - position results in reduction of potency, owing to steric hindrance in receptor binding interactions
3. Substituent at 6-position resulted with hydrogen bond accepting groups resulted in hydrogen bonding interactions with (hydrogen bond donating groups) in the receptors
4. The quaternary nitrogen present either as a aliphatic/heterocyclic substituent is involved in ionic interactions with the receptor.

6.2. Results

The final PC/molecular and human systemic PK/PD database consists of eight TRP. Based on the available information in the literature for TRP, four of them, namely, sumatriptan, almotriptan, rizatriptan and zolmitriptan are known to be substrates of monoamine oxidase (MAO), while there is sufficient evidence in the literature for the remaining three (i.e., non-MAO substrates), namely, naratriptan, frovatriptan and eletriptan. Further discussion of the property spaces for both PC/molecular and systemic PK/PD is presented comprehensively (i.e., all TRP) and also by MAO-substrate status.

6.2.1. PC/Molecular Property Space of TRP

The PC/molecular property space exhibited by TRP in the current dataset is presented in Table - 6.1. Structurally, all TRP in the current dataset show a 5-hydroxy-tryptamine scaffold (but vary in the substituents attached to it, see Figure 6.2); thus, they exhibit fairly similar values for PSA, nRot, HBA and HBD, as is evident from low diversity (2- to 4- fold, n = 8) of these PC properties, except for avitriptan which has higher values. All TRP have relatively low MW, ranging from 243 to 459 Da, n = 8. Although all the TRP in the current dataset show both pK_{a1} and pK_{a2}, only pK_{a2}, i.e., due to a weakly basic group (e.g., $-NH_2$ group) is relevant at physiological pH of 7.4. Therefore, all of them are bases (n = 8) and, at pH 7.4, they are completely ionized (~99% for all TRP except avitriptan, which is 60% ionized), i.e., they carry a (single) positive charge on nitrogen present in secondary form either in an aliphatic/heterocyclic side chain.

All the TRP in the current dataset are hydrophilic, i.e., $logD_{7.4} < 1.0$, and their (estimated $logD_{7.4}$) values are consistently lower than their respective (SciFinder-predicted) logP values, which is a consequence of complete ionization (see above). When they are further categorized based on

their known MAO-substrate status (shown in Tables 6.2 and 6.3), their respective molecular/PC property spaces overlap, suggesting that there are no meaningful differences in their PC properties due to MAO status. However, TRP that are MAO-substrates seem to be relatively more homogenous in their PC/molecular property space than the non-MOA substrates.

The descriptive statistics of PC/molecular properties are shown in Table 6.4, and their mean values are comparable to the median values. Based on the acceptance criteria set *a-priori* for collinearity, i.e., $r \geq 0.80$, MW is highly correlated with MV ($r = 0.99$, $n = 8$), MW with nRot ($r = 0.84$, $n = 8$), PSA with HBD ($r = 0.84$, $n = 8$), and nRot with MV ($r = 0.84$, $n = 8$) (shown in Table 6.5). Thus, $logD_{7.4}$, MW, HBA and HBD were used for subsequent analysis (i.e., PSA, MV and nRot were excluded).

Table 6.1 - Molecular/PC Property Space of TRP

		Drug	MW (Da)	logP	pK_{a1}	$pK_{a\ 2}$	LogD at pH 7.4	% Ionized at pH 7.4	Charge at pH 7.4	PSA (A^2)	MV (cm^3/ mol)	nRot	HBD	HBA
MAO Substrates	**1**	Sumatriptan	295	0.44	11.31	9.49	-1.65	99%	C	74	238	5	2	5
	2	Almotriptan	335	2.30	16.92	9.48	0.22	99%	C	65	264	6	1	5
	3	Rizatriptan	269	1.20	16.98	9.49	-0.89	99%	C	50	223	5	1	5
	4	Zolmitriptan	287	0.46	12.57	9.52	-1.66	99%	C	57	236	5	2	5
Non-MAO Substrates	**5**	Naratriptan	335	1.15	11.52	9.30	-0.76	99%	C	74	273	4	2	5
	6	Frovatriptan	243	0.93	16.39	10.38	-2.05	100%	C	71	192	2	4	4
	7	Eletriptan	383	2.98	17.14	10.35	0.03	100%	C	62	310	6	1	4
	8	Avitriptan	459	0.09	11.32	7.57	-0.30	60%	C	112	353	8	2	9
		N	8	8			8			8	8	8	8	8
		Mean	326	1.19			-0.88			71	261	5	2	5
		Maximum	459	2.98			0.22			112	353	8	4	9
		Minimum	243	0.09			-2.05			50	192	2	1	4
		-fold range	2	33			2			2	2	4	4	2

Table 6.2 - Molecular/PC Property Space of TRP - MAO Substrates

		Drug	MW (Da)	LogD at pH 7.4	PSA (A^2)	MV (cm^3/mol)	nRot	HBD	HBA
MAO Substrates	**1**	Sumatriptan	295	-1.65	74	238	5	2	5
	2	Almotriptan	335	0.22	65	264	6	1	5
	3	Rizatriptan	269	-0.89	50	223	5	1	5
	4	Zolmitriptan	287	-1.66	57	236	5	2	5
		N	4	4	4	4	4	4	4
		Mean	297	-1.00	62	240	5	1.5	5
		(95% CI)	*(252, 341)*	*(-2.41, 0.42)*	*(45, 78)*	*(213, 268)*	*(4, 6)*	*(0.6, 2.4)*	
		Maximum	335	0.22	74	264	6	2	5
		Minimum	269	-1.66	50	223	5	1	5
		-fold range	1.2	1.9	1.5	1.2	1.2	2	1

Table 6.3 - Molecular/PC Property Space of TRP - Non-MAO Substrates

		Drug	MW (Da)	LogD at pH 7.4	PSA (A^2)	MV (cm^3/mol)	nRot	HBD	HBA
Non-MAO Substrates	**1**	Naratriptan	335	-0.76	74	273	4	2	5
	2	Frovatriptan	243	-2.05	71	192	2	4	4
	3	Eletriptan	383	0.03	62	310	6	1	4
		N	3	3	3	3	3	3	3
		Mean	320	-0.93	69	258	4	2	4
		(95% CI)	*(144, 497)*	*(-3.53, 1.68)*	*(53, 84)*	*(108, 408)*	*(-1, 9)*	*(-1, 6)*	*(3, 6)*
		Maximum	383	0.03	74	310	6	4	5
		Minimum	243	-2.05	62	192	2	1	4
		-fold range	1.6	2.1	1.2	1.6	3.0	4.0	1.3

Table 6.4 - Descriptive Statistics of PC/Molecular Properties of TRP

	N	Mean	SD	95% CI	Minimum	10%	25%	Median	75%	90%	Maximum
MW (Da)	8	**326**	69	268, 384	243	243	274	**315**	371	459	459
$LogD_{7.4}$	8	**-0.88**	0.84	-1.6, -0.18	-2.1	-2.1	-1.7	**-0.83**	-0.053	0.22	0.22
PSA (A^2)	8	**71**	19	55, 86	50	50	58	**68**	74	112	112
MV (cm^3/mol)	8	**261**	51	218, 304	192	192	226	**251**	301	353	353
nRot	8	**5.1**	1.7	3.7, 6.6	2.0	2.0	4.2	**5.0**	6.0	8.0	8.0
HBA	8	**5.3**	1.6	3.9, 6.6	4.0	4.0	4.3	**5.0**	5.0	9.0	9.0
HBD	8	**1.9**	0.99	1.0, 2.7	1.0	1.0	1.0	**2.0**	2.0	4.0	4.0

Table 6.5 - Correlation Matrix for PC/Molecular Variables of TRP

	MW (Da)	$LogD_{7.4}$	PSA (A^2)	MV (cm^3/mol)	nRot	HBD	HBA
MW (Da)	1.00						
$LogD_{7.4}$	0.71	1.00					
PSA (A^2)	0.72	0.16	1.00				
MV (cm^3/mol)	**0.99**	0.73	0.66	1.00			
nRot	**0.84**	0.70	0.47	**0.84**	1.00		
HBA	-0.36	-0.74	0.27	-0.43	-0.66	1.00	
HBD	0.73	0.28	**0.84**	0.68	0.72	-0.07	1.00

6.2.2. Humans Systemic PK/PD Property Space of TRP

The final mean *in-vitro* and *in-vivo* human systemic PK and PD properties compiled from various studies in the literature are shown in Table - 6.6 and 6.12 respectively and the estimated biologically relevant PK properties are listed in Table 6.9. Appendix 3 contains all the supplemental information with respect to the *in-vitro*/*in-vivo* human systemic PK and *ex-vivo/in-vitro* PD data compiled for each of the compound from the literature.

Depending on the property, there is little to considerable diversity in the *in-vitro/ in-vivo* systemic and biologically relevant PK/PD properties of TRP in the current dataset, ranging from 3- to 21-fold (n = 7-8). Therefore, the systemic PK variables (except f_u, and PD variables) were log-transformed for further analysis. When classified based on MAO substrate status, it is observed that the diversity is reduced for the *in-vitro/in-vivo* systemic (shown in Tables 6.7 and 6.8), biologically relevant PK (shown in Tables 6.10 and 6.11) and for the PD property space (shown in Tables 6.13 and 6.14). When TRP were categorized by MAO-substrate status, it is observed that property spaces shown by MAO-substrates is relatively more homogenous than the non-MOA substrates, however, overall, no meaningful differences are observed in these property spaces.

The descriptive statistics for these PK/PD properties of all the TRP in the dataset (comprehensively) are shown in Table 6.15, and the mean values are comparable to the median values for the majority of them. Several correlations are observed between the *in-vitro*/*in-vivo* human systemic and biologically relevant PK variables of TRP (shown in Table 6.16). However, most of these correlations are mechanistically plausible, e.g., CL_{tot} is highly correlated with CL_{nonren} ($r = 0.98$, $n = 8$), and CL_{tot} is also highly correlated with CL_{ren} ($r = 0.80$, $n = 8$) suggesting that a few TRP show significant renal and the rest have significant non-renal

clearance pathways. Furthermore, f_u is highly negatively correlated with Vd_{ss}^u (r = -0.92, n = 7) and CL_{tot}^u (r = -0.82, n = 7), possibly because of a common underlying factor (e.g., $logD_{7.4}$ and/or MW) causing, counteracting effects on PPB and distribution/non-renal clearance of the unbound drug.

Overall, PPB varies 6-fold (n = 7), and the majority of TRP in the dataset are not extensively bound to plasma proteins, possibly because of their low lipophilicity and/or ionization. Most of the TRP show a low degree of PPB (median f_u = 75%, n = 7) with the exception of eletriptan (f_u = 15%). Furthermore, MAO substrates are fairly homogeneous in their f_u values (1.3-fold, n = 4), while the non-MAO substrates are quite heterogeneous (5.7-fold, n = 3). Vd_{ss}^u varies 8-fold (n = 7) compared to Vd_{ss} (6-fold, n = 7); after correcting for PPB, the mean value of Vd_{ss}^u (5.7 l/kg) is higher than the mean Vd_{ss} (2.3 l/kg). Therefore, it seems that the high Vd_{ss}^u values are offset by high PPB (i.e., low f_u), which resulted in lower Vd_{ss} values, suggesting that the extravascular tissue distribution is restricted by PPB. The majority of TRP have Vd_{ss}^u values greater than BW (70 kg), suggesting they undergo moderate extravascular distribution into tissues and/or binding to plasma membranes etc. (with the exception of eletriptan, which has Vd_{ss}^u value of 15.7 l/kg suggesting that it undergoes extensive extravascular distribution). This is true for both MAO and non-MAO substrates; however, the range of Vd_{ss}^u for the former (2-fold, n = 4) is relatively more homogeneous than for the latter (4-fold, n = 3).

Most of the TRP show clearance by renal pathways (with f_e ranging from 9% to 44%, n = 7); again, the range in CL_{ren} for MAO substrates is relatively more homogeneous (2-fold, n = 4) than for non-MAO substrates (5-fold, n = 3). CL_{ren}^u estimates for all the TRP (except frovatriptan) exceed GFR (1.7 ml/min/kg), suggesting they undergo net tubular secretion, potentially involving drug transporters (as they are all positively charged at physiological pH of 6.3 in urine

and 7.4 in the plasma). Naratriptan shows a CL_{ren}^{u} value (9 ml/min/kg) close to RPF (10 ml/min/kg). Although the mean estimates for CL_{ren}^{u} between MAO and non-MAO substrate classes are comparable, the range for former is more homogeneous (2-fold, n = 4) than for the latter (6-fold, n = 3).

Overall, CL_{nonren} varies 21-fold (n = 8). The CL_{tot} and CL_{nonren} values of MAO substrates are, in general, (a) on an average are higher, and (b) more heterogeneous than non-MAO substrates. However, after correcting for PPB, on an average, the CL_{tot}^{u} and CL_{nonren}^{u} values for non-MAO substrates are higher and more heterogeneous than MAO-substrates. This suggests that the PPB offset the high values of CL_{tot}^{u} and CL_{nonren}^{u} for non-MAO substrates. The pathways that encompass CL_{nonren} are known to include hepatic metabolism via enzymes e.g., CYP3A, 1A2 (and 2D6) and is also mediated by MAO, which is present both hepatically and extrahepatically (see Appendix 3). CL_{nonren} values (assuming a B:P ratio close to 1) for non-MAO substrates are lower than LBF (21 ml/min/kg), suggesting they are all low ER_{hep} drugs either because of low hepatic CL_{int} (e.g., frovatriptan) and/or (relatively) high PPB (e.g., eletriptan). Furthermore, owing to their positively charged nature, they may also be subject to hepato-biliary excretion, potentially involving transporters.

Based on the available *in-vivo* drug - drug interaction studies (i.e., in the presence of moclobemide, a MAO inhibitor), oral bioavailability studies and mass balance studies, the rank order for the contribution of MAO-mediated metabolic clearance towards the CL_{nonren} for MAO substrates is rizatriptan > almotriptan > zolmitriptan (see Appendix 3).

There is considerable diversity (7- to 11-fold, n = 7) in the *in-vitro/ex-vivo* PD properties, namely, receptor binding affinities at 5-$HT_{1B/1D}$ relative to [^{3}H] eletriptan and [^{3}H] sumatriptan. When they are classified based on MAO-substrate status, (a) in general, on an average, MAO-

substrates show high K_i (low affinity) values compared to non-MAO substrates, which show low K_i (high affinity) values, and (b) MAO-substrates, in general, show relatively larger diversity than non-MAO substrates.

Table 6.6 - *In-vitro* and *In-vivo* Human PK Systemic Properties of TRP

		In-vitro PK Variable	***In-vivo PK Variables***				
	Drug	**f_u [%]**	**Vd_{ss} [l/kg]**	**CL_{tot} [ml/min/kg]**	**f_e [%]**	**CL_{ren} [ml/min/kg]**	**CL_{nonren} [ml/min/kg]**
MAO Substrates	Sumatriptan	84%	2.6	16	23%	3.7	12
	Almotriptan	65%	2.3	9.0	42%	3.8	5.2
	Rizatriptan	86%	1.7	15	25%	3.7	11
	Zolmitriptan	75%	2.1	11	28%	3.0	7.5
Non-MAO Substrates	Naratriptan	28%	2.4	6.6	36%	2.4	4.2
	Frovatriptan	85%	3.6	2.8	44%	1.3	1.5
	Eletriptan	15%	2.4	6.3	9.0%	0.57	5.7
	Avitriptan	-	1.1	7.4	-	-	-
	N	7	8	8	7	7	7
	Mean	63%	2.3	9.2	30%	2.6	6.9
	Maximum	86%	3.6	16	44%	3.8	12
	Minimum	15%	1.1	2.8	9.0%	0.57	1.5
	-fold range	6	3	6	5	7	8

Table 6.7 - *In-vitro* and *In-vivo* Human PK Systemic Properties of TRP - MAO Substrates

		In-vitro PK Variable	***In-vivo PK Variables***				
	Drug	**f_u [%]**	**Vd_{ss} [l/kg]**	**CL_{tot} [ml/min/kg]**	**f_e [%]**	**CL_{ren} [ml/min/kg]**	**CL_{nonren} [ml/min/kg]**
MAO Substrates	Sumatriptan	84%	2.6	16.1	23%	3.7	12.4
	Almotriptan	65%	2.3	9.0	42%	3.8	5.2
	Rizatriptan	86%	1.7	15.2	25%	3.7	11.4
	Zolmitriptan	75%	2.1	10.5	28%	3.0	7.5
	N	4	4	4	4	4	4
	Mean	77%	2.1	12.7	30%	3.6	9.2
	(95% CI)	*(62%, 93%)*	*(1.6, 2.8)*	*(7.2, 18.2)*	*(16%, 43%)*	*(3.0, 4.1)*	*(3.8, 14.5)*
	Maximum	86%	2.6	16.1	42%	3.8	12.4
	Minimum	65%	1.7	9.0	23%	3.0	5.2
	-fold range	1.3	1.5	1.8	1.8	1.3	2.4

Table 6.8 - *In-vitro* and *In-vivo* Human PK Systemic Properties of TRP - Non-MAO Substrates

		In-vitro PK Variable	***In-vivo PK Variables***				
	Drug	**f_u [%]**	**Vd_{ss} [l/kg]**	**CL_{tot} [ml/min/kg]**	**f_e [%]**	**CL_{ren} [ml/min/kg]**	**CL_{nonren} [ml/min/kg]**
Non-MAO Substrates	Naratriptan	28%	2.4	6.6	36%	2.4	4.2
	Frovatriptan	85%	3.6	2.8	44%	1.3	1.5
	Eletriptan	15%	2.4	6.3	9.0%	0.57	5.7
	N	3	3	3	3	3	3
	Mean	43%	2.8	5.2	30%	1.4	3.9
	(95% CI)	*(-50%, 135%)*	*(1.0, 4.5)*	*(-0.01, 10.5)*	*(-15%, 75%)*	*(-0.9, 3.7)*	*(-1.3, 9.0)*
	Maximum	85%	3.6	6.6	44%	2.4	5.7
	Minimum	15%	2.4	2.8	9.0%	0.57	1.6
	-fold range	5.7	1.5	2.4	4.9	3.0	3.6

Table 6.9 - Biologically Relevant *In-vivo* Human PK Properties of TRP

	Drug	Vd_{ss}^{u} [l/kg]	CL_{tot}^{u} [ml/min/kg]	CL_{ren}^{u} [ml/min/kg]	CL_{nonren}^{u} [ml/min/kg]
MAO Substrates	Sumatriptan	3.1	19.2	4.4	14.8
	Almotriptan	3.5	13.8	5.8	8.0
	Rizatriptan	2.0	17.6	4.3	13.3
	Zolmitriptan	2.8	14.0	4.0	10.0
Non-MAO Substrates	Naratriptan	8.6	23.6	8.6	15.0
	Frovatriptan	4.2	3.2	1.4	1.8
	Eletriptan	15.7	42.0	3.8	38.2
	N	7	7	7	7
	Mean	5.7	19.2	4.6	14.4
	Maximum	15.7	42.0	8.6	38.2
	Minimum	2.0	3.2	1.4	1.8
	-fold range	8	13	6	21

Table 6.10 - Biologically Relevant *In-vivo* Human PK Properties of TRP - MAO Substrates

	Drug	Vd_{ss}^{u} [l/kg]	CL_{tot}^{u} [ml/min/kg]	CL_{ren}^{u} [ml/min/kg]	CL_{nonren}^{u} [ml/min/kg]
MAO Substrates	Sumatriptan	3.1	19.2	4.4	14.8
	Almotriptan	3.5	13.8	5.8	8.0
	Rizatriptan	2.0	17.6	4.3	13.3
	Zolmitriptan	2.8	14.0	4.0	10.0
	N	4	4	4	4
	Mean	2.9	16.2	4.6	11.5
	(95% CI)	*(1.8, 3.9)*	*(11.9, 20.4)*	*(3.3, 5.9)*	*(6.6, 16.5)*
	Maximum	3.5	19.2	5.8	14.8
	Minimum	2.0	13.8	4.0	8.0
	-fold range	1.8	1.4	1.5	1.9

Table 6.11 - Biologically Relevant *In-vivo* Human PK Properties of TRP - Non-MAO Substrates

	Drug	Vd_{ss}^{u} [l/kg]	CL_{tot}^{u} [ml/min/kg]	CL_{ren}^{u} [ml/min/kg]	CL_{nonren}^{u} [ml/min/kg]
Non-MAO Substrates	Naratriptan	8.6	23.6	8.6	15.0
	Frovatriptan	4.2	3.2	1.4	1.8
	Eletriptan	15.7	42.0	3.8	38.2
	N	3	3	3	3
	Mean	9.5	23.0	4.7	18.3
	(95% CI)	*(-4.8, 23.8)*	*(-25.1, 71.0)*	*(-4.3, 13.7)*	*(-27.1, 63.7)*
	Maximum	15.7	42.0	8.6	38.2
	Minimum	4.2	3.2	1.4	1.8
	-fold range	3.7	13.2	6.2	21.2

Table 6.12 - *In-vitro/Ex-vivo* Relative Receptor Binding Affinities of TRP at 5-HT$_{1B/1D}$

	Drug	5-HT$_{1B}$		5-HT$_{1D}$	
		[^{3}H] Eletriptan	**[^{3}H] Sumatriptan**	**[^{3}H] Eletriptan**	**[^{3}H] Sumatriptan**
MAO Substrates	Sumatriptan	22.4	8.7	10.0	10.2
	Almotriptan	10.0	10.0	10.0	10.0
	Rizatriptan	27.5	13.8	18.6	11.5
	Zolmitriptan	7.1	2.8	2.1	1.2
Non-MAO Substrates	Naratriptan	4.3	1.9	5.1	4.6
	Frovatriptan	2.5	2.5	4.0	4.0
	Eletriptan	4.5	3.2	1.6	1.7
	N	7	7	7	7
	Mean	11.2	6.1	7.4	6.2
	Maximum	27.5	13.8	18.6	11.5
	Minimum	2.5	1.9	1.6	1.2
	-fold range	11	7	11	9

Table 6.13 - *In-vitro/Ex-vivo* RRA of TRP - MAO Substrates

	Drug	5-HT$_{1B}$		5-HT$_{1D}$	
		[^{3}H] Eletriptan	**[^{3}H] Sumatriptan**	**[^{3}H] Eletriptan**	**[^{3}H] Sumatriptan**
MAO Substrates	Sumatriptan	22.4	8.7	10.0	10.2
	Almotriptan	10.0	10.0	10.0	10.0
	Rizatriptan	27.5	13.8	18.6	11.5
	Zolmitriptan	7.1	2.8	2.1	1.2
	N	4	4	4	4
	Mean	16.7	8.8	10.2	8.2
	(95% CI)	*(1.2, 32.3)*	*(1.6, 16.1)*	*(-0.52, 20.9)*	*(0.70, 15.8)*
	Maximum	22.4	13.8	18.6	11.5
	Minimum	7.1	2.8	2.1	1.2
	-fold range	3	5	9	9

Table 6.14 - *In-vitro/Ex-vivo* RRA of TRP - Non-MAO Substrates

	Drug	5-HT$_{1B}$		5-HT$_{1D}$	
		[^{3}H] Eletriptan	**[^{3}H] Sumatriptan**	**[^{3}H] Eletriptan**	**[^{3}H] Sumatriptan**
Non-MAO Substrates	Naratriptan	4.3	1.9	5.1	4.6
	Frovatriptan	2.5	2.5	4.0	4.0
	Eletriptan	4.5	3.2	1.6	1.7
	N	3	3	3	3
	Mean	3.8	2.5	7.5	5.8
	(95% CI)	*(1.1, 6.4)*	*(0.82, 4.3)*	*(-0.87, 8.0)*	*(-0.37, 7.2)*
	Maximum	4.5	3.2	5.1	4.6
	Minimum	2.5	1.9	1.6	1.7
	-fold range	2	2	3	3

Table 6.15 - Descriptive Statistics of Human Systemic PK/PD Variables of TRP

	N	Mean	SD	95% CI	Minimum	10%	25%	Median	75%	90%	Maximum
Vd_{ss} (L/kg)	8	**2.3**	0.71	1.7, 2.9	1.1	1.1	1.8	**2.3**	2.6	3.6	3.6
CL_{tot} (ml/min/kg)	8	**9.2**	4.5	5.4, 13.0	2.8	2.8	6.4	**8.2**	14.0	16.1	16.1
CL_{ren} (ml/min/kg)	7	**2.6**	1.3	1.4, 3.8	0.60	0.60	1.2	**3.0**	3.7	3.8	3.8
CL_{nonren} (ml/min/kg)	7	**6.9**	3.9	3.2, 10.5	1.6	1.6	4.2	**5.7**	11.5	12.4	12.4
f_u	7	**0.63**	0.29	0.36, 0.90	0.15	0.15	0.28	**0.75**	0.85	0.86	0.86
Vd_{ss}^u (L/kg)	7	**5.7**	4.9	1.2, 10.2	2.0	2.0	2.8	**3.5**	8.6	15.7	15.7
CL_{tot}^u (ml/min/kg)	7	**19.1**	11.90	8.1, 30.1	3.3	3.3	13.9	**17.7**	23.6	42.0	42.0
CL_{ren}^u (ml/min/kg)	7	**4.7**	2.17	2.6, 6.7	1.4	1.4	4.0	**4.3**	5.8	8.6	8.6
CL_{nonren}^u (ml/min/kg)	7	**14.4**	11.4	3.9, 24.9	1.9	1.9	8.0	**13.4**	15.0	38.0	38.0
5-HT_{1B} - RRA [^{3}H] Eletriptan	7	**11.2**	9.8	2.1, 20.3	2.5	2.5	4.3	**7.1**	22.4	27.5	27.5
5-HT_{1B} - RRA [^{3}H] Sumatriptan	7	**6.1**	4.7	1.8, 10.5	1.9	1.9	2.5	**3.2**	10.0	13.8	13.8
5-HT_{1D} - RRA [^{3}H] Eletriptan	7	**7.4**	6.0	1.8, 12.9	1.6	1.6	2.1	**5.1**	10.0	18.6	18.6
5-HT_{1D} - RRA [^{3}H] Sumatriptan	8	**6.7**	4.2	3.1, 10.2	1.2	1.2	2.3	**7.3**	10.2	11.5	11.5

Table 6.16 - Correlation Analysis of Human Systemic PK Variables of TRP

	Vd_{ss} (L/kg)	**CL_{tot} (ml/min/kg)**	**CL_{ren} (ml/min/kg)**	**CL_{nonren} (ml/min/kg)**	**f_u**	**Vd_{ss}^u (L/kg)**	**CL_{tot}^u (ml/min/kg)**	**CL_{ren}^u (ml/min/kg)**	**CL_{nonren}^u (ml/min/kg)**
Vd_{ss} (L/kg)	1.00								
CL_{tot} (ml/min/kg)	-0.37	1.00							
CL_{ren} (ml/min/kg)	-0.52	**0.79**	1.00						
CL_{nonren} (ml/min/kg)	-0.62	**0.98**	0.65	1.00					
f_u	0.13	0.46	0.56	0.38	1.00				
Vd_{ss}^u (L/kg)	0.05	-0.50	**-0.77**	-0.36	**-0.92**	1.00			
CL_{tot}^u (ml/min/kg)	-0.41	0.03	-0.37	0.16	**-0.82**	**0.85**	1.00		
CL_{ren}^u (ml/min/kg)	-0.47	0.12	0.33	0.04	-0.51	0.17	0.33	1.00	
CL_{nonren}^u (ml/min/kg)	-0.34	0.01	-0.45	0.16	-0.76	**0.85**	**0.98**	0.15	1.00

6.2.3. QSPKR Analysis, Model Building and Evaluation

The results of the univariate regression of the *in-vitro/(*log-transformed) *in-vivo* biologically relevant and reported PK/PD variables as a function of the molecular/PC variables of TRP, namely, MW, $logD_{7.4}$, HBD and HBA are shown in Table 6.17 to 6.24. MW shows significant univariate relationships ($r^2 \geq 0.3$, $p < 0.05$) with f_u, log (Vd_{ss}^u), log (CL_{tot}^u) and log (CL_{nonren}^u), HBD with log (CL_{tot}^u) and log (CL_{nonren}^u), and HBA with log (Vd_{ss}) and log (CL_{ren}). Lipophilicity ($logD_{7.4}$) did not show significant relationship ($p < 0.05$), although it explains ~ 35% of variability in the *in-vitro/in-vivo* systemic and/or biologically relevant PK variables. Similarly, HBA and HBD explain more than 30% of the variability in certain *in-vivo* and/or biologically relevant, but none of these relationships were significant. None of the PC/molecular variables show significant relationship with the PD variables of TRP; however, MAO substrates alone show significant relationships with HBA, potentially due to large range and/or limited sample size. During the final (multivariate) model building process (using MLLR with forward inclusion followed by backward elimination), MW was found to be the single most important determinant affecting biologically relevant systemic PK variable of TRP, and the final models are summarized in Table - 6.25. Overall, the final QSPKR models developed for TRP gave acceptable predictions ($q^2 \geq 0.40$) only for f_u only.

6.2.3.1. Effect of MW on Systemic and Biologically Relevant PK Variables of TRP

There is a significant negative association between MW and f_u, i.e., an increase in MW is associated with decrease in f_u (increase in PPB) for TRP (Slope = -0.0055, r^2 = 0.78, n = 7, shown in Figure - 6.1). A significant positive association is found with (each of log-transformed) Vd_{ss}^u (Slope = 0.0050, r^2 = 0.58, n = 7), CL_{tot}^u (Slope = 0.0057, r^2 = 0.65, n = 7), CL_{nonren}^u (Slope = 0.0064, r^2 = 0.58, n = 7) and MW of TRP (Figures - 6.2, 6.3 and 6.4 respectively). Due to the

offsetting effects of MW on f_u and $Vd_{ss}{}^u$, f_u and $CL_{tot}{}^u$, and f_u and $CL_{nonren}{}^u$, their uncorrected counterparts, Vd_{ss}, CL_{tot} and CL_{nonren}, respectively, did not depend on MW. Lastly, MW did not show a significant relationship with log-transformed $CL_{ren}{}^u$, probably because of the limited range in the MW and/or $CL_{ren}{}^u$ estimates of triptans in the current dataset. Therefore, it seems that the (significant) relationship of MW on $CL_{nonren}{}^u$ drive that of $CL_{tot}{}^u$. When the TRP are classified based on their MAO substrate status: (a) none of the relationships with MW are significant (except for the MW relationship with log $CL_{nonren}{}^u$), potentially because of reduction in the sample size and/or -fold range in the property space (e.g., $Vd_{ss}{}^u$); (b) a significant positive association between log ($CL_{nonren}{}^u$) and MW for non-MAO substrates (Slope = 0.009, r^2 = 0.99, n = 3) is observed and this seems to drive the overall TRP (comprehensive) relationship with MW (as their slopes are comparable) and (c) in general, the model fits with respect to MW (i.e., r^2) are comparatively better for both systemic and biologically relevant PK variables for the non-MAO substrates than MAO substrates and this is mechanistically plausible because the former is relatively more heterogeneous than the latter both in their molecular/PC as well as their PK property space.

6.2.3.2. Effect of Other PC/Molecular Variables on Systemic/Biologically Relevant PK Variables of TRP

None of systemic/biologically relevant PK/PD variables show significant relationship ($r^2 \geq 0.3$, $p < 0.05$) with $logD_{7.4}$, (for all TRP) or by MAO-substrate status. There is a significant negative association between HBD and log ($CL_{tot}{}^u$) (Slope = -0.26, r^2 = 0.68, n = 4), and also with log ($CL_{nonren}{}^u$) (Slope = -0.30, r^2 = 0.64, n = 7) comprehensively, and when classified there is a significant negative association with log ($CL_{nonren}{}^u$) (Slope = -0.44, r^2 = 0.99, n = 3) for non-MAO substrates. Frovatriptan (a non-MAO substrate) has the highest HBD (n = 4, while the rest

of TRP in the dataset have either n = 1 or 2) and it shows the lowest CL_{tot}^{u} and CL_{nonren}^{u} values and it seems to drive these relationships. There is a significant negative association between HBA and log (Vd_{ss}) (Slope = -0.08, r^2 = 0.73, n = 8) and significant positive association with log (CL_{ren}) (Slope = 0.59, r^2 = 0.87, n = 7) comprehensively. Although there are several relationships in which $logD_{7.4}$, HBD and HBA explained ≥ 30% variability in PK variables both comprehensively for all TRP and also when categorized based on MAO substrate status, none of the slopes for these relationships are different from zero. However, it is observed that, in general, the model fits (i.e., r^2) relative to these PC variables (as seen with MW) are comparatively better for both systemic and biologically relevant PK variables for the non-MAO substrates than MAO substrates and this is mechanistically plausible because the former is relatively more heterogeneous than the latter both in molecular/PC as well as PK property space.

Table 6.17 - Log-Linear Regression Between MW and Biologically Relevant/Systemic PK Variables of TRP

	f_u	Log (Vd_{ss}^u) [l/kg]	Log (CL_{tot}^u) [ml/min/kg]	Log (CL_{ren}^u) [ml/min/kg]	Log (CL_{nonren}^u) [ml/min/kg]	Log (Vd_{ss}) [l/kg]	Log (CL_{tot}) [ml/min/kg]	Log (CL_{ren}) [ml/min/kg]	Log (CL_{nonren}) [ml/min/kg]
All TRP	n = 7 r^2 = 0.78 Slope = -0.0055 -0.0088, -0.0022	n = 7 r^2 = 0.58 Slope = 0.0050 0.00015, 0.0010	n = 7 r^2 = 0.65 Slope = 0.0057 0.00085, 0.011	*n = 7* *r^2 = 0.37* *Slope = 0.0031* *N.S.*	n = 7 r^2 = 0.58 Slope = 0.0064 0.00021, 0.013	*n = 8* *r^2 = 0.48* *Slope =-0.0015* *N.S.*	N.S.	N.S.	N.S.
MAO Substrates	*n = 4* *r^2 = 0.76* *Slope = -0.0030* *N.S.*	*n = 4* *r^2 = 0.77* *Slope =0.0034* *N.S.*	N.S.	*n = 4* *r^2 = 0.80* *Slope =0.0023* *N.S.*	*n = 4* *r^2 = 0.54* *Slope = -0.0032* *N.S.*	*n = 4* *r^2 = 0.35* *Slope =0.0017* *N.S.*	*n = 4* *r^2 = 0.50* *Slope =-0.0031* *N.S.*	N.S.	*n = 4* *r^2 = 0.62* *Slope = -0.0049* *N.S.*
Non-MAO Substrates	*n = 3* *r^2 = 0.97* *Slope = -0.0051* *N.S.*	*n = 3* *r^2 = 0.98* *Slope =0.0039* *N.S.*	*n = 3* *r^2 = 0.98* *Slope =0.0080* *N.S.*	*n = 3* *r^2 = 0.51* *Slope =0.0039* *N.S.*	n = 4 r^2 = 0.99 Slope = 0.0094 0.0049, 0.014	*n = 3* *r^2 = 0.91* *Slope = -0.0014* *N.S*	*n = 3* *r^2 = 0.85* *Slope =0.0027* *N.S*	N.S.	*n = 3* *r^2 = 0.99* *Slope =0.0040* *N.S.*

In red: $r^2 \geq 0.30$ and $p<0.05$;
In italic and red: *$r^2 \geq 0.30$ but $p>0.05$ or $r^2 < 0.30$ but $p<0.05$;*
N.S = Not Significant ($r^2 < 0.30$ and $p>0.05$);

Table 6.18 - Log-Linear Regression Between $LogD_{7.4}$ and Biologically Relevant/Systemic PK Variables of TRP

	f_u	Log (Vd_{ss}^u) [l/kg]	Log (CL_{tot}^u) [ml/min/kg]	Log (CL_{ren}^u) [ml/min/kg]	Log (CL_{nonren}^u) [ml/min/kg]	Log (Vd_{ss}) [l/kg]	Log (CL_{tot}) [ml/min/kg]	Log (CL_{ren}) [ml/min/kg]	Log (CL_{nonren}) [ml/min/kg]
All TRP	*n = 7* *r^2 = 0.41* *Slope = -0.23* *N.S*	N.S	*n = 7* *r^2 = 0.39* *Slope = 0.24* *N.S*	*n = 7* *r^2 = 0.34* *Slope = 0.16* *N.S*	*n = 7* *r^2 = 0.32* *Slope = 0.26* *N.S*	N.S	N.S	N.S	N.S
Only MAO Substrates	*n = 4* *r^2 = 0.44* *Slope = -0.072* *N.S*	N.S.	N.S.	*n = 4* *r^2 = 0.84* *Slope = 0.075* *N.S*	*n = 4* *r^2 = 0.45* *Slope =-0.091* *N.S*	N.S.	*n = 4* *r^2 = 0.32* *Slope =-0.079* *N.S*	*n = 4* *r^2 = 0.35* *Slope =0.032* *N.S*	*n = 4* *r^2 = 0.46* *Slope =-0.13* *N.S*
Only Non-MAO Substrates	*n = 3* *r^2 = 0.96* *Slope =-0.35* *N.S*	*n = 3* *r^2 = 0.99* *Slope =0.27* *N.S*	*n = 3* *r^2 = 0.97* *Slope =0.54* *N.S*	*n = 3* *r^2 = 0.47* *Slope =0.26* *N.S*	*n = 3* *r^2 = 0.99* *Slope =0.63* *N.S*	*n = 3* *r^2 = 0.89* *Slope =-0.094* *N.S*	*n = 3* *r^2 = 0.82* *Slope =0.18* *N.S*	N.S.	*n = 3* *r^2 = 0.98* *Slope =0.27* *N.S*

Table 6.19 - Log-Linear Regression Between HBD and Biologically Relevant/Systemic PK Variables of TRP

	f_u	Log (Vd_{ss}^u) [l/kg]	Log (CL_{tot}^u) [ml/min/kg]	Log (CL_{ren}^u) [ml/min/kg]	Log (CL_{nonren}^u) [ml/min/kg]	Log (Vd_{ss}) [l/kg]	Log (CL_{tot}) [ml/min/kg]	Log (CL_{ren}) [ml/min/kg]	Log (CL_{nonren}) [ml/min/kg]
All TRP	N.S	N.S	n = 7 r^2 = 0.68 Slope = -0.26 -0.47, -0.053	*n = 7* *r^2 = 0.50* *Slope =-0.16* *N.S*	n = 7 r^2 = 0.64 Slope = -0.30 -0.55, -0.039	N.S	*n = 7* *r^2 = 0.45* *Slope =-0.16* *N.S*	N.S	*n = 7* *r^2 = 0.50* *Slope =-0.20* *N.S*
Only MAO Substrates	N.S.	N.S.	N.S.	*n = 4* *r^2 = 0.38* *Slope =-0.077* *N.S*	N.S.	*n = 4* *r^2 = 0.32* *Slope =0.077* *N.S.*	N.S.	*n = 4* *r^2 = 0.38* *Slope =-0.051* *N.S.*	N.S.
Only Non-MAO Substrates	*n = 3* *r^2 = 0.98* *Slope =0.24* *N.S*	*n = 3* *r^2 = 0.98* *Slope =-0.18* *N.S*	*n = 3* *r^2 = 0.99* *Slope =-0.38* *N.S*	*n = 3* *r^2 = 0.52* *Slope =-0.185* *N.S*	n = 3 r^2 = 0.99 Slope = -0.44 -0.59, -0.29	*n = 3* *r^2 = 0.92* *Slope =0.065* *N.S*	*n = 3* *r^2 = 0.86* *Slope =-0.13* *N.S*	N.S.	*n = 3* *r^2 = 0.99* *Slope =-0.19* *N.S*

Table 6.20 - Log-Linear Regression Between HBA and Biologically Relevant/Systemic PK Variables of TRP

	f_u	Log (Vd_{ss}^u) [l/kg]	Log (CL_{tot}^u) [ml/min/kg]	Log (CL_{ren}^u) [ml/min/kg]	Log (CL_{nonren}^u) [ml/min/kg]	Log (Vd_{ss}) [l/kg]	Log (CL_{tot}) [ml/min/kg]	Log (CL_{ren}) [ml/min/kg]	Log (CL_{nonren}) [ml/min/kg]
All TRP	N.S.	*n = 7* *r^2 = 0.33* *Slope = -0.37* *N.S*	N.S	*n = 7* *r^2 = 0.48* *Slope = 0.34* *N.S*	N.S	n = 8 r^2 = 0.73 Slope = -0.079 -0.13, -0.031	N.S	n = 7 r^2 = 0.87 Slope = 0.59 0.32, 0.85	*n = 7* *r^2 = 0.41* *Slope = 0.39* *N.S*
Only MAO Substrates	N.S.	N.S	N.S	N.S	N.S	N.S	N.S	N.S	N.S
Only Non-MAO Substrates	N.S.	N.S	N.S	*n = 3* *r^2 = 0.67* *Slope = 0.56* *N.S*	N.S	N.S	N.S	*n = 3* *r^2 = 0.75* *Slope = 0.45* *N.S*	N.S.

Table 6.21 - Linear Regression Between MW and PD Variables of TRP

	[^{3}H] Eletriptan	**[^{3}H] Sumatriptan**	**[^{3}H] Eletriptan**	**[^{3}H] Sumatriptan**
All TRP	N.S.	N.S.	N.S.	N.S.
Only MAO Substrates	N.S.	*n = 4* *r^2 = 0.72* *Slope = 0.13* *N.S.*	*n = 4* *r^2 = 0.52* *Slope = 0.082* *N.S.*	*n = 4* *r^2 = 0.53* *Slope = 0.088* *N.S.*
Only Non-MAO Substrates	N.S.	N.S.	N.S.	N.S.

Table 6.22 - Linear Regression Between Log$D_{7.4}$ and PD Variables of TRP

	[^{3}H] Eletriptan	**[^{3}H] Sumatriptan**	**[^{3}H] Eletriptan**	**[^{3}H] Sumatriptan**
All TRP	N.S.	N.S.	N.S.	N.S.
Only MAO Substrates	N.S.	N.S.	N.S.	N.S.
Only Non-MAO Substrates	N.S.	N.S.	N.S.	N.S.

Table 6.23 - Linear Regression Between HBD and PD Variables of TRP

	[^{3}H] Eletriptan	[^{3}H] Sumatriptan	[^{3}H] Eletriptan	[^{3}H] Sumatriptan
All TRP	N.S.	N.S.	N.S.	N.S.
Only MAO Substrates	N.S.	N.S.	N.S.	N.S.
Only Non-MAO Substrates	N.S.	N.S.	N.S.	N.S.

Table 6.24 - Linear Regression Between HBA and PD Variables of TRP

	[^{3}H] Eletriptan	[^{3}H] Sumatriptan	[^{3}H] Eletriptan	[^{3}H] Sumatriptan
All TRP	N.S.	N.S.	*n = 7* *r^2 = 0.39* *Slope = 7.7* *N.S.*	N.S.
Only MAO Substrates	N.S.	N.S.	N.S.	N.S.
Only Non-MAO Substrates	*n = 3* *r^2 = 0.99* *Slope = 21.8* *N.S.*	n = 3 r^2 = 0.99 Slope = 10.7 6.8, 14.7	n = 3 r^2 = 0.99 Slope = 16.7 11.0, 22.5	n = 3 r^2 = 0.99 Slope = 10.1 4.6, 15.6

Table 6.25 - Final QSPKR Models for TRP

Final QSPKR Model	N	Slope (95% CI)	r^2	q^2
f_u = 2.3 - 0.0054 * MW	7	-0.0054 (-0.0088, -0.0022)	0.78	**0.59**
Log (Vd_{ss}^u) = - 0.89 + 0.0050 * MW	7	0.0050 (0.00015, 0.0010)	0.58	-0.11
Log (CL_{tot}^u) = - 0.58 + 0.0058 * MW	7	0.0058 (0.00085, 0.010)	0.65	0.18
Log (CL_{nonren}^u) = - 0.93 + 0.0064 * MW	7	0.0064 (0.00021, 0.013)	0.58	0.11

$q^2 \geq 0.40$: Acceptable

Figure 6.3 - f_u vs. MW for TRP

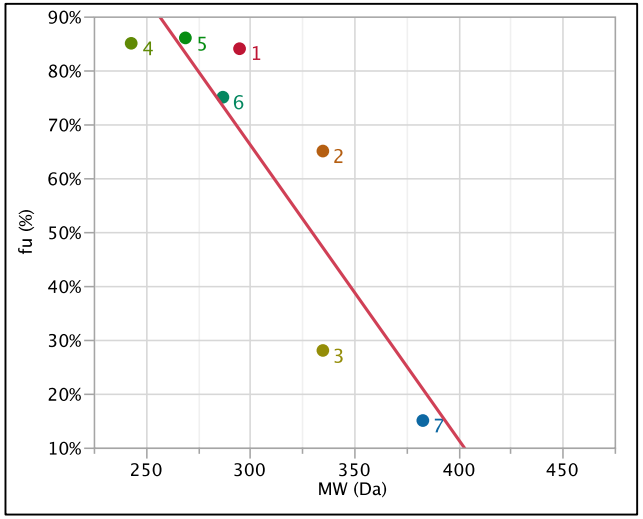

Figure 6.4 - Vd_{ss}^{u} vs. MW for TRP

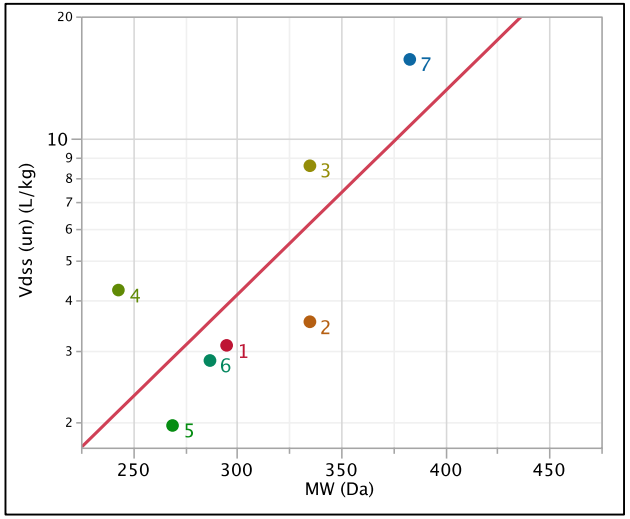

Figure 6.5 - CL_{tot}^{u} vs. MW for TRP

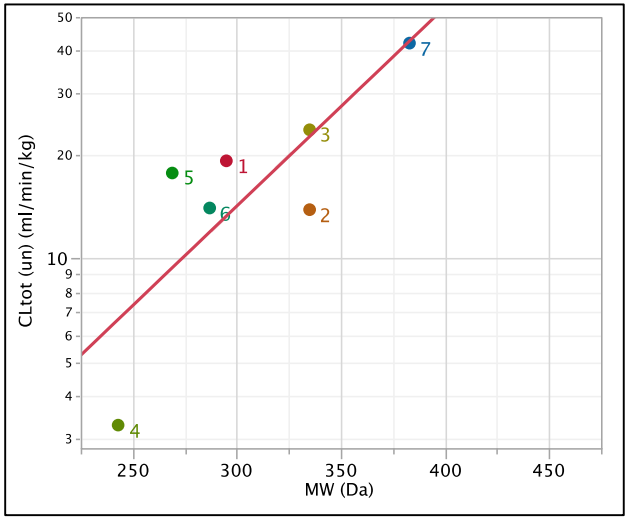

Figure 6.6 - CL_{nonren}^{u} vs. MW for TRP

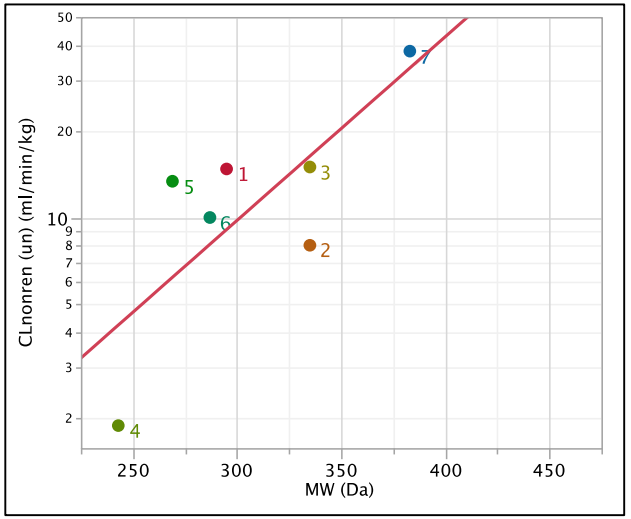

(Please refer Table 6.1 in Page 91, for the list of the individual compounds labeled in the figures 6.3 - 6.6)

Figure 6.7 - CL_{tot}^{u} vs. HBD for TRP

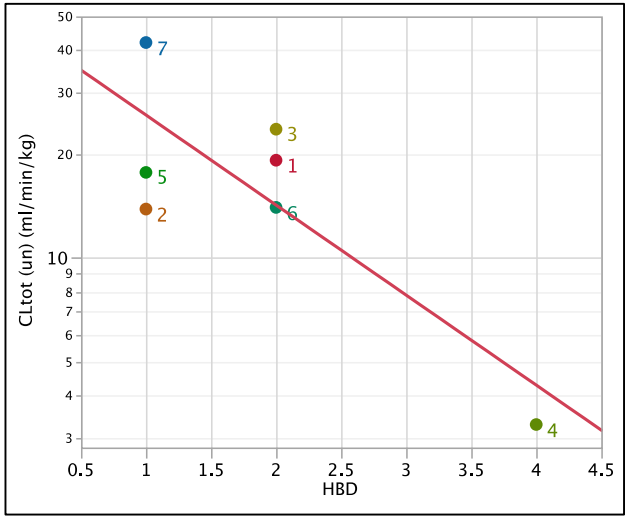

Figure 6.8 - CL_{tot}^{u} vs. HBD for TRP

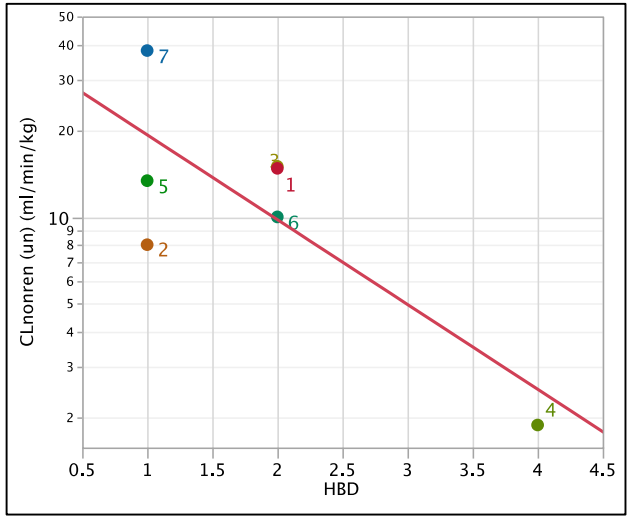

(Please refer Table 6.1 in Page 91, for the list of the individual compounds labeled in the figures 6.7 and 6.8)

Figure 6.9- CL_{nonren}^{u} vs. MW for TRP - MAO Substrates

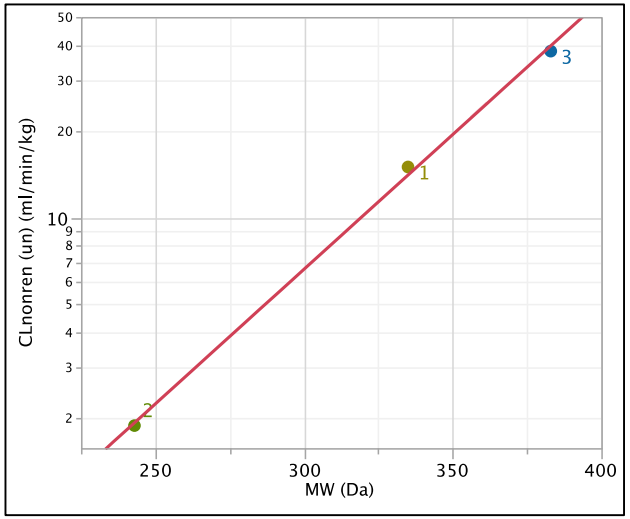

Figure 6.10 - CL_{nonren}^{u} vs. HBD for TRP - MAO Substrates

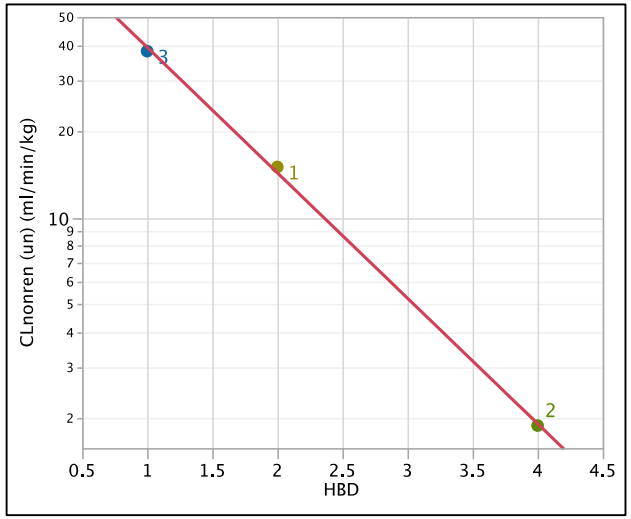

(Please refer Table 6.2 in Page 92, for the list of the individual compounds labeled in the figures 6.9 and 6.10)

6.3. Discussion

Structurally, TRP in the dataset show 5-hydroxy-tryptamine scaffold and exhibit low diversity (2- to 4- fold, n = 8) in their PC/molecular property space. They are relatively low MW (ranging from 243 to 459 Da, n = 8) hydrophilic bases, i.e., $logD_{7.4} < 1.0$ (ranging from 0.22 to -2.08, n = 8) and are (single) positively charged (~99% ionized for all TRP except avitriptan, which is 60% ionized). When they are classified based on MAO substrate status, although their respective PC/molecular property spaces overlap, MAO-substrates seem to be relatively more homogenous than the non-MOA substrates.

Most of the TRP in the dataset are not extensively PPB, and Vd_{ss}^{u} estimates suggest moderate extravascular distribution into tissues and/or binding to plasma membranes etc. High Vd_{ss}^{u} values are offset by high PPB resulting in lower Vd_{ss} values, suggesting that their distribution is restricted by PPB. CL_{ren}^{u} values for the available TRP in the dataset (except frovatriptan) suggest net tubular secretion, potentially involving drug transporters. Known pathways that encompass CL_{nonren} include hepatobiliary excretion and metabolism via enzymes e.g., CYP3A, 1A2 (and 2D6) and by MAO, which is present both hepatically and extra-hepatically. When they are classified based on MAO substrate status, although their respective PK/PD property spaces overlap, TRP that are MAO-substrates seem to be relatively more homogenous than the non-MOA substrates (except for CL_{nonren}). Based on the available *in-vivo* drug - drug interaction studies (i.e., in the presence of moclobemide, a MAO inhibitor), oral bioavailability studies and mass balance studies, the rank order for the contribution of MAO-mediated metabolic clearance towards the CL_{nonren} for MAO substrates is rizatriptan > almotriptan > zolmitriptan.

Overall, there is low to considerable diversity in the *in-vitro/in-vivo* systemic and biologically relevant PK/PD properties of TRP in the current dataset with available information, ranges from 3- to 21-fold (n = 7-8).

MW (which is highly correlated with $logD_{7.4}$) is found to be the important determinant affecting biologically relevant systemic PK properties, namely f_u, Vd_{ss}^u, CL_{tot}^u and CL_{nonren}^u. A significant negative association is observed between f_u and MW for TRP in the current dataset. A similar trend was observed between *in-vitro* PPB of diverse set of 2939 molecules in the GSK database[22]. Vd_{ss}^u of TRP in the current dataset show a significant positive association with MW. Similar positive trends were observed between Vd_{ss}^u and MV for cephalosporins[87]. Owing to the offsetting effects of MW on f_u and Vd_{ss}^u, Vd_{ss} did not show any relationship with MW. CL_{tot}^u and CL_{nonren}^u show a significant association with MW for TRP (comprehensively), and the slopes are quite similar, suggesting that the latter non-renal clearance drives the relationship for the total clearance. Furthermore, the slope of CL_{nonren}^u of non-MAO substrates with MW is comparable and seems to drive the comprehensive TRP CL_{nonren}^u relationship.

Cheng et al[88] carried out *in-vitro* OATP1A2-mediated uptake studies using six TRP, four of which are MAO substrates and the other two are not. In order to assess if hepatic excretion of TRP is dependent on OATP1A2-mediated uptake, CL_{nonren}^u values from the present work showed no (statistically significant, $p < 0.05$) relationship with the experimentally determined *in-vitro* OATP1A2-mediated uptake rates. This suggests that OATP1A2 may not be the primary route for cellular uptake for TRP.

So overall, MW (which is highly correlated with lipophilicity) is found to be the major determinant affecting the systemic disposition of (small MW, hydrophilic) TRP suggesting that they may be involved in more specific interactions with biological membranes, tissues, drug

metabolizing enzymes, both hepatic (e.g., CYP3A and extrahepatically (e.g., MAO), potentially involving drug transporters. Final QSPKR models gave acceptable predictions for f_u.

On the contrary, as evident from SAR studies, the receptor binding (PD) interactions encompass diverse interactions ranging from non-specific hydrogen bonding, ionic to more specific steric forces.

CHAPTER 7. QSPKR of Class III Anti-Arrhythmic Agents

7.1. Background

Cardiac arrhythmias result from abnormalities in the generation and/or conduction of impulses in the myocardium or pacemakers/conducting tissue and if untreated can prove to be fatal. AAR are classified broadly into four classes based on the mechanism of action[89,90]:

1. Class I AAR act by blocking voltage-sensitive sodium (Na^+) channels. They are further categorized depending on their effect on the cardiac action potential duration (APD) and the kinetics of Na^+ channel blockade:
   A. Class IA AAR prolong the APD by slowing phase 0 depolarization and dissociate from the channels with intermediate kinetics.
   B. Class IB AAR shorten the APD by shortening phase 3 repolarization and dissociate from the channels with rapid kinetics.
   C. Class IC AAR slow the phase 0 depolarization markedly but have minimal effects on the APD and dissociate from the channels with slow kinetics.
2. Class II AAR act by blocking β-adrenergic receptors and inhibiting the phase 4 depolarization in the SA and AV nodes.
3. Class III AAR act by blocking (delayed rectifier) potassium (K^+) channels and prolonging phase 3 repolarization (and thus APD, too).

4. Class IV AAR act by blocking calcium (Ca^{+}) channels and inhibiting the action potentials in SA and AV nodes.

Structure activity studies on the molecules of class III AAR[91,92] indicate that binding to K^{+} channels is characterized by the presence of a protonated nitrogen linked with two or three hydrophobic and/or aromatic moieties (with hydrogen bonding abilities). The charge of the N-atom is known to have a strong influence on the potency of the binding and is involved in hydrogen-bonding interaction[93]. The para-substituents of phenyl rings are involved in polar interactions, and the rank order of potency (of binding) was found to be nitro < chlorine < amine < amide. The ethyl group(s) attached to protonated N-atom are involved in hydrophobic interactions in the central cavity of K^{+} channels[94]. By study analogues of dofetilide, it was also found that the methanesulfonamide moieties (which are also present in ibutilide and sotalol) are involved in hydrogen bonding interactions[95].

Sotalol

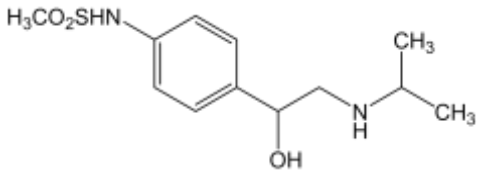

Dofetilide

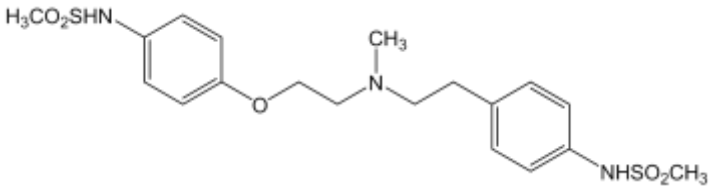

Ibutilide

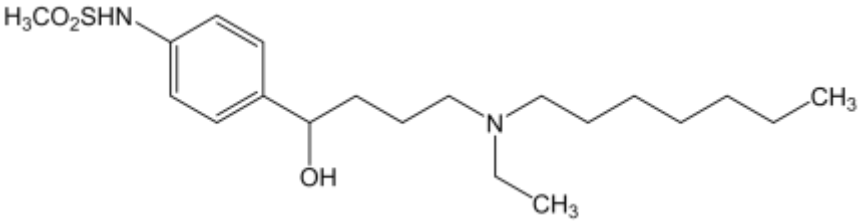

Bretylium

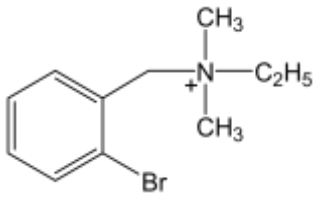

Amiodarone

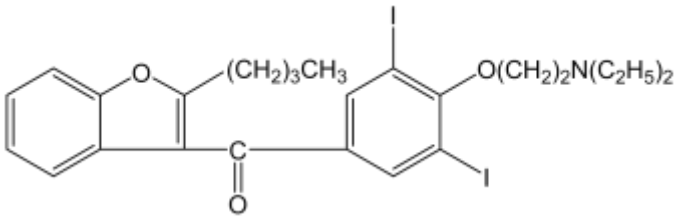

Dronedarone

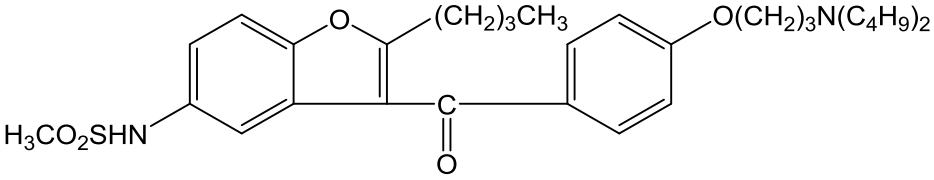

7.2. Results

7.2.1. PC/Molecular and Humans Systemic PK Property Space of Class III AAR

The final PC/molecular and human systemic PK database consisted of seven drugs that are/have been used clinically for treating arrhythmias. While bretylium[96] and sotalol[97] show both class II and III activity, dofetilide[98] and ibutilide[99] are selective class III drugs. Amiodarone[100] and dronedarone[101] (a derivative of desethyl metabolite of amiodarone) show broad spectrum (class I - IV) antiarrhythmic properties. The drugs included in the final database have been approved by US FDA for therapeutic use in the US and have also widely used over the past several decades.

The class III AAR in the final database represent quite a heterogeneous molecular/PC property space (Table - 7.1). Sotalol, dofetilide and ibutilide share a similar structural scaffold, while dronedarone is structurally related to amiodarone. Overall, they show relatively low to intermediate MW (243 - 645 Da). Sotalol has a low MW (272 Da) and is the least lipophilic ($logD_{7.4}$ = -1.7), while amiodarone and dronedarone have high MW (645, 559 Da respectively) and are the most lipophilic drugs in the final database ($logD_{7.4}$ = 5.9 and 5.8 respectively).

Although few of the drugs in the current dataset have two pK_as, $pK_{a2,}$ i.e., due to a basic (e.g., -NH_2) group, is the only relevant one for all the drugs in the database at the physiological pH of 7.4. Consequently, all the drugs in the database are almost entirely ionized, i.e., positively charged at physiologically relevant pH of 7.4. Ibutilide, azimilide, amiodarone and dronedarone exist at ≥ 70% as cationic species at pH of 7.4; however, all of them are lipophilic with $logD_{7.4}$ > 1.0, possibly owing to the presence of large aromatic and/or aliphatic functional groups (as evident from their higher MW relative to the more hydrophilic drugs in the database). Furthermore, the impact of the ionization on the estimated $logD_{7.4}$ is evident from their

(consistently) low values relative to the SciFinder-predicted logP, and this is more pronounced for hydrophilic drugs in the database. SciFinder-reported values for all the PC properties of Bretylium, except PSA and MV.

Descriptive statistics (Table 7.2) show that, for most of the molecular/PC properties, except $logD_{7.4}$, mean and median values were comparable. The wide dispersion (high standard deviations) is indicative of their diverse molecular/PC property space. Based on the acceptance criteria set *a-priori* for collinearity, (i.e., $r \geq 0.80$), MW is highly correlated with $logD_{7.4}$, MV and HBD; $logD_{7.4}$ with MV and HBD; PSA with MV and HBA; and MV with HBD (shown in Table 7.3). Thus, only $logD_{7.4}$ (and MW, just for the purpose of comparison), nRot and HBA were used for subsequent analysis.

Table 7.1 - Molecular/PC Properties of Class III AAR

	Drug	MW (Da)	logP	pK_{a1}	pK_{a2}	$LogD_{7.4}$	% Ionized at pH 7.4	Charge at pH 7.4	% Ionized at pH 6.3	Charge at pH 6.3	PSA (A^2)	MV (cm^3/ mol)	nRot	HBD	HBA
1	Sotalol	272	0.24	8.3	9.3	-1.68	99%	C	100%	C	87	220	6	3	5
2	Dofetilide	442	1.38	9.0	8.3	0.45	88%	C	99%	C	122	328	9	2	8
3	Ibutilide	385	3.72	8.5	9.9	1.17	100%	C	100%	C	78	350	14	2	5
4	Azimilide	458	3.33		7.7	2.84	68%	C	96%	C	73	346	8	0	8
5	Amiodarone	645	7.82		9.4	5.85	99%	C	100%	C	43	408	11	0	4
6	Dronedarone	557	7.98	7.4	9.4	5.94	99%	C	100%	C	97	487	17	1	7
7	Bretylium	243	-1.17			-1.17	100%	C	100%	C			3	0	1
	N	7	7	4	6	7					6	6	7	7	7
	Mean	429	3.3	8.3	9.0	1.9					83	357	10	1	5
	Maximum	645	8.0	9.0	10.0	5.9					122	487	17	3	8
	Minimum	243	-1.2	7.4	7.7	-1.7					43	220	3	0	1
	-fold range	3	9	1	1	8					3	2	6		8

C - Cationic

Table 7.2 - Descriptive Statistics of PC/Molecular Properties of Class III AAR

	N	Mean	SD	95% CI	Minimum	10%	25%	Median	75%	90%	Maximum
MW (Da)	7	**429**	145	295, 563	243	243	272	**442**	557	645	645
$LogD_{7.4}$	7	**1.9**	3.1	-1.0, 4.8	-1.7	-1.7	-1.2	**-1.2**	5.9	5.9	5.9
PSA (A^2)	6	**83**	26	56, 111	43	43	66	**83**	103	122	122
MV (cm^3/mol)	6	**357**	89	263, 450	220	220	301	**348**	428	487	487
nRot	7	**10**	5	5.3, 14.1	3	3	3	**9**	14	17	17
HBA	7	**5**	2.5	3.1, 7.7	1	1	4	**5**	8	8	8
HBD	7	**1**	1.2	0.020, 2.3	0	0	0	**1**	2	3	3

Table 7.3 - Correlation Matrix of PC/Molecular Variables of Class III AAR

	MW (Da)	$LogD_{7.4}$	PSA (A^2)	MV (cm^3/mol)	nRot	HBD	HBA
MW (Da)	1.00						
$LogD_{7.4}$	0.98	1.00					
PSA (A^2)	0.70	0.71	1.00				
MV (cm^3/mol)	0.92	0.95	0.88	1.00			
nRot	-0.25	-0.24	-0.49	-0.38	1.00		
HBD	-0.90	-0.93	-0.76	-0.94	0.54	1.00	
HBA	0.62	0.63	0.86	0.74	-0.33	-0.66	1.00

The final *in-vitro* f_u and *in-vivo* human systemic PK variables compiled from various studies in the literature are shown in Table - 7.4 and the corresponding estimated biologically relevant PK variables are shown in Table 7.5. There was considerable to large diversity in the *in-vitro* f_u (99-fold), *in-vivo* PK variables, namely, Vd_{ss} (50-fold), CL_{tot} (15-fold), CL_{ren} (351-fold) and CL_{nonren} (66-fold). After correcting for PPB, the biologically relevant PK variables showed relatively higher mean values and larger diversity (except CL_{ren}^{u}) compared to their respective uncorrected counterparts, e.g., Vd_{ss}^{u} (1650-fold), CL_{tot}^{u} (1500-fold) and CL_{nonren}^{u} (6522-fold) suggesting that class III ARR, on an average, show PPB-restricted distribution and clearance pathways (both total and nonrenal).

PPB of class III AAR in the current dataset varied from 1% to 99%, with the lipophilic drugs showing low f_u values, e.g., dronedarone (f_u = 1%, $logD_{7.4}$ = 5.9), amiodarone (f_u = 3%, $logD_{7.4}$ = 5.8) and azimilide (f_u = 6%, $logD_{7.4}$ = 2.8), while the hydrophilic drugs show high f_u values, e.g., sotalol (f_u = 99%, $logD_{7.4}$ = -1.7) and bretylium (f_u = 97%, $logD_{7.4}$ = -1.2). Vd_{ss}^{u} estimates for all the drugs in the database exceeded the BW, indicating moderate to extensive extravascular tissue distribution, potential binding to cell surface membranes etc., with the lipophilic drugs (dronedarone Vd_{ss}^{u} = 2000 L/kg) showing several fold higher values compared to the hydrophilic ones (sotalol Vd_{ss}^{u} = 1.2 L/kg). Also, the lipophilic drugs in the final database (with $logD_{7.4}$ > 1.0) showed f_e values $\leq$ 10%, suggesting they are highly metabolized, while renal clearance seems to be the major pathway ($f_e \geq 50\%$) of elimination for the more hydrophilic drugs ($logD_{7.4}$ < 1.0). The CL_{ren}^{u} value for amiodarone was less than GFR suggesting (a) it may have low glomerular filtration, potentially due to its large MW and/or high PPB or (b) it may undergo net tubular reabsorption potentially due to its lipophilic nature. Sotalol shows CL_{ren}^{u} value that is comparable to GFR suggesting that is excreted by net glomerular filtration. Dofetilide and

bretylium have CL_{ren}^{u} values that approach RPF, indicating that they undergo significant net renal tubular secretion. Both these drugs are hydrophilic, and are ≥ 90% positively charged at physiological pH of 7.4 (plasma) and 6.3 (urine), suggesting a potential role of the organic cationic transport (OCT) system. While dofetilide[102,103] is known to be a substrate for OCTs and is contraindicated with OCT inhibitors such as cimetidine, ketoconazole, trimethoprim, megestrol etc., there is no literature on the renal disposition of bretylium. Ibutilide and azimilide have CL_{ren}^{u} values greater than GFR, indicating that they are excreted by net tubular secretion, potentially involving OCTs.

Except for ibutilide and dronedarone, the rest of the drugs in the database have CL_{nonren} values lower than LBF, suggesting they are all low ER_{hep} drugs. For the hydrophilic drugs, e.g., sotalol and bretylium, the PPB is negligible and; therefore, they are low ER_{hep} drugs owing to low hepatic CL_{int}, while the lipophilic drugs e.g., azimilide and amiodarone, show low ER_{hep} because they undergo PPB-restricted hepatic metabolism. CL_{nonren} values for ibutilide and dronedarone are greater than LBF, suggesting they undergo extra-hepatic clearance pathways. Ibutilide[104] is metabolized primarily by ω-oxidation and sequential β-oxidation of the hepatyl side chain, but no further metabolic mechanisms have been reported in the literature. Dronedarone[105,106] is reported to undergo extensive metabolism, mainly by CYP3A, but exact mechanism of the extra-hepatic pathways is not known.

Table 7.4 - *In-vitro* and *In-vivo* Human PK Systemic Properties of Class III AAR

	***In-vitro* PK Variable**	***In-vivo PK Variable***				
Drug	**f_u [%]**	**Vd_{ss} [l/kg]**	**CL_{tot} [ml/min/kg]**	**f_e [%]**	**CL_{ren} [ml/min/kg]**	**CL_{nonren} [ml/min/kg]**
Sotalol	99%	1.2	2.2	77%	1.7	0.51
Dofetilide	36%	3.4	5.3	52%	2.7	2.5
Ibutilide	60%	12	29	6%	1.7	27.3
Azimilide	6%	12	2.2	10%	0.21	2.0
Amiodarone	3%	59	2.5	1.0%	0.025	2.4
Dronedarone	1.0%	20	33	.	.	33.3
Bretylium	97%	7.2	11.3	76%	8.6	2.7
N	7	7	7	6	6	7
Mean	43%	16.4	12.3	37%	2.5	10.1
Maximum	99%	59.5	33	77%	8.6	33
Minimum	1.0%	1.2	2.2	1.0%	0.025	0.51
-fold range	99	50	15	77	351	66

Table 7.5 - Biologically Relevant *In-vivo* Human PK Variables of Class III AAR

Drug	**Vd_{ss}^{u} [l/kg]**	**CL_{tot}^{u} [ml/min/kg]**	**CL_{ren}^{u} [ml/min/kg]**	**CL_{nonren}^{u} [ml/min/kg]**
Sotalol	1.2	2.2	1.7	0.51
Dofetilide	9.4	15	7.6	7.0
Ibutilide	20	48	2.9	45
Azimilide	193	37	3.5	33
Amiodarone	1725	71	0.71	70
Dronedarone	2000	3333		3333
Bretylium	7.4	12	8.9	2.8
N	7	7	6	7
Mean	565.1	502.6	4.1	498.8
Maximum	2000.0	3333.3	8.9	3333.3
Minimum	1.2	2.2	0.71	0.51
-fold range	1650	1500	13	6522

Table 7.6 - Descriptive Statistics of Human Systemic PK Variables of Class III AAR

	N	Mean	SD	95% CI	Minimum	10%	25%	Median	75%	90%	Maximum
Vd_{ss} (L/kg)	7	**16**	20	-2.1, 35	1.2	1.2	3.4	**11.6**	20	59	59
CL_{tot} (ml/min/kg)	7	**12**	13	-0.093, 25	2.2	2.2	2.2	**5.3**	29	33	33
CL_{ren} (ml/min/kg)	6	**2.5**	3.2	-0.83, 5.8	0.020	0.020	0.15	**1.7**	4.2	8.6	8.6
CL_{nonren} (ml/min/kg)	7	**10**	14	-2.7, 23	0.50	0.50	2.0	**2.6**	27	33	33
f_u	7	**0.43**	0.43	0.034, 0.83	0.010	0.010	0.035	**0.36**	0.97	0.99	0.99
Vd_{ss}^u (L/kg)	7	**565**	892	-260, 1390	1.2	1.2	7.4	**20**	1725	2000	2000
CL_{tot}^u (ml/min/kg)	7	**502**	1247	-651, 1656	2.2	2.2	11.7	**36**	73	3333.3	3333
CL_{ren}^u (ml/min/kg)	6	**4.1**	3.3	0.67, 7.6	0.58	0.58	1.4	**3.1**	7.8	8.9	8.9
CL_{nonren}^u (ml/min/kg)	7	**499**	1249	-656, 1654	0.51	0.51	2.9	**33**	73	3333	3333

Table 7.7 - Correlation Analysis of Human Systemic PK Variables of Class III AAR

	Vd_{ss} (L/kg)	**CL_{tot} (ml/min/kg)**	**CL_{ren} (ml/min/kg)**	**CL_{nonren} (ml/min/kg)**	**f_u**	**Vd_{ss}^u (L/kg)**	**CL_{tot}^u (ml/min/kg)**	**CL_{ren}^u (ml/min/kg)**	**CL_{nonren}^u (ml/min/kg)**
Vd_{ss} (L/kg)	1.00								
CL_{tot} (ml/min/kg)	-0.07	1.00							
CL_{ren} (ml/min/kg)	-0.40	0.21	1.00						
CL_{nonren} (ml/min/kg)	0.02	0.98	-0.09	1.00					
f_u	-0.58	-0.12	0.68	-0.27	1.00				
Vd_{ss}^u (L/kg)	0.75	0.33	-0.43	0.43	-0.69	1.00			
CL_{tot}^u (ml/min/kg)	0.10	0.70	-0.54	0.74	-0.45	0.72	1.00		
CL_{ren}^u (ml/min/kg)	-0.54	0.10	0.83	-0.15	0.35	-0.55	-0.57	1.00	
CL_{nonren}^u (ml/min/kg)	0.10	0.70	-0.60	0.74	-0.45	0.72	1.00	-0.65	1.00

7.2.2. QSPKR Analysis, Model Building and Evaluation

The results of the univariate regression of the log-transformed *in-vivo* systemic and biologically relevant PK variables as a function of the molecular/PC descriptors are shown in Table 7.8. MW shows significant univariate relationship ($r^2 \geq 0.30$ and $p < 0.05$) with f_u, log (Vd_{ss}^u), log (CL_{nonren}^u), log (Vd_{ss}) and log (CL_{ren}) (Figures 7.1 - 7.5 respectively); while $logD_{7.4}$ is related with f_u, log (Vd_{ss}^u), log (CL_{tot}^u), log (CL_{nonren}^u), log (Vd_{ss}) and log (CL_{ren}) (Figures 7.6 - 7.11 respectively). Although MW and $logD_{7.4}$ are highly correlated ($r = 0.98$), univariate relationships for both these descriptors were presented for the purpose of comparing them with those obtained for other pharmacological classes (see Chapter 8). Only $logD_{7.4}$ was considered for further model building because it described greater variability in the biologically relevant as well as systemic PK variables. nRot shows significant univariate relationship with log (CL_{tot}^u), log (CL_{nonren}^u) and log (CL_{nonren}) (Figures 7.12 - 7.14, respectively). During the final (multivariate) model building process (using MLLR with forward inclusion followed by backward elimination), $logD_{7.4}$ was found to be the single most important determinant affecting biologically relevant systemic PK of Class III AAR, and the final models are summarized in Table 7.9. Overall, the final QSPKR models developed for Class III AAR gave acceptable predictions ($q^2 \geq 0.40$) for f_u, Vd_{ss}^u and CL_{nonren}^u

7.2.2.1. Effect of $LogD_{7.4}$

$LogD_{7.4}$ shows a significant positive association with f_u, log (Vd_{ss}^u), log (CL_{tot}^u), log (CL_{nonren}^u), log (Vd_{ss}), i.e., an increase in $logD_{7.4}$ is associated with increase in those PK variables; while a negative association is observed with log (CL_{ren}^u). Furthermore, it explains ≥ 70% variability in the biologically relevant PK variables (range: 70% for log CL_{tot}^u, n = 7 to 97% for log Vd_{ss}^u, n = 7) and ≥ 75% variability in the systemic PK. Despite the offsetting effects of $logD_{7.4}$ on f_u and

log (Vd_{ss}^{u}), there was still a positive association with uncorrected counterpart - log (Vd_{ss}). This might be due to the predominant effects of $logD_{7.4}$ on Vd_{ss}^{u} (especially for the lipophilic compounds, namely, azimilide, amiodarone and dronedarone) that drive the relationship with Vd_{ss} than that on f_u (although it offsets the trend, evident from statistically significant shallower slope relative to that obtained with log Vd_{ss}^{u}). On the other hand, due to the offsetting effects of $logD_{7.4}$ on f_u and CL_{tot}^{u}, and f_u and CL_{nonren}^{u}, their uncorrected counterparts, CL_{tot} and CL_{nonren}, respectively, did not depend on $logD_{7.4}$. Lastly, for the compounds in the final dataset, $logD_{7.4}$ did not show a significant relationship with log (CL_{ren}^{u}), but showed a negative association with log (CL_{ren}). Therefore, the (significant) relationship of $logD_{7.4}$ on log (CL_{nonren}^{u}) seem to drive those on log (CL_{tot}^{u}), as also evident from the high correlation (r = 1.00) between CL_{nonren}^{u} and CL_{tot}^{u}.

Table 7.8 - Log-Linear Regression Between PC/Molecular Descriptors and PK Variables of Class III AAR

	f_u	Log (Vd_{ss}^u) [l/kg]	Log (CL_{tot}^u) [ml/min/kg]	Log (CL_{ren}^u) [ml/min/kg]	Log (CL_{nonren}^u) [ml/min/kg]	Log (Vd_{ss}) [l/kg]	Log (CL_{tot}) [ml/min/kg]	Log (CL_{ren}) [ml/min/kg]	Log (CL_{nonren}) [ml/min/kg]
MW (Da)	n = 7 r^2 = 0.87 Slope = -0.0028 -0.0040, -0.0015	n = 7 r^2 = 0.81 Slope = 0.00078 0.0034, 0.012	*n =7* *r^2 = 0.47* *Slope = 0.0047* *N.S*	*n =6* *r^2 = 0.39* *Slope = -0.019* *N.S*	n = 7 r^2 = 0.57 Slope = 0.0064 0.000060, 0.013	n = 7 r^2 = 0.62 Slope = 0.0029 0.00027, 0.0056	N.S	n = 6 r^2 = 0.79 Slope = -0.0058 -0.010, -0.0017	N.S
LogD$_{7.4}$	n = 7 r^2 = 0.83 Slope = -0.13 -0.19, -0.061	n = 7 r^2 = 0.97 Slope = 0.39 0.32, 0.47	n = 7 r^2 = 0.71 Slope = 0.27 0.070, 0.46	*n =6* *r^2 = 0.43* *Slope = -0.10* *N.S*	n = 7 r^2 = 0.79 Slope = 0.35 0.14, 0.56	n = 7 r^2 = 0.74 Slope = 0.15 0.048, 0.25	N.S	n = 6 r^2 = 0.86 Slope = -0.32 -0.49, -0.14	N.S
nRot	*n = 7* *r^2 = 0.41* *Slope =-0.058* *N.S.*	*n = 7* *r^2 = 0.42* *Slope = 0.17* *N.S.*	n = 7 r^2 = 0.69 Slope = 0.17 0.040, 0.30	N.S.	n = 7 r^2 = 0.74 Slope = 0.22 0.074, 0.37	N.S.	*n = 7* *r^2 = 0.33* *Slope =0.062* *N.S.*	N.S.	n = 7 r^2 = 0.66 Slope = 0.11 0.018, 0.20
HBA	*n = 7* *r^2 = 0.37* *Slope =-0.10* *N.S.*	N.S.	N.S.	N.S.	N.S	N.S	N.S	N.S	N.S

In red: $p<0.05$ and $r^2 \geq 0.30$; *In italic and red*: *$r^2 \geq 0.30$ but $p>0.05$;* N.S = Not Significant ($p>0.05$ and $r^2 < 0.30$);

Table 7.9: Final QSPKR Models for Class III AAR

Final QSPKR Model	N	Slope (95% CI)	r^2	q^2
$f_u = 0.67 - 0.13 * LogD_{7.4}$	7	- 0.13 (-0.19, -0.061)	0.83	**0.71**
$Log\ (Vd_{ss}^{u}) = 0.97 + 0.39 * LogD_{7.4}$	7	0.39 (0.32, 0.47)	0.97	**0.94**
$Log\ (CL_{tot}^{u}) = 1.1 + 0.27 * LogD_{7.4}$	7	0.27 (0.070, 0.46)	0.71	0.21
$Log\ (CL_{nonren}^{u}) = 0.70 + 0.35 * LogD_{7.4}$	7	0.35 (0.14, 0.56)	0.79	**0.45**

$q^2 \geq 0.40$: Acceptable

Figure 7.1 - f_u vs. MW for Class III AAR

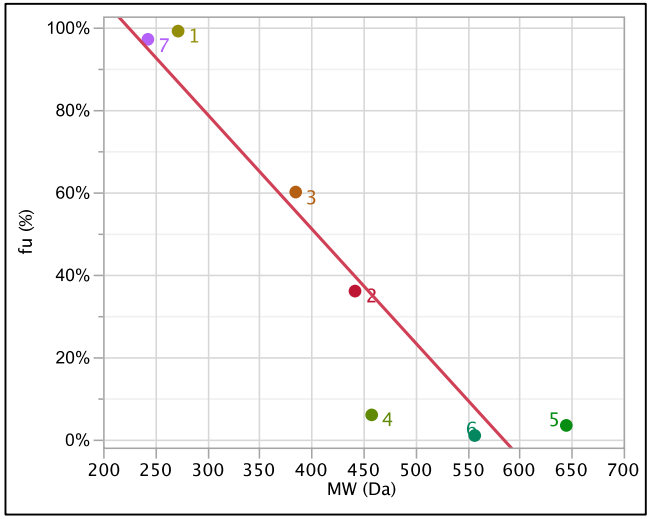

Figure 7.2 - Vd_{ss}^{u} vs. MW for Class III AAR

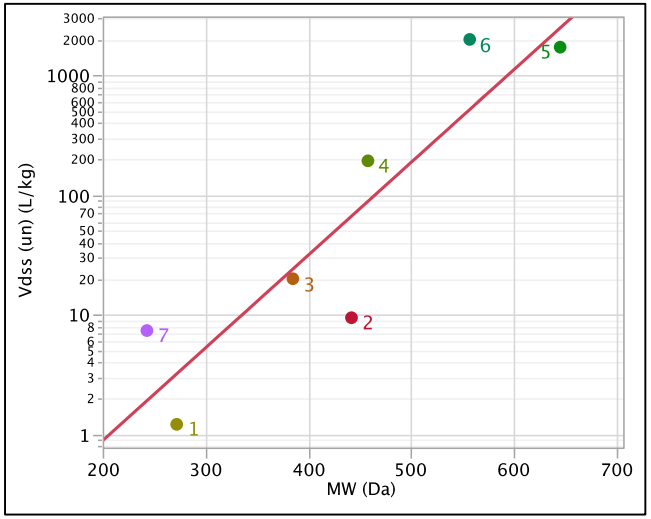

Figure 7.3 - CL_{nonren}^{u} vs. MW for Class III AAR

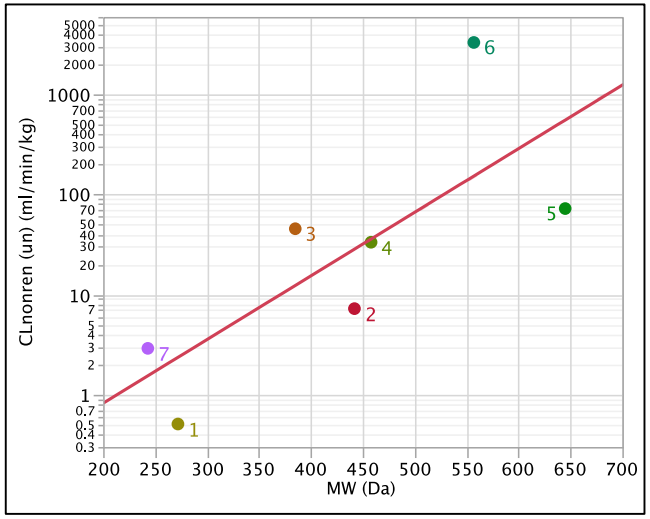

(Please refer Table 7.1 in Page 128, for the list of the individual compounds labeled in the figures 7.1 to 7.3)

Figure 7.4 - Vd_{ss} vs. MW for Class III AAR

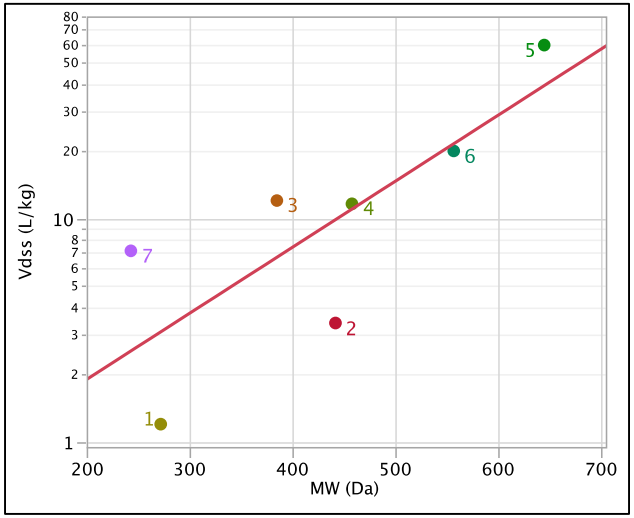

Figure 7.5 - CL_{ren} vs. MW for Class III AAR

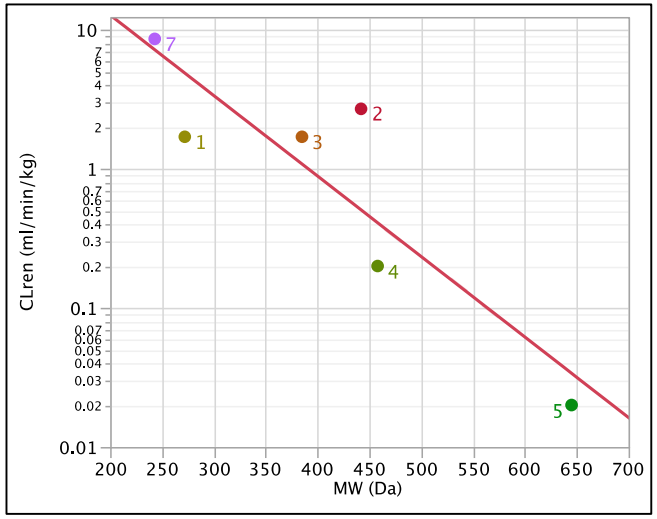

(Please refer Table 7.1 in Page 128, for the list of the individual compounds labeled in the figures 7.4 and 7.5)

Figure 7.6 - f_u vs. $logD_{7.4}$ for Class III AAR

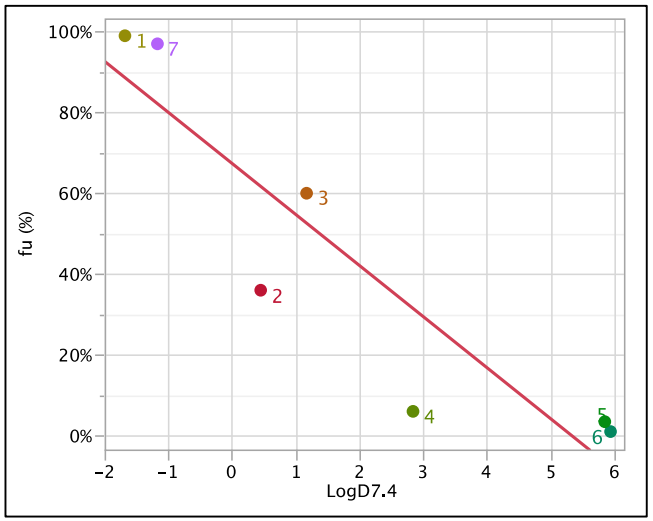

Figure 7.7 - Vd_{ss}^{u} vs. $logD_{7.4}$ for Class III AAR

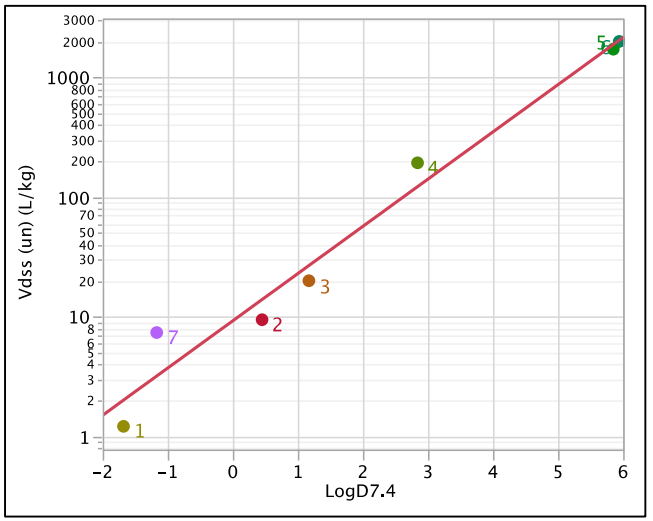

Figure 7.8 - CL_{tot}^{u} vs. $logD_{7.4}$ for Class III AAR

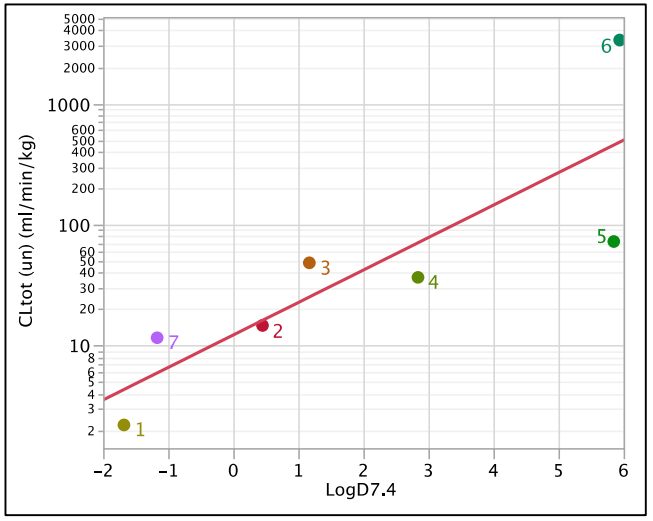

Figure 7.9 - CL_{nonren}^{u} vs. $logD_{7.4}$ for Class III AAR

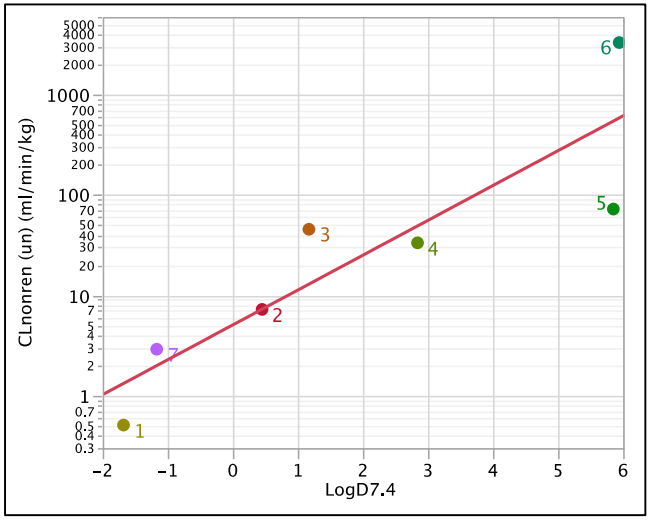

(Please refer Table 7.1 in Page 128, for the list of the individual compounds labeled in the figures 7.6 to 7.9)

Figure 7.10 - Vd_{ss}^{u} vs. $logD_{7.4}$ for Class III AAR

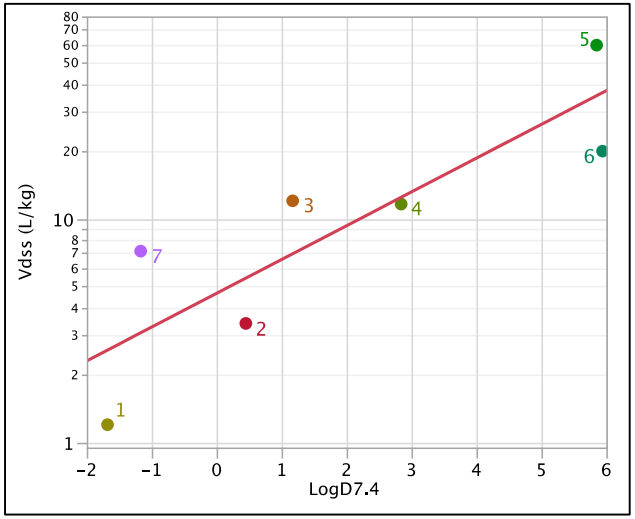

Figure 7.11 - CL_{ren} vs. $logD_{7.4}$ for Class III AAR

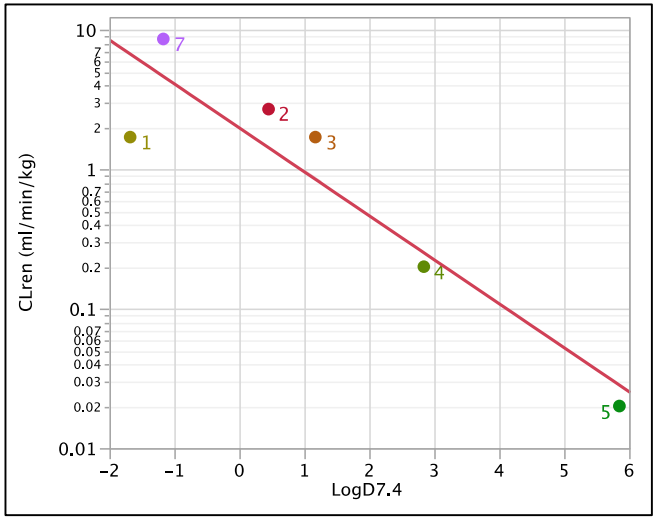

(Please refer Table 7.1 in Page 128, for the list of the individual compounds labeled in the figures 7.10 and 7.11)

Figure 7.12 - CL_{tot}^{u} vs. nRot for Class III AAR

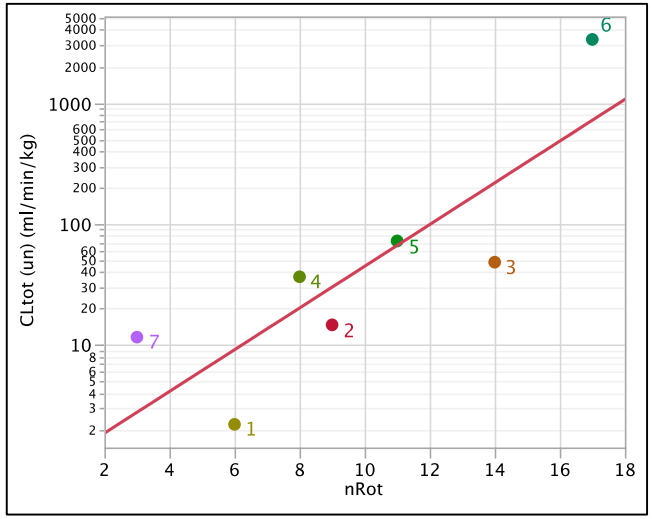

Figure 7.13 - CL_{nonren}^{u} vs. nRot for Class III AAR

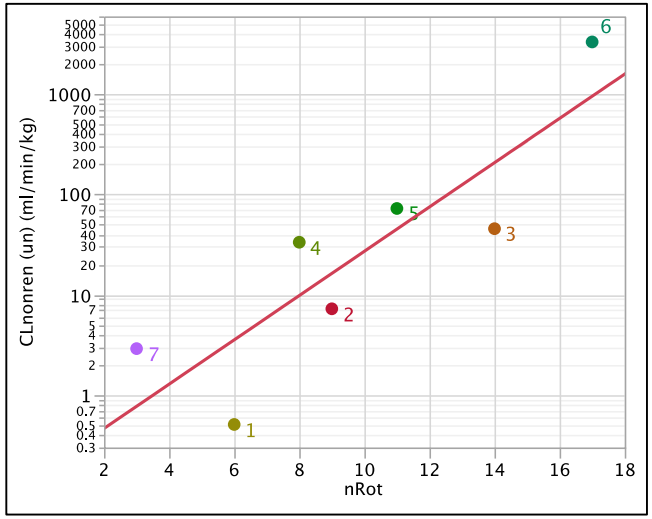

Figure 7.14 - CL_{nonren} vs. nRot for Class III AAR

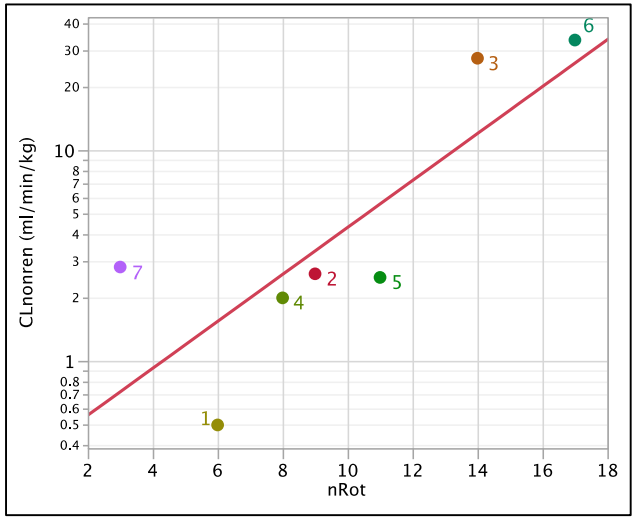

(Please refer Table 7.1 in Page 128, for the list of the individual compounds labeled in the figures 7.12 to 7.14)

7.3. Discussion

Few of the class III AAR in the final database share a similar structural scaffold (e.g., sotalol, dofetilide and ibutilide; amiodarone and dronedarone); however, they show very large diversity in the molecular/PC property space, e.g., MW ranged between 243 - 645 Da (3-fold, n = 7) and $logD_{7.4}$ ranged between -1.7 to 5.9 (8-fold, n = 7). All compounds in the final dataset are bases and predominantly (>70%) positively charged at physiological pH. They show an even larger diversity in the systemic PK (15- to 351-fold) and biologically relevant PK (13- to 6522-fold) variables. Vd_{ss} varies 50-fold, while f_u varies 99-fold across the compounds in the database. Vd_{ss}^u values (varies 1650-fold) were greater than BW, suggesting extensive extravascular distribution, which was counteracted by high PPB that led to lower values of Vd_{ss}. Except for ibutilide and dronedarone, the rest of the compounds in the database show CL_{nonren} values much lower LBF, suggesting that they are all low ER_{hep} drugs. Ibutilide[104] and dronedarone[105,106], on the other hand show CL_{nonren} values exceeding LBF suggesting they are subject to (not fully understood) extra-hepatic clearance pathways. The CL_{ren}^u values of compounds are also heterogeneous with values lower than GFR (e.g., amiodarone), suggesting (binding-) restricted filtration and/or net tubular reabsorption; approximating GFR suggesting net filtration (e.g., sotalol) and values greater than GFR suggesting net tubular reabsorption (dofetilide and bretylium approaching RPF, the former involving OCTs).

To characterize the large variability in the systemic and biologically relevant PK variables, the effect of molecular/PC descriptors were explored. Overall, $logD_{7.4}$ was found to be the most important determinant affecting biologically relevant PK properties, namely, f_u, Vd_{ss}^u, CL_{tot}^u and CL_{nonren}^u. Since, $logD_{7.4}$ is found to be highly correlated with MW, the trends observed by each of them cannot be distinguished. Non-specific hydrophobic interactions with plasma proteins

(potentially with α-acid glycoprotein, since they are all positively charged bases), seems to be a plausible explanation for the (significant) negative association of $logD_{7.4}$ with f_u. These findings are consistent with barbiturates in rats[68], β-adrenergic blockers in man[39,107], corticosteroids in man (in addition to polarizability)[40]. Obach et al[29] studied a heterogeneous dataset comprising of 554 drugs, and concluded that (non-specific) hydrophobic interactions with albumin and α-acid glycoprotein drive the negative trend of f_u as a function of $logD_{7.4}$.

Non-specific hydrophobic interactions with extravascular tissues/plasma membranes seem to be the plausible explanation for the (significant) positive association - of $logD_{7.4}$ with Vd_{ss}^u. PPB-restriction seems to lessen the Vd_{ss} values, and this is even more pronounced for highly PPB, lipophilic compounds. Furthermore, correction for the free fraction (i.e., PPB), increased the slope estimate for effect of $logD_{7.4}$ on Vd_{ss}^u. Although there was a reduction in that trend, there is still a positive association observed between $logD_{7.4}$ and Vd_{ss}, suggesting the predominant hydrophobic interactions with Vd_{ss}^u drive the relationships with Vd_{ss} as well. Similar trends were observed with Vd_{ss}^u of sulfonamides in rat[82] and β-adrenergic blockers in man[39] and heterogeneous dataset of 670 drugs (159 acids, 267 bases, 173 neutrals and 68 zwitterions).

Non-specific hydrophobic interactions with hepatic and possibly extrahepatic drug-metabolizing-enzymes seem to be plausible explanation for effect of $logD_{7.4}$ on CL_{nonren}^u. Ibutilide and dronedarone seem to have extra-hepatic clearance pathways and even with the exclusion of these drugs, the relationships of $logD_{7.4}$ with biologically relevant PK variables log CL_{tot}^u and log CL_{nonren}^u still hold true, with a slight improvement in the goodness of fit (r^2) but without any effect on the slope, suggesting that $logD_{7.4}$ is still the important determinant affecting the (unknown) extra-hepatic clearance pathways of those drugs in the same way as seen with hepatic clearance pathways.

A (significant) negative association is observed for CL_{ren} with $logD_{7.4}$ but there was no effect on CL_{ren}^{u}. This may be due to (a) large diversity in CL_{ren} (351-fold) vs. CL_{ren}^{u} (15-fold) and/or (b) from a mechanistic standpoint, all the drugs in the current dataset are positively charged at physiological pH of 7.4 and 6.3 - the hydrophilic compounds, e.g., dofetilide (for which CL_{ren}^{u} approaches RPF) undergo net tubular secretion possibly involving on the OCT system that don't depend on $logD_{7.4}$ but may rely on more specific molecular properties. On the other hand, the more lipophilic compounds, e.g., amiodarone show CL_{ren}^{u} values lower than GFR suggesting they undergo net tubular reabsorption, possibly by passive tubular reabsorption owing to their high degree of lipophilicity. Varma et al[23] reported a negative association of CL_{ren} with $logD_{7.4}$ for set of 391 compounds, while Hinderling et al[39] found a similar trend with β-adrenergic blockers in humans. Furthermore, van de Waterbeemd et al[108] found the relationship of CL_{ren}^{u} as a function of lipophilicity to be insignificant for β-adrenergic blockers in humans.

Overall, $logD_{7.4}$ was found to be the most important descriptor for predicting the biologically relevant PK variables of Class III AAR based on the compounds within the dataset. Thus, the disposition of these drugs depends on the hydrophobic interactions to pass through tissues/plasma membranes, hepatocytes and binding to drug metabolizing enzymes. The final QSPKR models gave acceptable predictions for f_u, Vd_{ss}^{u} and CL_{nonren}^{u}.

CHAPTER 8. OVERALL QSPKR DISCUSSION

8.1. Molecular/PC Property Space

8.1.1. BZD, NMB, TRP and Class III AAR

The distribution of the molecular/PC variables for BZD, NMB, TRP and Class III AAR is shown in Figures 8.1 - 8.7, and the ranges in these respective properties in Table - 8.1. BZD with their 5-aryl, 1, 4-benzodiazepine structural scaffold and TRP with 5-hydroxy-tryptamine scaffold, based on the substituents attached to the scaffold, show relatively small values in nRot, HBA, PSA and MV and little diversity. On the other hand, although, there are missing values for few compounds, NMB, are structurally diverse compounds with either an aminosteroid (ASN) nucleus, (n = 9) or with a benzylisoquinolinium (BIQ) nucleus, consisting of large, fused aromatic rings and, therefore, show higher values for nRot, HBA PSA and MV and greater diversity. Likewise, Class III AAR compounds are heterogeneous with large diversity in their molecular/PC properties. While BZD (271 - 412 Da, n = 20) and TRP (243 - 459 Da, n = 8) are relatively low MW compounds, Class III AAR (243 - 645 Da, n = 7) seem to be skewed towards intermediate - high MW, and a majority of NMB - with the exception of succinylcholine - are high MW compounds (290 - 1035 Da, n = 16). Similar trends, i.e., lower values for BZD and TRP (in general), while Class III AAR and NMB have higher values for MV, PSA and nRot, which is also evident from their high correlations with MW.

BZD in the database consist of both weakly acidic (n = 7) and weakly basic (n = 16), lipophilic compounds ($logD_{7.4}$ > 1.0, n = 19, except N-DMAD whose $logD_{7.4}$ is 0.75), and all of them are unionized at physiological pH of 7.4. In contrast, NMB (n = 16), TRP (n = 8) and Class III AAR (n = 7) are all weakly basic compounds, charged with either one (e.g., TRP, and Class III AAR) or two positive charges (e.g., NMB) at pH of 7.4. Furthermore, while TRP are hydrophilic ($logD_{7.4}$ < 1.0, n = 8); NMB ($logD_{7.4}$ ranges from -5.0 to 2.1, n = 16) and Class III AAR ($logD_{7.4}$ ranges from -1.7 to 5.9, n = 7) show a wide dispersion in the $logD_{7.4}$ values, consisting of a combination of hydrophilic as well as lipophilic compounds (despite being positively charged, possibly because of their large aromatic functional groups).

Figure 8.1 - MW Distribution By Pharmacological Class

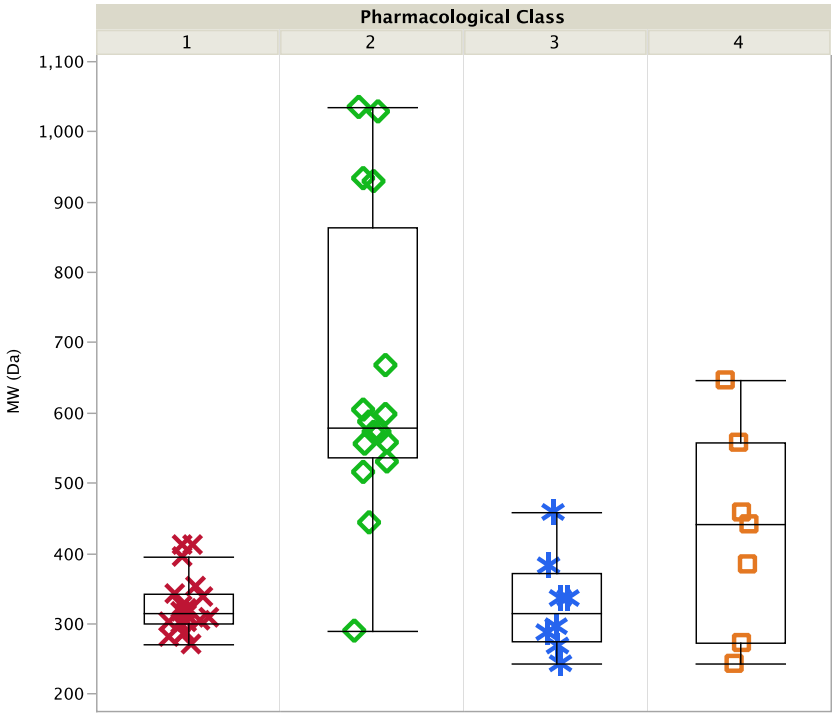

Figure 8.2 - LogD$_{7.4}$ Distribution By Pharmacological Class

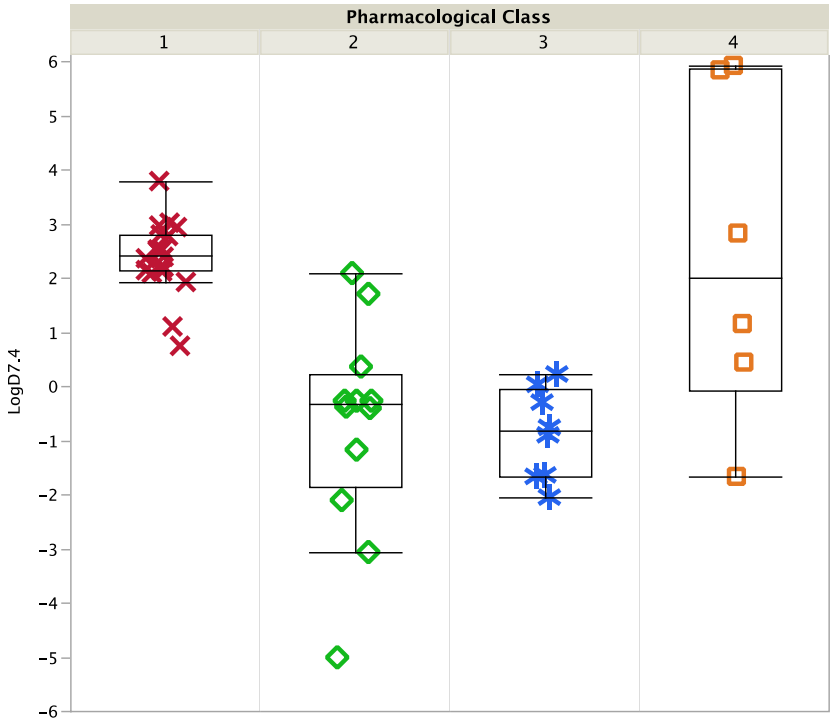

1 - BZD (X); 2 - NMB (◊); 3 - TRP (*) and 4 - Class III AAR (□)

Figure 8.3 - PSA Distribution By Pharmacological Class

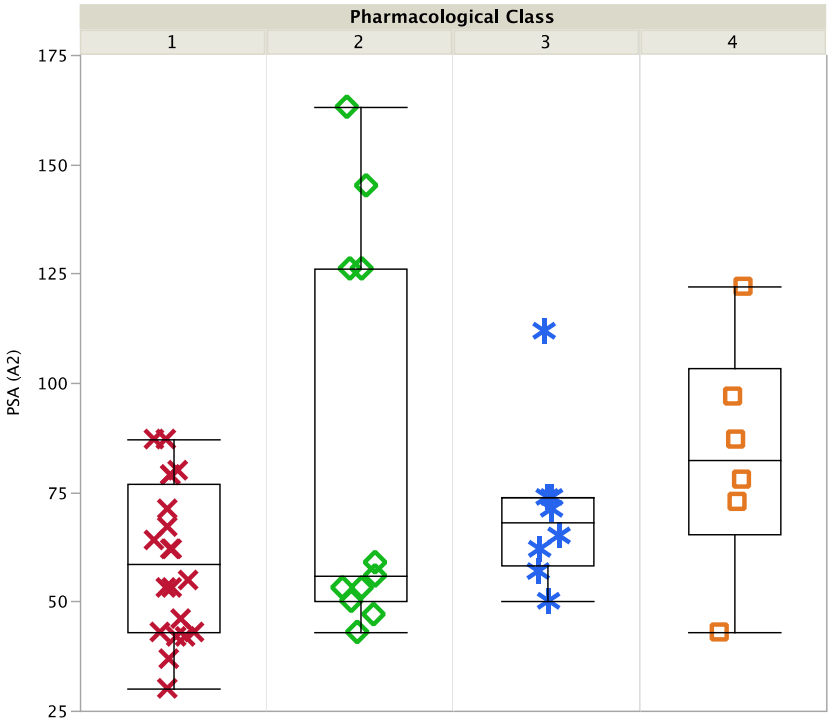

Figure 8.4 - nRot Distribution By Pharmacological Class

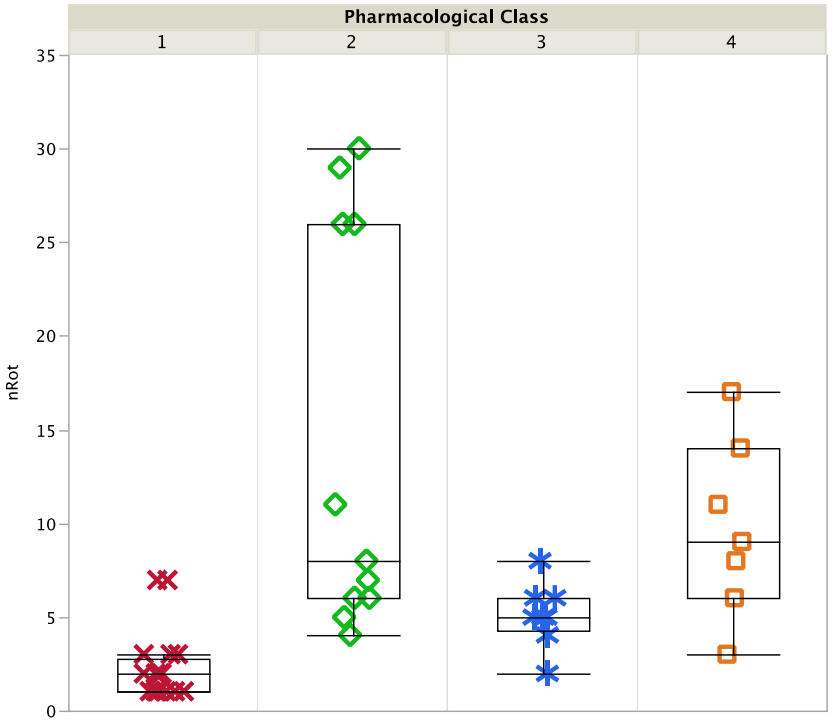

1 - BZD (X); 2 - NMB (◊); 3 - TRP (*) and 4 - Class III AAR (□)

Figure 8.5 - HBA Distribution By Pharmacological Class

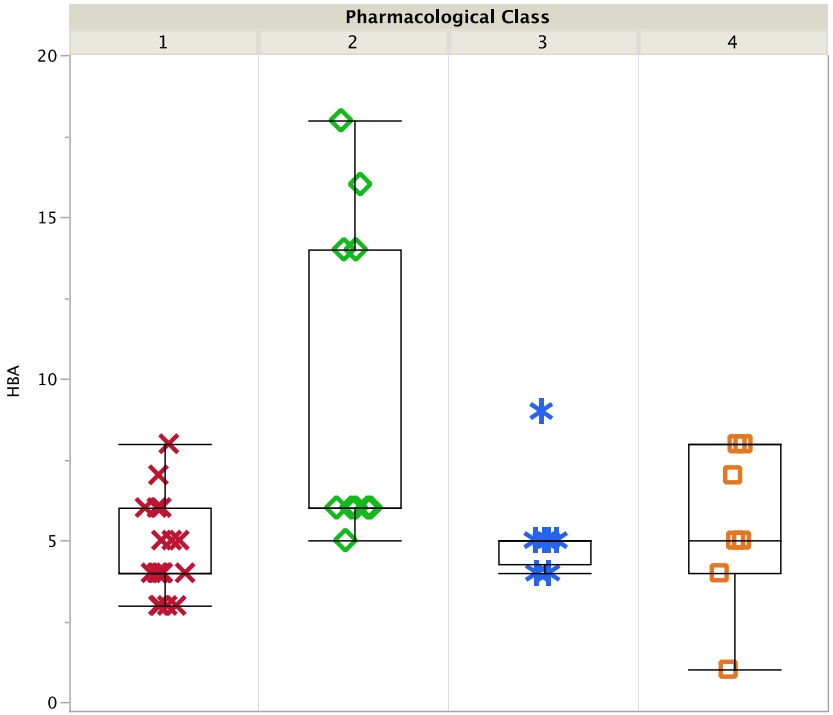

Figure 8.6 - HBD - Distribution By Pharmacological Class

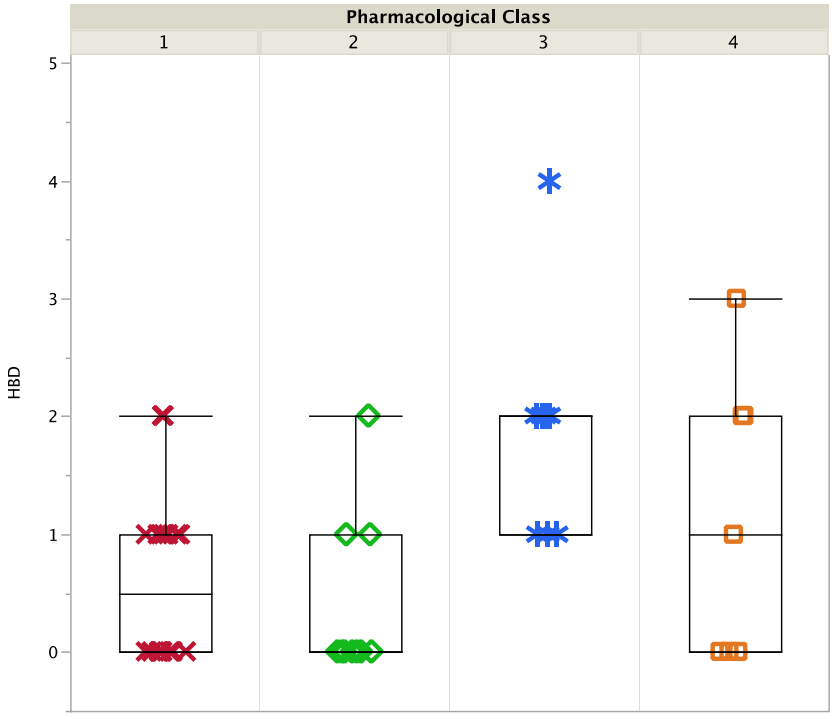

1 - BZD (X); 2 - NMB (◊); 3 - TRP (*) and 4 - Class III AAR (□)

Figure 8.7 - MV Distribution by Pharmacological Class

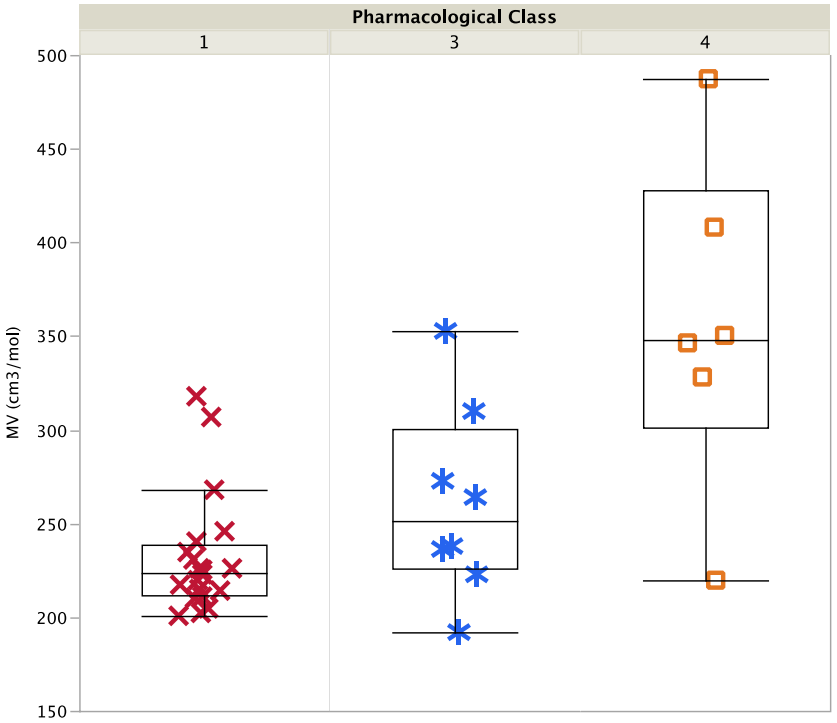

1 - BZD (X); 3 - TRP (*) and 4 - Class III AAR (□)

Table 8.1 - Molecular/PC Property Space of BZD, NMB, TRP and Class III AAR

PC Property	BZD (n)	NMB (n)	TRP (n)	Class III AAR (n)
MW (Da)	271 - 412 (20)	290 - 1035 (16)	243 - 459 (8)	243 - 645 (7)
$LogD_{7.4}$	0.75 to 3.8 (20)	-5.0 to 2.1 (12)	-2.1 to 0.22 (8)	-1.7 to 5.9 (7)
nRot	1.0 - 7.0 (20)	4.0 - 30 (11)	2.0 - 8.0 (8)	3.0 - 17 (7)
HBA	3.0 - 8.0 (20)	5.0 - 18 (11)	4.0 - 9.0 (8)	1.0 - 8.0 (7)
HBD	0 - 2.0 (20)	0 - 2.0 (11)	1.0 - 4.0 (8)	0 - 3.0 (7)
PSA (A^2)	30 - 87 (20)	43 - 163 (11)	50 - 112 (8)	43 - 122 (6)
MV (cm^3/mol)	201 - 318 (20)	-	192 - 353 (8)	220 - 487 (6)

Table 8.2 - Molecular/PC Property Space of Opioids, β-ARLs, β-LAs and CCB

PC Property	Opioids (n)	β-ARLs (n)	β-LAs (n)	CCB (n)
MW (Da)	221 - 496 (38)	225 - 510 (48)	199 - 672 (60)	315 - 496 (14)
$LogD_{7.4}$	-4.1 to 3.7 (38)	-2.9 to 3.1 (48)	-7.3 to 2.5 (60)	1.5 to 5.1 (14)
nRot	1.0 - 9.0 (38)	6.0 - 15 (48)	1.0 - 12.0 (60)	6.0 - 13 (14)
HBA	0 - 10.0 (38)	3.0 - 11 (48)	6.0 - 17 (60)	1.0 - 9.0 (14)
HBD	0 - 7.0 (38)	2.0 - 5.0 (48)	1.0 - 6.0 (60)	0 - 3.0 (14)
PSA (A^2)	5.8 - 248 (38)	45 - 228 (48)	118 - 447 (60)	12 - 120 (14)
MV (cm^3/mol)	198 - 467 (37)	192 - 424 (48)	120 - 364 (54)	272 - 429 (14)

8.1.2. Comparison with Opioids, β-ARLs, β-LAs and CCB

The ranges of the molecular/PC variables for available datasets of opioids[109], β-ARLs[109], β-LAs[109] and CCB[110] are shown in Table 8.2. CCB have a similar molecular/PC property space to BZD, i.e., they are relatively low MW, weakly basic, lipophilic compounds and also show relatively low diversity. Both opioids and β-ARLs are weakly basic compounds with MW ranging between 221 and 510 Da (n = 38 - 48), comparable to that observed for weakly acidic/basic BZD (271 - 412 Da, n = 20), weakly basic TRP (243 - 549 Da, n = 8) and weakly basic CCB (315 - 496 Da, n = 14). β-LAs (are weakly acidic) show diverse MW range that is comparable (199 - 672 Da, n = 60) to that of weakly basic Class III AAR (243 - 645 Da), while NMB show the most diverse range (290 - 1035 Da, n = 16) and the largest MW amongst all the eight classes.

The opioids dataset, in general, is relatively skewed towards lipophilic compounds, comparable to BZD and CCB; however, the overall range in the $logD_{7.4}$ values (-4.1 to 3.7, n = 38) suggests that it is quite heterogeneous. $LogD_{7.4}$ values of β-ARLs are also heterogeneous (ranging from -2.9 to 3.1, n = 48), consisting a combination of hydrophilic as well as lipophilic compounds, which is comparable to the (smaller) heterogeneous dataset of Class III AAR (ranging from -1.7 to 5.9, n = 7). TRP (-2.1 to 0.22, n = 8), NMB (-5.0 to 2.1, n = 12) and β-LAs (-7.3 to 2.5, n = 60) are all predominantly hydrophilic compounds in increasing order of diversity in $LogD_{7.4}$ values. Except for TRP, none of the other classes show high correlations between MW and $logD_{7.4}$. In general, there are several other correlations that are consistent across pharmacological classes, e.g., MW with MV, PSA, nRot, HBA, which is mechanistically plausible, owing to addition of substituents that not only add to the molecular size but also affect the increase hydrogen bonding ability (HBA, HBD), flexibility of bond rotation etc.

8.1.3. Discussion

Lipinski et al[27] investigated the *in-vitro* gastrointestinal solubility and permeability for a 2245 compounds in a United States Adopted Database (USAN) and proposed the "rule of five" cutoffs for log (P), MW, HBA and HBD. The rule states that a compound is likely to have poor oral absorption if (a) MW > 500 Da, (b) log (P) > 5, (c) HBD > 5.0 and HBA > 10.0. The majority of the compounds belonging to BZD, TRP and Class III AAR concur with the "rule of five", suggesting that, in general, they are less likely to show poor oral bioavailability due to poor solubility and/or permeability if administered by oral routes, as they are in clinical practice. However, the majority of NMB are exception to the Lipinski's "rule of five". In general, few NMB, especially the newer generations, show high MW and they show significant extrahepatic metabolism via chemical degradation. This is mechanistically plausible, because they are designed with the intent of having a short plasma half-life, facilitating quicker recovery from the neuromuscular blockade. Since, the intent of (exclusive) administration of NMB by I.V. route is to facilitate quick onset of neuromuscular blockade during surgical procedures, and they have been approved for clinical use, adequate oral bioavailability (and Lipinski's rule) is considered irrelevant.

Veber et al[28] studied oral bioavailability in rats of 1100 drug candidates in GSK database and suggested that there is high probability of acceptable oral bioavailability in rats if (a) nRot is ≤ 10, (b) PSA ≤ 140 A^2, and (c) sum of HBA and HBD is ≤ 12. The majority of the compounds belonging to BZD, TRP and Class III AAR meet these criteria, suggesting that they are likely to show acceptable oral bioavailability in rats, while NMB seem to have values that are outside of these criteria.

Obach et al[29] investigated the trend analysis of human systemic PK for 670 drugs (159 acids, 271 bases, 173 neutrals and 67 zwitterions) following I.V. administration, and is the only study that looked at human systemic and biologically relevant PK properties. They found that the typical 'drug-like' space for MW lies between 200 to 600 Da and is represented by 80% of the compounds in the dataset with a median value of 342 Da. Furthermore, they reported median value for logD (at pH = 7.0) of 0.42, PSA is 87 A^2, nRot is 5.0, HBA is 6.0 and HBD is 2.0. The database in the present work consists primarily of bases (n = 43), the majority of which are predominantly positively charged (Class III AAR show two positive charges) at physiological pH of 7.4, and only a few (n = 7) acids (all BZD). The median values of these molecular/PC properties for the compounds in the database of the present work, in general, are comparable to those shown in Obach et al.'s database, namely MW (352 Da), PSA (62 A^2), nRot (5.0), HBA (5.0) and HBD (1.0). However, in case of logD, in the present work, it was estimated at pH of 7.4 unlike at 7.0 and it tends to be skewed towards lipophilic side (median = 1.4) compared to Obach et al's database, in which it tends to be skewed towards hydrophilic side (median = 0.46). Overall, the molecular/PC property space in the present work is relatively less diverse compared to that of Obach et al.

8.2. Systemic and Biologically Relevant PK Property Space

8.2.1. BZD, NMB, TRP and Class III AAR

The statistical distribution of the *in-vivo* systemic and biologically relevant PK variables for BZD, NMB, TRP and Class III AAR are shown in Figures 8.8 - 8.16, and the ranges in these respective properties are listed in Table 8.3. There are missing values for several compounds in each class and therefore, the results should be interpreted with caution. On average, the majority of BZD show high PPB (i.e., low f_u values), owing to their lipophilic nature and low diversity in lipophilicity. The remaining three classes, in general, show greater diversity in the PPB values, possibly due to their relatively higher dispersion in lipophilicity.

In general, NMB and TRP show higher f_u values (i.e., skewed towards lower PPB) possibly owing to their predominantly hydrophilic nature, while Class III AAR show a wide dispersion in f_u values, due to the heterogeneous dataset of hydrophilic and lipophilic compounds with the latter showing a greater impact and thus skewing the distribution towards smaller f_u values (i.e., higher PPB). As a result of the (relatively) high PPB of (lipophilic) BZD, the impact of f_u correction of *in-vivo* systemic PK is more pronounced (i.e., in general, higher values for biologically relevant PK properties suggesting they are subject to binding - restricted distribution and clearance mechanisms) for BZD than for (hydrophilic) NMB and TRP. However, since Class III AAR are a heterogeneous dataset, there are no obvious conclusions, although, in general, the f_u correction increases the diversity of biologically relevant PK properties. The Vd_{ss}^u values for the lipophilic BZD (1.0 - 124 L/kg, n = 16) suggest moderate to extensive extravascular distribution and/or sequestration to tissues/membranes, low MW, hydrophilic TRP (2.0 - 16 L/kg, n = 7) also show moderate to extensive extravascular distribution. In contrast, the majority of the Vd_{ss}^u values for NMB (0.10 - 1.2 L/kg, n = 14) suggest that their distribution is

restricted to the intracellular/extracellular (0.26/0.34 L/kg) and total body water (0.60 L/kg) spaces owing to their large, charged and hydrophilic nature.

Except for the (most hydrophilic) N-DMAD and clorazepate, the remaining seven compounds in BZD dataset with available information show negligible contribution of renal clearance (f_e < 1%), i.e., they are all subject to extensive hepatic metabolism (with no obvious extra-hepatic pathways reported in literature); their high degree of lipophilicity is a plausible explanation for this finding. CYP3A, CYP2C19 and UGTs are the major known phase I and phase II metabolic pathways involved in the metabolism of BZD.

The compounds in NMB and TRP datasets with available information show considerable diversity in f_e and relatively higher values ranging from 5% - 58% (n = 12) and 9% - 44% (n = 5), respectively, compared to BZD. Although compounds belonging to these two classes are predominantly hydrophilic, their renal handling o is quite different. With the exception of mivacurium, CL_{ren}^{u} values of the remaining NMB with available information are lower than GFR (1.7 ml/min/kg) suggesting (a) they are potentially poorly filtered, due to their large size and/or (b) they undergo net tubular reabsorption, possibly involving transporters. On the other hand, with the exception of frovatriptan, CL_{ren}^{u} values for TRP exceed GFR, suggesting they undergo net tubular secretion, potentially involving drug transporters owing to the positive charge they show at physiological pH. Finally, Class III AAR show the highest diversity in f_e values (ranging from 1% to 77%, n = 6) amongst the four pharmacological classes. Within the Class III AAR, relatively hydrophilic ones show CL_{ren}^{u} values comparable to GFR suggesting filtration, potentially involving drug transporters, while the lipophilic ones have CL_{ren}^{u} < GFR, suggesting net renal tubular reabsorption. The compounds in NMB, TRP and Class III AAR datasets are known to undergo diverse nonrenal clearance mechanisms: A few NMB show

CL_{nonren} values exceeding the cardiac output, suggesting the presence of extra-hepatic pathways such as chemical (e.g., cisatracurirum and atracurium) and enzymatic degradation (e.g., mivacurium and succinylcholine) in plasma and/or tissues. A few others have CL_{nonren} values lower than LBF, suggesting they are low ER_{hep} drugs and may subject to hepato-biliary clearance mechanisms. Likewise, a few compounds in the TRP dataset are metabolized by mono amine oxidase (MAO) which is present both hepatically as well as extra-hepatically, while the remaining ones may be subject to hepato-biliary excretion, potentially involving drug transporters, owing to their positive charge and hydrophobicity. Except for ibutilide and dronedarone, the rest of the drugs in the Class III AAR dataset have CL_{nonren} values lower than the LBF, suggesting they are all low ER_{hep} ratio drugs. For the hydrophilic ones, e.g., sotalol and bretylium, PPB is negligible and they are low ER_{hep} drugs, owing to their low hepatic CL_{int}, while the lipophilic drugs e.g., azimilide and amiodarone, show low ER_{hep} because they undergo PPB-restricted hepatic metabolism. CL_{nonren} values for ibutilide and dronedarone are greater than LBF suggesting that they exhibit extra-hepatic clearance pathways.

Figure 8.8 - f_u Distribution by Pharmacological Class

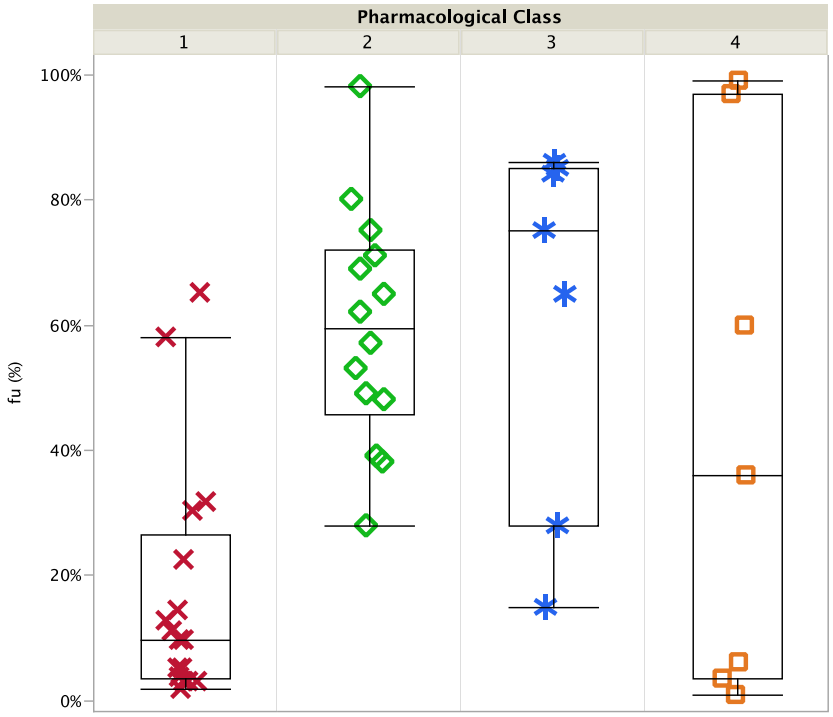

1 - BZD (X); 2 - NMB (◊); 3 - TRP (*) and 4 - Class III AAR (□)

Figure 8.9 - Vd_{ss}^{u} Distribution by Pharmacological Class

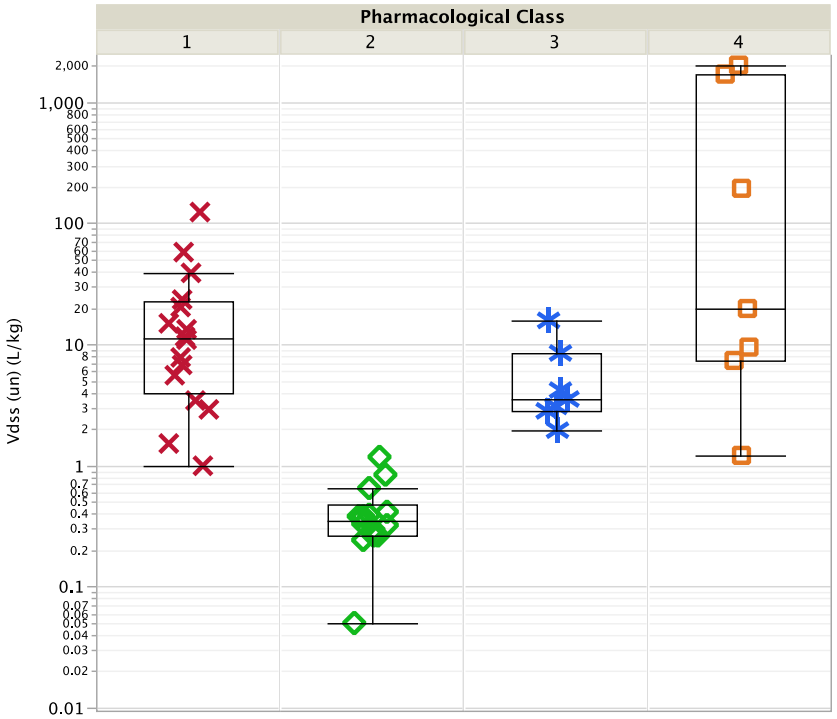

Figure 8.10 - Vd_{ss} Distribution by Pharmacological Class

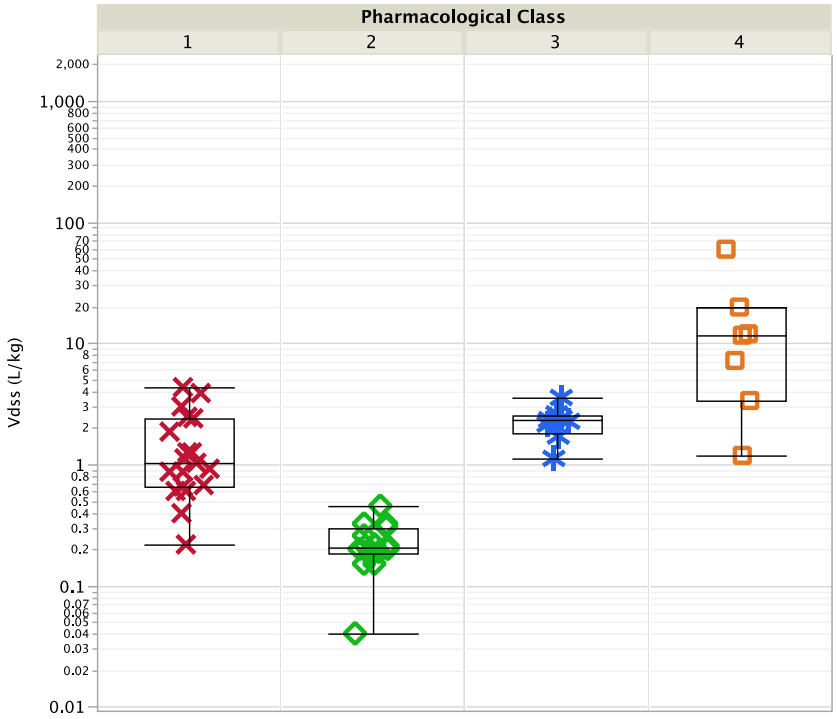

1 - BZD (X); 2 - NMB (◊); 3 - TRP (*) and 4 - Class III AAR (□)

Figure 8.11 - CL_{tot}^{u} Distribution by Pharmacological Class

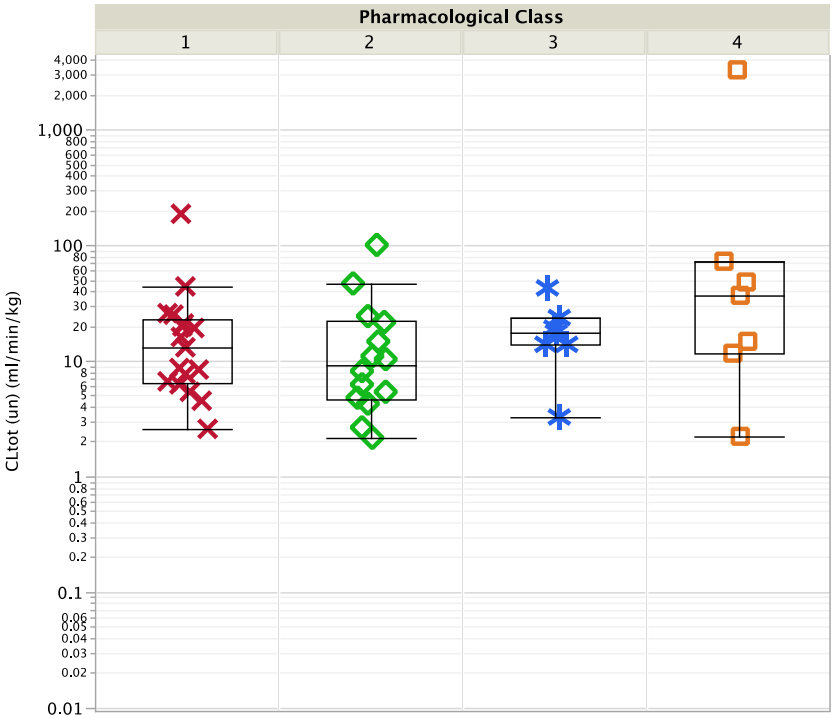

Figure 8.12 - CL_{tot} Distribution by Pharmacological Class

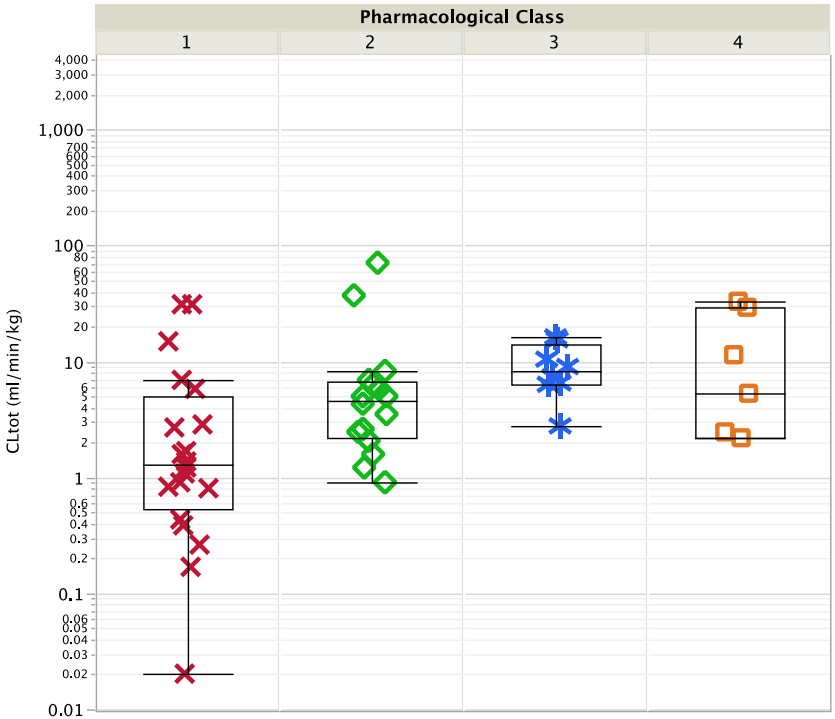

1 - BZD (X); 2 - NMB (◊); 3 - TRP (*) and 4 - Class III AAR (□)

Figure 8.13 - CL_{ren}^{u} Distribution by Pharmacological Class

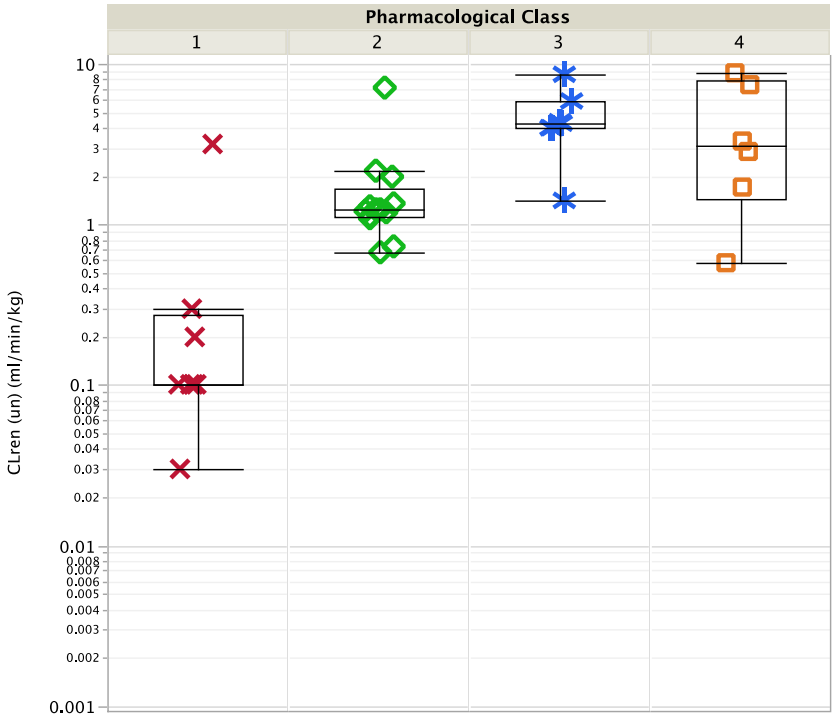

Figure 8.14 - CL_{ren} Distribution by Pharmacological Class

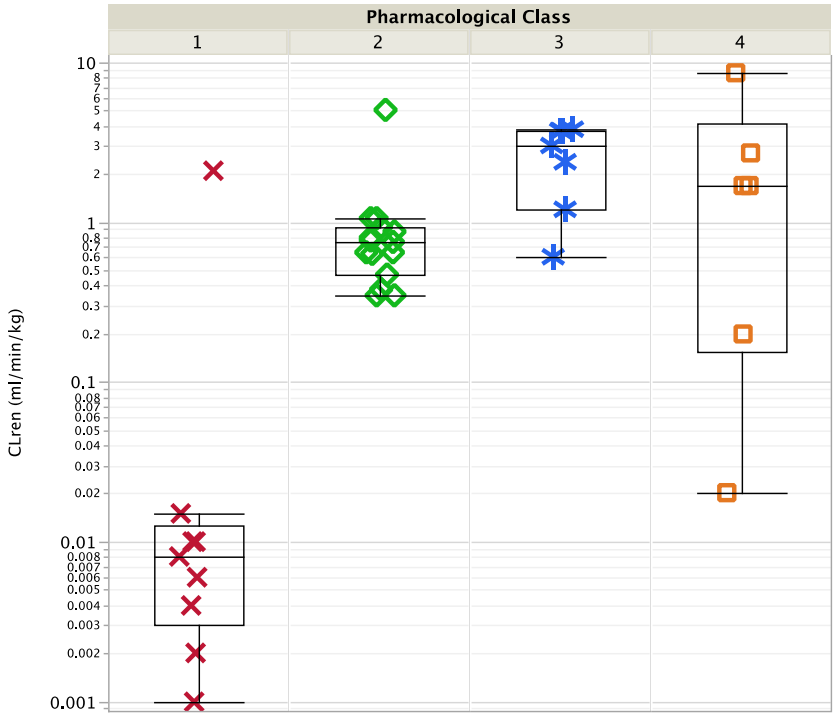

1 - BZD (X); 2 - NMB (◊); 3 - TRP (*) and 4 - Class III AAR (□)

Figure 8.15- CL_{nonren}^{u} Distribution by Pharmacological Class

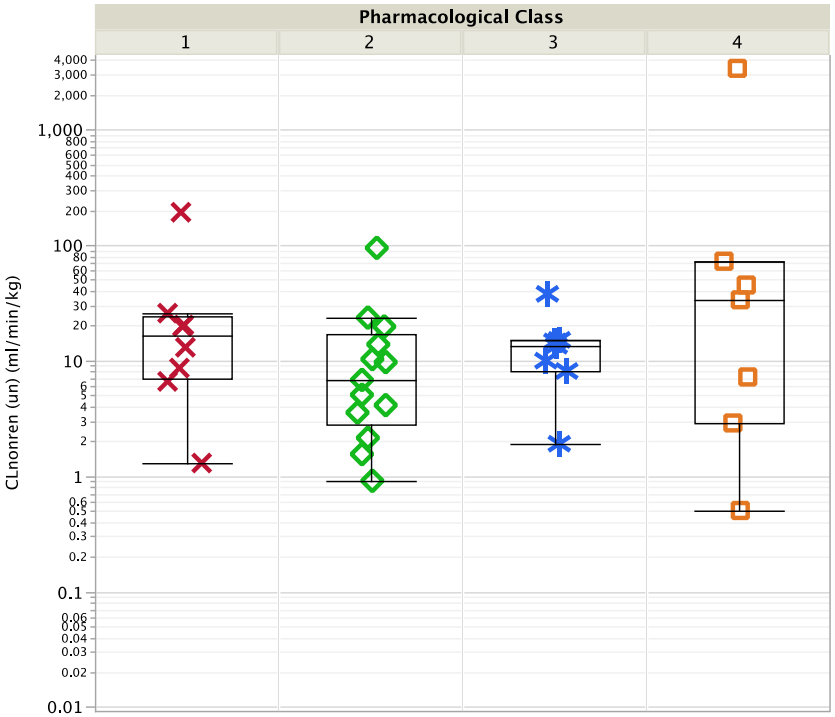

Figure 8.16 - CL_{nonren} Distribution by Pharmacological Class

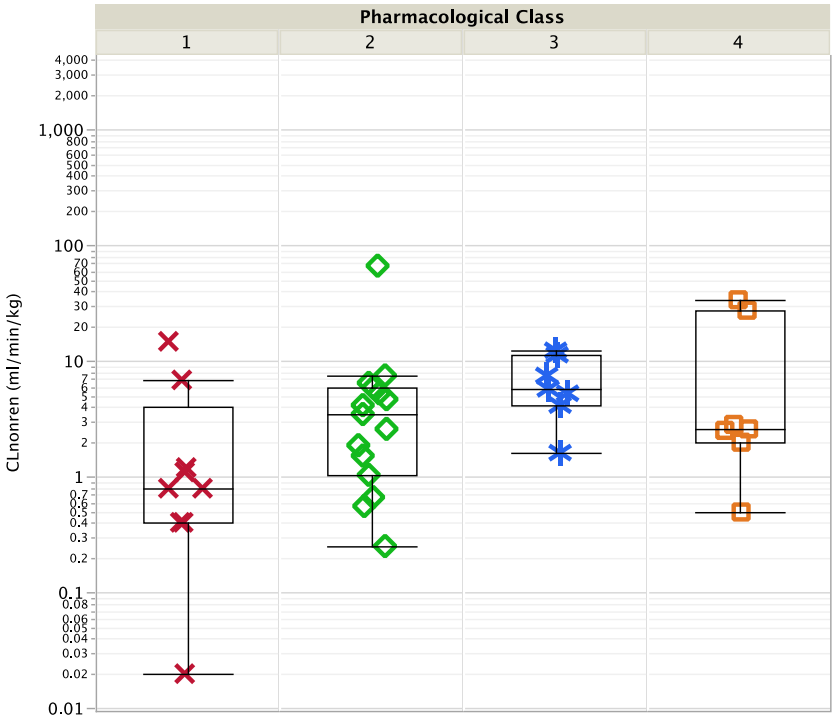

1 - BZD (X); 2 - NMB (◊); 3 - TRP (*) and 4 - Class III AAR (□)

Table 8.3 - Systemic and Biologically Relevant Property Space of BZD, NMB, TRP and Class III AAR

PK Property	BZD (n)	NMB (n)	TRP (n)	Class III AAR (n)
f_u (%)	2.0 - 65 (17)	28 - 98 (14)	15 - 86 (7)	1.0 - 99 (7)
Vd_{ss}^{u} (L/kg)	1.0 - 124 (16)	0.10 - 1.2 (14)	2.0 - 16 (7)	1.2 - 2000 (7)
CL_{ren}^{u} (ml/min/kg)	0.030 - 3.2 (8)	0.70 - 7.1 (13)	1.4 - 8.6 (7)	0.70 - 8.9 (6)
CL_{nonren}^{u} (ml/min/kg)	1.3 - 189 (8)	0.90 - 95 (13)	1.9 - 38 (7)	0.50 - 3333 (7)
Vd_{ss} (L/kg)	0.20 - 4.3 (19)	0.040 - 0.50 (16)	1.1 - 3.6 (8)	1.2 - 60 (7)
CL_{ren} (ml/min/kg)	0.0010 - 2.1 (9)	0.36 - 5.1 (15)	0.60 - 3.8 (7)	0.020 - 8.6 (6)
CL_{nonren} (ml/min/kg)	0.020 - 15 (9)	0.38 - 67 (15)	1.6 - 12 (7)	0.56 - 33 (7)

Table 8.4 - Systemic and Biologically Relevant Property Space of Opioids, β-ARLs, β-LAs and CCB

PK Property	Opioids (n)	β-ARLs (n)	β-LAs (n)	CCB (n)
f_u (%)	4.0 - 92 (29)	2.0 - 99 (34)	3.0 - 96 (57)	0.20 - 20 (13)
Vd_{ss}^{u} (L/kg)	0.10 - 96 (28)	0.30 - 590 (34)	0.13 - 4.5 (57)	14 - 4391 (13)
CL_{ren}^{u} (ml/min/kg)	0.40 - 4.4 (18)	0.20 - 13 (29)	0.18 - 12 (57)	0.30 - 14 (4)
CL_{nonren}^{u} (ml/min/kg)	0.80 - 283 (18)	0.18 - 462 (29)	0.080 - 26 (57)	51 - 41904 (13)
Vd_{ss} (L/kg)	0.010 - 13 (36)	0.30 - 14 (46)	0.11 - 0.46 (60)	0.60 - 20 (14)
CL_{ren} (ml/min/kg)	0.090 - 11 (21)	0.020 - 12 (38)	0.090 - 4.5 (60)	0.0030 - 0.72 (4)
CL_{nonren} (ml/min/kg)	0.70 - 198 (21)	0.18 - 284 (38)	0.080 - 4.8 (60)	6.7 - 132 (9)

8.2.2. Comparison with Opioids, β-ARLs, β-LAs and CCB

The ranges of the *in-vivo* systemic and biologically relevant PK variables for opioids, β-ARLs, β-LAs[109] and CCB[110] are shown in Table 8.3. On average, the BZD, CCB and opioids datasets consist of lipophilic compounds, and as a result, they show high PPB (i.e., low f_u), high Vd_{ss}^u suggesting extensive extravascular distribution and sequestration to body tissues/membranes etc.; (in general) the majority of them are cleared by nonrenal pathways, i.e., hepatic and extrahepatic pathways with little/negligible renal contribution (f_e < 10%) for BZD and CCB, while slightly higher for opioids (but the majority of them show f_e < 50%).

Except clevidine (whose CL_{nonren} values exceeds LBF, due to known extra-hepatic plasma/tissue ester hydrolysis) and amlodipine (whose CL_{nonren} is below LBF, suggesting low ER_{hep}), the rest of CCB in the dataset with available information are moderate to high ER_{hep} compounds with CL_{nonren} values approaching LBF. Furthermore, oxidative metabolism via phase I pathways, e.g., CYP3A, seem to be the major hepatic route for CCB.

In general, CL_{nonren} values of majority of opioids approach LBF, suggesting they are high ER_{hep} drugs. Glucuronidation via UGT2B7 and phase I pathways mediated by CYP2D6, CYP3A, CYP2C9, and CY2C19 are known to be involved in opioid metabolism. β-ARLs are heterogeneous dataset, consisting of both hydrophilic as well as lipophilic compounds; as a result they show diverse PK property space, i.e., low to extensive extravascular tissue distribution (skewed towards higher values) and the majority of them have f_e values less than 50% (35 out of 47), suggesting CL_{tot} is primarily due to elimination by nonrenal pathways, i.e., hepatic and extrahepatic clearance. CL_{ren}^u values exceed the GFR suggesting that they undergo net tubular secretion involving drug transporters; P-gp, OCTs and MRP2 are knownto be involved in transport of (positively) charged β-ARLs[111,112].

On the other hand, β-LAs are, in general, hydrophilic compounds like TRP and NMB, but differ from TRP in being intermediate to high MW (unlike NMB that are higher MW). Their Vd_{ss}^{u} values are low, suggesting little extravascular distribution, possibly owing to their molecular size and/or charged hydrophilic nature. Owing to their hydrophilicity, the contribution of renal pathways for β-LAs is significant (f_e exceeds 50%) for a large number of compounds. CL_{ren}^{u} values exceed GFR, suggesting that they undergo net tubular secretion; interactions of cephalosporins with hOATs is documented in the literature[113,114]. The majority of them show CL_{nonren} values less than LBF, suggesting that they are low ER_{hep} drugs subject to hepatobiliary, which may be excretion potentially mediated by hepatic drug transporters owing to their molecular size and (positive) charge.

8.2.3. Discussion

In the database that was used for investigating the trend analysis of human systemic PK for 670 drugs following I.V. administration, Obach et al[29] reported that (a) two-thirds of the compounds in their dataset are less than 90% PPB, with median f_u of 26%, (b) Vd_{ss} values ranged between 0.035 and 700 L/kg, with a median value of 0.96 L/kg, and the vast majority (90%) of the compounds lying between 0.10 and 10 L/kg (biologically relevant Vd_{ss}^{u} is not reported), and (c) CL_{tot} values ranged from 0.0037 ml/min/kg to 1070 ml/min/kg, with a median value of 4.0 ml/min/kg, and three-fifths of the compounds having values within the range 1.0 to 10 ml/min/kg and about fifty six (8.4% of the total number of the) compounds potentially cleared by extrahepatic pathways (i.e., based on the clearance values exceeding the LBF).

In the present work, the median values for the reported systemic PK variables are comparable, in general, e.g., (a) median f_u = 38% (ranging from 1% to 99%, n = 45), (b) median

Vd_{ss} = 0.98 L/kg (ranging from 0.04 to 59.5 L/kg, n = 50), while Vd_{ss}^{u} = 3.5 L/kg (ranging from 0.05 to 2000 L/kg, n = 44), suggesting that, on an average, the compounds in the current dataset show binding-restricted extravascular distribution, and this trend seem to be driven by more lipophilic compounds in the current dataset (concurrent with the median lipophilic $logD_{7.4}$ of 1.4) and, (d) median CL_{tot} of 3.5 ml/min/kg (ranging from 0.02 and 72.2 ml/min/kg, n = 51). Overall, the *in-vitro* PPB/*in-vivo* systemic PK property space in the present work is relatively less diverse compared to that of Obach et al[29].

CHAPTER 9. INTERSPECIES PHARMACOKINETIC ALLOMETRIC SCALING

Using the publicly available PK information on the drugs/compounds belonging to BZD and NMB:

9.1. Research Hypothesis II

Human systemic PK properties can be quantitatively predicted by scaling from available *in-vivo* animal systemic PK properties using interspecies PK-AS approaches. In order to test this hypothesis, the following specific aims were pursued:

e. Pertinent animal *in-vivo* systemic PK properties of the BZD and NMB were collected from the biomedical literature, and, subsequently, their biologically relevant animal PK properties were estimated.

f. PK properties of BZD were compared across different animal species

g. Allometric relationships were explored statistically using systemic and biologically relevant animal PK for BZD and NMB.

h. Different allometric-based prediction methods were assessed and validated based on their predictive performance.

9.2. Methods

9.2.1. Data Collection - Animal PK Studies

A comprehensive and exhaustive search was carried out for original research and/or review articles on animal systemic PK properties of BZD and NMB, in which the compounds of interest are administered exclusively by the I.V. route. Furthermore, urinary excretion studies, subject to availability were also compiled. The *in-vitro* PPB and *in-vivo* systemic and biologically relevant PK properties were compiled as described in detail in Chapter - 3.

Using these methods, the final BZD database consists of up to ten BZD including one metabolite, N-DMD and flumazenil, a $GABA_A$ antagonist in up to six species (i.e., including humans); the final NMB database consists of six NMB, including one metabolite, Org 7268 (vecuronium metabolite), all having aminosteroid structural scaffold, mostly in cats (and dogs for pipercuronium).

9.2.2. Descriptive PK Across Species

Interspecies comparison: The *in-vitro* PPB and *in-vivo* systemic and biologically relevant PK properties for each compound were compared across the different animal. Furthermore, the -fold range across all available the species was calculated to assess variation across all available species for each PK variable. Since the majority of BZD undergo hepatic extraction (and show negligible renal clearance), they were stratified as low, intermediate and high clearance drugs based on the LBF in the respective animal species and see Table 3.2 for the criteria.

Since NMB show significant renal clearance pathways, no such stratification was performed.

9.2.3. Simple Allometry

Simple PK-AS uses power functions to explore the relationship of PK variables (e.g., CL_{tot}, Vd_{ss}; their biologically relevant counterparts, CL_{tot}^{u}, Vd_{ss}^{u}) as a function of BW (in kg) across the animal species with available information.

Table 9.1 - Concentration of Plasma Proteins in Various Animal Species[55]

Variable	**Mouse**	**Rat**	**Rabbit**	**Dog**	**Human**
Weight (kg)	0.02	0.25	2.5	10	70
Plasma Albumin (μM)	495	479	586	398	633
Plasma α-Acid Glycoprotein (μM)	313	453	33	93	45

From Table 9.1, it can be observed that plasma albumin (which, in general, binds weak acids) concentrations are fairly similar across the various animal species. However, there are significant interspecies differences in the concentrations of plasma α-acid glycoprotein (which, in general, binds weak bases), with the smaller animal species (e.g., mice and rats) higher concentrations than bigger animal species (e.g., dogs and humans). Since most of the BZD and NMB are weak bases that (potentially) bind to α-acid glycoprotein, indicating that the PPB-correction could potentially account (at least in part) for interspecies differences in the systemic PK properties.

9.2.4. Prediction Methods

Single-species methods:

BW-Based Scaling: Human PK variables (PKV), namely, Vd_{ss} (and Vd_{ss}^{u}), CL_{tot} (and CL_{tot}^{u}), were predicted from the available (corresponding) single animal species PK based on BW, for BZD and NMB. The following equation was used:

$$PKV^{Humans} = PKV^{Animals} * \left(\frac{BW^{Humans}}{BW^{Animals}}\right) \ldots. \text{Eq 9.1}$$

Where, the units of Vd_{ss} and Vd_{ss}^{u}, are in l; and, CL_{tot} and CL_{tot}^{u} are in ml/min

LBF-Based Scaling: Selected human PK variables, namely, CL_{tot} (and CL_{tot}^{u}) were predicted from the available (corresponding) single animal species PK based on LBF for BZD and NMB. This prediction method is based on the assumption that renal elimination is negligible, and CL_{tot} (in plasma) approaches $CL_{hepatic}^{blood}$. The following equation was used[11]:

$$CL^{Humans}(ml/min/kg) = \frac{CL^{Animals}(ml/min)}{BW^{Animals}(kg)} * \left(\frac{LBF^{Humans}(ml/min/kg)}{LBF^{Animals}(ml/min/kg)}\right) \ldots \text{Eq 9.2}$$

GFR-Based Scaling: For compounds that are eliminated primarily by the kidneys, selected human PK variables, namely, CL_{ren} (and CL_{ren}^{u}), were predicted from the available single animal species (corresponding) PK based on GFR. The important underlying assumption (in this GFR-based prediction of CL_{ren}) is that the drugs are renally cleared by net glomerular filtration, without differences in tubular handling across the species. The following equation was used[115]:

$$CL_{ren}^{Humans}(ml/min/kg) = \frac{CL_{ren}^{Animals}(ml/min)}{BW^{Animals}(kg)} * \left(\frac{GFR^{Humans}(ml/min/kg)}{GFR^{Animals}(ml/min/kg)}\right) \ldots \text{Eq 9.3}$$

Two-species methods:

Log-log regression of PKV from at least two animal species (other than humans) were used to develop the PK-AS relationship (AS exponent and intercept), and the corresponding human PKV was predicted using the equation:

$$\text{Log (PKV)} = b*\text{Log (BW)} + \text{Log } a; \ldots. \text{ Eq 9.4}$$

where a the intercept and b is the AS exponent obtained from the PK-AS relationship based on at least two animal species.

9.2.5. Validation of the Predictive Performance of Different Prediction Methods

The predictive performance of the different PK-AS methods was assessed using % mean prediction error (%MPE) for bias and % root mean square error (%RMSE) for imprecision.

The respective equations that were used[116]:

$$\%\text{MPE} = \sum \left(\frac{(\text{Predicted} - \text{Observed})}{\text{Observed}} * 100 \right) \div n \quad \ldots \text{ Eq 9.5}$$

$$\%\text{RMSE} = \sqrt{\sum \left(\frac{(\text{Predicted} - \text{Observed})}{\text{Observed}} * 100 \right)^2 \div n} \quad \ldots \text{ Eq 9.6}$$

Furthermore, MPE values between -50% and 100% (i.e., a 0.5- to 2.0-fold prediction error) was considered as an acceptable range of prediction[11]. The number (or percentage) of compounds whose predicted values fall within this range were considered acceptable predictions, which were then used to compare the accuracy of the predictions based on the different methods.

CHAPTER 10. INTERSPECIES SCALING OF BZD

10.1. Results

10.1.1. Comparative PK of BZD Across Different Species

The final animal systemic PK database consists of ten BZD, including one metabolite, N-DMD and flumazenil, a $GABA_A$ antagonist. There are several missing values, i.e., for most of the BZD in the database, there is limited information available in a few preclinical species.

Overall, there are large interspecies differences in the BW-corrected *in-vivo* systemic animal PK properties, namely, CL_{tot} (mean values across the available animal species ranges from 1.7 ml/min/kg for N-DMD to 36.7 ml/min/kg for midazolam with an overall 1 to 200-fold range) and Vd_{ss} (mean values across the available animal species ranges from 0.5 l/kg for chlordiazepoxide to 4.7 l/kg for clonazepam and a 1 to 17-fold overall range) as represented in Table - 10.1. There are even larger interspecies differences in BW-corrected unbound *in-vivo* systemic PK animal properties, namely, CL_{tot}^{u} (mean values across the available animal species ranges from 18.2 ml/min/kg for N-DMD to 973.4 ml/min/kg for midazolam and a 1 to 272-fold overall range) and Vd_{ss}^{u} (mean values across the available animal species ranges from 4.8 l/kg for triazolam to 39.4 l/kg for diazepam and a 1 to 18-fold overall range) as represented in Table 10.1. *In-vitro* f_u values for most BZD with available information also show interspecies differences, i.e., in general, larger animal species showing lower f_u, e.g., diazepam and N-DMD showed highest PPB in humans and (see Table 10.2 and Figure 10.1 & 10.2 for diazepam, and N-DMD respectively).

Further, BZD in the dataset are categorized (Table 10.3) as low, intermediate and high ER_{hep} drugs in each animal species with available information by comparing the reported systemic CL_{tot} in plasma to the LBF in the respective animal species (shown in Table 10.3). However, two important assumptions in the estimation of ER_{hep} include (a) renal elimination is considered negligible, and (b) systemic CL_{tot} in plasma is considered equivalent to CL_{nonren}^{blood} (i.e., B:P ratio is assumed to be close to 1.0 across the species). Certain BZD, e.g., temazepam, diazepam, midazolam, triazolam, etc., show higher ER_{hep} in smaller animal species and lower ER_{hep} in larger animal species. This is a plausible explanation for (plasma protein) binding-restricted hepatic extraction (low ER_{hep}) in larger animal species, e.g., humans, for certain BZD, e.g., diazepam.

Table 10.1 - *In-vitro* and *In-vivo* Systemic and Biologically Relevant PK Variables Across Different Animal Species

Compound	Species	BW (kg)	Mean Dose (mg/kg)	CL_{tot} (ml/min/kg)	CL_{tot} (ml/min)	Vd_{ss} (L/kg)	Vd_{ss} (L)	f_u (%)	CL_{tot}^u (ml/min/kg)	Vd_{ss}^u (L/kg)
Alprazolam	Dogs	10	8.9					43		
	Humans	70	0.50					32		
Chlordiazepoxide	Dogs	12	8.9	4.4	52	0.52	6.2			
	Humans	70	0.50	0.44	31	0.39	27			
Clonazepam	Mice	0.020	2.0	32	0.65	6.4	0.13			
	Humans	70	0.030	0.90	63	3.0	210			
Diazepam	Rats	0.25	5.0	82	20	1.7	0.43	14	582	12
	Guinea Pigs	0.85	2.5	19	16	1.6	1.4	9.0	211	18
	Cats	4.0	12.5	3.4	14	1.6	6.4	-	-	-
	Rabbits	2.5	1.8	24	60	4.1	10	11	218	37
	Dogs	10	1.0	19	190	3.0	30	4.0	475	75
	Humans	70	0.20	0.40	28	1.1	77	2.0	20	55
Minimum		**0.25**	**0.20**	**0.40**	**14**	**1.1**	**0.43**	**2.0**	**20**	**12**
Maximum		**70**	**12.5**	**82**	**190**	**4.1**	**77**	**14**	**582**	**75**
Mean		**15**	**3.8**	**25**	**55**	**2.2**	**21**	**8.0**	**251**	**33**
SD		**27**	**4.6**	**29**	**68**	**1.1**	**29**	**4.9**	**236**	**28**
Fold-range		**280**	**63**	**205**	**14**	**3.7**	**179**	**7.0**	**29**	**6.3**
COV		**187%**	**119%**	**120%**	**125%**	**52%**	**141%**	**62%**	**94%**	**86%**

N-DMD	Cats	4.0	7.5	0.50	2.0	1.0	4.0	14	3.6	7.1
	Dogs	8.3	1.5	4.5	37	1.2	10	10	45	12
	Humans	70	0.10	0.24	14	1.2	84	3.0	6.7	40
Minimum		**4.0**	**0.10**	**0.24**	**2.0**	**1.0**	**4.0**	**3.0**	**3.6**	**7.1**
Maximum		**70**	**7.5**	**4.5**	**37**	**1.2**	**84**	**14**	**45**	**40**
Mean		**27**	**3.0**	**1.7**	**18**	**1.1**	**33**	**10**	**18**	**20**
SD		**37**	**3.9**	**2.4**	**18**	**0.12**	**45**	**5.6**	**23**	**18**
Fold-range		**17**	**75**	**19**	**19**	**1.2**	**21**	**4.7**	**13**	**5.6**
COV		**135%**	**130%**	**139%**	**101%**	**10%**	**136%**	**62%**	**125%**	**90%**
Lorazepam	Cats	4.0	0.50	-		-		12		
	Rabbits	2.5	0.20	22		1.7		-		
	Humans	70	0.040	1.2		1.3		10		
Midazolam	Rats	0.25	7.5	72	18	1.8	0.45	3.0	2410	60
	Cats	4.0	10	30	121	2.4	9.6	9.0	336	27
	Humans	70	0.15	7.0	490	1.0	70	4.0	175	25
Minimum		**0.25**	**0.15**	**7.0**	**18**	**1.0**	**0.45**	**3.0**	**175**	**25**
Maximum		**4.0**	**10**	**72**	**490**	**2.4**	**70**	**9.0**	**2410**	**60**
Mean		**25**	**5.9**	**37**	**210**	**1.7**	**27**	**5.3**	**974**	**37**
SD		**39**	**5.1**	**33**	**248**	**0.70**	**38**	**3.2**	**1247**	**20**
Fold-range		**16**	**67**	**10**	**27**	**2.4**	**156**	**3.0**	**14**	**2.4**
COV		**159%**	**87%**	**91%**	**118%**	**41%**	**142%**	**60%**	**128%**	**3%**
Triazolam	Rats	0.25	9.3	50	13	2.5	0.63	-		
	Cats	4.0	0.30	15	60	1.4	5.6	33	45	4.2

	Humans	70	0.0030	2.8	196	0.60	42	11	25	5.4
Minimum		**0.25**	**0.0030**	**2.8**	**13**	**0.60**	**0.63**			
Maximum		**4.0**	**9.3**	**50**	**196**	**2.5**	**42**			
Mean		**25**	**3.2**	**23**	**90**	**1.5**	**16**			
SD		**39**	**5.3**	**25**	**95**	**1.0**	**23**			
Fold-range		**16**	**3100**	**18**	**15**	**4.2**	**67**			
COV		**159%**	**165%**	**108%**	**106%**	**64%**	**141%**			
Flunitrazepam	Rats	0.25	2.5					15		
	Cats	4.0	0.30					32		
	Humans	70	0.020					23		
Minimum		**0.25**	**0.020**					**15**		
Maximum		**4.0**	**2.5**					**32**		
Mean		**25**	**0.94**					**23**		
SD		**39**	**1.4**					**8.5**		
Fold-range		**16**	**125**					**2.1**		
COV		**159%**	**144%**					**36%**		
Oxazepam	Rats	0.25	7.5	24	6.0	1.9	0.48	9.0	267	21
	Dogs	10	1.3	5.1	51	1.4	14	10	51	14
	Humans	70	0.20	1.1	77	0.60	42	5.0	22	12
Minimum		**0.25**	**0.20**	**1.1**	**6.0**	**0.60**	**0.48**	**5.0**	**22**	**12**
Maximum		**10**	**7.5**	**5.1**	**77**	**1.9**	**42**	**10**	**267**	**21**
Mean		**27**	**3.0**	**10**	**45**	**1.3**	**19**	**8.0**	**113**	**16**
SD		**38**	**4.0**	**12**	**36**	**0.66**	**21**	**2.6**	**134**	**4.8**

Fold-range **COV**		**40** **141%**	**38** **132%**	**4.6** **122%**	**13** **80%**	**3.2** **50%**	**29** **113%**	**2.0** **33%**	**12** **118%**	**1.8** **30%**
Temazepam	Cats	6.0	5.0	6.5		1.7				
	Humans	70	0.40	1.4		-				
Flumazenil	Dogs	10	0.010	37		2.5				
	Humans	70	0.030 - 0.54	15		0.90				

Table 10.2 - Plasma Protein Binding (f_u %) of BZD in Most Common Animal Species

Compound	Species			
	Rat	Cat	Dog	Human
Alprazolam			43%	32%
Diazepam	14%		4%	2%
N-DMD		14%	10%	3%
Lorazepam		12%		10%
Midazolam	3%	9%		4%
Triazolam		33%		11%
Flunitrazepam	15%	32%		23%
Oxazepam	9%		10%	5%

Figure 10.1 - Diazepam: f_u (%) vs. BW (kg) in log scale in Various Animal Species

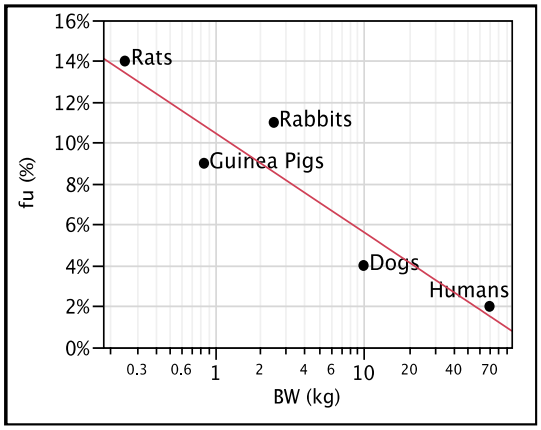

Figure 10.2 - N-DMD: f_u (%) vs. BW (kg) in log scale in Various Animal Species

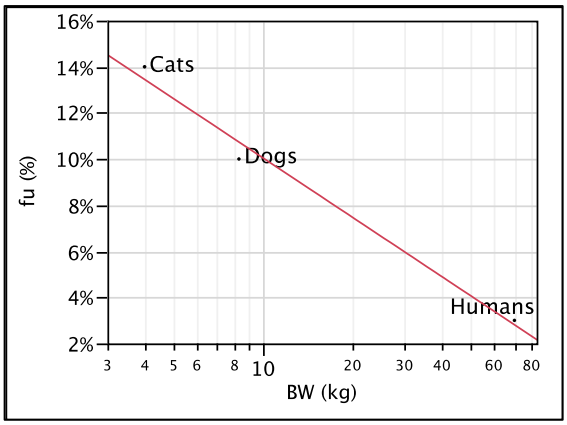

Table 10.3 - Categorization of BZD Into Low/Intermediate/High ER_{hep} in Various Animal Species

Compound	Rats		Rabbits		Cats		Dogs		Humans	
	CL_{tot} (ml/min/kg)	ER_{hep}	CL_{tot} (ml/min/kg)	ER_{hep}	CL_{tot} (ml/min/kg)	ER_{hep}	CL_{tot} (ml/min/kg)	ER_{hep}	CL_{tot} (ml/min/kg)	ER_{hep}
Temazepam					6.5	Intermediate			1.7	Low
Diazepam	81.6	High	24	Low	3.4	Low	19	Intermediate	0.4	Low
N-DMD					0.5	Low	4.5	Low	0.2	Low
Midazolam	72.3	High			30.2	High			7.0	Intermediate
Triazolam	50	High			15	High			2.7	Low
Oxazepam	24	Low					5.1	Low	1.1	Low
Chlordiazepoxide							4.4	Low	0.4	Low
Flumazenil							37.4	High	14.8	Intermediate
Lorazepam			21.7	Low					1.2	Low

10.1.2. Simple PK Allometry

Allometric relationships were studied for ten BZD, using information available in various animal species including humans. The exponents of these allometric relationships i.e., logarithm of each of Vd_{ss} (L), Vd_{ss}^{u} (L), CL_{tot} (ml/min), CL_{tot}^{u} (ml/min) plotted as a function of logarithm of BW (in kg) in various animal species are shown in Tables 10.4 - 10.7 respectively. They were compared with widely reported PK scaling factors in literature[117] - 0.75 for CL_{tot} (and CL_{tot}^{u}) and 1.0 for Vd_{ss} (and Vd_{ss}^{u}). Figures 10.3 - 10.6 show the interspecies PK-AS plots of Vd_{ss}, Vd_{ss}^{u}, CL_{tot} and CL_{tot}^{u} respectively, for a prototypical BZD, namely diazepam. The mean (range, n) AS coefficients for Vd_{ss} and Vd_{ss}^{u} are found to be 0.84 (0.48 - 1.1, n = 9) and 1.1 (0.90 - 1.6, n = 5), respectively; and (log - log) correlation coefficients are high (r^2>0.93), suggesting a good fit of the allometric relationships. The physiological body compartments, namely, total body water, intracellular and extracellular water, plasma and blood volumes have been shown[55] to scale with an AS coefficient of around 1.0 across the animal species (see Chapter 9); and the obtained mean AS coefficient for Vd_{ss}^{u} close to 1.0, suggests that distribution volumes for BZD scale well with physiological body compartments across the animal species. Mean (range, n) AS coefficients for CL_{tot} and CL_{tot}^{u} for BZD with available information in various animal species are 0.42 (0.13-0.60, n = 9) and 0.68 (0.53-0.97, n = 5), respectively; and goodness of fit (r^2) ranges from 0.11-0.99. Chlordiazepoxide was excluded from estimation of the mean slope, since it scales with an AS of -0.3, i.e., it shows a value higher CL_{tot} (in ml/min/kg) in smaller animal species (dogs) than larger animal species (humans) - potentially due to intrinsic species differences in clearance pathways. CL_{tot}^{u} scaling for BZD is less than the (expected[41,118]) AS coefficient of 0.7 to 0.8 (depending on the organ flow rates, e.g., LBF, RPF, GFR etc., as shown in Chapter 9), which suggests that even after accounting for the interspecies differences in PPB, qualitative and/or

quantitative interspecies differences in intrinsic (hepatic/metabolic) clearance seem to exist, i.e., smaller species showing higher metabolic clearance than larger species, especially humans. Furthermore, the biologically relevant PK properties, Vd_{ss}^{u} and CL_{tot}^{u}, for most of the BZD in the dataset with available information show higher AS coefficients (1.14 and 0.53) than those obtained for uncorrected counterparts (0.84 and 0.42 respectively). A plausible explanation is the (plasma protein) binding-restricted tissue distribution and hepatic extraction, which seem to affect the PK-AS relationships and lower the allometric coefficients for uncorrected Vd_{ss} and CL_{tot}.

Table 10.4 - Allometric PK Scaling of BZD - Log Vd_{ss} vs. Log BW

Compound	n	BW range (kg)	r^2	Slope ± SE
Chlordiazepoxide	2	12 - 70	.	0.84
Clonazepam	2	0.02 - 70	.	0.91
Diazepam	6	0.25 - 70	0.93	0.94 ± 0.13
N-DMD	3	4 - 70	0.99	1.05 ± 0.05
Lorazepam	2	2.5 - 70	.	0.92
Midazolam	3	0.25 - 70	0.98	0.90 ± 0.12
Triazolam	3	0.25 - 70	0.99	0.75 ± 0.03
Oxazepam	3	0.25 - 70	0.99	0.81 ± 0.09
Flumazenil	2	10 - 70	.	0.48
		Mean Slope ± SD (n = 9)		***0.84 ± 0.16***

Figure 10.3 - Diazepam: log (Vd_{ss} in l) vs. log (BW in kg) in Various Animal Species

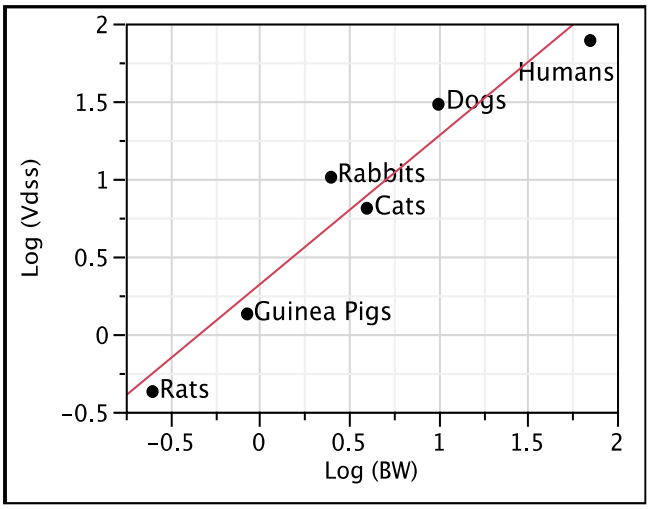

Table 10.5 - Allometric PK Scaling of BZD - log Vd_{ss}^{u} vs. Log BW

Compound	n	BW range (kg)	r^2	Slope ± SE
Diazepam	5	0.25 - 70	0.99	1.3 ± 0.03
N-DMD	3	4 - 70	0.99	1.6 ± 0.03
Midazolam	3	0.25 - 70	0.99	0.84 ± 0.08
Triazolam	2	0.25 - 70	.	1.1
Oxazepam	3	0.25 - 70	0.99	0.90 ± 0.08
		Mean Slope ± SD (n=5)		***1.1 ± 0.32***

Figure 10.4 - Diazepam: log (Vd_{ss}^{u} in l) vs. log (BW in kg) in Various Animal Species

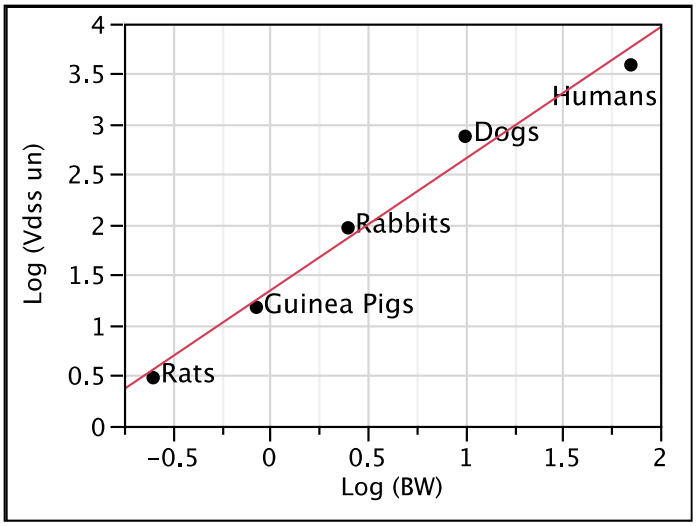

Table 10.6 - Allometric PK Scaling of BZD - log CL_{tot} vs. log BW

Compound	n	BW range (kg)	r^2	Slope ± SE
Chlordiazepoxide	2	12 - 70	.	-0.30
Clonazepam	2	0.02 - 70	.	0.56
Diazepam	6	0.25 - 70	0.11	0.17 ± 0.24
N-DMD	3	4 - 70	0.18	0.42 ± 0.90
Lorazepam	2	2.5 - 70	.	0.13
Midazolam	3	0.25 - 70	0.99	0.60 ± 0.06
Triazolam	3	0.25 - 70	0.99	0.49 ± 0.05
Oxazepam	3	0.25 - 70	0.96	0.47 ± 0.06
Temazepam	2	6 - 70	.	0.36
Flumazenil	2	10 - 70	.	0.52
		Mean Slope* ± SD (n = 9)		***0.42 ± 0.17***

**Excluding Chlordiazepoxide*

Figure 10.5 - Diazepam: log (CL_{tot} in ml/min) vs. log (BW in kg) in Various Animal Species

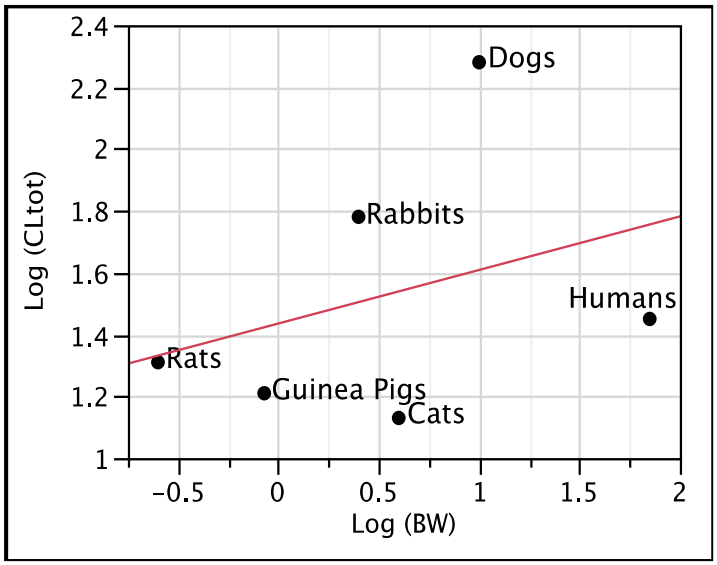

Table 10.7 - Allometric PK Scaling of BZD - log CL_{tot}^{u} vs. log BW

Compound	n	BW range (kg)	r^2	Slope ± SE
Diazepam	5	0.25 - 70	0.64	0.53 ± 0.23
N-DMD	3	4 - 70	0.54	0.97 ± 0.88
Midazolam	3	0.25 - 70	0.93	0.54 ± 0.14
Triazolam	2	0.25 - 70	.	0.80
Oxazepam	3	0.25 - 70	0.99	0.56 ± 0.14
		Mean Slope ± SD (n = 5)		***0.68 ± 0.20***

Figure 10.6 - Diazepam: log (CL_{tot}^{u} in ml/min) vs. log (BW in kg) in Various Animal Species

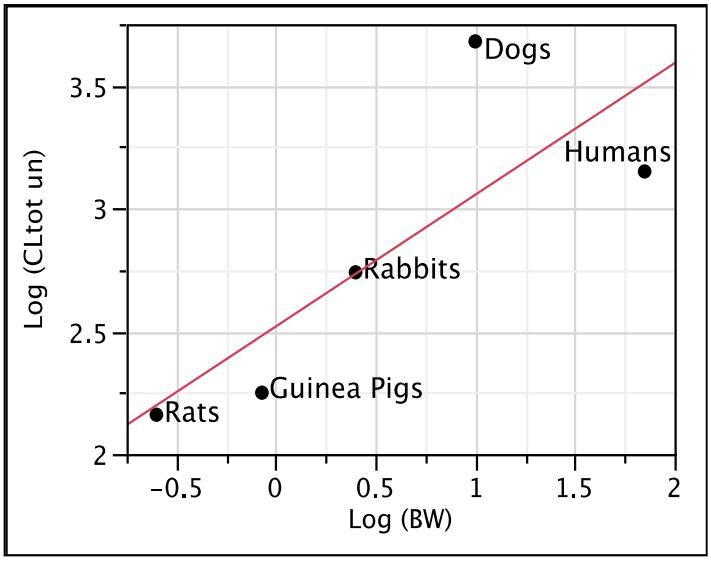

10.1.3. Prediction Methods

Single-species methods:

BW-Based Scaling:

This method assumes an AS exponent of 1.0 for both Vd_{ss} (and Vd_{ss}^{u}) as well as CL_{tot} (and CL_{tot}^{u}). However, as discussed above, although the mean AS exponents for Vd_{ss} and Vd_{ss}^{u} are comparable to 1.0, the mean AS exponents for CL_{tot} and CL_{tot}^{u} are lower than 1.0, suggesting that the CL_{tot} and CL_{tot}^{u} predictions will be prone to errors. Single-species BW-based predictions (and % prediction errors, %PE) of Vd_{ss}, Vd_{ss}^{u}, CL_{tot} and CL_{tot}^{u} for individual BZD in the common preclinical species with available information are shown in Tables 10.8, 10.10, 10.12 and 10.14 respectively. Additionally, bias (measured by % mean prediction error, MPE) and imprecision (measured by % root mean square error, RMSE) and number of compounds (and percentage of predictions) within 'acceptable' range of -50% to 100% are summarized in Tables 10.9, 10.11, 10.13 and 10.15 for Vd_{ss}, Vd_{ss}^{u}, CL_{tot} and CL_{tot}^{u}, respectively.

BW-based scaling of Vd_{ss} for BZD shows systematic positive bias, i.e., consistent over-prediction, regardless of the species used. However, after correcting for f_u, Vd_{ss}^{u} for BZD shows significant improvement in the MPE in all the species, and a slightly higher percentage of the compounds within the acceptable range of MPE - if cat and dog PK is used for the prediction of Vd_{ss}^{u}, compared to the Vd_{ss} predictions (although this is based on a limited sample size). This suggests that the prediction of Vd_{ss}^{u} is improved after accounting for interspecies differences in PPB. BW-based scaling of CL_{tot} for BZD also shows a systemic bias (much higher than for Vd_{ss}) regardless of the species used. Likewise, after correcting for f_u, CL_{tot}^{u} for BZD shows significant improvement in MPE in all species, but still, consistently overpredicting from rats and dogs.

The plausible explanation for this can be because (a) the underlying assumption of AS exponent for single-species based approaches is equal to 1.0, which is not the case for BZD as discussed above; and (b) even after correcting for species differences in PPB, there are qualitative/quantitative species differences in clearance mechanisms, independent of body size. CL_{tot}^{u} predictions from cats, however, are acceptable for all the three compounds with available information in the current dataset.

LBF-Based Scaling:

The results CL_{tot} and CL_{tot}^{u} predictions for individual compounds based on LBF scaling are shown in Table 10.16 and 10.18, respectively, while prediction errors, bias and imprecision are summarized in Table 10.17 and 10.19, respectively.

The AS exponent for LBF across different species is 0.85 (see Chapter 9), which is lower than that assumed for BW-based scaling (1.0). Therefore, in general, the prediction errors obtained from LBF-based scaling are relatively lower than those obtained from BW-based scaling but still were unacceptable.

Two-species methods:

Due the limited availability of in-vivo systemic PK data in a sufficient number of animal species for most of the BZD in the database (only five BZD), the results for the two-species PK-AS approaches could not be interpreted adequately.

Table 10.8 - Prediction of Human Vd_{ss} - BW based Scaling

Compound	From Rats PK			From Cats PK			From Dogs PK		
	Obs.	**Pred.**	**%PE**	**Obs.**	**Pred.**	**%PE**	**Obs.**	**Pred.**	**%PE**
Diazepam	77	119	**55%**	77	112	**45%**	77	1330	1627%
NDMD				84	70	**-17%**	84	84	**0%**
Midazolam	70	126	**80%**	70	168	140%			
Triazolam	42	175	317%	42	98	133%			
Chlordiazepoxide							27	36	**33%**
Flumazenil							63	175	178%
Oxazepam	42	133	217%				42	98	133%

Table 10.9 - Summary of Predictions of Human Vd_{ss} - BW based Scaling

Species	n	Prediction Error		No. of Compounds in -50% to 100% error range
		Bias	**Imprecision**	
		%MPE	**%RMSE**	
Rats PK	4	167 (± 61%)	198	2/4 (**50%**)
Cats PK	4	75 (± 38%)	100	2/4 (**50%**)
Dogs PK	5	394 (± 310%)	735	2/5 (**40%**)

Table 10.10 - Prediction of Human Vd_{ss}^{u} - BW based Scaling

Compound	From Rats PK			From Cats PK			From Dogs PK		
	Obs.	**Pred.**	**%PE**	**Obs.**	**Pred.**	**%PE**	**Obs.**	**Pred.**	**%PE**
Diazepam	3850	850	-78%				3850	5250	**36%**
NDMD				2800	500	-82%	2800	840	-70%
Midazolam	1750	4200	140%	1750	1867	**7%**			
Triazolam				3812	297	**-22%**			
Oxazepam	840	1478	**76%**				840	980	**17%**

Table 10.11 - Summary of Predictions of Human Vd_{ss}^{u} - BW based Scaling

Species	n	Prediction Errors		No. of Compounds in -50% to 100% error range
		Bias	**Imprecision**	
		%MPE	**%RMSE**	
Rats PK	3	46 (± 65%)	103	1/3 (**33%**)
Cats PK	3	-32 (± 26%)	49	2/3 (**66%**)
Dogs PK	3	-10 (± 33%)	53	2/3 (**66%**)

Table 10.12 - Prediction of Human CL_{tot} - BW based Scaling

Compound	From Rats PK			From Cats PK			From Dogs PK		
	Obs.	**Pred.**	**%PE**	**Obs.**	**Pred.**	**%PE**	**Obs.**	**Pred.**	**%PE**
Temazepam				98	455	364%			
Diazepam	28	5712	20300%	28	238	750%	28	1330	4650%
NDMD				14	35	150%	14	35	150%
Midazolam	490	5061	933%	490	2114	331%			
Triazolam	196	3500	1686%	196	1050	436%			
Chlordiazepoxide							31	306	893%
Flumazenil							1036	2618	153%
Oxazepam	77	1680	2082%				77	357	364%

Table 10.13 - Summary of Predictions of Human CL_{tot} - BW based Scaling

Species	n	Prediction Errors		No. of Compounds in -50% to 100% error range
		Bias	Imprecision	
		%MPE	%RMSE	
Rats PK	4	6250 (± 4689%)	10249	0/4 (**0%**)
Cats PK	5	406 (± 98%)	451	0/5 (**0%**)
Dogs PK	5	1242 (± 828%)	2126	0/5 (**0%**)

Table 10.14 - Prediction of Human CL_{tot}^{u} - BW based Scaling

Compound	From Rats PK			From Cats PK			From Dogs PK		
	Obs.	**Pred.**	**%PE**	**Obs.**	**Pred.**	**%PE**	**Obs.**	**Pred.**	**%PE**
Diazepam	1400	40800	2814%				1400	33250	2275%
NDMD				467	250	**-46%**	466.7	3150	575%
Midazolam	12250	168700	1277%	12250	23500	**92%**			
Triazolam				1782	3182	**79%**			
Oxazepam	1540	18667	1112%				1540	3570	132%

Table 10.15 - Summary of Predictions of Human CL_{tot}^{u} - BW based Scaling

Species	n	Prediction Errors		No. of Compounds in -50% to 100% error range
		Bias	Imprecision	
		%MPE	%RMSE	
Rats PK	3	1734 (± 542%)	1896	0/3 (**0%**)
Cats PK	3	42 (± 44%)	75	3/3 (**100%**)
Dogs PK	3	994 (± 653%)	1357	0/3 (**0%**)

Table 10.16 - Prediction of Human CL_{tot} - LBF based Scaling

Compound	From Rats PK			From Cats PK			From Dogs PK		
	Obs.	**Pred.**	**%PE**	**Obs.**	**Pred.**	**%PE**	**Obs.**	**Pred.**	**%PE**
Diazepam	28	9	-69%	28	122	335%	28	133	375%
NDMD				14	18	**28%**	14	26	**87%**
Midazolam	490	8	-98%	490	1083	121%			
Triazolam	196	5	-97%	196	538	174%			
Chlordiazepoxide							31	37	**19%**
Flumazenil							1036	262	-75%
Oxazepam	77	2	-97%				77	36	-54%
Temazepam				98	233	138%			

Table 10.17 - Summary of Predictions of Human CL_{tot} - LBF based Scaling

Species	n	Prediction Errors		No. of Compounds in -50% to 100% error range
		Bias	Imprecision	
		%MPE	%RMSE	
Rats PK	4	-90 (± 7%)	91	0/4 (0%)
Cats PK	5	159 (± 206%)	188	1/5 (**20%**)
Dogs PK	5	70 (± 81%)	177	2/5 (**40%**)

Table 10.18 - Prediction of Human CL_{tot}^{u} - LBF based Scaling

Compound	From Rats PK			From Cats PK			From Dogs PK		
	Obs.	**Pred.**	**%PE**	**Obs.**	**Pred.**	**%PE**	**Obs.**	**Pred.**	**%PE**
Diazepam	1400	61	-96%				1400	3325	138%
NDMD				467	128	-73%	467	261	**-44%**
Midazolam	12250	253	-98%	12250	12031	**-2%**			
Triazolam				1782	1630	**-9%**			
Oxazepam	1540	28	-98%				1540	357	-77%

Table 10.19 - Summary of Predictions of Human CL_{tot}^{u} - LBF based Scaling

Species	n	Prediction Errors		No. of Compounds in -50% to 100% error range
		Bias	Imprecision	
		%MPE	%RMSE	
Rats PK	3	-97 (± 1%)	97	0/3 (0%)
Cats PK	3	-28 (± 92%)	42	2/3 (**66%**)
Dogs PK	3	6 (± 67%)	95	1/3 (**33%**)

Table 10.20 - Predictions based Two Species Method - Cats and Dogs

Compound	Human CL_{tot} (ml/min)			Human CL_{tot}^{u} (ml/min)			Human Vd_{ss} (L)			Human Vd_{ss}^{u} (L)		
	Obs.	**Pred.**	**%PE**	**Obs.**	**Pred.**	**%PE**	**Obs.**	**Pred.**	**%PE**	**Obs.**	**Pred.**	**%PE**
Diazepam	28	51393	183448%				77	798	936%			
N-DMD	14	192994	1378426%	467	5158616	1105318%	84	143	**70%**	2800	3823	**37%**

Table 10.21 - Prediction based on Two Species Method - Cats and Rats

Compound	Human CL_{tot} (ml/min)			Human CL_{tot}^{u} (ml/min)			Human Vd_{ss} (L)			Human Vd_{ss}^{u} (L)		
	Obs.	**Pred.**	**%PE**	**Obs.**	**Pred.**	**%PE**	**Obs.**	**Pred.**	**%PE**	**Obs.**	**Pred.**	**%PE**
Diazepam	28	9	-68%				77	105	**37%**			
Midazolam	490	858	**75%**	12250	3070	-75%	70	226	223%	1750	808	-54%
Triazolam	196	303	**55%**				42	54	**28%**			

Table 10.22 - Prediction based on Two Species Method - Rats and Dogs

Compound	Human CL_{tot} (ml/min)			Human CL_{tot}^{u} (ml/min)			Human Vd_{ss} (L)			Human Vd_{ss}^{u} (L)		
	Obs.	**Pred.**	**%PE**	**Obs.**	**Pred.**	**%PE**	**Obs.**	**Pred.**	**%PE**	**Obs.**	**Pred.**	**%PE**
Diazepam	28	616	2101%	1400	29833	2031%	77	283	268%	3850	13719	256%
Oxazepam	77	158	105%	1540	1492	**-3%**	42	83	**99%**	840	789	**-6%**

10.2. Discussion

There are large differences in the reported, BW-corrected, CL_{tot} and Vd_{ss} values across various preclinical species with available information (range 1 - 200 fold and 1 - 17 fold respectively). Furthermore, *in-vitro* f_u values for most BZD with available information also show interspecies differences in PPB, i.e., in general, larger animal species showing lower f_u; e.g., diazepam shows a negative allometric relationship with BW (shown in Figure 10.1).

In general, BZD are relatively small MW acids and bases, which are mostly lipophilic ($logD_{7.4}$ > 1.0, except for N-DMAD) and unionized at physiological pH. The two main plasma proteins to which the drugs bind are α-acid glycoprotein (AAG, which binds with weakly basic drugs), and albumin (which binds with weakly acidic and neutral drugs). The concentrations of these plasma proteins is known to be different across the animal species[55] (see Chapter 9). Age and gender are important covariates that could potentially affect PPB, especially the concentration of plasma proteins[119,120]. Therefore, these factors may contribute to the observed interspecies differences in PPB, if the life-span expectancy (and/or gender) is not considered while AS. Lastly, the observed species differences in PPB may also reflect qualitative differences[121] in binding affinity and/or the number of binding sites on the protein molecule. Sawada et al[122] studied PPB of ten basic drugs across various preclinical species and reported that the interspecies differences in distribution may be attributed to differences in f_u.

Categorization of BZD based on their hepatic extraction suggests that certain BZD, e.g., temazepam, diazepam, midazolam, triazolam, etc., show higher ER_{hep} in smaller animal species and lower ER_{hep} in larger animal species. A plausible explanation for this finding is (plasma protein) binding-restricted hepatic extraction (low ER_{hep}) in larger animal species, e.g., humans, for certain BZD, e.g., diazepam. Furthermore, the underlying assumptions in the estimation of

(and categorization of compounds based on) hepatic extraction ratio are (a) the renal elimination is considered negligible, and (b) systemic CL_{tot} in plasma is considered to be equivalent to CL_{nonren}^{blood}, that is, there are no interspecies differences B:P ratio and also that there is/are no extrahepatic clearance pathway(s). Diazepam has been extensively studied across various preclinical species and it is reported to show[123] (a) different values of B:P in different species and (b) the systemic CL_{tot} exceeds the LBF in rats, suggesting there are extrahepatic pathways unlike other species. Similarly, systemic CL_{tot} exceeds LBF in dogs for flumazenil[124], suggesting extrahepatic clearance pathway(s). Boxenbaum et al[125] investigated PK of BZD (n = 12) in humans and dogs and reported that, in general, they exhibit greater tissue distribution and are metabolized more rapidly in dog than in man. Most of BZD are subject to phase I metabolism e.g., CYP3A, CYP2D isoforms while lorazepam undergoes phase II metabolism by glucuronidation via UGTs. Both qualitative (e.g., genetic polymorphisms, substrate specificity, catalytic activity, etc.) as well as quantitative differences (expression levels of the enzyme, etc.) in CYP isoforms[45–47] and UGTs[126] has been widely documented in literature.

The mean (range, n) AS coefficients for Vd_{ss} and Vd_{ss}^{u} are found to be 0.84 (0.48 - 1.1, 9) and 1.1 (0.90 - 1.6, 5), respectively, and both of them are comparable to 1.0, which the various physiological body compartments, namely, total body water, intracellular and extracellular water, plasma and blood volumes across the animal species (see Chapter 9). The plausible explanation for such an occurrence may be attributed to the lipophilic nature of most of BZD, because of which they undergo moderate to extensive extravascular distribution/binding to membranes/tissues across the various preclinical species.

Mean (range, n) AS coefficients for CL_{tot} and CL_{tot}^{u} for BZD with available information in various animal species scales with exponents 0.42 (0.13-0.60, n = 9) and 0.68 (0.53-0.97, n = 5),

suggesting there are qualitative and/or quantitative interspecies differences in intrinsic (hepatic/metabolic) clearance that are independent of body size even after accounting for the interspecies differences in PPB. Mahmood et al[117] reported AS exponents for systemic CL_{tot} ranging between 0.42 to 1.2 for heterogeneous dataset of fifty compounds that were administered by I.V route to various animal species including humans.

BW-based scaling of Vd_{ss} for BZD shows systematic positive bias, i.e., consistent over-prediction, compared to Vd_{ss} predictions, regardless of the species used. However, after correcting for f_u, Vd_{ss}^u prediction shows significant improvement in accuracy and precision of the predictions from all species as well as higher r^2, indicating better goodness of fit and a slightly higher percentage of the compounds within the acceptable range of MPE - if cat and dog PK was used for prediction of Vd_{ss}^u,. BW-based scaling for CL_{tot} for BZD also shows a systemic bias (much higher than for Vd_{ss}) regardless of the species used. Likewise, after correcting for f_u, CL_{tot}^u for BZD shows significant improvement in the accuracy and precision of prediction from all species, higher r^2 but still consistently overpredicting from rats and dogs. Overall, the number of acceptable predictions for Vd_{ss} and Vd_{ss}^u seem to be relatively higher than those compared to CL_{tot} and CL_{tot}^u for BW-based scaling (which is expected because of implicit assumption of 1.0 that is not true with BZD in the current dataset).

LBF has been shown to scale across several species (n = 11), including humans with AS exponent of 0.85[127]. Because of the limited sample size, adequate interpretation could not made for LBF-based predictions. However, within the limitation of a small sample size, in general, (a) the prediction errors in CL_{tot} and CL_{tot}^u seem to be lower for LBF-based scaling compared to BW-based scaling, possibly owing relatively higher AS exponent (implicit) assumption of 0.85

compared to 1.0 respectively; and (b) PPB correction seem to improve the prediction errors and also higher number of acceptable predictions.

LBF-based predictions are more likely to be accurate if the drugs show high ER_{hep} (i.e., flow-limited hepatic clearance[127]) across all animal species. However, intrinsic species differences in PPB and/or ER_{hep} are particularly evident for BZD. Thus, overall, neither CL_{tot} nor CL_{tot}^{u} was predicted adequately for BZD based on BW- or LBF-based scaling, suggesting intrinsic quantitative and/or qualitative species differences in hepatic metabolism and/or B:P ratios that are independent of size.

Ward et al[10] investigated the BW-based prediction of human systemic Vd_{ss} from respective values in preclinical species (i.e., I.V administration in all animal species including humans), for a heterogeneous dataset of 103 compounds; they found that predictions across the compounds were within 1.4, 1.3 and 1.0-fold error range when rats, dogs and monkeys' systemic Vd_{ss} values were used for prediction, respectively. In a study carried out by Obach et al[3], human systemic Vd_{ss} was predicted from dog systemic Vd_{ss} (collected after I.V administration in both the species) for 16 compounds from Pfizer's proprietary database by BW-based scaling methods, i.e., assuming AS exponent of 1.0. They reported that 81% of the compounds (13 of 16) were within the 2-fold error range and concluded that human systemic Vd_{ss} can be predicted reasonably well from systemic dog Vd_{ss}. Tang et al[128] investigated using a heterogeneous database of 102 compounds (57 metabolized by liver - 29 low, 17 intermediate and 11 high ER_{hep}; 33 excreted by kidneys; and 11 by both renal and metabolism), for the prediction of human systemic CL_{tot} from rats and they reported two potential rules for the occurrence of large overprediction, (1) ratio of unbound fraction of drug in plasma (f_u) between rats and humans greater than 5; and (2) (predicted) logP greater than 2. They also concluded that metabolic

elimination could also serve as an additional indicator for expecting large vertical allometry. BZD within the dataset with available information on f_u in rats and humans, diazepam shows large vertical allometry and meets both these criteria. Tang et al[129] investigated the role of the selection of "best" or optimal combination of preclinical species by carrying out Monte Carlo simulations for different combinations and found that the predicted values were heavily dependent on certain species like dog, whereas, parameter values from rat made no contribution to the predicted human values, as long as the rat was not the smallest species used. In the prediction of human systemic Vd_{ss}, $Vd_{ss}{}^{u}$, CL_{tot} and $CL_{tot}{}^{u}$ of BZD within the dataset with available information, cats, in general, seems to show better (acceptable) predictions compared to other preclinical species.

CHAPTER 11. INTERSPECIES SCALING OF NMB

11.1. Results

11.1.1. Comparative PK of NMB

The final preclinical systemic PK database consists of six NMB, including one metabolite, Org 7268 (Vecuronium metabolite), all having the aminosteroid structural scaffold, mostly in cats (and dogs for Pipercuronium). For these six NMB, there was information on urinary excretion data but PPB values were not found in the literature. There are considerable interspecies differences in the reported BW-corrected *in-vivo* systemic animal PK properties (shown in Table 11.1), namely, CL_{tot} (2 to 10 fold) while Vd_{ss} and CL_{ren} were comparable (except for CL_{ren} of pipercuronium) to respective *in-vivo* human systemic PK.

Table 11.1 - Summary of *In-vivo* Systemic PK of NMB Cats (&Dogs)

	Species	**Vd_{ss} (L/kg)**	**CL_{tot} (ml/min/kg)**	**f_e (%)**	**CL_{ren} (ml/min/kg)**	**CL_{nonren} (ml/min/kg)**	**ER_{hep}****
Rocuronium	Cats	0.25	31	2.0%	0.56	30	High
	Humans	0.21	3.5	25%	0.88	2.6	
Org 9489	Cats	0.19	33	5.0%	1.8	31	High
	Humans	0.46	5.8	8.0%	0.46	5.3	
Org 9453	Cats	0.14	35	3.0%	1.1	34	High
	Humans	0.18	6.9	5.0%	0.35	6.6	
Org 7268	Cats	0.22	58	4.0%	2.1	56	Extrahepatic?
	Humans	0.26	4.3	18%	0.77	3.5	
Vecuronium	Cats	0.23	12	14%	1.7	10	Low
	Humans	0.20	5.0	7.0%	0.35	4.7	
Pipercuronium	Cats	0.36	5.0	54%	2.7	2.3	Low
	Dogs	0.30	6.0	78%	4.7	1.3	Low
	Humans	0.32	2.6	41%	1.1	1.5	

***ER_{hep} is estimated as CL_{nonren}/LBF, and the cut-off are discussed in Table 3.2; LBF in cats is 41 ml/min/kg*

11.1.2. Prediction Methods

Single-species methods:

BW-Based Scaling:

The results of BW-based scaling of human systemic Vd_{ss} and CL_{tot} from the respective cat PK variables are shown in Table - 11.1 and summarized in Table - 11.2. Except for Org 9489, all Vd_{ss} predictions for the remaining NMB in the dataset are within the acceptable range. The plausible mechanistic explanation for such a high percentage (83%) of acceptable BW-based prediction of Vd_{ss} of the compounds within the dataset could be due to the limited extravascular distribution of NMB both in humans as well as preclinical species, potentially due to their large MW and/or (positively charged) hydrophilic nature. Further, the systematic bias is found to be insignificant and the imprecision in predictions for Vd_{ss} is quite low (< 30%).

On the other hand, none of the CL_{tot} predictions for NMB in the current dataset, except Pipercuronium, are within the acceptable range. Also, there is a significant positive systematic bias (i.e., consistent over-prediction) and high imprecision in the CL_{tot} predictions. This suggests that even after correcting for BW, there are interspecies differences in CL_{tot}. After accounting for the individual clearance pathways, i.e., renal and nonrenal, it is evident from Table - 11.1 that, the interspecies differences are more likely to exist in the nonrenal pathways, since the BW-corrected CL_{ren} are comparable between cats/dogs and humans for most of the NMB within the dataset. Mechanistically, apart from potential species differences in hepatobiliary clearance pathways, cats may also show certain extrahepatic clearance pathways (unlike humans), evident from CL_{nonren} values for certain NMB, which exceed the LBF. Also, BW-based scaling implies

an AS exponent of 1.0, which may or may not hold true for NMB (with the available information for limited number of NMB and only in cats, it is difficult to estimate the AS exponent for CL_{tot}).

LBF-Based Scaling:

The results for LBF-based human systemic CL_{tot} predictions from cats are shown in Table - 11.3 and summarized in Table - 11.4 below. There is a significant positive systematic bias (i.e., consistent over-prediction) and high imprecision in the CL_{tot} predictions. It is observed that most of the NMB in the current dataset (except pipercuronium) are primarily cleared by nonrenal pathways (i.e., relatively low CL_{ren}) in cats (which is the underlying assumption for the LBF-based prediction method). The plausible mechanistic explanation for unacceptable, consistent (positively) biased and imprecise LBF-based predictions for CL_{tot} could be due to the significant qualitative and/or quantitative interspecies differences in CL_{tot}, more specifically in CL_{nonren}.

The results of LBF-based human CL_{nonren} predictions from cats are shown in Table - 11.5 and summarized in Table - 11.6 below. There is a significant positive systematic bias (i.e., consistent over-prediction) and high imprecision in CL_{nonren} predictions. The imprecision in the CL_{nonren} predictions is higher than those obtained for CL_{tot} predictions, suggesting that there are potential qualitative and/or quantitative interspecies differences. The CL_{nonren} value for Org 7268 in cats exceed the LBF, suggesting it may be subject to extrahepatic pathways. Assuming that there are no significant extrahepatic clearance pathways, the CL_{nonren} values for the rest of NMB in cats, rocuronium, Org 9489 and Org 9453 approach the LBF, suggesting that they are likely to be intermediate - high ER_{hep} drugs, while vecuronium and pipercuronium are low ER_{hep} drugs in cats. On the other hand, CL_{nonren} values for all the NMB in the current dataset are lower than LBF, suggesting that they are likely to be low ER_{hep} drugs.

GFR-Based Scaling:

The results for GFR-based human systemic CL_{ren} predictions from cats are shown in Table - 11.7 and summarized in Table - 11.8 below. The majority (67%) of GFR-based CL_{ren} predictions for NMB in the current dataset are within the acceptable range. Additionally, there was significant positive bias, i.e., consistent overprediction and high imprecision. The plausible mechanistic explanation is the 1.5- to 3.4- fold difference with respect to cats and dogs in the GFR relative to that in humans (more specifically, species differences[55,130] in the number of nephrons per kg of BW).

Table 11.2 - Prediction of Human Systemic PK - BW-Based Scaling From Cat PK

Compound	CL_{tot}			Vd_{ss}		
	Obs.	**Pred.**	**%PE**	**Obs.**	**Pred.**	**%PE**
Rocuronium	245	2170	786%	15	18	**19%**
Org 9489	406	2310	469%	32	13	-59%
Org 9453	483	2450	407%	13	10	**-22%**
Org 7268	301	4060	1249%	18	15	**-15%**
Vecuronium	350	826	136%	14	16	**15%**
Pipercuronium	182	350	**92%**	22	25	**13%**
***** In Dogs***	*182*	*413*	*127%*	*22*	*21*	***-6%***

Table 11.3 - Summary of BW - Based Predictions of Human Systemic PK Variables

PK Variable	n	Prediction Errors		No. of Compounds in -50% to 100% error range
		Bias	**Imprecision**	
		%MPE	**%RMSE**	
CL_{tot}	6	523 (± 178%)	657	1/6 (**17%**)
Vd_{ss}	6	-8 (± 12%)	29	5/6 (**83%**)

Table 11.4 - Prediction of Human CL_{tot} - LBF-Based Scaling

Compound	Obs.	Pred.	%PE
Rocuronium	3.5	16	354%
Org 9489	5.8	17	191%
Org 9453	6.9	18	160%
Org 7268	4.3	30	591%
Vecuronium	5.0	6.2	**23%**
Pipercuronium	2.6	2.6	**-2%**
*****In Dogs***	*2.6*	*4.2*	***62%***

Table 11.5 - Summary of CL_{tot} Predictions - LBF-Based Scaling From Cat PK

PK Variable	n	Prediction Errors		No. of Compounds in -50% to 100% error range
		Bias	Imprecision	
		%MPE (± SE)	%RMSE	
CL_{tot}	6	220 (± 91%)	299	2/6 (**33%**)

Table 11.6 - Prediction of Human CL_{nonren} - LBF-Based Scaling

Compound	Obs.	Pred.	%PE
Rocuronium	2.62	15.59	495%
Org 9489	5.34	15.99	199%
Org 9453	6.55	17.39	165%
Org 7268	3.53	28.63	711%
Vecuronium	4.65	5.30	**14%**
Pipercuronium	1.53	1.19	**-22%**
*****In Dogs***	*1.53*	*0.92*	***-40%***

Table 11.7 - Summary of CL_{nonren} Predictions - LBF-Based Scaling From Cat PK

PK Variable	n	Prediction Errors		No. of Compounds in -50% to 100% error range
		Bias	Imprecision	
		%MPE (± SE)	%RMSE	
CL_{tot}	6	260 (± 117%)	369	2/6 (**33%**)

Table 11.8 - Prediction of Human CL_{ren} - GFR-Based Scaling

Compound	Obs.	Pred.	%PE
Rocuronium	0.88	0.25	-72%
Org 9489	0.46	0.80	**74%**
Org 9453	0.35	0.47	**34%**
Org 7268	0.77	0.95	**23%**
Vecuronium	0.35	0.74	111%
Pipercuronium	1.1	1.2	**13%**
*****In Dogs***	*1.1*	*1.2*	***31%***

Table 11.9 - Summary of CL_{ren} Predictions - GFR - Based Scaling From Cat PK

PK Variable	n	Prediction Errors		No. of Compounds in -50% to 100% error range
		Bias	Imprecision	
		%MPE (± SE)	%RMSE	
CL_{ren}	6	31 (± 25%)	64	4/6 (**67%**)

11.2. Discussion

Overall, the prediction of human systemic Vd_{ss} of NMB from respective cat PK seem to be the most accurate (i.e., lowest bias and imprecision) compared to (BW-based and LBF-based) CL_{tot} and (GFR-based) CL_{ren} predictions. The plausible explanation could be due to the limited extravascular distribution of NMB both in humans as well as preclinical species, owing to large size and (positively charged) hydrophilic nature at physiological pH.

The bias and imprecision of CL_{tot} predictions were lower for LBF-based scaling relative to BW-based scaling, suggesting that hepato(biliary) route(s) could be the major clearance pathways while the contribution of renal clearance be low. However, the predictions are still biased and imprecise, suggesting likely qualitative and/or quantitative differences in the clearance mechanisms, e.g., few NMB show extra-hepatic pathways (as evident from plasma CL_{nonren} values exceeding the LBF, assuming B:P ratio close to 1.0) in cats.

Within the limitation of a small sample size, majority of the GFR-based CL_{ren} predictions were acceptable, possibly because they are all subject to net tubular reabsorption (CL_{ren} values lower than the respective GFR values, assuming that NMB show negligible PPB), but they are biased and imprecise, potentially due to differences in the GFR.

11.3. Summary of AS-PK Findings - Comparison with BZD

NMB and BZD differ dramatically in their respective PC/molecular and human systemic PK property spaces (see chapter 8). In general, BZD, are relatively small MW, weakly acidic or basic, unionized (at physiological pH of 7.4) lipophilic compounds, while, NMB, are relatively large MW, weakly basic, positively charged (at physiological pH of 7.4) hydrophilic compounds. For both classes the prediction of human systemic PK from preclinical species seem to be

relatively better for Vd_{ss} (using BW-based scaling) compared to the CL_{tot} (BW-based or LBF-based scaling). NMB show higher percentage of predictions within the acceptable range for BW-based scaling of Vd_{ss} (using cats), which is mechanistically plausible because of their limited extravascular distribution owing to the PC/molecular properties discussed above, unlike BZD, which undergo moderate to extravascular tissue distribution/binding to membranes possibly because of their PC molecular property space discussed above.

For NMB with available information in total systemic clearance in cats encompasses renal and hepatobiliary pathways, while for BZD there is inadequate information in the literature about the detailed mechanisms involved in the systemic CL_{tot}. Overall, majority of the BW-based systemic CL_{tot} (or CL_{tot}^{u}) predictions from preclinical species were systematically (positively) biased and unacceptable (except from cats) suggesting even after correcting for species differences in PPB, there are qualitative/quantitative species differences in clearance mechanisms, independent of body size. Similar results were obtained for NMB, suggesting the positively biased and imprecise BW-based systemic CL_{tot} predictions could be due to the significant qualitative and/or quantitative interspecies differences in CL_{tot}, more specifically in CL_{nonren} as the CL_{ren} values were comparable for majority of them between cats and humans.

CHAPTER 12. COMPARATIVE ANALYSIS ACROSS PHARMACOLOGICAL CLASSES OF COMPOUNDS

12.1. Comparison of the QSPKR Relationships Across Pharmacological Classes

Overall, QSPKR of a total of eight pharmacological classes of compounds, namely, BZD, NMB, TRP and Class III AAR (in this research project); opioids, β-ARLs and β-LAs; and CCB have been investigated so far in this and previous research[109,110]. For the purpose of comparison of these relationships across classes, they are first grouped based on the molecular/PC property space as follows:

a) Group I: consisting of BZD and CCB, the majority of which are of relatively low MW and lipophilic;
b) Group II: consisting of heterogeneous pharmacological classes of Class III AAR, opioids and β-ARLs, which are of low to intermediate MW and include both hydrophilic as well as lipophilic compounds (although the former two classes are slightly skewed towards more lipophilic ones), and
c) Group III: consisting of TRP, NMB and β-LAs, the majority of which are hydrophilic compounds, but vary in MW ranging from low (TRP) - intermediate/high (β-LAs and NMB).

Next, the slope (or sensitivity) of the QSPKR relationships, i.e., *in-vivo* systemic as well as biologically relevant PK variables as a function of the molecular/PC variables is compared across these eight pharmacological classes, primarily focusing on the effects of $logD_{7.4}$ and MW (as they were found to be the major determinants affecting the systemic disposition across

classes). Additionally, mechanistic plausibility and the potential significance of these relationships is also discussed.

12.1.1. Effect of Molecular/PC Variables on f_u Across Pharmacological Classes

The effect of molecular/PC variables, namely, $logD_{7.4}$ and MW on PPB (i.e., f_u) across the eight pharmacological classes of compounds, which are categorized by different groups I - III is shown in Table 12.1.

Within group I, the trend is similar (i.e., negative) in direction, suggesting that for small MW, lipophilic compounds such as BZD and CCB, an increase in $logD_{7.4}$ is associated with increase in PPB (or decrease in f_u). However, the slope (or the sensitivity) of this relationship seems to be (relatively) steeper for CCB than BZD, potentially because CCB in general, are (a) relatively more lipophilic ($logD_{7.4}$ ranges from 1.5 to 5.1, n = 14 compared to 0.75 to 3.8, n = 20 for BZD) and/or (b) on an average, they are highly PPB and also show limited range (f_u ranges from 0.20 to 20%, n = 13 compared to 2.0 to 65%, n = 17 for BZD) compared to BZD (and also to compounds belonging to other groups II and III).

Within group II, the trend seems to be consistent both in direction and magnitude. This is mechanistically plausible because of the heterogeneous nature of the molecular/PC as well as *in-vitro* PPB property space for these three classes of compounds, namely, Class III AAR (f_u ranges between 1.0 - 99%, n = 7), opioids (f_u ranges between 4.0 - 92%, n = 29) and β-ARLs (f_u ranges between 3.0 - 96%, n = 57).

Class III AAR within group II shows a significant negative association between f_u and MW; the likely explanation for this trend is the high correlation between $logD_{7.4}$ and MW (r = 0.98, n = 7). Furthermore, it is observed that the slope is (significantly) steeper for the trend with $logD_{7.4}$ than with MW; the potential reason for such a finding is the larger diversity in $logD_{7.4}$

values (-1.7 to 5.9, n = 7) than MW values (243 - 645 Da, n = 7). Within group III - consisting of relatively hydrophilic compounds; namely TRP and β-LAs, f_u shows a significant negative association with MW (rather than $logD_{7.4}$), and slopes are comparable; however, for β-LAs, the variability explained by MW is lower than the criteria set *a-priori* ($r^2 > 0.3$). For relatively large MW and hydrophilic NMB, f_u shows a significant negative association with $logD_{7.4}$ (and not with MW). The possible reasons for such a trend are (a) a large range in PPB (f_u ranging between 28 and 98%, n = 14), (b) despite a few missing values in $logD_{7.4}$, NMB show larger range (ranging between -5.0 and 2.1, n = 12) than in MW (ranging between 290 and 1035 Da, n = 16).

The majority of the compounds in the database of the present work are bases that are, in general, skewed towards the relatively lipophilic side, although the majority of them are positively charged at physiological pH. Albumin is the major drug-binding protein in adult humans, and, in general, it binds weakly acidic drugs, while weakly basic drugs (in general) bind to alpha-1 acid glycoprotein (AAG)[131]. The trends observed in f_u as a function of $logD_{7.4}$ for compounds within group I and II in the present work, were comparable to those reported by Obach et al[29] in their trend analysis of human systemic PK database of 670 compounds, where they expressed PPB as the logarithm of the apparent affinity constant, logK (or log[bound/free]) as a function of logP and it was consistent across all the charge types, acids, bases, neutral and zwitterions.

In another study by Valko et al[132], logP was found to predict the drug binding to serum albumin for neutrals and ionized molecules, with the similar affinity[133]. A plausible explanation for higher PPB with higher lipophilicity is hydrophobic interactions with plasma proteins. Furthermore, based on *in-vitro* studies, acids are reported to show relatively higher PPB relative to bases and neutrals, due to an ion-pair interaction with basic residue within albumin; while

electrostatic interactions seem to drive the high affinity interactions between bases and acidic residues within AAG[2,29,134].

Table 12.1 - Effect of $LogD_{7.4}$ and MW on f_u by Group

Group		$LogD_{7.4}$	MW
I	**BZD**	n = 17 r^2 = 0.51 Slope = - 0.20	N.S.
	CCB	n = 12 r^2 = 0.40 Slope = - 0.04	N.S.
II	**Class III AAR**	n = 7 r^2 = 0.83 Slope = - 0.13	n = 7 r^2 = 0.87 Slope = -0.0028
	Opioids	n = 29 r^2 = 0.42 Slope = - 0.13	N.S.
	β - ARLs	n = 34 r^2 = 0.63 Slope = - 0.23	N.S.
III	**TRP**	*n = 7* *r^2 = 0.41* *Slope = -0.21* *N.S*	n = 7 r^2 = 0.78 Slope = -0.0055
	NMB	n = 11 r^2 = 0.42 Slope = - 0.044	N.S.
	β - LAs	N.S.	*n = 57* *r^2 = 0.24* *Slope = -0.0020*

12.1.2. Effect of Molecular/PC Variables on Vd_{ss}^{u} (and Vd_{ss})

The effect of molecular/PC variables, namely, $logD_{7.4}$ and MW on Vd_{ss}^{u} and Vd_{ss} across the eight pharmacological classes of compounds categorized by groups I - III is shown in Table 12.2. Within group I, Vd_{ss}^{u} (but not Vd_{ss}) values of BZD shows a significant positive association with $logD_{7.4}$. CCB, on the other hand, do not show significant trends with Vd_{ss}^{u} or Vd_{ss}.

Within group II, the trends for Vd_{ss}^{u} as a function of $logD_{7.4}$ for Class III AAR, opioids and β-ARLs seem to be consistent both in direction and magnitude, and also comparable with BZD (from group I). This is mechanistically plausible because of the heterogeneous nature of the molecular/PC as well as Vd_{ss}^{u} property space (although the rank order of diversity is Class III AAR > β-ARLs > opioids) shown by these three classes of compounds, namely, Class III AAR (Vd_{ss}^{u} ranges between 1.2 - 2000 L/kg n = 7), β-ARLs (Vd_{ss}^{u} ranges between 0.30 - 590 L/kg, n = 34) and opioids (Vd_{ss}^{u} ranges between 0.10 - 96 L/kg, n = 28).

Vd_{ss} values do not show any significant trend with $logD_{7.4}$ for opioids, β-ARLs and BZD, suggesting that the counteracting effects of $logD_{7.4}$ on f_u and Vd_{ss}^{u} resulted in no net change in the observed values of Vd_{ss}, while the net effect of $logD_{7.4}$ on Vd_{ss}^{u} seem to drive the positive association of Vd_{ss} with $logD_{7.4}$ for Class III AAR. Class III AAR also show significant positive association between Vd_{ss}^{u} (and Vd_{ss}) and MW; the most likely explanation for this trend is the high correlation between $logD_{7.4}$ and MW ($r = 0.98$, $n = 7$). Furthermore, it can be observed that the slope is (significantly) steeper for the trend with $logD_{7.4}$ than MW; the potential reason for such an occurrence is the larger diversity in $logD_{7.4}$ values (-1.7 to 5.9, n = 7) than MW values (243 - 645 Da, n = 7). Within group III consisting of relatively hydrophilic compounds, namely TRP and β-LAs, Vd_{ss}^{u} shows significant negative association with MW (rather than $logD_{7.4}$) and; the slopes are comparable; however, for β-LAs, the variability explained by MW is lower than

the criteria set *a-priori* ($r^2 > 0.3$). On the other hand, for relatively large MW and hydrophilic NMB, which have low Vd_{ss}^u values, suggesting very limited extravascular distribution, $logD_{7.4}$ shows significant positive association with Vd_{ss}^u (but not Vd_{ss}); this trend is possibly driven by succinylcholine, the most hydrophilic NMB with the lowest Vd_{ss}^u in the dataset (it should also be noted that there were several missing $logD_{7.4}$ values for NMB). Lastly, the slope of the effect of $logD_{7.4}$ on Vd_{ss}^u seems to be shallower to those shown by compounds belonging to pharmacological classes in groups I and II; a plausible explanation may be due to the limited range (0.10 - 1.2 L/kg, n = 14) and in general low values in Vd_{ss}^u compared to those in groups I and II

Overall, non-specific hydrophobic interactions with tissue components and/or membranes[2,133], is plausible explanation for the positive trends shown by BZD (in group I), Class III AAR, which on average, appears to be skewed more towards the lipophilic side. It is speculated that bases are involved in ionic interactions with the charged polar heads in the phospholipids, resulting in higher tissue binding and thus higher Vd_{ss}^u (and Vd_{ss})[22,135]. Furthermore, basic lipophilic compounds are also known to bind extensively to cellular components, such as mitochondria and lysosomes, which are believed to be the result of pH differences with the cytoplasm (pH 4 - 5 and 6.7 - 7.0 in lysosomes and mitochondria versus pH 7.2 to 7.3 in cytoplasm respectively), commonly referred to 'ion-trapping'[20,29]. The extent of ion-trapping is dependent on the lipophilicity and pKa of the drug, and the pH of and fraction of the hepatocyte volume occupied by these organelles[20].

Obach et al[29], in their trend analysis of human systemic PK database of 670 compounds, reported a 2.5- to 10-fold increase in the median Vd_{ss}^u relative to median Vd_{ss} depending on the charge

type, suggesting that on an average, the drugs in the comprehensive dataset show PPB-restricted distribution (primarily due to the highly PPB drugs).

The Vd_{ss}^{u} (but not Vd_{ss}) values of TRP, show a positive association with MW, suggesting that molecular size (which is highly correlated with nRot and $logD_{7.4}$), is important for tissue distribution via passive or transporter-mediated uptake (which may rely on the flexibility of the drug molecule), but the exact mechanism is not fully understood.

Table 12.2 - Effect of $LogD_{7.4}$ and MW on Vd_{ss}^{u} and Vd_{ss} by Group

Group	Pharmacological Class	$LogD_{7.4}$		MW	
		Log (Vd_{ss}^{u})	Log (Vd_{ss})	Log (Vd_{ss}^{u})	Log (Vd_{ss})
I	**BZD**	n = 16 r^2 = 0.57 Slope = 0.60	N.S.	N.S.	N.S.
	CCB	N.S.	N.S.	N.S.	N.S.
II	**Class III AAR**	n = 7 r^2 = 0.97 Slope = 0.39	n = 7 r^2 = 0.74 Slope = 0.15	n = 7 r^2 = 0.81 Slope = 0.0078	n = 7 r^2 = 0.62 Slope = 0.0029
	Opioids	n = 28 r^2 = 0.49 Slope = 0.30	N.S.	N.S.	*n = 36* *r^2 = 0.22* *Slope =-0.004*
	β - ARLs	n = 34 r^2 = 0.75 Slope = 0.45	N.S.	N.S.	N.S.
III	**TRP**	N.S.	N.S.	n = 7 r^2 = 0.58 Slope = 0.0050	*n = 8* *r^2 = 0.48* *Slope =-0.0015* *N.S.*
	NMB	n = 11 r^2 = 0.68 Slope = 0.13	*n = 12* *r^2 = 0.33* *Slope = 0.069* *N.S.*	N.S.	N.S.
	β - LAs	N.S.	N.S.	*n = 57* *r^2 = 0.19* *Slope = 0.0010*	N.S.

12.1.3. Effect of Molecular/PC Variables on CL_{tot}^{u}, (and CL_{tot})

The effect of molecular/PC variables, namely, $logD_{7.4}$ and MW on CL_{tot}^{u} and CL_{tot} across the eight pharmacological classes of compounds categorized by groups I - III is shown in Table 12.3. In general, the interpretation is limited because (a) CL_{tot} encompasses various pathways depending on the pharmacological class, which is briefly summarized in Table 12.4 and (b) there are several missing values in the f_e and f_u data which reduced the number of compounds with information on CL_{ren} and CL_{nonren}, their unbound PK counterparts, namely, CL_{ren}^{u} and CL_{nonren}^{u}. Within group I, in general, the contribution of renal pathways is negligible and, there is limited confidence in the CL_{ren} estimates. Neither CL_{tot}^{u} nor CL_{tot} show any significant trend with $logD_{7.4}$ while CL_{nonren}^{u} (but not CL_{nonren}) show a significant positive trend with $logD_{7.4}$ for BZD. For CCB, on the other hand, both the large spread (and in general higher values) in the CL_{nonren}^{u} values and/or higher $logD_{7.4}$ values seem to drive the positive trend of CL_{tot}^{u} versus $logD_{7.4}$. The slopes for these significant trends of CL_{nonren}^{u} of BZD, CL_{tot}^{u} and CL_{nonren}^{u} of CCB with $logD_{7.4}$ are comparable. A plausible explanation for the observed trend of CL_{nonren}^{u} as a function of $logD_{7.4}$ for BZD and CCB is non-specific hydrophobic interactions with hepatic membranes/drug metabolizing enzymes (e.g., CYP3A and CYP2C19 etc.) increasing hepatic uptake and/or enzymatic metabolism with increasing lipophilicity.

Owing to the diverse nature of the clearance mechanisms in which compounds belong pharmacological classes in group II, no further interpretation for $CL_{nonren}^{u}/CL_{nonren}$ can be made. Although few of these compounds show significant renal contribution, none of the molecular/PC variables in the current dataset with available information could explain the relationships for CL_{ren}^{u} or CL_{ren} suggesting that they may driven by more specific molecular interactions with drug metabolizing enzymes and drug transporters.

Within group III, the significant positive trend of CL_{nonren}^{u} (and more specifically, due to the MAO-substrates TRP) seems to drive the overall trend of CL_{tot}^{u} as a function of MW. While none of the molecular/PC variables in the current dataset with available information could explain the relationships with the total systemic clearance or its mechanistic renal/nonrenal pathways, suggesting that they may be driven by more specific molecular interactions with drug metabolizing enzymes and drug transporters; CL_{nonren} values seem to show significant negative trend with MW for β-LAs but MW could explain 30% or more of variability in neither of these relationships based on the criteria set *a-priori* ($r^2 > 0.3$). Tables 12.5 and 12.6 show the relationships of CL_{ren}^{u} and CL_{ren}; and CL_{nonren}^{u} and CL_{nonren} respectively.

Table 12.3 - Effect of $LogD_{7.4}$ and MW on CL_{tot}^{u} and CL_{tot} By Group

Group	Pharmacological Class	$LogD_{7.4}$		MW	
		Log (CL_{tot}^{u})	**Log (CL_{tot})**	**Log (CL_{tot}^{u})**	**Log (CL_{tot})**
I	**BZD**	N.S.	N.S.	N.S.	n = 20 r^2 = 0.40 Slope = 0.012 0.0048, 0.019
	CCB	n = 12 r^2 = 0.61 Slope = 0.97	N.S.	N.S.	N.S.
II	**Class III AAR**	n = 7 r^2 = 0.71 Slope = 0.27 0.072, 0.46	N.S.	*n =7* *r^2 = 0.47* *Slope = 0.0050* *N.S*	N.S.
	Opioids	n = 29 r^2 = 0.31 Slope = 0.21	N.S.	N.S.	N.S.
	β - ARLs	n = 34 r^2 = 0.54 Slope = 0.41	N.S.	N.S.	N.S.
III	**TRP**	*n = 7* *r^2 = 0.39* *Slope = 0.24* *N.S*	N.S.	n = 7 r^2 = 0.65 Slope = 0.0058 0.00085, 0.011	N.S.
	NMB	N.S.	N.S.	N.S.	N.S.
	β - LAs	N.S.	N.S.	N.S.	*n = 60* *r^2 = 0.23* *Slope = -0.002*

Table 12.4 - Mechanistic Pathways of CL_{tot} By Group

Group	Pharmacological Class	CL_{ren}^{u}	CL_{nonren}
I	**BZD**	Majority show negligible renal clearance (and imprecisely estimated) Net tubular reabsorption	Extensive hepatic metabolism (primarily by CYP3A and 2C9 and a few by UGTs) No evidence of extrahepatic pathways
	CCB	Majority show negligible renal clearance (and imprecisely estimated)	Extensive hepatic metabolism (primarily by CYP3A and 2C9)
II	**Class III AAR**	A few show net tubular reabsorption, while the rest show net tubular secretion	Hepatobiliary excretion (drug transporters?) Hepatic metabolism Extrahepatic (unknown?)
	Opioids	A few show net tubular reabsorption, while the rest show net tubular secretion	Hepatobiliary excretion (drug transporters?) Hepatic metabolism Extrahepatic metabolism
	β - ARLs	A few show net tubular reabsorption, while the rest show net tubular secretion	Hepatobiliary excretion (drug transporters?) Hepatic metabolism Extrahepatic metabolism
III	**TRP**	Majority show net tubular secretion (drug transporters?)	Hepatic metabolism (?) Extrahepatic metabolism (MAO) Hepatobiliary excretion (drug transporters?)
	NMB	Majority show net glomerular filtration, while a few show net tubular secretion (drug transporters?)	Hepatobiliary excretion (drug transporters?) Hepatic metabolism (?) Extrahepatic - chemical/enzymatic degradation in plasma/tissues
	β - LAs	Renal pathways is the major elimination pathway	N.S.

Table 12.5 - Effect of $LogD_{7.4}$ and MW on CL_{ren}^{u} and CL_{ren} By Group

Group	Pharmacological Class	$LogD_{7.4}$		MW	
		Log (CL_{ren}^{u})	**Log (CL_{ren})**	**Log (CL_{ren}^{u})**	**Log (CL_{ren})**
I	**BZD**	N.S.	n = 9 r^2 = 0.56 Slope = -0.88	*n =8* *r^2 = 0.40* *Slope = 0.019* *N.S*	*n = 9* *r^2 = 0.35* *Slope = 0.028* *N.S.*
	CCB	n = 3 r^2 = 0.91 Slope = -0.66	*n = 3* *r^2 = 0.80* *Slope = -1.1* *N.S*	*n = 3* *r^2 = 0.49* *Slope = -0.016* *N.S*	*n =3* *r^2 = 0.66* *Slope = -0.033* *N.S*
II	**Class III AAR**	*n =6* *r^2 = 0.43* *Slope = -0.10* *N.S*	n = 6 r^2 = 0.86 Slope = -0.32	*n =6* *r^2 = 0.39* *Slope = -0.0019* *N.S*	n = 6 r^2 = 0.79 Slope = -0.0058
	Opioids	N.S.	*n = 21* *r^2 = 0.22* *Slope =-0.12*	N.S.	N.S.
	β - ARLs	N.S.	*n = 38* *r^2 = 0.17* *Slope = -0.25*	N.S.	N.S.
III	**TRP**	*n = 7* *r^2 = 0.34* *Slope = 0.16* *N.S*	N.S.	*n = 7* *r^2 = 0.37* *Slope = 0.0031* *N.S.*	N.S.
	NMB	N.S.	N.S.	N.S.	N.S.
	β - LAs	N.S.	N.S.	N.S.	*n = 60* *r^2 = 0.26* *Slope = -0.002*

Table 12.6 - Effect of $LogD_{7.4}$ and MW on CL_{nonren}^{u} and CL_{nonren} by Group

Group	Pharmacological Class	$LogD_{7.4}$		MW	
		Log (CL_{nonren}^{u})	Log (CL_{nonren})	Log (CL_{nonren}^{u})	Log (CL_{nonren})
I	**BZD**	n = 8 r^2 = 0.81 Slope = 0.66	N.S.	N.S.	N.S.
	CCB	n = 8 r^2 = 0.77 Slope = 1.1	N.S	N.S.	N.S.
II	**Class III AAR**	n = 7 r^2 = 0.79 Slope = 0.35	N.S.	n = 7 r^2 = 0.57 Slope = 0.0064	N.S
	Opioids	n = 18 r^2 = 0.73 Slope = 0.34	n = 21 r^2 = 0.35 Slope = 0.19	N.S.	*n = 21* *r^2 = 0.19* *Slope = - 0.004*
	β - ARLs	n = 29 r^2 = 0.43 Slope = 0.51	*n = 38* *r^2 = 0.15* *Slope = 0.22*	N.S.	N.S.
III	**TRP**	*n = 7* *r^2 = 0.32* *Slope = 0.26* *N.S*	N.S.	n = 7 r^2 = 0.58 Slope = 0.0064	N.S.
	NMB	N.S.	N.S.	N.S.	N.S.
	β - LAs	N.S.	N.S.	N.S.	*n = 60* *r^2 = 0.08* *Slope = -0.001*

CHAPTER 13. OVERALL CONCLUSIONS

This research project focuses on investigating two approaches of predicting PK properties, namely, QSPKR and AS-PK, for four pharmacological classes of compounds, namely, BZD, NMB, TRP and Class III AAR, selected based on the availability of pertinent human PK information after I.V. administration. Biologically relevant, i.e, PPB-corrected, PK properties for drug distribution (Vd_{ss}^{u}) and elimination (CL_{tot}^{u}, CL_{ren}^{u}, CL_{nonren}^{u}) were evaluated consistently.

Overall, with the final QSPKR database that was compiled, the hypotheses investigated were: (1) if molecular/PC properties can be used for the quantitative prediction of *in-vivo* systemic and biologically relevant PK in humans; and if these relationships are consistent across the pharmacological classes; and (2) if *in-vivo* systemic and biologically relevant PK in humans can be successfully predicted from preclinical species using allometric approaches.

The present work focuses on testing the first hypothesis on four pharmacological classes of compounds namely, BZD, NMB, TRP and Class III AAR and comparing the results of previous work[109, 110] carried out on opioids, β-ARLs, β-LAs and CCB. These classes were chosen, (a) based on the availability of systemic PK information for an adequate number of compounds following the I.V. route of administration, and, more importantly, (b) with the intent of exploring the property spaces (both in terms of molecular/PC as well as PK) which are relatively distinct from that shown by the previous four classes. This is particularly relevant in

the context of comparing the results and determining if they are generalizable across pharmacological classes.

Overall, lipophilicity ($logD_{7.4}$) was found to be the major molecular/PC determinant affecting f_u, Vd_{ss}^u and CL_{nonren}^u for low MW, lipophilic molecules such as BZD, as well as for f_u and Vd_{ss}^u for large MW, hydrophilic molecules such as NMB. On the other hand, for intermediate MW and hydrophilic molecules such as TRP and the heterogeneous class III AAR, although $logD_{7.4}$ was the important molecular/PC determinant, affecting f_u, Vd_{ss}^u, CL_{tot}^u and CL_{nonren}^u, $logD_{7.4}$ and MW were highly correlated (and similar trends are observed for both these descriptors), indicating that an independent effect of MW rather than logD7,4 cannot ruled out,

Across the different pharmacological classes of drugs, the slopes of the effect of $logD_{7.4}$ on f_u and Vd_{ss}^u were similar in direction; however, in general, the magnitude of these slopes appear to be sensitive to the lipophilic nature of the molecules, i.e., for lipophilic molecules such as BZD, the slopes were found to be relatively steeper than those obtained for hydrophilic molecules such as TRP and NMB.

The final validated QSPKR models gave acceptable predictions only for:

(1) Vd_{ss}^u and CL_{nonren}^u (each as a function of $logD_{7.4}$) for BZD;

(2) f_u, Vd_{ss}^u and CL_{nonren}^u (each as a function of $logD_{7.4}$) for Class III AAR, and

(3) f_u (as function of MW) for TRP.

None of the other QSPKR models developed gave acceptable predictions.

In order to elicit an *in-vivo* PD response, a drug molecule must reach its biophase, and during this process, (a) it has to cross biological membranes composed of phospholipid layers (via passive and/or transporter-mediated uptake), (b) it interacts with extra- and intracellular proteins, such as, plasma proteins, membrane-bound proteins such as DT and DME[2,29] etc.

From the present work, it can be concluded that lipophilicity, a bulk molecular/PC property, drives the nonspecific hydrophobic interactions of drug molecules with plasma proteins, cell membranes and proteins in extravascular tissues; this mechanism is a plausible explanation for the observed trends and final validated QSPKR models for f_u and Vd_{ss}^u, regardless of drug target (or pharmacological class).

Lipophilicity also seems to be responsible for the partitioning into the hepatocytes and/or nonspecific hydrophobic interactions with the hepatic drug metabolizing enzymes (e.g., CYP3A and 2C19), and this mechanism is a plausible explanation for the observed trends and final validated QSPKR model of CL_{nonren}^u for BZD. On the other hand, although similar trends were observed for CL_{tot}^u and/or CL_{nonren}^u as a function of $logD_{7.4}$ (and/or MW) for BZD, TRP and Class III AAR, these trends cannot be mechanistically interpreted, as the underlying clearance mechanisms are highly diverse, e.g., extrahepatic via chemical/enzymatic degradation for NMB, enzymatic degradation by MAO for certain TRP, hepatobiliary pathways for Class III AAR, etc.

Lastly, none of the *in-vitro/ex-vivo* PD properties for BZD or TRP and *in-vivo* PD properties for NMB showed any significant trends with any of the molecular/PC descriptors, suggesting that these drug molecule-PD target interactions are driven by specific molecular interactions, presumably involving steric molecular properties, and cannot be explained by the bulk molecular/PC properties investigated in the present work.

The second hypothesis was tested for BZD using systemic and biologically relevant PK information in different animal species and for NMB in cats.

Within the limitations of the methods (and sample size), 'acceptable' predictions for BZD were obtained only for Vd_{ss}^u and Vd_{ss}, and the f_u-correction resulted in an improvement in the prediction; however, none of the CL_{tot}^u or CL_{tot} predictions were acceptable. This suggests that -

for lipophilic BZD - Vd_{ss}^{u} (and Vd_{ss}) values scale well across species because of the underlying, similar nonspecific hydrophobic interactions with plasma membranes and extravascular tissues across animal species. However, quantitative species differences observed in f_u values were observed across species, in general, with high values in smaller animals and low values in larger animals (e.g., humans). The prediction of Vd_{ss}^{u} values was improved by f_u correction because it accounts for the differences in PPB.

Furthermore, owing to quantitative and/or qualitative interspecies differences in drug metabolism, e.g., less phase I, oxidative metabolism of diazepam in humans relative to preclinical animal species[136], that exist even after correcting for BW, CL_{tot} predictions are unacceptable.

NMB are intermediate to large MW, hydrophilic compounds that are restricted to blood or plasma volume in humans as well as in the preclinical animal species; as a result, relatively little distribution to extravascular spaces occurs across animal species, Vd_{ss} predictions (based on BW) were acceptable for 83% of the compounds in the dataset. CL_{ren} (based on GFR) predictions were acceptable in 67% of the compounds, suggesting that NMB are cleared by GFR across all animal species, and there are no interspecies differences in tubular handling. The low percentage of acceptable predictions for CL_{tot} (based on BW and LBF) and CL_{nonren} (based on LBF) suggests that interspecies differences in clearance mechanisms resulted in poor CL_{tot} (and CL_{nonren}) predictions.

References

1. Arrowsmith, J. A decade of change. *Nat. Rev. Drug Discov.* **11,** 17–8 (2012).

2. Arnott, J. a & Planey, S. L. The influence of lipophilicity in drug discovery and design. *Expert Opin. Drug Discov.* **7,** 863–75 (2012).

3. Obach, R. S. *et al.* The prediction of human pharmacokinetic parameters from preclinical and in vitro metabolism data. *J. Pharmacol. Exp. Ther.* **283,** 46–58 (1997).

4. Paul, S. M. *et al.* How to improve R&D productivity: the pharmaceutical industry's grand challenge. *Nat. Rev. Drug Discov.* **9,** 203–14 (2010).

5. Chohan, K., Paine, S. & Waters, N. Advancements in Predictive In Silico Models for ADME. *Curr. Chem. Biol.* **44,** 215–228 (2008).

6. Mager, D. E. Quantitative structure-pharmacokinetic/pharmacodynamic relationships. *Adv. Drug Deliv. Rev.* **58,** 1326–56 (2006).

7. Xu, C. & Mager, D. E. Quantitative structure-pharmacokinetic relationships. *Expert Opin. Drug Metab. Toxicol.* **7,** 63–77 (2011).

8. Mahmood, I. & Balian, J. D. The pharmacokinetic principles behind scaling from preclinical results to phase I protocols. *Clin. Pharmacokinet.* **36,** 1–11 (1999).

9. Gleeson, M. P., Waters, N. J., Paine, S. W. & Davis, A. M. In silico human and rat Vss quantitative structure-activity relationship models. *J. Med. Chem.* **49,** 1953–63 (2006).

10. Ward, K. W. & Smith, B. R. A comprehensive quantitative and qualitative evaluation of extrapolation of intravenous pharmacokinetic parameters from rat , dog , and monkey to humans . II . Volume of distribution and mean residence time. *Drug Metab. Dispos.* **32,** 612–9 (2004).

11. Ward, K. W. & Smith, B. R. A comprehensive quantitative and qualitative evaluation of extrapolation of intravenous pharmacokinetic parameters from rat, dog, and monkey to humans. I. Clearance. *Drug Metab. Dispos.* **32,** 603–11 (2004).

12. Mahmood, I. & Balian, J. D. Interspecies scaling: predicting clearance of drugs in humans. Three different approaches. *Xenobiotica.* **26,** 887–95 (1996).

13. Mahmood, I. Interspecies scaling of renally secreted drugs. *Life Sci.* **63,** 2365–71 (1998).

14. Espié, P., Tytgat, D., Sargentini-Maier, M.-L., Poggesi, I. & Watelet, J.-B. Physiologically based pharmacokinetics (PBPK). *Drug Metab. Rev.* **41,** 391–407 (2009).

15. Hansch, C. & Fujita, T. p -σ-π Analysis. A Method for the Correlation of Biological Activity and Chemical Structure. *J. Am. Chem. Soc.* **86,** 1616–1626 (1964).

16. Van De Waterbeemd, H., Smith, D. a, Beaumont, K. & Walker, D. K. Property-based design: optimization of drug absorption and pharmacokinetics. *J. Med. Chem.* **44,** 1313–33 (2001).

17. Lombardo, F., Obach, R. S., Shalaeva, M. Y. & Gao, F. Prediction of volume of distribution values in humans for neutral and basic drugs using physicochemical measurements and plasma protein binding data. *J. Med. Chem.* **45,** 2867–76 (2002).

18. Van de Waterbeemd, H. & Gifford, E. ADMET in silico modelling: towards prediction paradise? *Nat. Rev. Drug Discov.* **2,** 192–204 (2003).

19. Lombardo, F., Obach, R. S., Shalaeva, M. Y. & Gao, F. Prediction of human volume of distribution values for neutral and basic drugs. 2. Extended data set and leave-class-out statistics. *J. Med. Chem.* **47,** 1242–50 (2004).

20. Fagerholm, U. Prediction of human pharmacokinetics--evaluation of methods for prediction of volume of distribution. *J. Pharm. Pharmacol.* **59,** 1181–90 (2007).

21. Sui, X. *et al.* Predicting the volume of distribution of drugs in humans. *Curr. Drug Metab.* **9,** 574–80 (2008).

22. Gleeson, M. P. Generation of a set of simple, interpretable ADMET rules of thumb. *J. Med. Chem.* **51,** 817–34 (2008).

23. Varma, M. V. S. *et al.* Physicochemical determinants of human renal clearance. *J. Med. Chem.* **52,** 4844–52 (2009).

24. Berellini, G., Waters, N. J. & Lombardo, F. In silico prediction of total human plasma clearance. *J. Chem. Inf. Model.* **52,** 2069–78 (2012).

25. Yu, M. J. Predicting total clearance in humans from chemical structure. *J. Chem. Inf. Model.* **50,** 1284–95 (2010).

26. Gleeson, M. P. Plasma protein binding affinity and its relationship to molecular structure: an in-silico analysis. *J. Med. Chem.* **50,** 101–12 (2007).

27. Lipinski, C. a. Drug-like properties and the causes of poor solubility and poor permeability. *J. Pharmacol. Toxicol. Methods* **44,** 235–49 (2001).

28. Veber, D. F. *et al.* Molecular properties that influence the oral bioavailability of drug candidates. *J. Med. Chem.* **45,** 2615–23 (2002).

29. Obach, R. S., Lombardo, F. & Waters, N. J. Trend Analysis of a Database of Intravenous Pharmacokinetic Parameters in Humans for 670 Drug Compounds. *Drug Metab. Dispos.* **36,** 1385 (2008).

30. Gleeson, M. P., Hersey, A., Montanari, D. & Overington, J. Probing the links between in vitro potency, ADMET and physicochemical parameters. *Nat. Rev. Drug Discov.* **10,** 197–208 (2011).

31. McGinnity, D. F., Collington, J., Austin, R. P. & Riley, R. J. Evaluation of human pharmacokinetics, therapeutic dose and exposure predictions using marketed oral drugs. *Curr. Drug Metab.* **8,** 463–79 (2007).

32. Mahmood, I. Interspecies scaling: predicting oral clearance in humans. *Am. J. Ther.* **9,** 35–42 (2002).

33. Greenblatt, D. J. *et al.* Pharmacokinetic and electroencephalographic study of intravenous diazepam, midazolam, and placebo. *Clin. Pharmacol. Ther.* **45,** 356–65 (1989).

34. Greenblatt, D. J. *et al.* Desmethyldiazepam pharmacokinetics: studies following intravenous and oral desmethyldiazepam, oral clorazepate, and intravenous diazepam. *J. Clin. Pharmacol.* **28,** 853–9 (1988).

35. Giles, H. G., Sellers, E. M., Naranjo, C. a, Frecker, R. C. & Greenblatt, D. J. Disposition of intravenous diazepam in young men and women. *Eur. J. Clin. Pharmacol.* **20,** 207–13 (1981).

36. Ochs, H. R. *et al.* Diazepam kinetics in relation to age and sex. *Pharmacology* **23,** 24–30 (1981).

37. Moolenaar, F., Bakker, S., Visser, J. & Huizinga, T. Biopharmaceutics of rectal administration of drugs in man IX. Comparative biopharmaceutics of diazepam after single rectal, oral, intramuscular and intravenous administration in man. *Int. J. Pharm.* **5,** 127–137 (1980).

38. Mandelli, M., Tognoni, G. & Garattini, S. Clinical Pharmacokinetics of Diazepam. *Clin. Pharmacokinet.* **3,** 72 (1978).

39. Hinderling, P. H., Schmidlin, O. & Seydel, J. K. Quantitative relationships between structure and pharmacokinetics of beta-adrenoceptor blocking agents in man. *J. Pharmacokinet. Biopharm.* **12,** 263–87 (1984).

40. Mager, D. E. & Jusko, W. J. Quantitative structure-pharmacokinetic/pharmacodynamic relationships of corticosteroids in man. *J. Pharm. Sci.* **91,** 2441–51 (2002).

41. Adolph, E. F. Quantitative Relations in the Physiological Constitutions of Mammals. *Science* **109,** 579–85 (1949).

42. Mordenti, J. Man versus beast: pharmacokinetic scaling in mammals. *J. Pharm. Sci.* **75,** 1028–40 (1986).

43. Mahmood, I. & Sahajwalla, C. Interspecies scaling of biliary excreted drugs. *J. Pharm. Sci.* **91,** 1908–14 (2002).

44. Mahmood, I. & Balian, J. D. Interspecies scaling: a comparative study for the prediction of clearance and volume using two or more than two species. *Life Sci.* **59,** 579–85 (1996).

45. Martignoni, M., Groothuis, G. M. M. & de Kanter, R. Species differences between mouse, rat, dog, monkey and human CYP-mediated drug metabolism, inhibition and induction. *Expert Opin. Drug Metab. Toxicol.* **2,** 875–94 (2006).

46. Baillie, T. & Rettie, A. Role of Biotransformation in Drug-Induced Toxicity : Influence of Intra- and Inter-Species Differences in Drug Metabolism. *Drug Metab. Pharmacokinet.* **26,** 15–29 (2011).

47. Pasanen, M. Species differences in CYP enzymes. *Monogr. la Real Acad. Nac. Farm.* 63–90 (2009). at <http://93.189.33.183/index.php/mono/article/view/516/534>

48. Zwart, L., Rompelberg, C. & Sips, A. Anatomical and physiological differences between various species used in studies on the pharmacokinetics and toxicology of xenobiotics. A review of literature. (1999). at <http://rivm.openrepository.com/rivm/handle/10029/10210>

49. Lin, J. Applications and Limitations of Interspecies Scaling and In Vitro Extrapolation in Pharmacokinetics. *Drug Metab. Dispos.* **26,** 1202–1212 (1998).

50. Ng, C., Xiao, Y., Putnam, W., Lum, B. & Tropsha, A. Quantitative structure-pharmacokinetic parameters relationships (QSPKR) analysis of antimicrobial agents in humans using simulated annealing k-nearest-neighbor and partial least-square analysis methods. *J. Pharm. Sci.* **93,** 2535–44 (2004).

51. Singh, B., Paul, Y. & Dhake, A. In silico quantitative structure pharmacokinetic relationship modeling of quinolones: Apparent volume of distribution. *Asian J. Pharm.* **3,** 202 (2009).

52. Karalis, V., Tsantili-Kakoulidou, A. & Macheras, P. Quantitative structure-pharmacokinetic relationships for disposition parameters of cephalosporins. *Eur. J. Pharm. Sci.* **20,** 115–23 (2003).

53. Herman, R. a & Veng-Pedersen, P. Quantitative structure-pharmacokinetic relationships for systemic drug distribution kinetics not confined to a congeneric series. *J. Pharm. Sci.* **83,** 423–8 (1994).

54. Rowland, Malcolm, and T. T. *Clinical Pharmacokinetics: Concepts and Applications.* (Lippincott Williams & Wilkins,, 1995).

55. Davies, B. & Morris, T. Physiological parameters in laboratory animals and humans. *Pharm. Res.* **10,** 1093–5 (1993).

56. Ferrari, M. D., Goadsby, P. J., Roon, K. I. & Lipton, R. B. Triptans (serotonin, 5-HT1B/1D agonists) in migraine: detailed results and methods of a meta-analysis of 53 trials. *Cephalalgia* **22,** 633–58 (2002).

57. Hamel, E., & Saxena, P. R. in *The Headaches* 275–281 (Lippincott Williams & Wilkins, 2006).

58. Humphrey, P. P. 5-Hydroxytryptamine and the pathophysiology of migraine. *J. Neurol.* **238 Suppl,** S38–44 (1991).

59. Hinderling, P. H. Red blood cells: a neglected compartment in pharmacokinetics and pharmacodynamics. *Pharmacol. Rev.* **49,** 279–95 (1997).

60. Pang, K. S. & Rowland, M. Hepatic clearance of drugs. I. Theoretical considerations of a "well-stirred" model and a "parallel tube" model. Influence of hepatic blood flow, plasma and blood cell binding, and the hepatocellular enzymatic activity on hepatic drug clearance. *J. Pharmacokinet. Biopharm.* **5,** 625–53 (1977).

61. Gramatica, P. Principles of QSAR models validation: internal and external. *QSAR Comb. Sci.* **26,** 694–701 (2007).

62. Starckweather, J. Cross Validation in R: A brief overview of some methods, packages, and functions for assessing prediction models. at <http://www.unt.edu/rss/class/Jon/Benchmarks/CrossValidation1_JDS_May2011.pdf >

63. Goodman, L. S., Hardman, J. G., Limbird, L. E. & Gilman, A. G. *Goodman & Gilman's The Pharmacological Basis of Therapeutics*. *Goodman Gilman's Pharmacol. Basis Ther.* **10th,** 1841 (McGraw-Hill, 2011).

64. Moody, D. in *Handb. Drug Interact.* (Mozayani, A. & Raymon, L. P.) 3 – 88 (Humana Press, 2004). doi:10.1007/978-1-59259-654-6_1

65. Guentert, T. W. Pharmacokinetics of benzodiazepines and of their metabolites. *Prog. Drug Metab.* **8,** 241 – 386 (1984).

66. Wang, Q., Han, Y. & Xue, H. Ligands of the GABA-A Receptor Benzodiazepine Binding Site. *CNS Drug Rev.* **5,** 125–144 (1999).

67. Van der Graaf, P. H., Nilsson, J., Van Schaick, E. a & Danhof, M. Multivariate quantitative structure-pharmacokinetic relationships (QSPKR) analysis of adenosine A1 receptor agonists in rat. *J. Pharm. Sci.* **88,** 306–12 (1999).

68. Toon, S. & Rowland, M. Structure-pharmacokinetic relationships among the barbiturates in the rat. *J. Pharmacol. Exp. Ther.* **225,** 752–63 (1983).

69. Lucek, R. W. & Countinho, C. B. The Role of Substituents in the Hydrophobic binding of 1, 4 Benzodiazepines by Human plasma proteins. *Mol. Pharmacol.* **12,** 612 (1976).

70. Arendt, R. M. *et al.* In vitro correlates of benzodiazepine cerebrospinal fluid uptake, pharmacodynamic action and peripheral distribution. *J. Pharmacol. Exp. Ther.* **227,** 98–106 (1983).

71. Greenblatt, D. J. *et al.* In vitro quantitation of benzodiazepine lipophilicity: relation to in vivo distribution. *Br. J. Anaesth.* **55,** 985–9 (1983).

72. Hunter, J. M. New neuromuscular blocking drugs. *N. Engl. J. Med.* **332,** 1691–9 (1995).

73. Gyermek, L. Development of ultra short-acting muscle relaxant agents: history, research strategies, and challenges. *Med. Res. Rev.* **25,** 610–54 (2005).

74. Lee, C. Conformation, action, and mechanism of action of neuromuscular blocking muscle relaxants. *Pharmacol. Ther.* **98,** 143–169 (2003).

75. Lee, C. Structure, conformation, and action of neuromuscular blocking drugs. *Br. J. Anaesth.* **87,** 755–69 (2001).

76. Lacroix, M., Donati, F. & Varin, F. Pharmacokinetics of mivacurium isomers and their metabolites in healthy volunteers after intravenous bolus administration. *Anesthesiology* **86,** 322–30 (1997).

77. Savarese, J. J. *et al.* The clinical neuromuscular pharmacology of mivacurium chloride (BW B1090U). A short-acting nondepolarizing ester neuromuscular blocking drug. *Anesthesiology* **68,** 723–32 (1988).

78. Kisor, D. F. *et al.* Importance of the organ-independent elimination of cisatracurium. *Anesth. Analg.* **83,** 1065–71 (1996).

79. Roy, J. J. & Varin, F. Physicochemical properties of neuromuscular blocking agents and their impact on the pharmacokinetic-pharmacodynamic relationship. *Br. J. Anaesth.* **93,** 241–8 (2004).

80. Neef, C. & Meijer, D. Structure-pharmacokinetics relationship of quaternary ammonium compounds. *Naunyn. Schmiedebergs. Arch. Pharmacol.* **328,** 103–110 (1984).

81. Proost, J. H., Roggeveld, J., Wierda, J. M. & Meijer, D. K. Relationship between chemical structure and physicochemical properties of series of bulky organic cations and their hepatic uptake and biliary excretion rates. *J. Pharmacol. Exp. Ther.* **282,** 715–26 (1997).

82. Kaul, S. & Ritschel, W. A. Quantitative structure--pharmacokinetic relationship of a series of sulfonamides in the rat. *Eur. J. Drug Metab. Pharmacokinet.* **15,** 211–7

83. Wierda, J. M. & Proost, J. H. Structure-pharmacodynamic-pharmacokinetic relationships of steroidal neuromuscular blocking agents. *Eur. J. Anaesthesiol. Suppl.* **11,** 45–54 (1995).

84. Ramzan, I. M. Molecular weight of cation as a determinant of speed of onset of neuromuscular blockade. *Anesthesiology* **57,** 247–8 (1982).

85. Peterlin, B. L. & Rapoport, A. M. Clinical pharmacology of the serotonin receptor agonist, zolmitriptan. *Expert Opin. Drug Metab. Toxicol.* **3,** 899–911 (2007).

86. Yevich, J. & Yocca, F. Second generation antimigraine 5-HT1B/D agonists: structure activity relationship and preclinical pharmacological distinctions. *Curr. Med. Chem.* **4,** 295–312 (1997).

87. Turner, J. V, Maddalena, D. J., Cutler, D. J. & Agatonovic-Kustrin, S. Multiple pharmacokinetic parameter prediction for a series of cephalosporins. *J. Pharm. Sci.* **92,** 552–9 (2003).

88. Cheng, Z. *et al.* Hydrophilic anti-migraine triptans are substrates for OATP1A2, a transporter expressed at human blood-brain barrier. *Xenobiotica.* **42,** 880–90 (2012).

89. Nattel, S. & Singh, B. N. Evolution, mechanisms, and classification of antiarrhythmic drugs: focus on class III actions. *Am. J. Cardiol.* **84,** 11R–19R (1999).

90. Katzung, G. B. *Basic and Clinical Pharmacology*. (Lange Medical Books/McGraw-Hill, 2010).

91. Jitendra N Singh, S. S. S. in *Ion Channels Their Inhib.* (Gupta, S. P.) (Springer Berlin Heidelberg, 2011). doi:10.1007/978-3-642-19922-6

92. Qidong You, Qian Yang, X. W. in *Ion Channels Their Inhib.* (Gupta, S. P.) (Springer Berlin Heidelberg, 2011). doi:10.1007/978-3-642-19922-6

93. Perry, M., Stansfeld, P. & Leaney, J. Drug binding interactions in the inner cavity of HERG channels: molecular insights from structure-activity relationships of clofilium and ibutilide analogs. *Mol. …* **69,** 509–519 (2006).

94. Perry, M., Groot, M. de & Helliwell, R. Structural determinants of HERG channel block by clofilium and ibutilide. *Mol. …* **66,** 240–249 (2004).

95. Singleton, D. H. *et al.* Fluorescently labeled analogues of dofetilide as high-affinity fluorescence polarization ligands for the human ether-a-go-go-related gene (hERG) channel. *J. Med. Chem.* **50,** 2931–41 (2007).

96. Rapeport, W. G. Clinical pharmacokinetics of bretylium. *Clin. Pharmacokinet.* **10,** 248–56 (1985).

97. Hanyok, J. J. Clinical pharmacokinetics of sotalol. *Am. J. Cardiol.* **72,** 19A–26A (1993).

98. Lenz, T. L. & Hilleman, D. E. Dofetilide, a new class III antiarrhythmic agent. *Pharmacotherapy* **20,** 776–86 (2000).

99. Kowey, P. R., Marinchak, R. A., Rials, S. J. & Bharucha, D. Pharmacologic and pharmacokinetic profile of class III antiarrhythmic drugs. *Am. J. Cardiol.* **80,** 16G–23G (1997).

100. Nolan, P. E. Pharmacokinetics and pharmacodynamics of intravenous agents for ventricular arrhythmias. *Pharmacotherapy* **17,** 65S–75S; discussion 89S–91S (1997).

101. Pamukcu, B. & Lip, G. Y. H. Dronedarone as a new treatment option for atrial fibrillation patients: pharmacokinetics, pharmacodynamics and clinical practice. *Expert Opin. Pharmacother.* **12,** 131–40 (2011).

102. Dofetilide FDA Label. at <http://www.accessdata.fda.gov/drugsatfda_docs/label/2013/020931s007lbl.pdf>

103. Yamreudeewong, W. & DeBisschop, M. Potentially Significant Drug Interactions of Class III Antiarrhythmic Drugs. *Drug Saf.* **26,** 421–438 (2003).

104. Foster, R. H., Wilde, M. I. & Markham, A. Ibutilide. A review of its pharmacological properties and clinical potential in the acute management of atrial flutter and fibrillation. *Drugs* **54,** 312–30 (1997).

105. Dronedarone FDA Label. at <http://www.accessdata.fda.gov/drugsatfda_docs/label/2014/022425s023lbl.pdf>

106. Dronedarone FDA Approval Package. at <http://www.accessdata.fda.gov/drugsatfda_docs/nda/2009/022425s000_ClinPharm_P1.pdf>

107. Drayer, D. E. Clinical consequences of the lipophilicity and plasma protein binding of antiarrhythmic drugs and active metabolites in man. *Ann. N. Y. Acad. Sci.* **432,** 45–56 (1984).

108. Van De Waterbeemd, H., Smith, D. a, Beaumont, K. & Walker, D. K. Property-based design: optimization of drug absorption and pharmacokinetics. *J. Med. Chem.* **44,** 1313–33 (2001).

109. Badri, P. Prediction of Human Systemic, Biologically Relevant Pharmacokinetic (PK) Properties Based on Quantitative Structure Pharmacokinetic Relationships (QSPKR) and Interspecies Pharmacokinetic Allometric Scaling. (2010).

110. Al-Tafif, A. Prediction of Human Systemic, Biologically Relevant Pharmacokinetic Properties Based on Physicochemical Properties of Calcium Channel Blockers. (2012).

111. Bachmakov, I., Werner, U., Endress, B., Auge, D. & Fromm, M. F. Characterization of beta-adrenoceptor antagonists as substrates and inhibitors of the drug transporter P-glycoprotein. *Fundam. Clin. Pharmacol.* **20,** 273–82 (2006).

112. Bachmakov, I. *et al.* Interaction of beta-blockers with the renal uptake transporter OCT2. *Diabetes. Obes. Metab.* **11,** 1080–3 (2009).

113. Takeda, M., Babu, E., Narikawa, S. & Endou, H. Interaction of human organic anion transporters with various cephalosporin antibiotics. *Eur. J. Pharmacol.* **438,** 137–42 (2002).

114. Khamdang, S. *et al.* Interaction of human and rat organic anion transporter 2 with various cephalosporin antibiotics. *Eur. J. Pharmacol.* **465,** 1–7 (2003).

115. Kang, H. E. & Lee, M. G. Approaches for predicting human pharmacokinetics using interspecies pharmacokinetic scaling. *Arch. Pharm. Res.* **34,** 1779–88 (2011).

116. Sheiner, L. B. & Beal, S. L. Some suggestions for measuring predictive performance. *J. Pharmacokinet. Biopharm.* **9,** 503–12 (1981).

117. Mahmood, I. *Interspecies Pharmacokinetic Scaling - Principles and Application of Allometric Scaling*. (Pine House, 2005).

118. Boxenbaum, H. Interspecies pharmacokinetic scaling and the evolutionary-comparative paradigm. *Drug Metab. Rev.* **15,** 1071–121 (1984).

119. Bender, A. D., Post, A., Meier, J. P., Higson, J. E. & Reichard, G. Plasma protein binding of drugs as a function of age in adult human subjects. *J. Pharm. Sci.* **64,** 1711–3 (1975).

120. Verbeeck, R. K., Cardinal, J. A. & Wallace, S. M. Effect of age and sex on the plasma binding of acidic and basic drugs. *Eur. J. Clin. Pharmacol.* **27,** 91–7 (1984).

121. Lin, J. H. Applications and limitations of interspecies scaling and in vitro extrapolation in pharmacokinetics. *Drug Metab. Dispos.* **26,** 1202–12 (1998).

122. Sawada, Y., Hanano, M., Sugiyama, Y., Harashima, H. & Iga, T. Prediction of the volumes of distribution of basic drugs in humans based on data from animals. *J. Pharmacokinet. Biopharm.* **12,** 587–96 (1984).

123. Klotz, U., Antonin, K. H. & Bieck, P. R. Pharmacokinetics and plasma binding of diazepam in man, dog, rabbit, guinea pig and rat. *J. Pharmacol. Exp. Ther*. **199,** 67–73 (1976).

124. Oliver, F. M. *et al.* Comparative pharmacokinetics of submucosal vs. intravenous flumazenil (Romazicon) in an animal model. *Pediatr. Dent.* **22,** 489–93 (2000).

125. Boxenbaum, H. Comparative pharmacokinetics of benzodiazepines in dog and man. *J. Pharmacokinet. Biopharm.* **10,** 411–26 (1982).

126. Clarke, D. *The uridine diphosphate glucuronosyltransferase multigene family: Function and regulation*. (Springer-Verlag, 1994).

127. Boxenbaum, H. Interspecies variation in liver weight, hepatic blood flow, and antipyrine intrinsic clearance: extrapolation of data to benzodiazepines and phenytoin. *J. Pharmacokinet. Biopharm.* **8,** 165–76 (1980).

128. Tang, H. & Mayersohn, M. A global examination of allometric scaling for predicting human drug clearance and the prediction of large vertical allometry. *J. Pharm. Sci.* **95,** 1783–99 (2006).

129. Tang, H. & Mayersohn, M. Accuracy of allometrically predicted pharmacokinetic parameters in humans: role of species selection. *Drug Metab. Dispos.* **33,** 1288–93 (2005).

130. Lin, J. H. Species similarities and differences in pharmacokinetics. *Drug Metab. Dispos.* **23,** 1008–21 (1995).

131. Israili, Z. H. & Dayton, P. G. Human alpha-1-glycoprotein and its interactions with drugs. *Drug Metab. Rev.* **33,** 161–235 (2001).

132. Valko, K., Nunhuck, S., Bevan, C., Abraham, M. H. & Reynolds, D. P. Fast gradient HPLC method to determine compounds binding to human serum albumin. Relationships with octanol/water and immobilized artificial membrane lipophilicity. *J. Pharm. Sci.* **92,** 2236–48 (2003).

133. Waring, M. J. Lipophilicity in drug discovery. *Expert Opin. Drug Discov.* **5,** 235–48 (2010).

134. Ghuman, J. *et al.* Structural basis of the drug-binding specificity of human serum albumin. *J. Mol. Biol.* **353,** 38–52 (2005).

135. Van de Waterbeemd, H., Smith, D. a & Jones, B. C. Lipophilicity in PK design: methyl, ethyl, futile. *J. Comput. Aided. Mol. Des.* **15,** 273–86 (2001).

136. Boxenbaum, H. & DiLea, C. First-time-in-human dose selection: allometric thoughts and perspectives. *J. Clin. Pharmacol.* **35,** 957–66 (1995).

Appendix 1.1 - Human PK Study Summaries of BZD

Chlordiazepoxide

Study	Population	BW	Dose (I.V.)	Rate	PK Sampling Schedule		Assay Method	Analytical Method Parameters		PK Analysis	Urine Collection Method	Vd_{ss}/ Vd_{pss}	CL_{tot}	CL_{ren}
		(kg)	(mg/kg)		Plasma	Urine		Plasma	Urine			(L/kg)	[ml/min/kg]	[ml/min/kg]
Boxenbaum et al[1]	Healthy subjects, n = 6, Mean (SD) Age = 27 (2) years	81 (12)	0.34	1 min	-	0 - 48 hrs	Fluorescence	Limit of sensitivity = 0.2 µg/ml	Limit of sensitivity = 0.2 µg/ml	Compartmental (2)	Fractionated	0.30 (± 0.03)	0.37 (± 0.06)	0.04
Sellers et al[2]	Healthy males, n = 14, Mean Age = 25 years	73	0.61	10 min	0 - 48 hrs	-	Fluorescence	Limit of sensitivity = 0.2 µg/ml	-	Compartmental (2)	-	0.48 (± 0.04)	0.54 (± 0.1)	-
Greenblatt et al[3]	Healthy males, n = 14, Mean Age = 27 years	67	0.67	60 min	0 - 72 hrs	-	Fluorescence	Limit of sensitivity = 0.2 µg/ml	-	Compartmental (2)	-	-	0.41 (± 0.06)	-

Urinary Excretion Studies

1. Boxenbaum et al[1] calculated the CL_{ren} by using CL_{ren} = Ae/AUC (Urine was collected in 2 fractions for 0-24 and 24 - 48 hrs); f_e < 1%

Plasma Protein Binding Studies

Study	Subjects	Method	Concentration Range	Assay	f_u (%)
Boxenbaum et al[1]	Healthy humans, n = 3	Equilibrium dialysis	0.8 - 240.0 µg/ml	-	7 (± 2)
Moschitto et al[4]	*In-vitro*	Equilibrium dialysis	10 - 10000 ng/ml	Liquid Scintillation	4.1

B:P Ratio

Study	Method	Concentration Range	Assay	B:P
Boxenbaum et al[1]	*In-vitro*	1 - 2 µg/ml	-	0.7

Metabolism

Early studies of the fate of chlordiazepoxide in humans elucidated the metabolic scheme[5] shown in Figure -1 below. Furthermore, it has been reported that all the four metabolites (shown in figure -1) have psychopharmacological activity similar to that of the parent compound.

Schematic of Metabolism of Chlordiazepoxide[5]

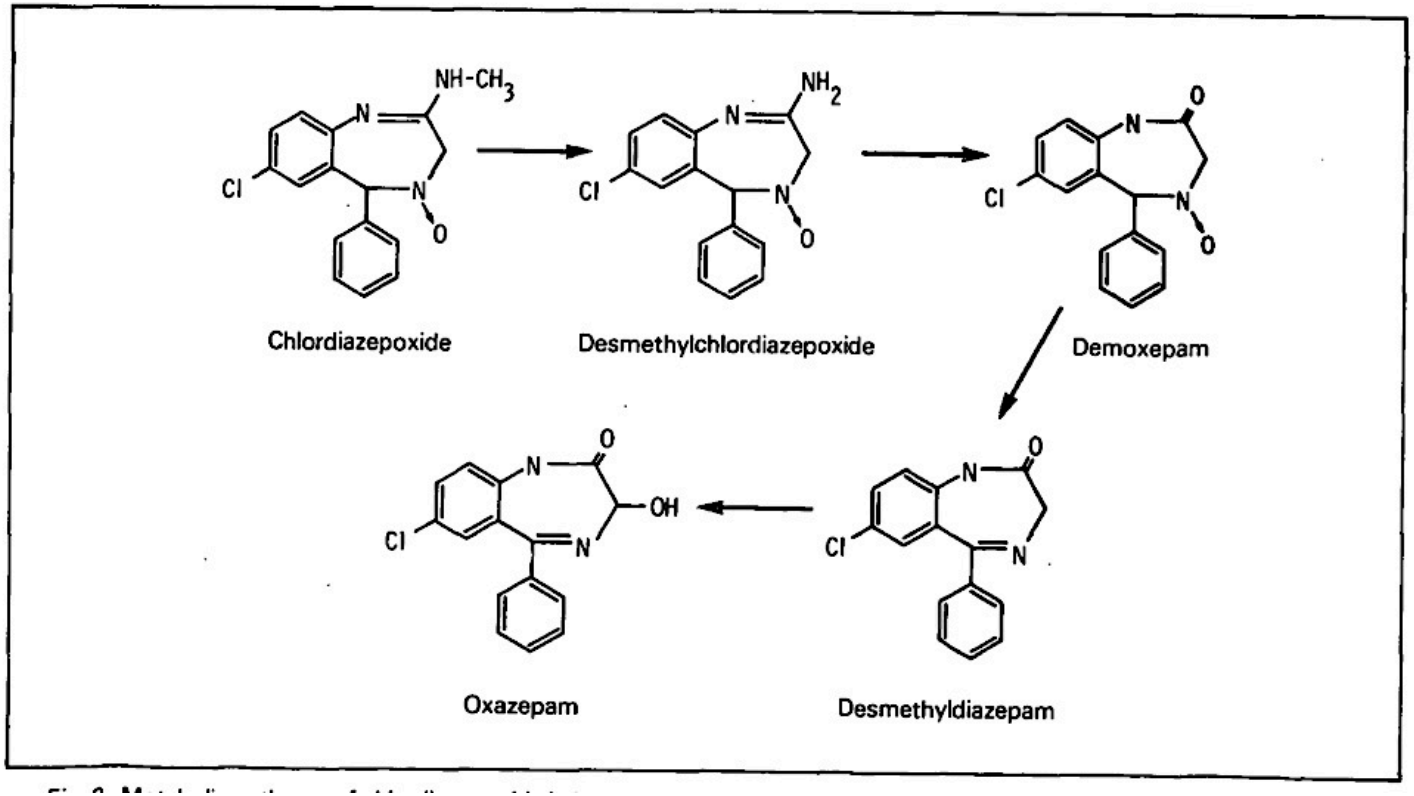

Clonazepam

Study	Population	BW	Dose (I.V.)	Rate	PK Sampling Schedule		Assay Method	Analytical Method Parameters		PK Analysis	Urine Collection Method	Vd_{ss}/ Vd_{pss}	CL_{tot}	CL_{ren}
		(kg)	(mg/kg)		Plasma	Urine		Plasma	Urine			(L/kg)	[ml/min/kg]	[ml/min/kg]
Berlin et al[6]	Healthy subjects, n = 8, Mean (SD) Age = 42 (14) years	68 (10)	0.03	Bolus	0 - 96 h	-	GC-EC	Sensitivity limit = 0.5 ng/ml	-	NCA	-	3.28 (± 1.1)	0.95 (± 0.2)	-
Crevoisier et al[7]	Healthy subjects, n = 12, Mean (Range) Age = 30 (23-50) years	63 (52-90)	0.03	4 min Infusion	0 - 120 hrs	-	GC-EC	LLOQ = 0.5 ng/ml	-	NCA	-	2.68 (± 0.7)	0.87 (± 0.1)	-

Plasma Protein Binding Studies

Study	Subjects	Method	Concentration Range	Assay	f_u (%)
Pacifici et al[8]	Healthy subjects, n = 6	Equilibrium dialysis	Up to 0.2 µg/ml	Liquid scintillation	13.9
Lucek et al[9]	Healthy subjects, n = 3	Equilibrium dialysis	5 - 15 µg/ml	Liquid scintillation	14.6 ± 1.5
Moschitto et al[4]	*In-vitro*	Equilibrium dialysis	10 - 10000 ng/ml	Liquid Scintillation	14.9

Clorazepate

Study	Population	BW	Dose (I.V.)	Rate	PK Sampling Schedule		Assay Method	Analytical Method Parameters		PK Analysis	Urine Collection Method	Vd_{ss}/ Vd_{pss}	CL_{tot}	CL_{ren}
		(kg)	(mg/kg)		Plasma	Urine		Plasma	Urine			(L/kg)	[ml/min/kg]	[ml/min/kg]
Bertler et al[10]	Healthy subjects, n = 8, Mean (Range) Age = 28 (23-37) years	-	0.3	2 min Infusion	0 - 96 hrs	0 - 24 h	HPLC	Limit of sensitivity = 10 ng/ml	Limit of sensitivity = 10 ng/ml	Compartmetal (2)	Cumulative	0.22 (± 0.01)	0.02 (± 0.001)	0.002

Urinary Excretion Studies

1. Bertler et al[10] calculated the CL_{ren} by using $CL_{ren} = f_e * CL_{tot}$ (f_e is the fraction of the dose that is excreted unchanged in the urine; urine samples were collected 0 - 3.5, 3.5 - 9 and 9 - 24 hrs), $f_e = 11.2\%$

Diazepam

Study	Population	BW	Dose (I.V.)	Rate	PK Sampling Schedule		Assay Method	Analytical Method Parameters		PK Analysis	Urine Collection Method	Vd_{ss}/ Vd_{pss}	CL_{tot}	CL_{ren}
		(kg)	(mg/ kg)		Plasma	Urine		Plasma	Urine			(L/kg)	[ml/min/kg]	[ml/min/kg]
Klotz et al[11]	Healthy subjects, n = 5	-	0.1	2 min Infusion	0 - 72 hrs	0 - 72 hrs	GC-EC	Calibration curve linear from 1 - 50 ng/ml	Calibration curve linear from 1 - 50 ng/ml	Compartmental (2)	Cumulative	1.13 (± 0.3)	0.38 (± 0.06)	0.001
Klotz et al[12]	Healthy volunteers, n = 10, Age range = 23 - 35 years	-	0.1	2 min Infusion	0 - 72 hrs	-	GC-EC	Calibration curve linear from 1 - 50 ng/ml	-	Compartmental (2)	-	0.89 (± 0.18)	0.35 (± 0.11)	-
Cloyd et al[13]	Healthy subjects, n = 20, Mean (SD) Age = 29 (9) years	73 (9)	0.1	2 min Infusion	0 - 240 hrs	-	GC-EC	LLOQ = 2 ng/ml	-	NCA	-	1.33	0.27 (± 0.09)	-
Greenblatt et al[14]	Healthy subjects, n = 12, Mean (Range) Age = 62 (34 - 79) years	-	5 - 15 mg/ 70 kg	1 min Infusion	0 - 72 hrs, then q.d. for 7 days	-	GC-EC	LLOQ = 2 ng/ml	-	Compartmental (2 or 3)	-	-	0.40 (± 0.20)	-

Ochs et al[15]	Healthy subjects, n = 10, Mean (Range) Age = 27 (22-37) years	66	5 - 10 mg/ 66 kg	1 min Infusion	0 - 24 hrs, then q.d. for 7 days	-	GC-EC	LLOQ = 2 ng/ml	-	Compartmental (2 or 3)	-	-	0.44 (± 0.16)	-
Locniskar et al[16]	Healthy subjects, n = 10, Age Range = 18 - 44 years	68 (14)	0.1	1 min Infusion	0 - 168 hrs	-	GC-EC	LLOQ = 2 ng/ml	-	Compartmental (2 or 3)	-	-	0.47 (± 0.16)	-
Giles et al[17]	Healthy subjects, n = 11, Age Range = 20 - 32 years	65 (11)	0.1	20 min Infusion	0 - 24 hrs, up to 28 days	-	GC-EC	LLOQ = 2 ng/ml	-	NCA	-	-	0.39 (± 0.10)	-
Divoll et al[18]	Healthy subjects, n = 11, Mean (Range) Age = 30 (20 - 39) years	65 (48 - 86)	0.1	1 min Infusion	0 - 336 hrs	-	GC-EC	LLOQ = 2 ng/ml	-	NCA	-	-	0.41 (0.22 - 0.66)	-

Urinary Excretion Studies

1. Klotz et al[11] calculated the CLren by using CLren = fe*CLtot (fe = % of the dose excreted unchanged in the urine; urine was sampled up to 72 hrs). f_e = 0.3%

Plasma Protein Binding Studies

Study	Subjects	Method	Concentration Range	Assay	f_u (%)
Klotz et al[11]	Healthy humans	Equilibrium dialysis	100 ng/ml	GC-EC	2.2 (± 1.0)
Klotz et al[12]	Healthy humans	Equilibrium dialysis	100 ng/ml	GC-EC	3.2 (± 0.8)
Ochs et al[15]	Healthy humans	Equilibrium dialysis	-	GC-EC	1.4 (± 0.2)
Divoll et al[19]	*In-vitro*	Equilibrium dialysis	0.2 - 20 µg/ml	GC-EC	2.3
Moschitto et al[4]	*In-vitro*	Equilibrium dialysis	10 - 10000 ng/ml	Liquid Scintillation	1.6 (± 0.01)

B:P Ratio

Study	Method	Concentration Range	Assay	B:P
Klotz et al[11]	*In-vitro*	100 ng/ml	GC-EC	0.58 (± 0.18)
Klotz et al[12]	*In-vitro*	100 ng/ml	GC-EC	0.58 (± 0.11)

Metabolism Schematic

The schematic of the metabolism for diazepam[20] in shown below:

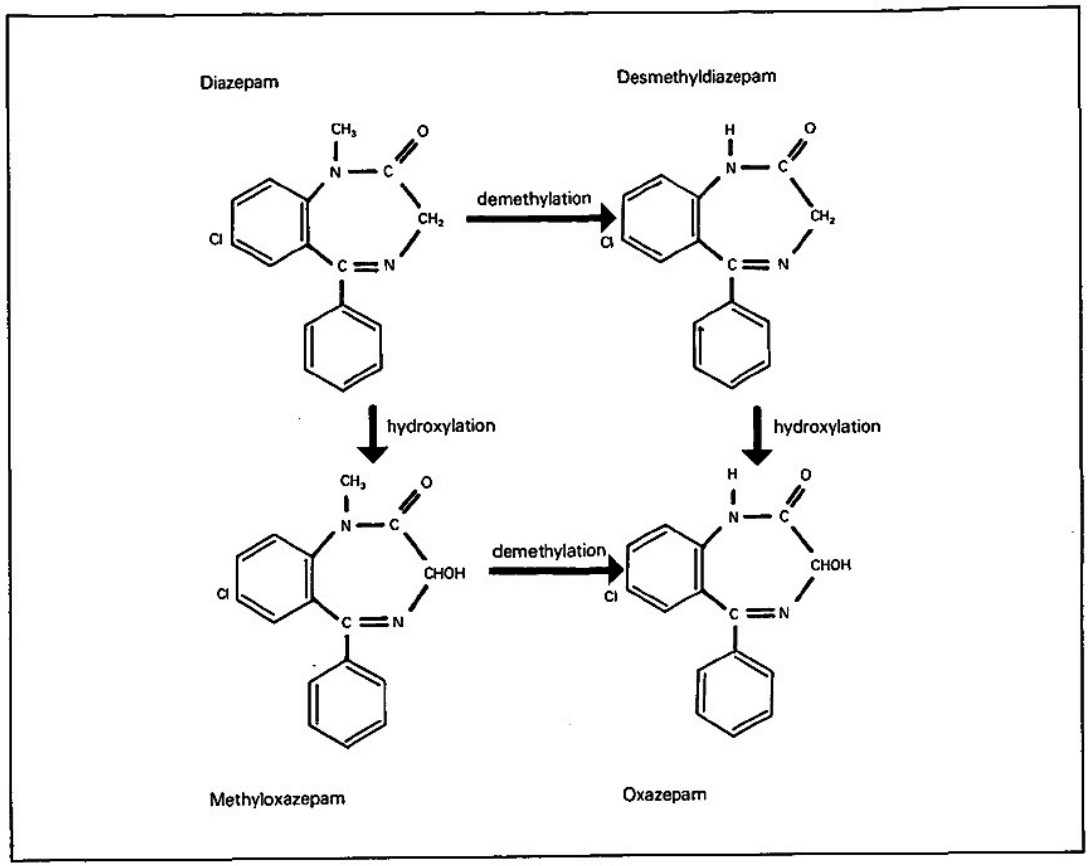
Diazepam
Desmethyldiazepam
demethylation
hydroxylation
hydroxylation
demethylation
Methyloxazepam
Oxazepam

N-DesmethylDiazepam

Study	Population	BW	Dose (I.V.)	Rate	PK Sampling Schedule		Assay Method	Analytical Method Parameters		PK Analysis	Urine Collection Method	Vd_{ss}/ Vd_{pss}	CL_{tot}	CL_{ren}
		(kg)	(mg/kg)		Plasma	Urine		Plasma	Urine			(L/kg)	[ml/min/kg]	[ml/min/kg]
Greenblatt et al[14]	Healthy subjects, n = 12, Mean (Range) Age = 62 (34 - 79) years	-	5 - 15 mg/ 70 kg	1 min Infusion	0 - 72 hrs, then q.d. for 7 days	-	GC-EC	LLOQ = 1 ng/ml	-	Compartmental (2 or 3)	-	*1.24 (± 0.31)*	0.17 (± 0.20)	-

Plasma Protein Binding Studies

Study	Subjects	Method	Concentration Range	Assay	f_u (%)
Divoll et al[19]	*In-vitro*	Equilibrium dialysis	0.2 - 20 μg/ml	GC-EC	3.0
Moschitto et al[4]	*In-vitro*	Equilibrium dialysis	10 - 10000 ng/ml	Liquid Scintillation	3.5 (± 0.05)

ChlordesmethylDiazepam

Study	Population	BW	Dose (I.V.)	Rate	PK Sampling Schedule		Assay Method	Analytical Method Parameters		PK Analysis	Urine Collection Method	Vd_{ss}/ Vd_{pss}	CL_{tot}	CL_{ren}
		(kg)	(mg/kg)		Plasma	Urine		Plasma	Urine			(L/kg)	[ml/min/kg]	[ml/min/kg]
Sennesael et al[21]	Healthy subjects, n = 11, Mean (SD) Age = 51 (6) years	63 (12)	0.03	Bolus	0 - 21 days	-	GC-EC	LLOQ = 0.2 ng/ml	-	Compartmental (2)	-	*3.80 (± 1.32)*	0.26 (± 0.06)	-
Bareggi et al[22]	Healthy subjects, n = 12, Mean (SD) Age = 56 (7) years	70 (9)	0.01	Bolus	0 - 15 days	-	GC-EC	LLOQ = 0.2 ng/ml	-	Compartmental (2)	-	*4.00 (± 1.67)*	0.25 (± 0.07)	-

Plasma Protein Binding Studies

Study	Subjects	Method	Concentration Range	Assay	f_u (%)
Sennesael et al[21]	Healthy subjects	Ultrafiltration	-	GC-EC	2.9
Bareggi et al[22]	Healthy subjects	Ultrafiltration	-	GC-EC	3.4

Lorazepam

Study	Population	BW	Dose (I.V.)	Rate	PK Sampling Schedule		Assay Method	Analytical Method Parameters		PK Analysis	Urine Collection Method	Vd_{ss}/ Vd_{pss}	CL_{tot}	CL_{ren}
		(kg)	(mg/kg)		Plasma	Urine		Plasma	Urine			(L/kg)	[ml/min/kg]	[ml/min/kg]
Greenblatt et al[23]	Healthy subjects, n = 7, Mean (SD) Age = 27 (3) years	66 (10)	2 mg, 4 mg/66 kg	5 min Infusion	0 - 48 h	0 - 72 h	GC - EC	Limit of sensitivity = 1 ng/ml	Limit of sensitivity = 1 ng/ml	Compartmental (2)	Cumulative	1.14 (± 0.08)	1.05 (± 0.40)	0.006
Greenblatt et al[24]	Healthy subjects, n = 6, Mean (Range) Age = 35 (28 - 33) years	69	0.02 - 0.05	1 min Infusion	0 - 24 hr	-	GC - EC	Limit of sensitivity = 1 ng/ml	-	Compartmental (2 - 3)	-	1.37 (± 0.12)	1.98 (± 0.54)	-
Wermeling et al[25]	Healthy subjects, n = 7, Mean (SD) Age = 22 (3) years	70 (9)	0.03	5 min Infusion	0 - 36 hrs	-	LC - MS/MS	LLOQ = 0.1 ng/ml	-	NCA	-	1.32 (± 0.23)	1.98 (± 0.53)	-
Kudsk et al[26]	Healthy subjects, n = 6, Mean (SD) Age = 30 (7) years	71 (12)	0.03	10 min Infusion	0 - 48 h	-	GC- EC	LLOD = 1 ng/ml	-	Compartmental (2)	-	1.21 (± 0.17)	1.04 (± 0.15)	-

Ochs et al[15]	Healthy subjects, n = 10, Mean (Range) Age = 27 (22-37) years	66	0.03	1 min Infusion	0 - 72 hrs	-	GC-EC	LLOQ = 2.5 ng/ml	-	Compartmental (2 or 3)	-	-	0.96 (± 0.28)	-
Abernethy et al[27]	Healthy subjects, n = 14	63 (8)	0.03	Bolus	0 - 72 hrs	-	GC - EC	LLOQ = 1 ng/ml	-	Compartmental (2 or 3)	-	-	1.00 (± 0.27)	-
Greenblatt et al[28]	Healthy subjects, n = 6, Mean (SD) Age = 27 (5) years	-	0.03	5 min Infusion	0 - 72 hrs	-	GC - EC	LLOQ = 1 ng/ml	-	Compartmental (2 or 3)	-	-	0.96	-

Urinary Excretion Studies

1. Greenblatt et al[23] calculated the CLren by using CLren = fe*CLtot (fe = % of the dose excreted unchanged in the urine; urine was collected in intervals: 0 - 4, 4 - 8, 8 - 24, 24 - 48, 48 - 72 hrs). f_e = 0.5%

Plasma Protein Binding Studies

Study	Subjects	Method	Concentration Range	Assay	f_u (%)
Ochs et al[15]	Healthy humans	Equilibrium dialysis	-	GC-EC	8.0 (± 0.9)
Abernerthy et al[27]	*In-vitro*	Equilibrium dialysis	-	GC-EC	10.0 (± 0.7)
Moschitto et al[4]	*In-vitro*	Equilibrium dialysis	10 - 10000 ng/ml	Liquid Scintillation	9.7 (± 0.04)

Nitrazepam

Study	Population	BW	Dose (I.V.)	Rate	PK Sampling Schedule		Assay Method	Analytical Method Parameters		PK Analysis	Urine Collection Method	Vd_{ss}/ Vd_{pss}	CL_{tot}	CL_{ren}
		(kg)	(mg/kg)		Plasma	Urine		Plasma	Urine			(L/kg)	[ml/min/kg]	[ml/min/kg]
Jochemsen et al[29]	Healthy subjects, n = 7, Age Range = 23 - 27 years	72 (6)	0.07	Bolus	0 - 80 h	-	GC-EC	Limit of sensitivity = 1 ng/ml	-	Compartmental (2)	-	*1.90 (± 0.18)*	0.84 (± 0.15)	-
Jochemsen et al[30]	Healthy subjects, n = 8, Mean (SD) Age = 27 (9) years	73 (7)	0.07	Bolus	0 - 96 h	-	GC-EC	Limit of detection = 1 ng/ml	-	NCA	-	*1.83 (± 0.25)*	0.83 (± 0.17)	-

Urinary Excretion Studies

1. Jochemsen et al[30] calculated fraction of the dose excreted unchanged in the urine to be ~1.0%

Plasma Protein Binding Studies

Study	Subjects	Method	Concentration Range	Assay	f_u (%)
Jochemsen et al[29]	Healthy subjects	Equilibrium dialysis	75 ng/ml	GC-EC	12.3
Jochemsen et al[30]	Healthy subjects	Equilibrium dialysis	-	GC-EC	13
Moschitto et al[4]	*In-vitro*	Equilibrium dialysis	10 - 10000 ng/ml	Liquid Scintillation	12.7

Flunitrazepam

Study	Population	BW	Dose (I.V.)	Rate	PK Sampling Schedule		Assay Method	Analytical Method Parameters		PK Analysis	Urine Collection Method	Vd_{ss}/ Vd_{pss}	CL_{tot}	CL_{ren}
		(kg)	(mg/ kg)		Plasma	Urine		Plasma	Urine			(L/kg)	[ml/min/kg]	[ml/min/kg]
Kanto et al[31]	Healthy subjects, n = 20, Mean (SD) = 51 (19) years	79 (9)	0.02	10 min Infusion	0 - 70 h	-	GC-EC	Limit of sensitivity = 0.2 ng/ml	-	NCA	-	2.44 (± 1.22)	1.70 (± 0.67)	-

Plasma Protein Binding Studies

Study	Subjects	Method	Concentration Range	Assay	f_u (%)
Moschitto et al[4]	*In-vitro*	Equilibrium dialysis	10 - 10000 ng/ml	Liquid Scintillation	22.5 (± 0.40)

B:P Ratios

Study	Method	Concentration Range	Assay	B:P Ratio
Kanto et al[31]	*In-vitro*	-	GC-EC	0.75

Oxazepam

Study	Population	BW	Dose (I.V.)	Rate	PK Sampling Schedule		Assay Method	Analytical Method Parameters		PK Analysis	Urine Collection Method	Vd_{ss}/ Vd_{pss}	CL_{tot}	CL_{ren}
		(kg)	(mg/kg)		Plasma	Urine		Plasma	Urine			(L/kg)	[ml/min/kg]	[ml/min/kg]
Sonne et al[32]	Healthy subjects, n =6, Age range = 26 - 38 years	56 - 87	0.22	15 min Infusion	0 - 24 h	0 - 48 h	HPLC - UV	LLOD = 5 ng/ml	-	NCA	Cumulative	0.60 (± 0.19)	1.05 (± 0.36)	-

Urinary Excretion Studies

1. Sonne et al[32] calculated renal clearance as $CL_{ren} = f_e * CL_{tot}$ (f_e is the fraction of the dose that is excreted unchanged, urinary samples collected from 0 -4, 4 - 8, 8 - 24 and 24 - 48 h after dose), f_e = ~1%

Plasma Protein Binding Studies

Study	Subjects	Method	Concentration Range	Assay	f_u (%)
Abernerthy et al[27]	*In-vitro*	Equilibrium dialysis	-	GC-EC	4.0 ± (0.7)
Kanto et al[31]	*In-vitro*	-	-	-	4.5
Moschitto et al[4]	*In-vitro*	Equilibrium dialysis	10 - 10000 ng/ml	Liquid Scintillation	5.12 (± 0.08)
Sonne et al[32]	Healthy subjects	Equilibrium dialysis	1 µg/ml	HPLC	4.5 (3.7 - 5.5)

B:P Ratios

Study	Method	Concentration Range	Assay	B:P Ratio
Shull et al[33]	*In-vitro*	-	GC-EC	1.04

Temazepam

Study	Population	BW	Dose (I.V.)	Rate	PK Sampling Schedule		Assay Method	Analytical Method Parameters		PK Analysis	Urine Collection Method	Vd_{ss}/ Vd_{pss}	CL_{tot}	CL_{ren}
		(kg)	(mg/ kg)		Plasma	Urine		Plasma	Urine			(L/kg)	[ml/min/kg]	[ml/min/kg]
van Steveninck et al[34]	Healthy subjects, n = 9, Age Range = 18 - 24 years	66 (11)	0.4	30 min Infusion	0 - 24 hrs	-	HPLC	Limit of sensitivity = 1.1 ng/ml	-	NCA	-	-	1.4	-

Urinary Excretion Study

1. Ghabrial et al[35] estimated f_e for temazepam to be 0.80% in the control group.

Plasma Protein Binding Studies

Study	Subjects	Method	Concentration Range	Assay	f_u (%)
van Steveninck et al[34]	*In-vitro*	Equilibrium dialysis	-	GC-EC	2.3
Moschitto et al[4]	*In-vitro*	Equilibrium dialysis	10 - 10000 ng/ml	Liquid Scintillation	3.6 (± 0.07)

Adinazolam

Study	Population	BW	Dose (I.V.)	Rate	PK Sampling Schedule		Assay Method	Analytical Method Parameters		PK Analysis	Urine Collection Method	Vd_{ss}/ Vd_{pss}	CL_{tot}	CL_{ren}
		(kg)	(mg/kg)		Plasma	Urine		Plasma	Urine			(L/kg)	[ml/min/kg]	[ml/min/kg]
Venkatakrishnan et al[36]	Healthy subjects, n = 9, Mean (Range) Age = 29 (20 - 40) years	80	0.1	30 min Infusion	0 - 24 h	-	HPLC-UV	Limit of sensitivity = 5 ng/ml	-	Compartmental (2)	-	0.84	5.55 (± 1.31)	-
Fleishaker et al[37]	Healthy subjects, n = 14, Age Range = 20 - 48 years	67 - 95	0.06	10 min Infusion	0 - 24 h	-	HPLC-UV	LLOQ = 2 ng/ml	-	NCA	-	1.13 (± 0.19)	7.11 (± 1.61)	-
Ajir et al[38]	Healthy subjects, n = 39, Mean (SD) Age = 39 (8) years	75 (8)	0.11	30 min Infusion	0 - 24 h	-	HPLC-UV	LLOQ = 2 ng/ml	-	NCA	-	0.74	4.72 (± 1.18)	-
Fleishaker et al[39]	Healthy subjects, n = 18, Age Range = 21 - 36 years	52 - 90	0.17	30 min Infusion	0 - 24 h	-	HPLC-UV	LLOQ = 2 ng/ml	-	NCA	-	1.58 (± 0.58)	6.87 (± 2.40)	-
Fleishaker et al[40]	Healthy subjects, n = 16, Mean (Range) Age = 28 (19 - 54) years	73 (58 - 91)	0.16	30 min Infusion	0 - 24 h	-	HPLC-UV	LLOQ = 2 ng/ml	-	NCA	-	0.91 (± 0.13)	4.88 (± 0.75)	-

Fleishaker et al[41]	Healthy subjects, n = 24, Age Range = 18 - 50 years	68 (64 - 94	5, 10, 15, 20 mg/ 67.7 kg	30 min Infusion	0 - 24 h	-	HPLC-UV	LLOQ = 2 ng/ml	-	NCA	-	-	5.55 (± 1.19)	-

Plasma Protein Binding Studies

Study	Subjects	Method	Concentration Range	Assay	f_u (%)
Fleishaker et al[37]	Healthy humans	Equilibrium dialysis	50 ng/ml	HPLC - UV	31 (± 3)
Fleishaker et al[39]	Healthy humans	Equilibrium dialysis	75 - 150 ng/ml	HPLC - UV	31 (± 4)
Fleishaker et al[40]	*In-vitro*	Equilibrium dialysis	50 - 750 ng/ml	HPLC - UV	29 (± 2)

B:P Ratio

Study	Subjects	Method	Concentration Range	Assay	B:P Ratio
Fleishaker et al[37]	Healthy Humans	*In-vitro*	-	HPLC - UV	0.70 (0.60 - 0.84)

N-DesmethylAdinazolam

Study	Population	BW	Dose (I.V.)	Rate	PK Sampling Schedule		Assay Method	Analytical Method Parameters		PK Analysis	Urine Collection Method	Vd_{ss}/ Vd_{pss}	CL_{tot}	CL_{ren}
		(kg)	(mg/kg)		Plasma	Urine		Plasma	Urine			(L/kg)	[ml/min/kg]	[ml/min/kg]
Venkatakrishnan et al[36]	Healthy subjects, n = 9, Mean (Range) Age = 29 (20 - 40) years	80	0.1	30 min Infusion	0 - 24 h	-	HPLC-UV	Limit of sensitivity = 5 ng/ml	-	Compartmental (1)	-	0.74	4.0 (± 0.4)	-
Ajir et al[38]	Healthy subjects, n = 39, Mean (SD) Age = 39 (8) years	75 (8)	0.3	30 min Infusion	0 - 24 h	-	HPLC-UV	LLOQ = 10 ng/ml	-	NCA	-	0.54	2.43 (± 0.32)	-
Fleishaker et al[40]	Healthy subjects, n = 16, Mean (Range) Age = 28 (19 - 54) years	73 (58 - 91)	0.3	30 min Infusion	0 - 24 h	-	HPLC-UV	LLOQ = 2 ng/ml	-	NCA	-	0.62 (± 0.08)	2.47 (± 0.30)	-
Fleishaker et al[41]	Healthy subjects, n = 24, Age Range = 18 - 50 years	68 (64 - 94	10, 20, 30, 40 mg/68 kg	30 min Infusion	0 - 24 h	0 - 36 hrs	HPLC - UV	LLOQ = 10 ng/ml	LLOQ = 10 ng/ml	NCA	Cumulative	0.83	2.83	2.0

Urinary Excretion Studies

1. Fleishaker et al[41] calculated the CL_{ren} by using CL_{ren} = Ae/AUC (Urine was collected in intervals 0 - 2, 2 - 4, 4 - 8, 8 - 12, 12 - 24 and 24 - 36 hrs); f_e = 71%

Plasma Protein Binding Studies

Study	Subjects	Method	Concentration Range	Assay	f_u (%)
Fleishaker et al[40]	*In-vitro*	Equilibrium dialysis	50 - 750 ng/ml	HPLC - UV	65 (± 2)

Alprazolam

Study	Population	BW	Dose (I.V.)	Rate	PK Sampling Schedule		Assay Method	Analytical Method Parameters		PK Analysis	Urine Collection Method	Vd_{ss}/ Vd_{pss}	CL_{tot}	CL_{ren}
		(kg)	(mg/kg)		Plasma	Urine		Plasma	Urine			(L/kg)	[ml/min/kg]	[ml/min/kg]
Smith et al[42]	Healthy subjects, n = 9, Mean (Range) Age = 29 (20 - 40) years	80	0.01	1 min Infusion	10 min - 36 h	-	GC - EC	Limit of sensitivity = 0.25 ng/ml	-	NCA	-	0.80	0.74 (0.56 - 1.05)	-
Fleishaker et al[43]	Healthy subjects, n = 42, Age range = 18 - 54 years		0.01	1 min Infusion	5 min - 36 h	-	HPLC-UV	LLOD = 1 ng/ml	-			1.03 (± 0.13)	0.89 (±0.28)	

Plasma Protein Binding Studies

Study	Subjects	Method	Concentration Range	Assay	f_u (%)
Moschitto et al[4]	*In-vitro*	Equilibrium dialysis	10 - 10000 ng/ml	Liquid Scintillation	31.6 (± 0.6)

Midazolam

Study	Population	BW	Dose (I.V.)	Rate	PK Sampling Schedule		Assay Method	Analytical Method Parameters		PK Analysis	Urine Collection Method	Vd_{ss}/ Vd_{pss}	CL_{tot}	CL_{ren}
		(kg)	(mg/kg)		Plasma	Urine		Plasma	Urine			(L/kg)	[ml/min/kg]	[ml/min/kg]
Greenblatt et al[44]	Healthy subjects, n = 11, Age Range = 28 - 42 years	-	0.1	1 min Infusion	0 - 24 h	-	GC-EC	LLOQ = 1.5 ng/ml	-	Compartmental (2)	-	1.6	11.0 (± 3.6)	-
Heizmann et al[45]	Healthy subjects, n = 6, Age Range = 22 - 27 years	66	0.15	Bolus	0 - 12 h	-	GC-EC	Limit of Detection = 4 ng/ml	-	Compartmental (2)	-	0.72 (± 0.16)	4.6 (± 1.2)	-
Smith et al[46]	Healthy subjects, n = 6, Mean (SD) Age = 22 (0.5) years	73 (6)	0.07	Bolus	0 - 8 hrs	0 - 8 h	GC - EC	Limit of Detection = 0.5 ng/ml	-	NCA	Cumulative	0.85 (± 0.42)	6.39 (± 1.57)	-
Thummel et al[47]	Healthy subjects, n = 20, Mean (SD) Age = 32 (7) years	77 (13)	0.01	Bolus	0 - 6 hrs	0 -24 hours	GC - MS	-	-	NCA	Cumulative	0.90 (± 0.39)	4.62 (± 1.00)	0.013
Allonen et al[48]	Healthy subjects, n = 6, Mean (SD) Age = 30 (4) years	70 (8)	0.08	1 min Infusion	0 - 7 hrs	-	GC - EC	Sensitivity limit = 5 ng/ml	-	NCA	-	0.68 (± 0.15)	4.12 (± 0.94)	-

Clausen et al[49]	Healthy subjects, n = 6, Mean (Range) Age = 27 (23 - 37) years	68 (6)	0.3	Bolus	0 - 12 hrs	-	GC - EC	Limit of detection = 5 ng/ml	-	Compartmental (3)	-	1.10 (± 0.20)	6.28 (± 1.03)	-
Macgilchrist et al[50]	Healthy subjects, n = 8, Age Range = 37 - 42 years	61 (11)	0.08	1 min Infusion	0 - 24 h	-	GC - EC	Sensitivity limit = 5 ng/ml	-	Compartmental (2)	-	0.87	10.4 (± 3.7)	-
Ochs et al[15]	Healthy subjects, n = 10, Mean (Range) Age = 27 (22-37) years	66	0.08	1 min Infusion	0 - 24 hrs	-	GC-EC	LLOQ = 2.5 ng/ml	-	Compartmental (2 or 3)	-	-	9.6 (± 3.8)	-

Urinary Excretion Studies

1. Smith et al[46] calculated the CLren by using CLren = fe*CLtot (fe = % of the dose excreted unchanged in the urine; urine was sampled up to 8 hrs). f_e = 0.02%
2. Thummel et al[47] calculated the CLren by using CLren = fe*CLtot (fe = % of the dose excreted unchanged in the urine; urine was sampled up to 8 hrs). f_e = 0.28%

Plasma Protein Binding Studies

Study	Subjects	Method	Concentration Range	Assay	f_u (%)
Thummel et al[47]	Healthy humans	Equilibrium dialysis	-	GC - MS	1.9 (± 0.7)
Allonen et al[48]	Healthy humans	Equilibrium dialysis	130 ng/ml	GC - EC	6.0 (± 1.9)
Ochs et al[15]	Healthy humans	Equilibrium dialysis	-	GC-EC	3.4 (± 0.3)
Moschitto et al[4]	*In-vitro*	Equilibrium dialysis	10 - 10000 ng/ml	Liquid Scintillation	3.7 (± 0.03)

B:P Ratio

Study	Subjects	Method	Concentration Range	Assay	B:P Ratio
Heizmann et al[45]	Healthy humans	*In-vitro*	-	GC-EC	0.53
Allonen et al[48]	Healthy humans	*In-vitro*	130 ng/ml	GC-EC	0.57 (± 0.06)

Triazolam

Study	Population	BW	Dose (I.V.)	Rate	PK Sampling Schedule		Assay Method	Analytical Method Parameters		PK Analysis	Urine Collection Method	Vd_{ss}/ Vd_{pss}	CL_{tot}	CL_{ren}
		(kg)	(mg/kg)		Plasma	Urine		Plasma	Urine			(L/kg)	[ml/min/kg]	[ml/min/kg]
Kroboth et al[51]	Healthy subjects, n = 12, Mean (Range) Age = 23 (20 - 35)	83	0.003	Bolus	Up to 12 h	-	GC - EC	LLOD = 0.25 ng/ml	-	Non-compartmental	-	0.64 (± 0.18)	2.6 (± 1.0)	-
Pete Vanderveen[52]	Healthy subjects, n = 12, Mean (Range) Age = 35 (19 - 54)	79 (66 - 96)	0.003	5 min Infusion	Up to 12 h	-	HPLC	LLOQ = 0.2 ng/ml	-	Non-compartmental	-	0.59	2.7 (± 0.70)	-
Smith et et al[53]	Healthy subjects, n = 30, Mean (Range) Age = 28 (21 - 38)	74 (60 - 103)	0.125 - 1 mg	Bolus	Up to 8 h	-	GC - EC	Sensitivity limit = 0.25 ng/ml	-	Non-compartmental	-	0.67	2.9	-

Plasma Protein Binding Studies

Study	Subjects	Method	Concentration Range	Assay	f_u (%)
Moschitto et al[4]	*In-vitro*	Equilibrium dialysis	10 - 10000 ng/ml	Liquid Scintillation	11

B:P Ratio

Study	Subjects	Method	Concentration Range	Assay	B:P Ratio
Pete Vanderveen[52]	Healthy subjects	[^{14}C]-labelled Radioactivity	-	Liquid Scintillation Counter	0.76 (±0.050)

Ro 48 - 6791

Study	Population	BW	Dose (I.V.)	Rate	PK Sampling Schedule		Assay Method	Analytical Method Parameters		PK Analysis	Urine Collection Method	Vd_{ss}/ Vd_{pss}	CL_{tot}	CL_{ren}
		(kg)	(mg/kg)		Plasma	Urine		Plasma	Urine			(L/kg)	[ml/min/kg]	[ml/min/kg]
Dingemanse et al[54]	Healthy subjects, n = 10, Age range = 21 - 26 kg	64 - 78	0.1 - 3 mg	20 min Infusion	Up to 280 min	-	HPLC -MS/MS	LLOQ = 20 pg/ml	-	Compartmental (2)	-	2.41 (± 0.92)	30.99 (± 12.7)	-

B:P Ratio

Study	Subjects	Method	Concentration Range	Assay	B:P Ratio
Dingemanse et al[54]	-	-	-	-	1.33

Ro 48 - 8684

Study	Population	BW	Dose (I.V.)	Rate	PK Sampling Schedule		Assay Method	Analytical Method Parameters		PK Analysis	Urine Collection Method	Vd_{ss}/ Vd_{pss}	CL_{tot}	CL_{ren}
		(kg)	(mg/kg)		Plasma	Urine		Plasma	Urine			(L/kg)	[ml/min/kg]	[ml/min/kg]
van Gerven et al[55]	Healthy subjects, n = 10, Age range = 22 - 32 years	67 - 89	0.1 - 10 mg	20 min Infusion	Up to 300 min	-	HPLC -MS/MS	LLOQ = 50 pg/ml	-	Compartmental (2)	-	4.32 (± 1.46)	30.77 (± 6.41)	-

B:P Ratio

Study	Subjects	Method	Concentration Range	Assay	B:P Ratio
van Gerven et al[55]	-	-	-	-	1.36

Brotizolam

Study	Population	BW	Dose (I.V.)	Rate	PK Sampling Schedule		Assay Method	Analytical Method Parameters		PK Analysis	Urine Collection Method	Vd_{ss}/ Vd_{pss}	CL_{tot}	CL_{ren}
		(kg)	(mg/kg)		Plasma	Urine		Plasma	Urine			(L/kg)	[ml/min/kg]	[ml/min/kg]
Jochemsen et al[56]	Healthy subjects, n = 8, Age range = 21 - 26 years	69	0.004	4 min Infusion	Up to 48 h	-	GC - EC	Sensitivity limit = 0.1 ng/ml	-	Compartmental (2)	-	0.66 (± 0.19)	1.58 (± 0.39)	-

Plasma Protein Binding Studies

Study	Subjects	Method	Concentration Range	Assay	f_u (%)
Bechtel et al[57]	*In-vitro*	Equilibrium Dialysis	0.07 - 13.7 µg/ml	Liquid Scintillation	9.8%

Flumazenil

Study	Population	BW	Dose (IV)	Rate	PK Sampling Schedule		Assay Method	Analytical Method Parameters		PK Analysis	Urine Collection Method	Vd_{ss}	CL_{tot}	CL_{ren}
		(kg)	(mg/kg)		Plasma	Urine		Plasma	Urine			(L/kg)	[ml/min/kg]	[ml/min/kg]
Roncari et al[58]	Healthy subjects, n = 6; Mean (Range) Age = 26 (24 - 27) years	74 (65 - 79)	0.27	Bolus	Up to 6h	Up to 24 hrs	HPLC-UV	Sensitivity limit = 10 ng/ml	Sensitivity limit = 10 ng/ml	Non-Compartmental	Cumulative	1.1± 0.23	14.8± 2.3	
			0.54	Bolus								1.0± 0.17	16.2± 2.8	
Klotz et al[59]	Healthy subjects, n = 6; Age Range = 28 - 42 years	63 - 82 kg	0.04	Bolus	Up to 3h	-	HPLC-UV	Sensitivity limit = 2 ng/ml	-	Compartmental (2)	-	0.63 ±0.18	10.1± 3.2	-
Janssen et al[60]	Healthy subjects, n = 8; Mean (Range) Age = 50 (45 - 56) years	73 (57 - 87)	0.03	Bolus	Up to 4h	-	HPLC-UV	Sensitivity limit = 3 ng/ml	-	Non-Compartmental	-	0.97 ±0.19	16.5± 2.6	-
Pomier - Layrargues et al[61]	Healthy subjects, n = 8; Mean (SD) Age = 38 (1.6) years	76 (11)	0.03	5 min Infusion	Up to 7h	-	GC	Sensitivity limit = 0.05 ng/ml	-	Non-Compartmental	-	0.62 (± 0.090)	16.3 (±2.6)	-
Klotz et al[62]	Healthy subjects, n = 6; Age Range = 18 - 36 years	59 - 87	0.1	Bolus	Up to 5.75 h	-	HPLC-UV	Sensitivity limit = 2 ng/ml	-	Non-Compartmental	-	-	15.1 (±2.8)	-

Urinary Excretion Studies

1. Boncari et al[58] calculated the CLren by using CLren = fe*CLtot (fe = % of the dose excreted unchanged in the urine up to 24 hours = 0.1%)

Plasma Protein Binding Studies

Study	Subjects	Method	Concentration Range	Assay	f_u (%)
Klotz et al[59]	*In-vitro*	Equilibrium Dialysis	50 ng/ml	HPLC	60 (±8)
Pomier - Layrargues et al[61]	*In-vitro*	Equilibrium Dialysis	20 - 600 ng/ml	Liquid Scintillation	55 (±4)

B:P Ratio

Study	Subjects	Method	Concentration Range	Assay	B:P Ratio
Boncari et al[58]	Healthy subjects	[^{14}C]-labelled Radioactivity	-	Liquid Scintillation Counter	0.88
Klotz et al[59]	Healthy subjects	-	-	HPLC	0.99 (±0.26)

Metabolism

The schematic for metabolism of flumazenil[60,63] is shown in figure below.

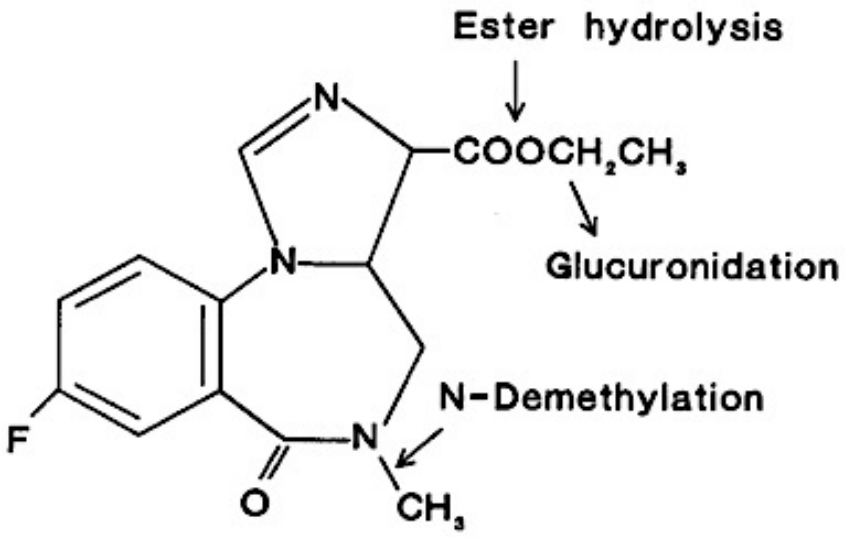

Structure of flumazenil and its metabolic sites.

Appendix 1.2 - Hepatic Metabolism

The contribution of a enzyme-specific metabolic pathway towards CL_{tot}, $f_{pathway}$ can be assessed by looking into drug-drug interaction studies in the presence of the specific inhibitor and genetic polymorphisms in the drug metabolizing enzyme. For example, ketoconazole is a selective and a potent CYP3A inhibitor, and since the majority of the BZD in the present work are metabolized by the CYP3A pathway, drug-drug interaction studies between BZD and ketoconazole were compiled in the Appendix below:

In the absence of inhibitor (Control):

$CL_{tot}^{I.V.}(Control) / F_{oral} = Dose/AUC_{0-\infty}(Control)$

$CL_{tot}^{I.V.}$ is the systemic total body clearance of BZD, which is primarily, CL_{nonren} (since CL_{ren} is, in general, negligible). Furthermore, since there are no significant extrahepatic pathways reported in the literature, CL_{nonren} is assumed to equal to the CL_{hep} (which is sum of all the metabolic pathways). The majority of the BZD are low ER_{hep} drugs and in general, they have high F_{oral}, and therefore, the systemic exposure depends on CL_{hep} only.

In the presence of inhibitor (I):

$CL_{tot}^{I.V.}(I) / F_{oral}(I) = Dose/AUC_{0-\infty}(I)$

The assumptions are: (a) CL_{ren} is negligible and there are no significant extrahepatic metabolic pathways; $CL_{tot} = \sim CL_{nonren} = \sim CL_{hep}$, (b) In the presence of inhibitor, only that specific pathway is inhibited (e.g., CYP3A for ketoconazole; genetic polymorphisms - poor versus extensive metabolizers), and (c) the inhibitor is selective and completely inhibits the specific metabolic pathway of interest.

The contribution of specific pathway of interest to the overall hepatic clearance (assumed to be CL_{tot} for BZD) can be estimated as (assuming the oral doses are identical):

$$f_{pathway} = 1 - (CL_{tot}^{I.V}(I) / CL_{tot}^{I.V.}(Control)) = 1 - (AUC_{0-\infty}(Control) / AUC_{0-\infty}(I))$$

Chlordiazepoxide

Study	Population	Inhibitor		Substrate	PK Sampling Schedule	Assay Method	Analytical Method Parameters	PK Analysis	$AUC_{0-\infty}$ (Control)	$AUC_{0-\infty}$ (+ Inhibitor)	(1 - AUC Con/In) $f_{pathway}$
		Name	**Dosing Regimen**	**Dosing Regimen**							
Brown et al[64]	Healthy subjects, n = 12, Age Range = 25 - 36 years	Ketoconazole	200 mg **P.O.** (1 dose)	0.6 mg/kg **I.V.** (1 dose 1h after Ketoconazole)	0 - 48 hrs	HPLC	Sensitivity limit = 50 ng/ml	Compartmental (2)	1684	2042	18%
			400 mg. **P.O.** (1 dose)	0.6 mg/kg **I.V.** (1 dose 1h after Ketoconazole)					1685	2076	19%
			400 mg. q.d for 6 days **P.O.** (6 doses)	0.6 mg/kg **I.V.** on day 6 (1 dose 1h after Ketoconazole)					1470	2262	35%

Midazolam

Study	Population	Inhibitor		Substrate	PK Sampling Schedule	Assay Method	Analytical Method Parameters	PK Analysis	$AUC_{0-\infty}$ (Control)	$AUC_{0-\infty}$ (+ Inhibitor)	(1 - AUC Con/ In) $f_{pathway}$
		Name	Dosing Regimen	Dosing Regimen							
Lam et al[65]	Healthy subjects, n = 10, Mean (SD) Age = 34 (8) years	Ketoconazole	200 mg q.d. for 12 days **P.O.** (12 doses)	10 mg **P.O.** (1 dose 1h after Ketoconazole)	0.25 - 24 hrs	HPLC - UV	LLOQ = 5 ng/ml	Non-Compartmental	195 (±115)	1280 (±617)	85%
Tsunoda et al[66]	Healthy subjects, n = 5, Mean (SD) Age = 26 (6) years	Ketoconazole	200 mg q.d. for 3 days **P.O.** (3 doses)	6 mg **P.O.** (1 dose on day 3)	Up to 24 hrs	GC - EC	LLOQ = 5 ng/ml	Non-Compartmental	54 (±37)	651 (±181)	92%
				2 mg **I.V.** (1 dose on day 3)					56 (±20)	222 (±65)	75%
Tsunoda et al[67]	Healthy subjects, n = 9, Age range = 19 - 41 years	Ketoconazole	200 mg b.i.d for 3 days **P.O.**	6 mg **P.O.** (1 dose 12 h after Ketoconazole)	Up to 24 hrs	GC - EC	LLOQ = 5 ng/ml	Non-Compartmental	54 (±28)	738 (±191)	93%
			200 mg b.i.d for 3 days **P.O.**	2 mg **I.V.** (1 dose 12 h after Ketoconazole)					70 (±26)	354 (±185)	**80%**

Olkkola et al[68]	Healthy subjects, n = 9, Age range = 19 - 26 years	Ketoconazole	400 mg q.d. for 4 days **P.O.** (4 doses)	7.5 mg **P.O.** (1 dose 1h after Ketoconazole)	Up to 17 hrs	GC - EC	LLOQ = 5 ng/ml	Non-Compartmental	4 (± 2)	42 (±18)	94%

Triazolam

Study	Population	Inhibitor		Substrate	PK Sampling Schedule	Assay Method	Analytical Method Parameters	PK Analysis	$AUC_{0-\infty}$ (Control)	$AUC_{0-\infty}$ (+ Inhibitor)	(1 - AUC Con/In) $f^{path\ way}$
		Name	Dosing Regimen	Dosing Regimen							
Greenblatt et al[69]	Healthy subjects, n = 7, Age Range = 21 - 44 years	Ketoconazole	200 mg b.i.d for 2.5 days **P.O.** (5 doses)	0.25 mg **P.O.** 1 dose on day 3 1 h after Ketoconazole	Up to 48 hrs	GC - EC	LLOQ = 0.1 - 0.2 ng/ml ng/ml	Non-Compartmental	11 (±4)	145 (±96)	92%
von Moltke et al[70]	Healthy subjects, n = 9, Age Range = 23 - 72 years	Ketoconazole	200 mg 1, 17h **P.O.** (2 doses)	0.125 mg **P.O.** 1 dose on day 2	Upto 24 hrs	GC - EC	LLOQ = 0.2 ng/ml	Non-Compartmental	7 (±2)	62 (±30)	89%
Varhe et al[71]	Healthy subjects, n = 9, Age Range = 20 - 26 years	Ketoconazole	400 mg q.d. for 4 days **P.O.** (4 doses)	0.25 mg **P.O.** 1 dose on day 4	Up to 17 hrs	GC - EC	LLOQ = 0.2 ng/ml	Non-Compartmental	6 (±2)	132 (±75)	95%

Alprazolam

Study	Population	Inhibitor		Substrate	PK Sampling Schedule	Assay Method	Analytical Method Parameters	PK Analysis	$AUC_{0-\infty}$ (Control)	$AUC_{0-\infty}$ (+ Inhibitor)	(1 - AUC Con/ In) $f_{pathway}$
		Name	Dosing Regimen	Dosing Regimen							
Greenblatt et al[69]	Healthy subjects, n = 7, Age Range = 21 - 44 years	Ketoconazole	200 mg b.i.d for 2.5 days **P.O.** (5 doses)	1 mg **P.O.** 1 dose on day 3 1 h after Ketoconazole	Up to 48 hrs	GC - EC	LLOQ = 0.1 - 0.2 ng/ml ng/ml	Non-Compartmental	237 (±114)	944 (±733)	75%
Schmider et al[72]	Healthy subjects, n = 7, Age Range = 22 - 55 years	Ketoconazole	200 mg b.i.d for 2 days **P.O.**	1 mg **P.O.** 1 dose on day 3 1 h after Ketoconazole	Up to 24 hrs	HPLC - UV	LLOQ = 0.5 ng/ml ng/ml	Non-Compartmental	242 (±114)	426 (±86)	43%

Brotizolam

Study	Population	Inhibitor		Substrate	PK Sampling Schedule	Assay Method	Analytical Method Parameters	PK Analysis	$AUC_{0-\infty}$ (Control)	$AUC_{0-\infty}$ (+ Inhibitor)	(1 - AUC Con/In) $f_{pathway}$
		Name	Dosing Regimen	Dosing Regimen							
Osanai et al[73]	Healthy subjects, n = 10, Mean (SD) Age = 34 (5) years	Itraconazole	200 mg q.d. for 4 days **P.O.** (4 doses)	0.5 mg **P.O.** 1 dose on day 4	Up to 24 hrs	HPLC - UV	LLOQ = 5 ng/ml	Non-Compartmental	33	169	80%

Diazepam

Study	Population	Genetic Polymorphisms	Substrate	PK Sampling Schedule	Assay Method	Analytical Method Parameters	PK Analysis	$AUC_{0-\infty}$ (Control)	$AUC_{0-\infty}$ (+ Inhibitor)	(1 - AUC Con/In) $f_{pathway}$
			Dosing Regimen							
Qin et al[74]	Healthy subjects, n = 18, Mean (SD) Age = 26 (6) years	Wild type reflect - poor metabolizers (Control) Double homozygous reflect - extensive metabolizers	5 mg **P.O.**	Up to 12 days	GC	LLOQ = 8 ng/ml	Non-Compartmental	5.3 (± 2.7)	32.4 (±10.1)	84%

Appendix 2 - Human PK Study Summaries of NMB

Rocuronium

Study	Population	BW	Dose (I.V.)	Rate	PK Sampling Schedule		Assay Method	Analytical Method Parameters		PK Analysis	Urine Collection Method	Vd_{ss}/ Vd_{pss}	CL_{tot}	CL_{ren}
		(kg)	(mg/kg)		Plasma	Urine		Plasma	Urine			(L/kg)	[ml/min/kg]	[ml/min/kg]
van Miert et al[75]	Healthy subjects, n = 21, Mean (SD) Age = 44 (12) years	73 (9)	0.60	Bolus	1 - 480 min	-	HPLC-Fluorescence	Assay range: 10 - 20000 ng/ml	-	Compartmental (2, 3)	-	0.21 (± 0.055)	3.7 (± 1.0)	-
McCoy et al[76]	Healthy subjects, n = 8, Age range = 18 - 65 years		0.45	Bolus followed by Infusion at 15 µg/kg/min	1 min - 6.5 h	-	HPLC - Fluorescence	LLOQ = 3 ng/ml	-	Compartmental (2, 3)	-	0.21 (± 0.040)	3.3 (± 0.77)	-

Wierda et al[77]	Healthy subjects, n = 10, Mean (Range) Age = 51 (30 - 60) years	69 (56 - 75)	1.00	60 min	1 min - 8h	Up to 24 hrs	HPLC - Fluorescence	LLOQ = 5 ng/ml	LLOQ = 5 ng/ml	Compartmental (2, 3)	Cumulative	0.27 (± 0.15)	4.0 (± 0.95)	1.32
Cooper et al[78]	Healthy subjects, n = 9, Mean (Range) Age = 51 (21 - 61) years	63 (19)	0.60	Bolus	1 min - 6.5 h	-	HPLC - Fluorescence	LLOQ = 10 ng/ml	-	Compartmental (2, 3)	-	0.21 (± 0.049)	3.7 (± 1.4)	-
Van den Broek et al[79]	Healthy subjects, n = 18	-	0.60	Bolus	1 min - 8 h	Up to 24 hrs	HPLC - Fluorescence	LLOQ = 10 ng/ml	LLOQ = 25 ng/ml	Compartmental (2, 3)	Cumulative	0.20 (± 0.079)	4.3 (± 0.99)	0.73
Khalil et al[80]	Healthy subjects, n = 8, Mean (SD) Age = 53 (13) years	72 (8)	0.60	3 min	2 min - 6 h	-	HPLC - Fluorescence	Sensitivity limit = 20 ng/ml	-	Compartmental (2)	-	0.18 (± 0.041)	2.8 (± 0.62)	-
Magorian et al[81]	Healthy subjects, n = 10, Mean (SD) Age = 44 (15) years	78 (12)	0.60	Bolus	2 min - 6 h	-	GC	Sensitivity limit = 10 ng/ml	-	Population PK	-	0.21	2.8	-

Urinary Excretion Studies

1. Wierda et al[77] calculated $CL_{ren} = f_e * CL_{tot}$ (f_e is the fraction of the dose that is excreted unchanged in the urine; urine samples were collected at 2, 4, 6, 9, 12, 18, 24 hrs), $f_e = 33\%$
2. Van den Broek et al[79] calculated $CL_{ren} = f_e * CL_{tot}$ (f_e is the fraction of the dose that is excreted unchanged in the urine; urine samples were collected up to 24 hrs), $f_e = 17\%$

Plasma Protein Binding Studies

Study	Subjects	Method	Concentration Range	Assay	f_u (%)
Proost et al[82]	*In-vitro*	Ultrafiltration	Up to 2000 ng/ml	HPLC - Fluorescence	75
Roy et al[83]	*In-vitro*	Ultrafiltration	Up to 2000 ng/ml	HPLC - Fluorescence	54 (4)

Metabolism

Of the 3 putative metabolites of rocuronium, measurable amount of only 17-desacetyl derivative was detected in plasma[84]. Biliary excretion and metabolism have not been detected in healthy human adults[84].

Pharmacodynamics

Study	Subjects	PD Endpoint	k_{eo} (min^{-1})	Cp^{ss}_{50} (µg/ml)	γ
van Miert et al[75]	Healthy subjects, n = 21, Mean (SD) Age = 44 (12) years	> 70% Depression in the muscle twitch following train of four stimulus	0.16 (± 0.060)	1.0 (± 0.29)	5.4 (±1.2)
Khalil et al[80]	Healthy subjects, n = 8, Mean (SD) Age = 53 (13) years	90% Depression in the muscle twitch following train of four stimulus	0.18 (± 0.058)	1.2 (± 0.25)	6.8 (±1.7)

Vecuronium

Study	Population	BW	Dose (I.V.)	Rate	PK Sampling Schedule		Assay Method	Analytical Method Parameters		PK Analysis	Urine Collection Method	Vd_{ss}/ Vd_{pss}	CL_{tot}	CL_{ren}
		(kg)	(mg/kg)		Plasma	Urine		Plasma	Urine			(L/kg)	[ml/min/kg]	[ml/min/kg]
Cronnelly et al[85]	Healthy subjects, n = 5	-	0.04	10 min	2 min - 24 h	-	LC - MS	Sensitivity limit of 2 ng/ml	-	Compartmental (2, 3)	-	0.27 (± 0.040)	5.2 (± 0.7)	-
Caldwell et al[86]	Healthy male subjects, n = 12, Mean (SD) Age = 26 (5) years	74 (8)	0.30	10 min	2 min - 6 h	360 - 480 min	GC-Nitrogen sensitive detector	Sensitivity limit of 5 ng/ml	Sensitivity limit of 5 ng/ml	Compartmental (2, 3)	Fractionated	0.15	5.7	0.40
Arden et al[87]	Healthy subjects, n = 10, Mean (SD) Age = 41 (9) years	70 (13)	0.10	Bolus	2 min - 8 h	-	GC-Nitrogen sensitive detector	Sensitivity limit of 5 ng/ml	-	Compartmental (2, 3)	-	0.18 (± 0.060)	4.5 (± 2.0)	-
Rupp et al[88]	Healthy subjects, n = 5, Mean (SD) Age = 36 (4) years	61 (10)	2.5 µg/kg/min)	T_{inf} based on PD endpoint	2 min - 6 h	-	LC - MS	Sensitivity limit of 2 ng/ml	-	Compartmental (2, 3)	-	0.24 (± 0.040)	5.2 (± 0.8)	-
van der Veen et al[89]	Healthy subjects, n = 6, Mean (SD) Age = 32 (16) years	-	0.11	80 - 202 min	Up to 60 min (B) and 125 min	-	HPLC	-	-	Compartmental (2)	-	0.18 (± 0.070)	6.1	-

					(Inf)									
Fahey et al[90]	Healthy subjects, n = 4	-	0.28	Bolus	4 min - 4 h	-	HPLC	Sensitivity limit of 50 ng/ml	-	Compartmental (2)	-	0.19 (± 0.040)	3.0 (± 0.3)	-

Urinary Excretion Studies

1. Caldwell et al[86] calculated CL_{ren} by using CL_{ren} = Ae/AUC (Urine was collected in intervals 6 - 8 hrs); f_e = 7%

Plasma Protein Binding Studies

Study	Subjects	Method	Concentration Range	Assay	f_u (%)
Proost et al[82]	*In-vitro*	Ultrafiltration	Up to 2000 ng/ml	HPLC - Fluorescence	43
Cameron et al[91]	Healthy subjects, n = 10	Ultrafiltration	0.5 - 2.0 µg/ml	HPLC - Fluorescence	31 (± 4)
Duvaldestin et al[92]	Healthy subjects, n = 6	Ultracentrifugation	0.3 µg/ml	Liquid scintillation counting	70 (± 9)

Pharmacodynamics

Study	Subjects	PD Endpoint	k_{eo} (min^{-1})	Cp^{ss}_{50} (µg/ml)	γ
Cronnelly et al[85]	Healthy subjects, n = 5	-	-	0.094 (± 0.033)	-

Caldwell et al[86]	Healthy male subjects, n = 12, Mean (SD) Age = 26 (5) years	>90% Depression in the muscle twitch following train of four stimulus	0.28	0.10	-
Rupp et al[88]	Healthy subjects, n = 5, Mean (SD) Age = 36 (4) years	-	0.17 (± 0.021)	0.092 (±0.037)	5.8 (± 0.95)
van der Veen et al[89]	Healthy subjects, n = 6, Mean (SD) Age = 32 (16) years	-	0.27 (±0.07)	0.14 (± 0.027)	5.7 (±1.5)

Org 7268 (Vecuronium Metabolite)

Study	Population	BW	Dose (I.V.)	Rate	PK Sampling Schedule		Assay Method	Analytical Method Parameters		PK Analysis	Urine Collection Method	Vd_{ss}/ Vd_{pss}	CL_{tot}	CL_{ren}
		(kg)	(mg/kg)		Plasma	Urine		Plasma	Urine			(L/kg)	[ml/min/kg]	[ml/min/kg]
Caldwell et al[86]	Healthy male subjects, n = 12, Mean (SD) Age = 26 (5) years	74 (8)	0.30	10 min	2 min - 6 h	360 - 480 min	GC-Nitrogen sensitive detector	Sensitivity limit of 5 ng/ml	Sensitivity limit of 5 ng/ml	Compartmental (2, 3)	Fractionated	0.26	4.3	0.77

Urinary Excretion Studies

1. Caldwell et al[86] calculated CL_{ren} by using CL_{ren} = Ae/AUC (Urine was collected in intervals 6 - 8 hrs); f_e = 18%

Plasma Protein Binding Studies

Study	Subjects	Method	Concentration Range	Assay	f_u (%)
Proost et al[82]	*In-vitro*	Ultrafiltration	Up to 2000 ng/ml	HPLC - Fluorescence	69

Pharmacodynamics

Study	Subjects	PD Endpoint	k_{eo} (min^{-1})	Cp^{ss}_{50} (µg/ml)	γ
Caldwell et al[86]	Healthy male subjects, n = 12, Mean (SD) Age = 26 (5) years	>90% Depression in the muscle twitch following train of four stimulus	0.26	0.13	-

Pancuronium

Study	Population	BW	Dose (I.V.)	Rate	PK Sampling Schedule		Assay Method	Analytical Method Parameters		PK Analysis	Urine Collection Method	Vd_{ss}/ Vd_{pss}	CL_{tot}	CL_{ren}
		(kg)	(mg/kg)		Plasma	Urine		Plasma	Urine			(L/kg)	[ml/min/kg]	[ml/min/kg]
Cronnelly et al[85]	Healthy subjects, n = 4	-	0.04	10 min	2 min - 24 h	-	LC - MS	Sensitivity limit of 2 ng/ml	-	Compartmental (2, 3)	-	0.26 (± 0.070)	1.8 (± 0.4)	-
Rupp et al[88]	Healthy subjects, n = 5, Mean (SD) Age = 36 (4) years	61 (10)	2.5 µg/kg/min)	T_{inf} based on PD endpoint	2 min - 6 h	-	LC - MS	Sensitivity limit of 2 ng/ml	-	Compartmental (2, 3)	-	0.21 (± 0.079)	1.5 (± 0.5)	-
Caldwell et al[93]	Healthy subjects, n = 18, Mean (SD) Age = 41 (15) years	75 (15)	0.10	Bolus	2 min - 6 h	-	GC - Nitrogen sensitive detector	Sensitivity limit of 2 ng/ml	-	Compartmental (2, 3)	-	0.20 (± 0.054)	1.5 (± 0.4)	-

Urinary Excretion Studies

Although the analytical method used for the quantification of the (parent) pancuronium was not specific, i.e., coloriemetry, from the urinary excretion studies carried out by Duvaldestin et al[94–96] (although they state that it was specific), the mean value calculated from these studies for the fraction that appears in the urine (f_e) was found to be **58%.** The underlying assumption is that there are no major metabolites in the urine, i.e., only the unchanged drug appears in the urine. The PK parameter estimates, namely, Vd_{ss} and CL_{tot} obtained for the parent

pancuronium from other studies (shown above) in which it was quantitated by specific and sensitive methods were similar to those obtained by Duvaldestin et al[94–96] suggesting that there are no (major) metabolites.

Plasma Protein Binding Studies

Study	Subjects	Method	Concentration Range	Assay	f_u (%)
Proost et al[82]	*In-vitro*	Ultrafiltration	Up to 2000 ng/ml	HPLC - Fluorescence	79
Duvaldestin et al[92]	Healthy subjects, n = 8	Ultracentrifugation	0.3 µg/ml	Liquid scintillation counting	71 (± 9)

Pharmacodynamics

Study	Subjects	PD Endpoint	k_{eo} (min^{-1})	Cp^{ss}_{50} (µg/ml)	γ
Cronnelly et al[85]	Healthy subjects, n = 4	-	-	0.088 (± 0.034)	-
Rupp et al[88]	Healthy subjects, n = 5, Mean (SD) Age = 36 (4) years	-	0.17 (± 0.075)	0.11 (±0.035)	4.8 (± 0.97)

Pipercuronium

Study	Population	BW	Dose (I.V.)	Rate	PK Sampling Schedule		Assay Method	Analytical Method Parameters		PK Analysis	Urine Collection Method	Vd_{ss}/ Vd_{pss}	CL_{tot}	CL_{ren}
		(kg)	(mg/kg)		Plasma	Urine		Plasma	Urine			(L/kg)	[ml/min/kg]	[ml/min/kg]
Caldwell et al[93]	Healthy subjects, n = 20, Mean (SD) Age = 46 (15) years	71 (13)	0.07	Bolus	2 min - 6 h	-	GC - Nitrogen sensitive detector	Sensitivity limit of 2 ng/ml	-	Compartmental (2, 3) and also NCA (similar results)	-	0.31 (± 0.054)	2.4 (± 0.60)	-
D'Honneur et al[97]	Healthy subjects, n = 8, Mean (SD) Age = 56 (12) years	64 (8)	0.10	Bolus	2 min - 5 h	-	HPLC - Fluorescence	LLOD = 20 ng/ml	-	Compartmental (2, 3)	-	0.35 (± 0.081)	3.0 (± 1.1)	-
Ornstein et al[98]	Healthy subjects, n = 10, Mean (SD) Age = 49 (7) years	82 (10)	0.07	Bolus	2 min - 6 h	-	GC - Nitrogen sensitive detector	Sensitivity limit of 5 ng/ml	-	Compartmental (2, 3)	-	0.39 (± 0.13)	2.5 (± 0.7)	-

Urinary Excretion Studies

Although the analytical method used for the quantification of the (parent) pipercuronium was not specific, i.e., coloriemetry, from the urinary excretion study carried out by Wierda et al[99] (although they state that it was specific), the fraction that appears in the urine (f_e) was found to be **41%.** The underlying assumption is that there are no major metabolites in the urine, i.e., only the unchanged drug appears in the urine. The PK parameter estimates, namely, Vd_{ss} and CL_{tot} obtained for the parent pipercuronium from other studies (shown above) in which it was quantitated by specific and sensitive methods were similar to those obtained by Wierda et al[99] suggesting that there are no (major) metabolites.

Plasma Protein Binding Studies

Study	Subjects	Method	Concentration Range	Assay	f_u (%)
Obach et al[100]	-	-	-	-	98

Rapacuronium

Study	Population	BW	Dose (I.V.)	Rate	PK Sampling Schedule		Assay Method	Analytical Method Parameters		PK Analysis	Urine Collection Method	Vd_{ss}/ Vd_{pss}	CL_{tot}	CL_{ren}
		(kg)	(mg/kg)		Plasma	Urine		Plasma	Urine			(L/kg)	[ml/min/kg]	[ml/min/kg]
Szenohradszky et al[101]	Healthy subjects, n = 10, Mean (Range) Age = 26 (20 - 42) years	69 (50 - 85)	1.5	Bolus	3 min - 8h	Up to 48 h	HPLC - MS	Sensitivity limit of 2 ng/ml	-	Compartmental (3)	Cumulative	0.41	9.4	0.75
van Den Broek et al[102]	Healthy subjects, n = 10, Mean (Range) Age = 28 (18 - 57) years	79 (6)	1.5	Bolus	2 min - 4h	Up to 24 h	HPLC - Fluorescence	LLOQ = 10 ng/ml	LLOQ = 10 ng/ml	Compartmental (2, 3)	Cumulative	0.29 (± 0.16)	8.5 (± 2.5)	1.3
Schiere et al[103]	Healthy subjects, n = 10, Mean (Range) Age = 54 (26 - 64) years	74 (62 - 88)	1.0	Bolus	1 min 4 h	Up to 24 h	HPLC - MS	LLOQ = 10 ng/ml	LLOQ = 50 ng/ml	Compartmental (3)	Cumulative	0.19 (0.11 - 0.25)	7.3 (3.9 - 8.9)	0.44
Duvaldestin et al[104]	Healthy subjects, n = 8, Mean (Range) Age = 49 (35 - 68) years	77 (59 - 83)	1.5	Bolus	2 min - 8h	-	HPLC - MS	LLOQ = 10 ng/ml	-	Compartmental	-	0.22 (0.12 - 0.29)	5.3 (4.2 - 8.4)	-
Wierda et al[105]	Healthy subjects, n = 3	-	1.5	Bolus	1 min - 8 h	Up to 24 h	HPLC - Fluorescence	LLOQ = 10 ng/ml	LLOQ = 10 ng/ml	Compartmental	Cumulative	0.46 (± 0.25)	11.1 (± 1.1)	0.56

Urinary Excretion Studies

1. Szenohradszky et al[101] calculated $CL_{ren} = f_e * CL_{tot}$ (f_e is the fraction of the dose that is excreted unchanged in the urine; urine samples were collected during the time periods 0 -2, 2 - 4, 4 - 6, 6 - 9, 12 - 18, 18 - 24, 24 - 36, 36 - 48h), $f_e = 8\%$
2. van Den Broek et al[102] calculated $CL_{ren} = f_e * CL_{tot}$ (f_e is the fraction of the dose that is excreted unchanged in the urine; urine samples were collected up to 24 h), $f_e = 15\%$
3. Schiere et al[103] calculated $CL_{ren} = f_e * CL_{tot}$ (f_e is the fraction of the dose that is excreted unchanged in the urine; urine samples were collected during the time periods 0 -2, 2 - 4, 4 - 6, 6 - 9, 12 - 18, 18 - 24, 24 - 36, 36 - 48h), $f_e = 6\%$
4. Wierda et al[105] calculated $CL_{ren} = f_e * CL_{tot}$ (f_e is the fraction of the dose that is excreted unchanged in the urine; urine samples were collected during the time periods 2, 4, 6, 9, 12, 18, 24 h), $f_e = 5\%$

Plasma Protein Binding Studies

Study	Subjects	Method	Concentration Range	Assay	f_u (%)
Proost et al[82]	*In-vitro*	Ultrafiltration	Up to 2000 ng/ml	HPLC - Fluorescence	38

Org 9488 (Rapacuronium Metabolite)

Study	Population	BW	Dose (I.V.)	Rate	PK Sampling Schedule		Assay Method	Analytical Method Parameters		PK Analysis	Urine Collection Method	Vd_{ss}/ Vd_{pss}	CL_{tot}	CL_{ren}
		(kg)	(mg/kg)		Plasma	Urine		Plasma	Urine			(L/kg)	[ml/min/kg]	[ml/min/kg]
Schiere et al[103]	Healthy subjects, n = 7, Mean (Range) Age = 45 (19 - 62) years	83 (68 - 99)	0.20	Bolus	2 min 6 h	Up to 24 h	HPLC - MS	LLOQ = 10 ng/ml	LLOQ = 50 ng/ml	Compartmental (3)	Cumulative	0.23 (0.14 - 0.31)	1.3 (0.76 - 1.9)	0.68
	Healthy subjects, n = 7, Mean (Range) Age = 49 (21 - 63) years	77 (68 - 100)	0.68	Tinf based on PD endpoint	1 min - 6 h	Up to 24 h	HPLC - MS	LLOQ = 10 ng/ml	LLOQ = 50 ng/ml	Compartmental (3)	Cumulative	0.18 (0.14 - 0.35)	1.1 (0.73 - 2.1)	0.59

Urinary Excretion Studies

1. Schiere et al[103] calculated $CL_{ren} = f_e * CL_{tot}$ (f_e is the fraction of the dose that is excreted unchanged in the urine; urine samples were collected during the time periods 0 -2, 2 - 4, 4 - 6, 6 - 9, 12 - 18, 18 - 24, 24 - 36, 36 - 48h), f_e = 52% (after I.V. bolus) and 54% (after short infusion)

Org 9489

Study	Population	BW	Dose (I.V.)	Rate	PK Sampling Schedule		Assay Method	Analytical Method Parameters		PK Analysis	Urine Collection Method	Vd_{ss}/ Vd_{pss}	CL_{tot}	CL_{ren}
		(kg)	(mg/kg)		Plasma	Urine		Plasma	Urine			(L/kg)	[ml/min/kg]	[ml/min/kg]
Wierda et al[105]	Healthy subjects, n = 3	-	0.90	Bolus	1 min - 8 h	Up to 24 h	HPLC - Fluorescence	LLOQ = 10 ng/ml	LLOQ = 25 ng/ml	Compartmental	Cumulative	0.46 (± 0.25)	5.8 (± 1.4)	0.46

Urinary Excretion Studies

1. Wierda et al[105] calculated $CL_{ren} = f_e * CL_{tot}$ (f_e is the fraction of the dose that is excreted unchanged in the urine; urine samples were collected during the time periods 2, 4, 6, 9, 12, 18, 24 h), f_e = 8%

Plasma Protein Binding Studies

Study	Subjects	Method	Concentration Range	Assay	f_u (%)
Proost et al[82]	*In-vitro*	Ultrafiltration	Up to 2000 ng/ml	HPLC - Fluorescence	37

Org 9453

Study	Population	BW	Dose (I.V.)	Rate	PK Sampling Schedule		Assay Method	Analytical Method Parameters		PK Analysis	Urine Collection Method	Vd_{ss}/ Vd_{pss}	CL_{tot}	CL_{ren}
		(kg)	(mg/kg)		Plasma	Urine		Plasma	Urine			(L/kg)	[ml/min/kg]	[ml/min/kg]
Wierda et al[105]	Healthy subjects, n = 3	-	1.3	Bolus	1 min - 8 h	Up to 24 h	HPLC - Fluorescence	LLOQ = 10 ng/ml	LLOQ = 10 ng/ml	Compartmental	Cumulative	0.18 (± 0.018)	6.9 (± 1.5)	0.35

Urinary Excretion Studies

1. Wierda et al[105] calculated $CL_{ren} = f_e * CL_{tot}$ (f_e is the fraction of the dose that is excreted unchanged in the urine; urine samples were collected during the time periods 2, 4, 6, 9, 12, 18, 24 h), $f_e = 5\%$

Plasma Protein Binding Studies

Study	Subjects	Method	Concentration Range	Assay	f_u (%)
Proost et al[82]	*In-vitro*	Ultrafiltration	Up to 2000 ng/ml	HPLC - Fluorescence	28

Alcuronium

Study	Population	BW	Dose (I.V.)	Rate	PK Sampling Schedule		Assay Method	Analytical Method Parameters		PK Analysis	Urine Collection Method	Vd_{ss}/ Vd_{pss}	CL_{tot}	CL_{ren}
		(kg)	(mg/kg)		Plasma	Urine		Plasma	Urine			(L/kg)	[ml/min/kg]	[ml/min/kg]
Diefenbach et al[106]	Healthy subjects, n = 10, Age Range = 18 - 70 years	50 - 90	0.25	Bolus	3 min - 720 min	Up to 24 hours	HPLC - UV	Sensitivity = 25 ng/ml	-	Non-Compartmental	Cumulative	0.31 (± 0.070)	0.90 (± 0.29)	-

Urinary Excretion Studies

1. Diefenbach et al[106] calculated $CL_{ren} = f_e * CL_{tot}$ (f_e is the fraction of the dose that is excreted unchanged in the urine; urine samples were collected up to 48 hrs), $f_e = 72\%$

Pharmacodynamics

Study	Subjects	PD Endpoint	k_{eo} (min^{-1})	Cp^{ss}_{50} (µg/ml)	γ
Diefenbach et al[106]	Healthy subjects, n = 10, Age Range = 18 - 70 years	-		0.54 (±0.1)	5

Doxacurium

Study	Population	BW	Dose (I.V.)	Rate	PK Sampling Schedule		Assay Method	Analytical Method Parameters		PK Analysis	Urine Collection Method	Vd_{ss}/ Vd_{pss}	CL_{tot}	CL_{ren}
		(kg)	(mg/kg)		Plasma	Urine		Plasma	Urine			(L/kg)	[ml/min/kg]	[ml/min/kg]
Dresner et al[107]	Healthy subjects, n = 8, Mean (SD) Age = 31 (9) years	77 (17)	0.03	Bolus	2 min - 6h	Up to 24 h	HPLC - UV	LLOQ = 10 ng/ml	LLOQ = 10 ng/ml	Compartmental (2, 3)	Cumulative	0.15 (± 0.04)	2.2 (± 1.1)	-
Gareipy et al[108]	Healthy subjects, n = 9, Mean (SD) Age = 27 (9) years	71 (15)	0.03	Bolus	2 min - 8 h	Up to 8 h	HPLC - UV	LLOQ = 4 ng/ml	LLOQ = 4 ng/ml	Compartmental (2)	Cumulative	0.23 (± 0.03)	2.5 (± 0.24)	-
Cook et al[109]	Healthy subjects, n = 9, Mean (SD) age = 32 (7)	82 (12)	0.02	Bolus	2 min - 6 hr	Up to 12 h	HPLC - UV	LLOQ = 10 ng/ml	-	NCA	Cumulative	0.22 (± 0.11)	2.7 (± 1.6)	-

Urinary Excretion Studies

1. Dresner et al[107] calculated the CL_{ren} by using $CL_{ren} = f_e * CL_{tot}$ (urine was sampled up to 24 hrs). $f_e = 31\%$
2. Gareipy et al[108] calculated the CL_{ren} by using $CL_{ren} = f_e * CL_{tot}$ (urine was sampled up to 8 hrs). $f_e = 25\%$
3. Cook et al[109] calculated the CL_{ren} by using $CL_{ren} = f_e * CL_{tot}$ (urine was sampled up to 12 hrs). $f_e = 21\%$

Plasma Protein Binding Studies

Study	Subjects	Method	Concentration Range	Assay	f_u (%)
Doxacurium FDA Label	-	-	-	-	53%

Pharmacodynamics

Study	Subjects	PD Endpoint	k_{eo} (min^{-1})	Cp^{ss}_{50} (µg/ml)	γ
Gareipy et al[108]	Healthy male subjects, n = 9, Mean (SD) Age = 27 (9) years	>90% Depression in the muscle twitch following train of four stimulus	0.051 (± 0.003)	0.054 (±0.0055)	5.46 (±0.34)

Atracurium

Study	Population	BW	Dose (I.V.)	Rate	PK Sampling Schedule		Assay Method	Analytical Method Parameters		PK Analysis	Urine Collection Method	Vd_{ss}/ Vd_{pss}	CL_{tot}	CL_{ren}
		(kg)	(mg/kg)		Plasma	Urine		Plasma	Urine			(L/kg)	[ml/min/kg]	[ml/min/kg]
Fahey et al[110]	Healthy subjects, n = 10	-	0.50	Bolus	2 min - 4 h	-	HPLC - Fluorescence	Sensitivity limit = 10 ng/ml	-	Compartmental (2, 3)	-	-	6.1 (± 0.95)	-
Parker et al[111]	Healthy subjects, n = 7, Mean (SD) Age = 56 (11) years	69 (15)	0.60	Bolus	2 min - 6 h	-	HPLC - Fluorescence	Sensitivity limit = 25 ng/ml	-	Compartmental (2)	-	-	6.6 (± 1.2)	-
Fisher et al[112]	Healthy subjects, n = 8, Age range = 22 - 43 years	-	0.15	Bolus	1 min - 2 hrs	-	HPLC - Fluorescence	Sensitivity limit = 10 ng/ml	-	Compartmental (2)	-	0.087 (± 0.031)	4.8 (± 1.1)	-
Ward et al[113]	Healthy subjects, n = 7 Age range = 24 - 69 years	75	0.3 or 0.6	Bolus	1 min - 2 hrs	-	HPLC - Fluorescence	Sensitivity limit = 50 ng/ml	-	Compartmental (2)	-	-	5.5 (± 0.69)	-
Ward et al[114]	Healthy subjects, n = 6	-	0.3 or 0.4	Bolus	2 - 500 min	Up to 500 min	HPLC - Fluorescence	LLOD = 10 ng/ml	LLOD = 10 ng/ml	Compartmental (2 or 3)	Cumulative	-	5.5 (± 0.73)	0.33
Smith et al[115]	Healthy subjects, n = 10, Mean (SD) age = 39 (15)	77 (14)	0.50	T_{inf} based on PD Endpoint	2 min - 8 hr	-	HPLC - Fluorescence	LLOQ = 10 ng/ml	-	Compartmental (2)	-	0.21	10	-

Kent et al[116]	Healthy subjects, n = 10, Mean (SD) age = 24 (4)	72 (12)	0.60	Bolus	2 min - 2 h	-	HPLC - Fluorescence	Sensitivity limit = 25 ng/ml	-	NCA	-	0.17 (± 0.034)	5.9 (± 0.9)	-

Urinary Excretion Studies

4. Ward et al[114] calculated the CL_{ren} by using $CL_{ren} = A_e/AUC_{0\text{-}500\ min}$ (urine was sampled up to 500 min). $f_e = 6\%$

Plasma Protein Binding Studies

Study	Subjects	Method	Concentration Range	Assay	f_u (%)
Cameron et al[91]	Healthy subjects, n = 10	Ultrafiltration	0.5 - 2.0 µg/ml	HPLC - Fluorescence	57 (±7)

Metabolism

Atracurium is eliminated through several pathways, including Hofmann elimination, i.e., by spontaneous degradation in plasma (central compartment) and tissue(s) (peripheral compartment) at normal body pH and temperature) and ester hydrolysis (catalysis by nonspecific esterases)[112,115]. Ward et al[114] proposed the pathways of breakdown of atracurium (shown below)

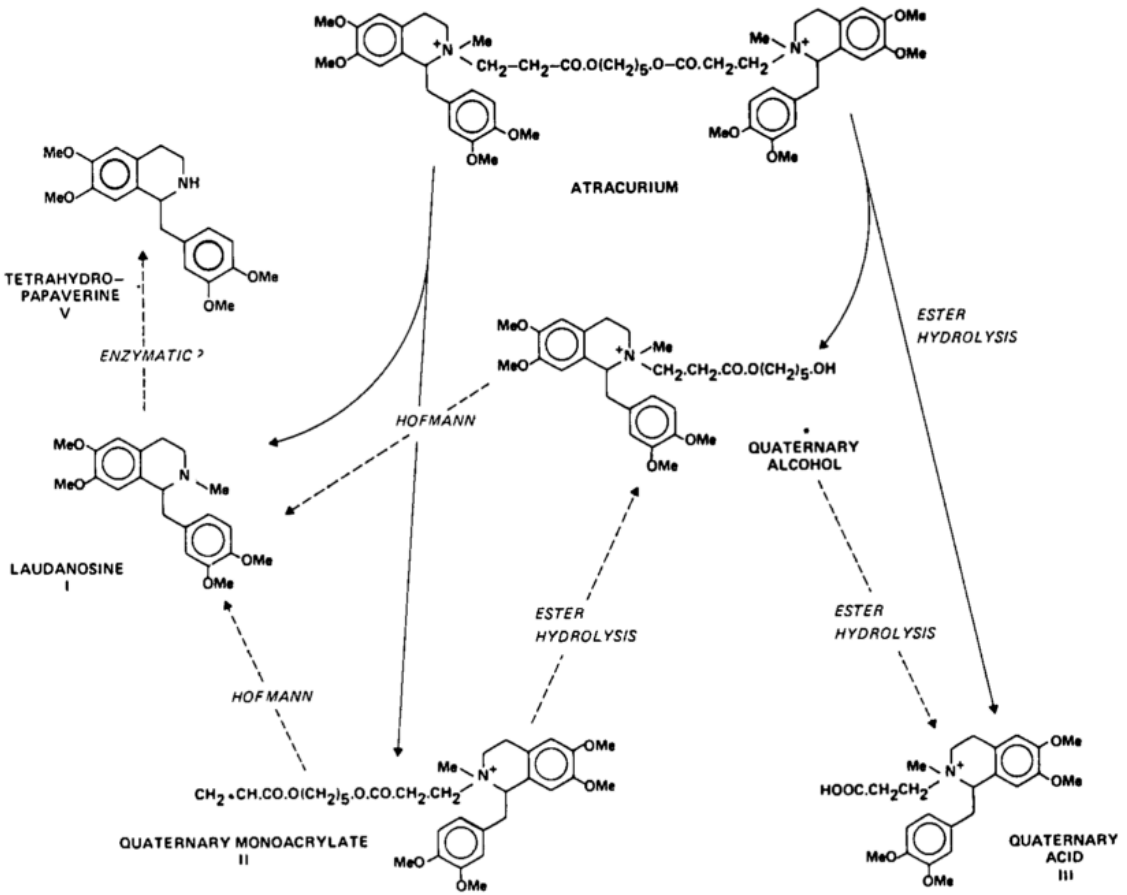
ATRACURIUM
TETRAHYDRO–
PAPAVERINE
V
ENZYMATIC ?
LAUDANOSINE
I
HOFMANN
HOFMANN
ESTER
HYDROLYSIS
ESTER
HYDROLYSIS
ESTER
HYDROLYSIS
QUATERNARY
ALCOHOL
QUATERNARY MONOACRYLATE
II
QUATERNARY
ACID
III

Cisatracurium

Study	Population	BW	Dose (I.V.)	Rate	PK Sampling Schedule		Assay Method	Analytical Method Parameters		PK Analysis	Urine Collection Method	Vd_{ss}	CL_{tot}	CL_{ren}
		(kg)	(mg/kg)		Plasma	Urine		Plasma	Urine			(L/kg)	[ml/min/kg]	[ml/min/kg]
Smith et al[115]	Healthy subjects, n = 10, Mean (SD) age = 50 (11)	66 (8)	0.10	T_{inf} based on PD Endpoint	2 min - 8 hr	-	HPLC - Fluorescence	LLOQ = 10 ng/ml	-	Compartmental (2)	-	0.21	6.44 (± 0.85)	-
Lien et al[117]	Healthy subjects, n = 10, Mean (SD) age = 37 (12)	73 (13)	0.10	Bolus	2 min - 8 hr	-	HPLC - Fluorescence	LLOQ = 10 ng/ml	-	Compartmental	-	0.18 (± 0.048)	5.1 (± 0.84)	-
	Healthy subjects, n = 10, Mean (SD) age = 39 (8)	87 (10)	0.20									0.16 (± 0.036)	4.9 (± 0.64)	
Ornstein et al[118]	Healthy subjects, n = 12, Mean (SD) age = 42 (5)	78 (16)	0.10	Bolus	2 min - 8 hr	Up to 10 h	HPLC - Fluorescence	Sensitivity limit = 10 ng/ml	Sensitivity limit = 10 ng/ml	Compartmental (2, 3)	Cumulative	0.11 (± 0.013	4.6 (± 0.8)	0.83
Tran et al[119]	Healthy subjects, n = 14, Mean (SD) age = 46 (12)	72 (15)	0.10	Bolus	2 min - 8 hr	-	HPLC - Fluorescence	-	-	Compartmental	-	0.12 (± 0.027)	3.7 (± 0.8)	-
Wolf et al[120]	Healthy subjects, n = 11, Mean (Range) age = 37 (21 - 65)	80 (12)	0.10	Bolus	2 min - 8 hr	Up to 10 h	HPLC - Fluorescence	LLOQ = 10 ng/ml	LLOQ = 10 ng/ml	NCA	Cumulative	0.16 (± 0.023)	5.7 (± 0.8)	0.80

Urinary Excretion Studies

1. Ornstein et al[118] calculated $CL_{ren} = f_e * CL_{tot}$ (f_e is the fraction of the dose that is excreted unchanged in the urine; urine samples were collected at up to 10 hrs), $f_e = 18\%$
2. Wolf et al[120] calculated $CL_{ren} = f_e * CL_{tot}$ (f_e is the fraction of the dose that is excreted unchanged in the urine; urine samples were collected at up to 10 hrs), $f_e = 14\%$

Plasma Protein Binding Studies

Study	Subjects	Method	Concentration Range	Assay	f_u (%)
Roy et al[83]	*In-vitro*	Ultrafiltration	Up to 2000 ng/ml	HPLC - Fluorescence	62 (9)

Metabolism

Cisatracurium undergoes pH and temperature-dependent Hofmann elimination in plasma and tissues[121]. The clearance of cisatracurium due to Hofmann elimination and organ elimination occurs from both central and peripheral compartments, i.e., in an organ independent manner[121]. Kisor et al[122] proposed the metabolic elimination pathway for cisatracurium besylate in human plasma, the schematic of which is shown below.

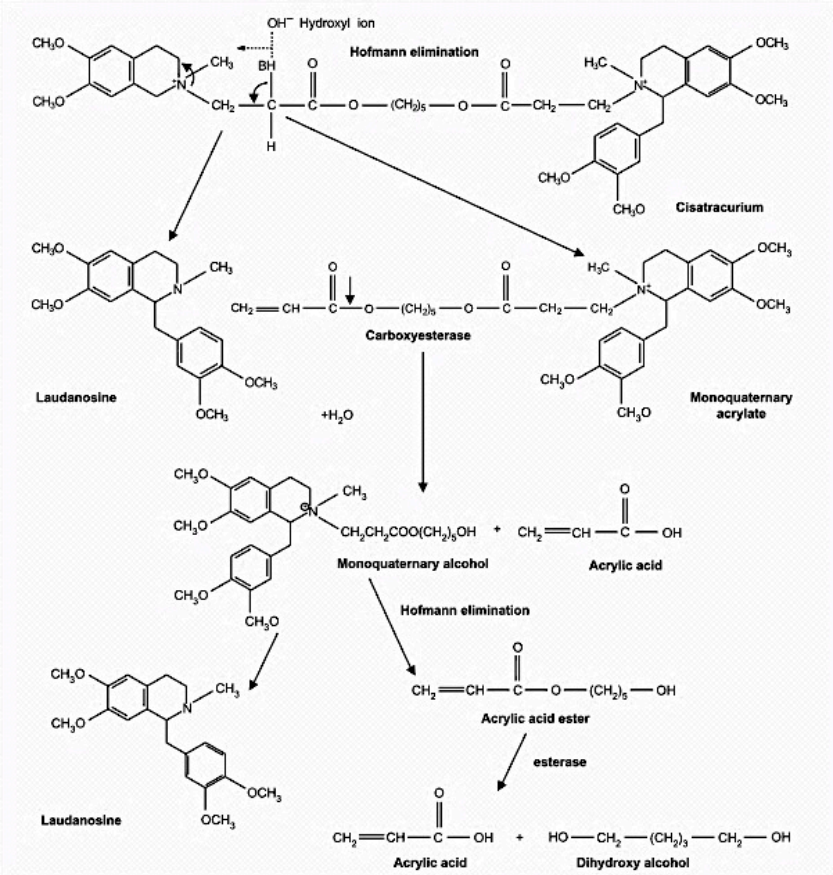

Pharmacodynamics

Study	Subjects	PD Endpoint	k_{eo} (min^{-1})	Cp^{ss}_{50} (µg/ml)	γ
Tran et al[119]	Healthy subjects, n = 14, Mean (SD) age = 46 (12)	75% Depression in the muscle twitch following train of four stimulus	0.054 (± 0.013)	0.15 (± 0.033)	6.9 (±1.3)

Mivacurium

Study	Population	BW	Dose (I.V.)	Rate	PK Sampling Schedule		Assay Method	Analytical Method Parameters		PK Analysis	Urine Collection Method	Vd_{ss}/ Vd_{pss}	CL_{tot}	CL_{ren}
		(kg)	(mg/kg)		Plasma	Urine		Plasma	Urine			(L/kg)	[ml/min/kg]	[ml/min/kg]
Head-Rapson et al[123]	Healthy subjects, n = 9, Mean (Range) Age = 40 (20 - 61) years	71 (48 - 84)	0.23	Inf	1 min - 5h	-	HPLC	LLOQ = 2 ng/ml	-	Compartmental	-	0.24	71	-
Cook et al[124]	Healthy subjects, n = 9, Mean (Range) Age = 27 (21 - 35) years	77 (12)	0.15	Bolus	1 min - 150 min	Up to 6h	HPLC	Sensitivity limit = 10 ng/ml	Sensitivity limit = 10 ng/ml	Compartmental	Cumulative	0.11 (± 0.072)	70 (± 28)	4.9
Head-Rapson et al[125]	Healthy subjects, n = 10, Mean (Range) Age = 47 (31 - 62) years	75 (52 - 107)	0.15	Boluses	1 min - 190 min	-	HPLC	LLOQ = 2.5 ng/ml	-	Compartmental	-	0.21	75	-

Plasma Protein Binding Studies

Study	Subjects	Method	Concentration Range	Assay	f_u (%)
Cameron et al[91]	Healthy subjects, n = 10	Ultrafiltration	0.5 - 2.0 μg/ml	HPLC - Fluorescence	71 (±7)

Metabolism

The schematic for the potential routes of metabolism for Mivacurium[126] is shown below.

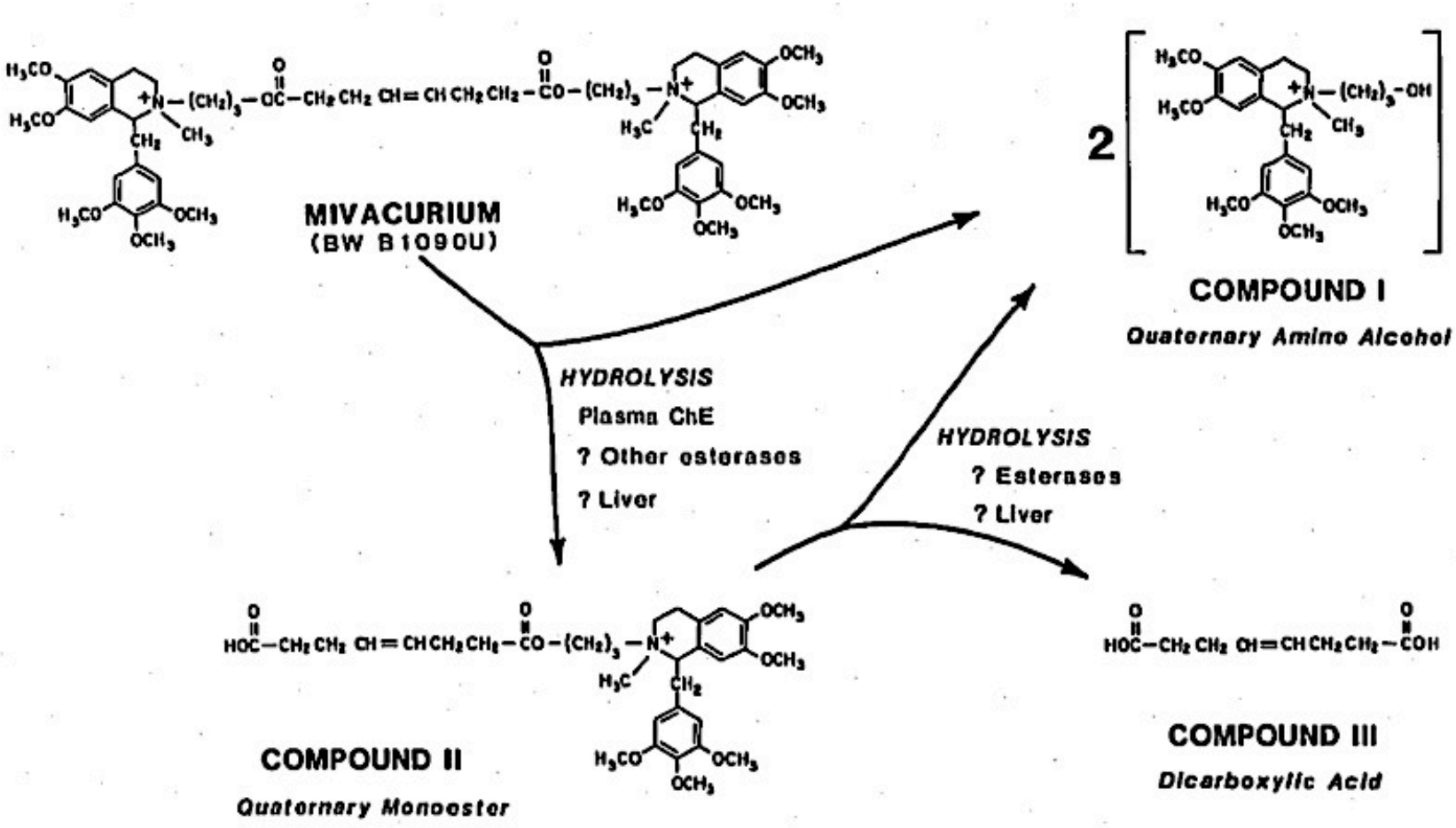

Fazadinium

Study	Population	BW	Dose (I.V.)	Rate	PK Sampling Schedule		Assay Method	Analytical Method Parameters		PK Analysis	Urine Collection Method	Vd_{ss}/ Vd_{pss}	CL_{tot}	CL_{ren}
		(kg)	(mg/kg)		Plasma	Urine		Plasma	Urine			(L/kg)	[ml/min/kg]	[ml/min/kg]
Duvaldestin et al[127]	Healthy subjects, n = 10, Mean (SD) Age = 33 (17)	63 (20)	1.5	Bolus	5 min - 5 h	Up to 24 h	Coloriemetry	Limit of sensitivity = 50 ng/ml	Limit of sensitivity = 40 ng/ml	Compartmental	Cumulative	0.19	2.10	-

Urinary Excretion Studies

1. Duvaldestin et al[127] calculated $CL_{ren} = f_e * CL_{tot}$ (f_e is the fraction of the dose that is excreted unchanged in the urine; urine samples were collected 24 h), f_e = 50%

Plasma Protein Binding Studies

Study	Subjects	Method	Concentration Range	Assay	f_u (%)
Hollander et al[128]	-	-	-	-	49

Succinylcholine

Study	Population	BW	Dose (I.V.)	Rate	PK Sampling Schedule		Assay Method	Analytical Method Parameters		PK Analysis	Urine Collection Method	Vd_{ss}/ Vd_{pss}	CL_{tot}	CL_{ren}
		(kg)	(mg/kg)		Plasma	Urine		Plasma	Urine			(L/kg)	[ml/min/kg]	[ml/min/kg]
Roy et al[129]	Healthy subjects	-	1.0	Bolus	Up to 10 min	-	LC - MS	Sensitivity limit = 25 ng/ml	-	Compartmental	-	0.04 (± 0.006)	37 (±9)	-

Plasma Protein Binding Studies

Study	Subjects	Method	Concentration Range	Assay	f_u (%)
Roy et al[129]	-	-	-	-	80

Pharmacodynamics

Study	Subjects	PD Endpoint	k_{eo} (min^{-1})	Cp^{ss}_{50} (µg/ml)	γ
Roy et al[129]	-	-	0.06 (±0.03)	0.76 (±0.21)	19.3 (±8.1)

Appendix 3.1 - Human PK Study Summaries of Triptans

5-HT

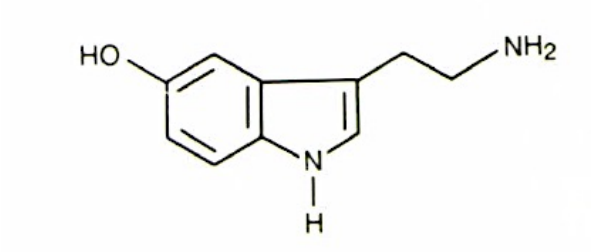

Sumatriptan

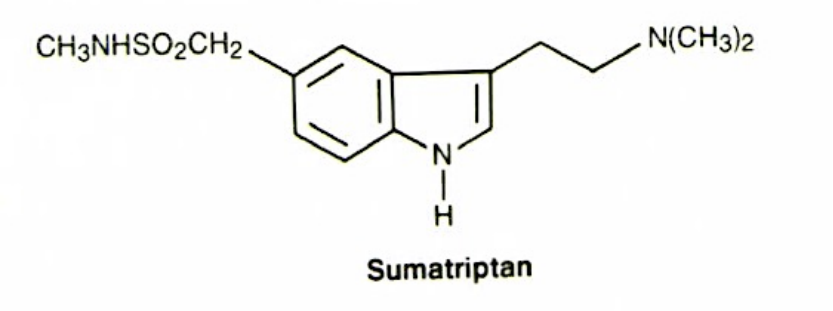

Study	Population	BW	Dose (IV/	Rate	PK Sampling	Assay Method	Analytical Method	PK Analy	Urine Collecti	Vd_{ss}	CL_{tot}	CL_{ren}

			***PO*)**		**Schedule**			**Parameters**		**sis**	**on Method**			
		(kg)	(mg/ kg)		**Plas ma**	**Urine**		**Plasma**	**Urine**			(L/k g)	[ml/m in/kg]	[ml/m in/kg]
Lacey., F. et al[130]	Healthy males, n = 18, Mean Age (Range) = 27 (19 - 40)	72 (58 - 88)	0.04	15 min Infus ion	Up to 12 hrs	-	HPLC - Electrochemical Detection	LLOQ = 1 ng/ml	LLOQ = 400 ng/ml	Comp artme ntal (3)	-	2.6 (1.3 - 4.4)	16.1 (8.8 - 21.9)	3.7 (2.0 - 6.5)

Plasma Protein Binding Studies

Study	Subjects	Method	Concentration Range	Assay	f_u (%)
Dixon. M. et al[131]	Healthy males, n = 4	Equilibrium dialysis	10 - 1000 ng/ml	Liquid Scintillation Counting	84

Metabolism

In-vivo, sumatriptan undergoes extensive first-pass metabolism primarily mediated by MAO-A and the major metabolite obtained is indole acetic acid analogue (which is then eliminated mainly in the urine either as a free acid or as an ester glucuronide)[132–134].

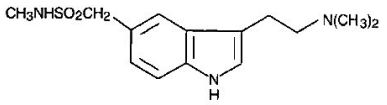

Sumatriptan

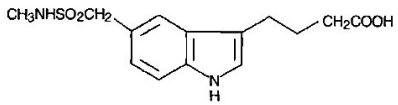

Major metabolite
(indole acetic acid analogue)

Almotriptan

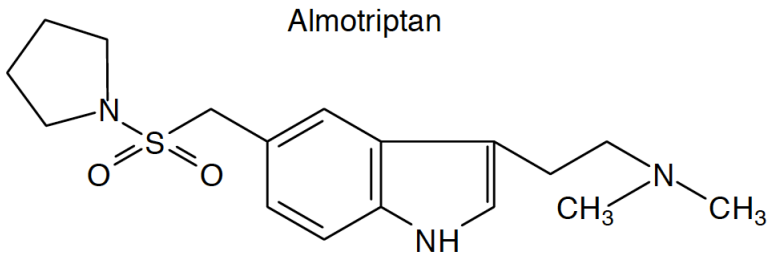

Study	Population	BW	Dose (IV/ *PO*)	Rate	PK Sampling Schedule		Assay Method	Analytical Method Parameters		PK Analysis	Urine Collection Method	Vd_{ss}	CL_{tot}	CL_{ren}
		(kg)	(mg/kg)		Plasma	Urine		Plasma	Urine			(L/kg)	[ml/min/kg]	[ml/min/kg]
Janset et al[135]	Healthy males, n = 18, Mean (Range) Age = 25 (20 - 33) years	74 (64 - 88)	0.04	15 min Infusion	15 min - 24 hrs	0 - 72 hrs	HPLC - UV	LLOQ = 1 ng/ml	LLOQ = 50 ng/ml	Compartmental (2)	Fractioned	2.3 (± 0.5)	9.0 (± 1.8)	5.6 (± 1.8)
McEwen et al[136]	Healthy males, n = 23, Mean (Range) Age = 29 (19 - 46) years	73 (52 - 101)	*0.07 - 2.74*	*P.O.*	15 min - 12 hrs	0 - 12 hrs	HPLC - Electrochemical for plasma and HPLC - UV for urine	LLOQ = 1 ng/ml	LLOQ = 1 µg/ml	NCA	Cumulative	-	-	3.8 (3.1 - 4.6)
Fleishaker et al[137]	Healthy subjects, n = 12, Mean (SD) Age = 34 (± 8)	67 (± 10)	*0.19*	*P.O.*	30 min - 24 hrs	0 - 24 hrs	LC/MS/MS for Plasma and HPLC - UV for Urine	LLOQ = 1 ng/ml	LLOQ = 50 ng/ml	NCA	Fractioned	-	-	3.2 (± 0.6)

	years													
Fleishaker et al[138]	Healthy subjects, n = 14, Mean (SD) Age = 35 (± 10) years	69 (± 10)	*0.18*	*P.O.*	30 min - 24 hrs	0 - 24 hrs	LC/MS/MS for Plasma and HPLC - UV for Urine	LLOQ = 0.5 ng/ml	LLOQ = 50 ng/ml	NCA	Fractioned	-	-	3.3 (± 0.9)
Fleishaker et al[139]	Healthy subjects, n = 12, Mean (SD) Age = 31 (± 11) years	74 (± 13)	*0.17*	*P.O.*	30 min - 24 hrs	0 - 24 hrs	LC/MS/MS for Plasma and HPLC - UV for Urine	LLOQ = 0.5 ng/ml	LLOQ = 50 ng/ml	NCA	Fractioned	-	-	4.4 (± 0.7)
Fleishaker et al[140]	Healthy subjects, n = 16, Mean (SD) Age = 28 (± 9) years	77 (± 12)	*0.16*	*P.O.*	30 min - 48 hrs	0 - 48 hrs	LC/MS/MS for Plasma and HPLC - UV for Urine	LLOQ = 0.5 ng/ml	LLOQ = 50 ng/ml	NCA	Fractioned	-	-	3.0 (± 0.4)
Baldwin et al[141]	Healthy subjects, n = 18, Mean (Range) Age = 37 (18 - 53) years	74 (53 - 94)	*0.17*	*P.O.*	30 min - 24 hrs	0 - 24 hrs	LC/MS/MS	LLOQ = 0.5 ng/ml	LLOQ = 50 ng/ml	NCA	Fractioned	-	-	3.3 (± 0.7)

Urinary Excretion Studies

2. Janset et al[135] calculated the CL_{ren} by using CL_{ren} = Ae/AUC (Urine was collected in 4 hr fractions for first 12 hrs, and then 12 hr fraction upto 24 hrs)
3. McEwen et al[136] calculated the CL_{ren} by using $CL_{ren} = A_e/AUC$ (Ae is the cumulative amount = % dose excreted unchanged in urine; urine was collected in 4 hr fractions for 12 hrs)
4. Fleishaker et al[137] calculated the CL_{ren} by using $CL_{ren} = A_e/AUC$ (Urine was collected in 4 hr fractions for first 12 hrs, and then 12 hr fraction upto 24 hrs)

5. Fleishaker et al[138] calculated the CL_{ren} by using $CL_{ren} = A_e/AUC$ (Urine was collected in 4 hr fractions for first 12 hrs, and then 12 hr fraction upto 24 hrs)
6. Fleishaker et al[139] calculated the CL_{ren} by using $CL_{ren} = A_e/AUC$ (Urine was collected in 4 hr fractions for first 12 hrs, and then 12 hr fraction upto 24 hrs)
7. Fleishaker et al[140] calculated the CL_{ren} by using $CL_{ren} = A_e/AUC$ (Urine was collected in 4 hr fractions for first 12 hrs, and then 12 hr fraction upto 48 hrs)
8. Baldwin et al[141] calculated the CL_{ren} by using $CL_{ren} = A_e/AUC$ (Urine was collected in 4 hr fractions for first 12 hrs, and then 12 hr fraction upto 24 hrs)

Plasma Protein Binding Studies

Study	Subjects	Method	Concentration Range	Assay	f_u (%)
Almotriptan FDA Label	-	-	-	-	65[142–144]

Metabolism

In-vivo, it is metabolized by two major pathways[144,145]: (1) Monoamine oxidase (MAO)-mediated oxidative deamination (and consequent oxidation by aldehyde dehydrogenase) to indolacetic acid metabolite (which then forms a glucuronide conjugate) and (2) Cytochrome-mediated (primarily involving CYP3A4, CYP2D6 and other CYP enzymes contributing to a minor extent) hydroxylation of the pyrrolidine ring to form and intermediate which is further oxidized by aldehyde dehydrogenase to form a gamma-aminobutyric acid derivative. Another minor pathway by which almotriptan is metabolized is flavin monooxygenase-mediated N-oxidation. The metabolic profile of almotriptan in urine, faeces and plasma show highest amounts of indolacetic acid and oxidized pyrrolidine product[146]. The scheme is shown in Figure - 1.

Figure 1 - Pathways of almotriptan metabolism in humans[144,146]

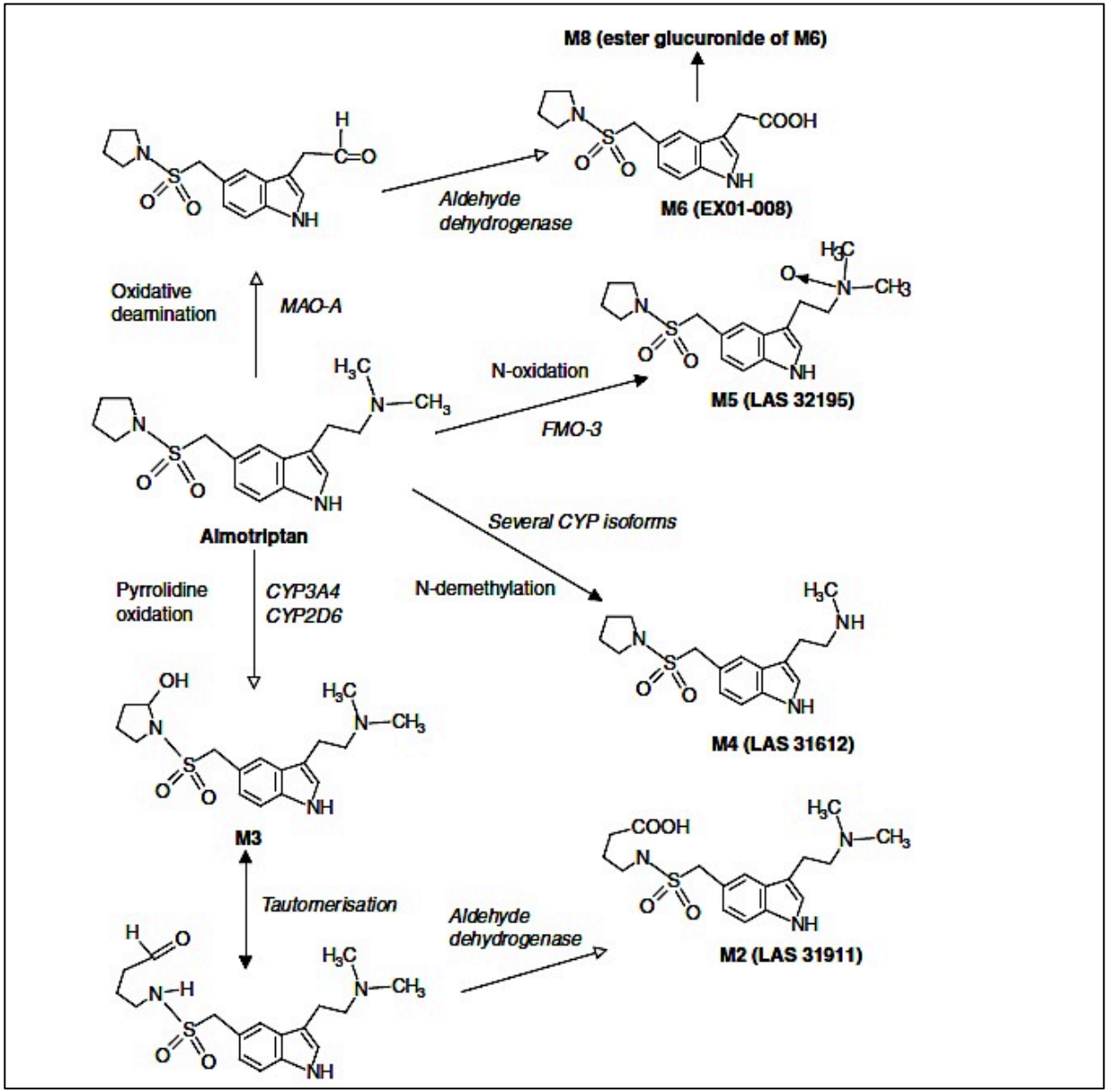

Naratriptan

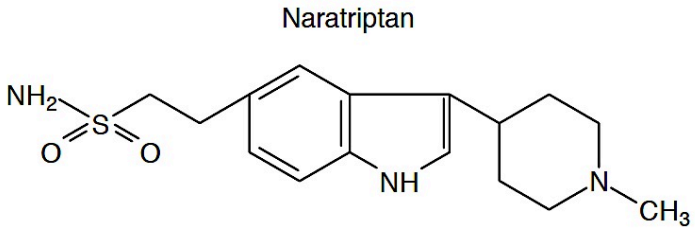

Study	Population	BW	Dose (IV/ *PO*)	Rate	PK Sampling Schedule		Assay Method	Analytical Method Parameters		PK Analysis	Urine Collection Method	Vd_{ss}	CL_{tot}	CL_{ren}
		(kg)	(mg/kg)		Plasma	Urine		Plasma	Urine			(L/kg)	[ml/min/kg]	[ml/min/kg]
Fuseau E., et al[147]	Healthy n = 23, Age range = 20 - 47 years	50 - 95	0.02	15 min Infusion	Up to 36 hrs	Up to 36 hrs	-	-	-	Compartmental (2)	-	-	-	-
Kempsford et al[148]	Healthy females n = 26, Age range = 18 - 45 years	50 - 78	*0.04 - 0.14*	*P.O.*	Up to 24 hrs	Up to 24 hrs	-	-	-	NCA	-	-	-	2.4 (± 0.1)
Naratriptan FDA Approval Package[149]			0.02	15 min Infusion	Up to 36 hrs	Up to 36 hrs	-	-	-	Compartmental (2)	-	2.4	6.6	-

Urinary Excretion Studies

2. Kempsford et al[148] calculated the CL_{ren} by using $CL_{ren} = A_e/AUC$ (Urine was collected upto 24 hrs)

Plasma Protein Binding Studies

Study	Subjects	Method	Concentration Range	Assay	f_u (%)
Naratriptan FDA Approval Package[149]	-	-	50 - 1000 ng/ml	-	25
FDA Label[150]	-	-	50 - 1000 ng/ml	-	28 - 31

Metabolism

In-vivo, the major metabolites found in human plasma and urine include N-oxide and piperidineone metabolite[149]. CYP450 enzyme system is believed to be involved in the metabolism of naratriptan[149–151] (and is not a substrate for MAO)[152].

Blood-to-Plasma Ratio Studies

Study	Subjects	Method	Concentration Range	Assay	B:P Ratio
Naratriptan FDA Approval Package[149]	-	-	-	Radioactivity	1.2

Frovatriptan

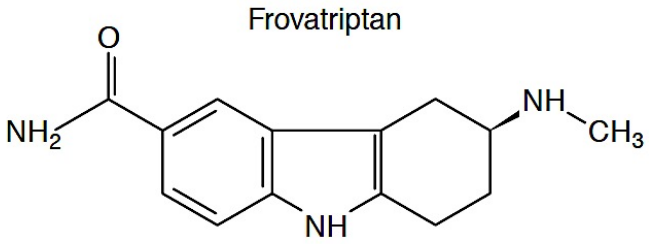

Study	Population	BW	Dose (IV/ *PO*)	Rate	PK Sampling Schedule		Assay Method	Analytical Method Parameters		PK Analysis	Urine Collection Method	Vd_{ss}	CL_{tot}	CL_{ren}
		(kg)	(mg/kg)		Plasma	Urine		Plasma	Urine			(L/kg)	[ml/min/kg]	[ml/min/kg]
Buchan et al[153]	Healthy males n = 6	-	0.01	15 min Infusion	-	-	LC-MS/MS	LLOQ = 0.5 ng/ml	LLOQ = 50 ng/ml	-	Cumulative	4.2 ± 1.4	3.2 ± 0.6	1.2
Buchan et al[154]	Healthy females n = 6	-	0.01	15 min Infusion	-	-	LC-MS/MS	LLOQ = 0.5 ng/ml	LLOQ = 50 ng/ml	-		3.0 ± 0.8	2.3 ± 0.9	1.1

Urinary Excretion Studies

1. Buchan et al[153,154] calculated the CL_{ren} by using $CL_{ren} = f_e * CL_{tot}$ (f_e is the percent of the dose excreted in urine to the administered dose, urine was collected up to 24 hrs)

Plasma Protein Binding Studies

Study	Subjects	Method	Concentration Range	Assay	f_u (%)
Frovatriptan FDA Approval Package[155] and FDA Label[156]	-	-	2 - 1220 ng/ml	-	85

Metabolism

In-vivo, the major metabolites of frovatriptan in blood, urine and feces are hydroxyl-, desmethyl-, N-acetyldesmethyl-, and hydroxyl-N-acetyldesmethyl-frovatriptan[154,156–159]. Additionally, indole acid of frovatriptan is found only in the feces[154,155]. The schematic for metabolism of frovatriptan is shown in Figure - 2 below. Cytochrome P450 enzymes, predominantly by CYP 1A2, mediate hepatic metabolism of frovatriptan[158–160] (and not a substrate for CYP3A4 and/or MAO)[161].

Figure 2 - Metabolic Scheme for Frovatriptan[154,155]

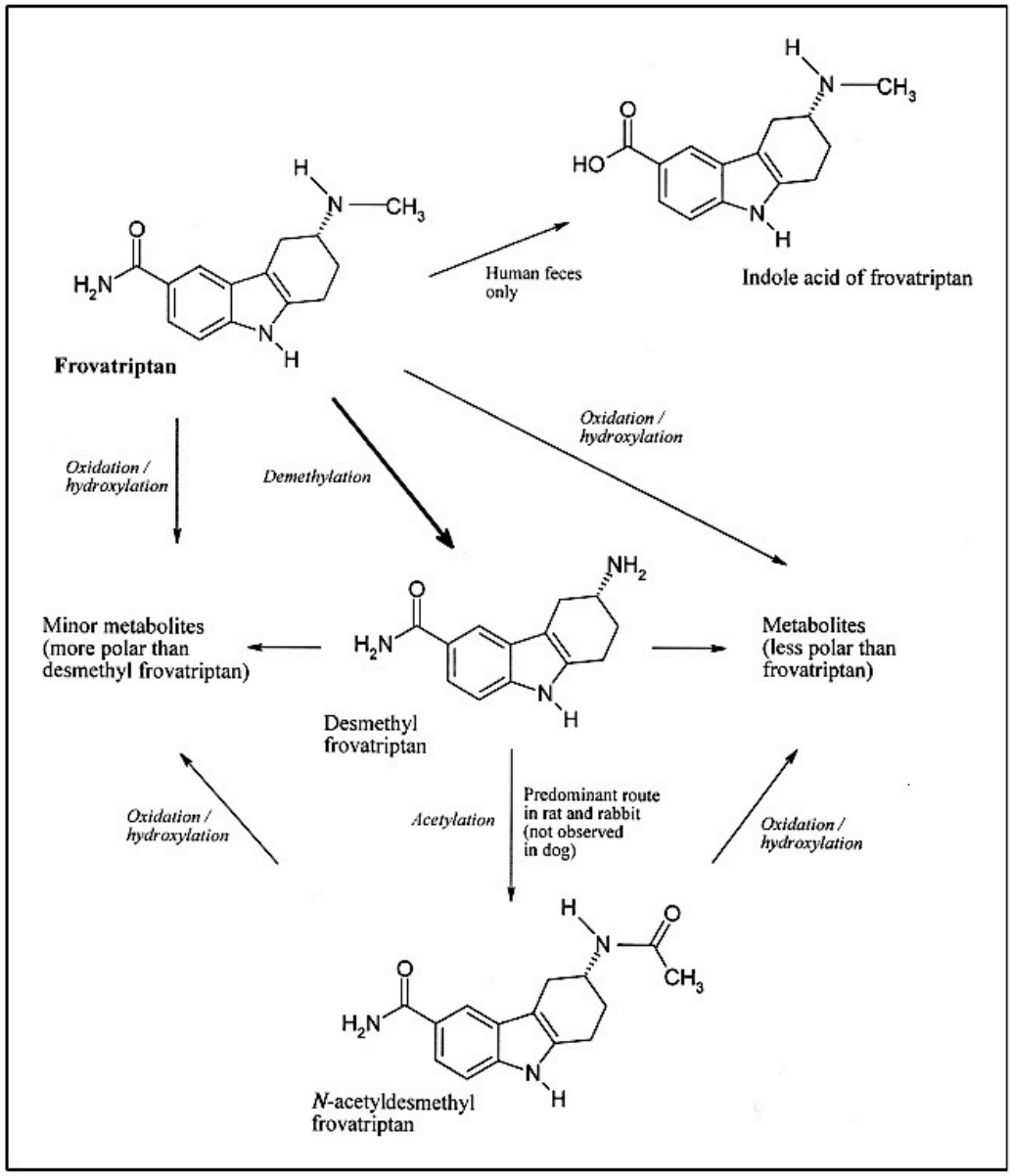

Blood-to-Plasma Ratio Studies

Study	Subjects	Method	Concentration Range	Assay	B:P Ratio
Frovatriptan FDA Approval Package[155] and FDA Label[156]	-	-	-	-	2.0

Rizatriptan

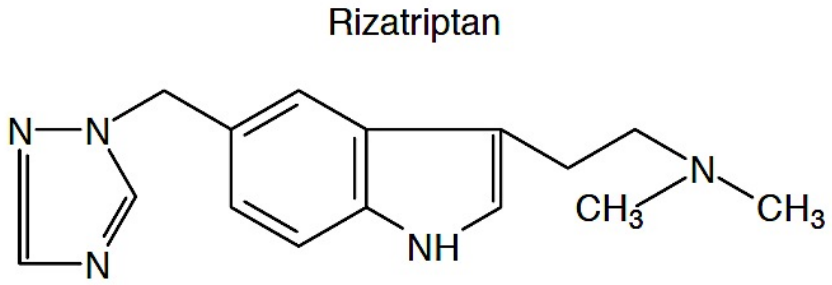

Study	Population	BW	Dose (IV/ *PO*)	Rate	PK Sampling Schedule		Assay Method	Analytical Method Parameters		PK Analysis	Urine Collection Method	Vd_{ss}	CL_{tot}	CL_{ren}
		(kg)	(mg/kg)		Plasma	Urine		Plasma	Urine			(L/kg)	[ml/min/kg]	[ml/min/kg]
Lee. Y., et al[162]	Healthy females, n=8, Age range = 21 - 30 years	59 - 77	0.007	30 min Infusion	15 min - 24 hrs	0 - 24 hrs	LC-MS/MS	LLOQ = 0.5 ng/ml	LLOQ = 5 ng/ml	NCA	Cumulative	1.3 (± 0.3)	13.4 (± 1.9)	2.0
			0.014									1.5 (± 0.4)	12.8 (± 1.4)	2.6
			0.04									1.5 (± 0.2)	12.3 (± 1.5)	3.4

Cheng. H., et al[163]	Healthy males, n = 6	-	0.01	15 min Infusion	15 min - 24 hrs	-	LC-MS/MS	LLOQ = 0.5 ng/ml	-	NCA	-	1.9 (± 0.4)	16.2 (± 3.2)	-
			0.02									1.5 (± 0.3)	16.7 (± 2.2)	-
			0.04									2.0 (± 0.5)	18.7 (± 4.1)	-
			0.06									1.7 (± 0.3)	17.0 (± 3.5)	-
Lee. Y., et al[164]	Healthy, n = 24, Age Range = 22 - 41 years	Males: 78 (61 - 93)	0.05	30 min Infusion	15 min - 12 hrs	0 - 24 hrs	LC-MS/MS	LLOQ = 0.5 ng/ml	LLOQ = 5 ng/ml	NCA	Fractioanted	1.8 (± 0.4)	13.4 (± 3.6)	2.9 (± 0.5)
		Females: 61 (54 - 71)	0.07									1.7 (± 0.5)	13.5 (± 2.4)	2.8 (± 0.5)
		Males: 78 (61 - 93)	*0.03*	*P.O*					LLOQ = 1 ng/ml			-	-	2.9 (± 1.1)
			0.06									-	-	4.4 (± 1.6)
			0.13						LLOQ = 5 ng/ml			-	-	3.8 (± 1.6)

		Females: 61 (54 - 71)	*0.04*						LLOQ = 1 ng/ml			-	-	2.9 (± 0.4)
			0.08									-	-	4.0 (± 0.9)
			0.16						LLOQ = 5 ng/ml			-	-	4.0 (± 2.2)
Vyas. P., et al[165]	Healthy males, n = 6	-	0.04	30 min Infusion	Up to 5 days	Up to 5 days	LC-MS/MS	-	-	NCA	-	2.0 (± 0.4)	17.6 (± 2.6)	4.5 (± 0.6)
			0.14	*P.O*								-	-	5.2 (± 1.5)

Urinary Excretion Studies

1. Lee. Y., et al[162] calculated the CL_{ren} by using CL_{ren} by using $CL_{ren} = f_e * CL_{tot}$ (f_e is the percent of the dose excreted in urine to the administered dose, urine was collected up to 24 hrs)
2. Lee. Y., et al[164] calculated the CL_{ren} by using $CL_{ren} = A_e/AUC$ (Urine was collected in 6 hr fractions for up to 12 hrs and a 12 hr fraction up to 24 hrs)
3. Vyas. P., et al[165] calculated the CL_{ren} by using $CL_{ren} = A_e/AUC$ (Urine was collected up to 5 days)

Plasma Protein Binding Studies

Study	Subjects	Method	Concentration Range	Assay	f_u (%)
Rizatriptan FDA Approval Package[166] and FDA Label[167]	-	-	50 - 5000 ng/ml	-	86

Metabolism

In-vivo, rizatriptan undergoes oxidative deamination mediated by MAO-A to indole acetic acid metabolite, which is primary route of metabolism[166,167]. N-monodesmethyl-rizatriptan is a metabolite, which has shown similar activity at 5-$HT_{1B/1D}$ receptors as the parent compound. Other minor metabolites include N-oxide, 6-hydroxy compound and its sulfate conjugate[166,167]. The schematic of metabolism of rizatriptan is shown in Figure - 3.

Figure 3 - Schematic of Metabolism of Rizatriptan[165,166]

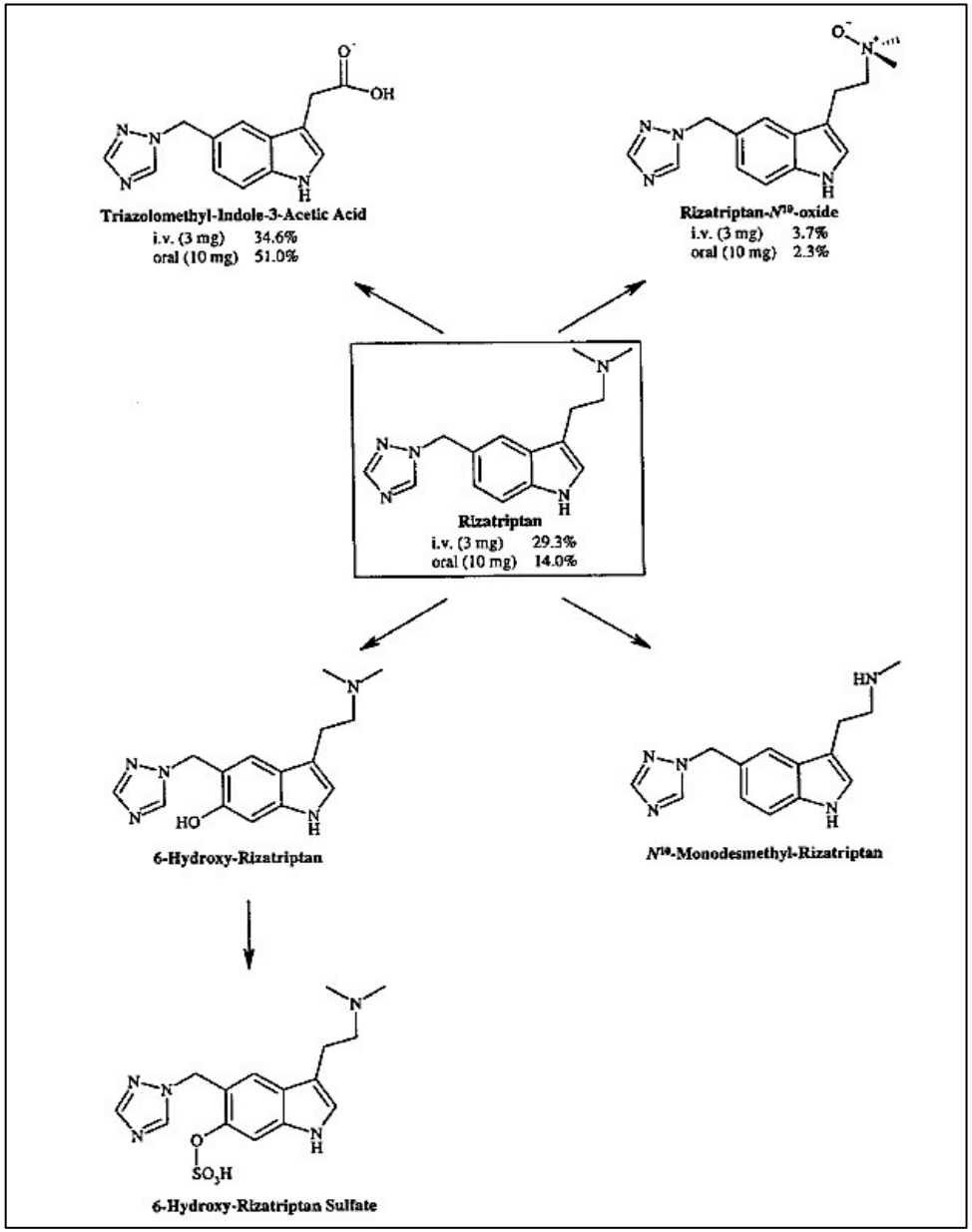

Zolmitriptan

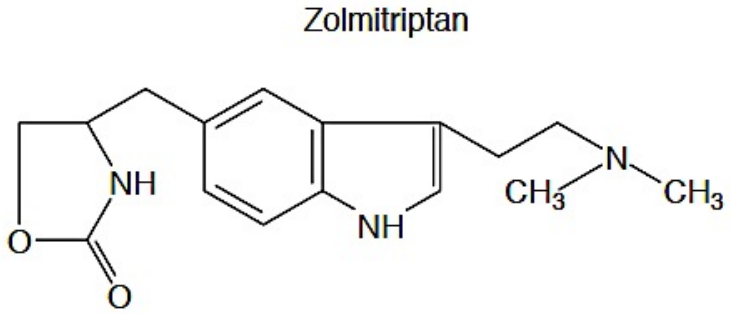

Study	Population	BW	Dose (IV/ *P.O.*)	Rate	PK Sampling Schedule		Assay Method	Analytical Method Parameters		PK Analysis	Urine Collection Method	Vd_{ss}	CL_{tot}	CL_{ren}
		(kg)	(mg/kg)		Plasma	Urine		Plasma	Urine			(L/kg)	[ml/min/kg]	[ml/min/kg]
Seaber. E., et al[168]	Healthy males, n = 6, Mean Age (Range) = 33 (25 - 38) years	78 (61 - 95)	0.04	240 min Infusion	15 min - 24 hrs	Up to 24 hrs	HPLC-Fluoroscence	LLOQ = 2 ng/ml	LLOQ = 100 ng/ml	NCA	Fractionated	4.2 ± 1.4	9.2 (± 1.7)	3.0 (± 0.5)
	Healthy females, n = 6, Mean Age (Range) = 27 (21 - 34) years	65 (58 - 72)	0.05									3.0 ± 0.8	8.3 (± 1.7)	3.0 (± 0.7)
	Healthy males, n = 6, Mean Age (Range) = 33 (25 - 38) years	78 (61 - 95)	*0.13*	*P.O.*		Up to 168 hrs						-	-	2.5 (± 1.0)

	Healthy females, n = 6, Mean Age (Range) = 27 (21 - 34) years	65 (58 - 72)	*0.15*	*P.O.*										2.5 (± 0.7)
Seaber. E., et al[169]	Healthy males, n = 10, Mean Age (Range) = 23 (20 - 28) years	78 (65 - 90)	0.01	120 min Infusion	30 min - 15 hrs	-	HPLC-MS	LLOQ = 0.1 ng/ml	-	NCA	-		11.8	-
			0.02										12.3	
	Healthy females, n = 10, Mean Age (Range) = 23 (19 - 34) years	69 (52 - 85)	0.02										11.2	
			0.04										10.2	
Peck., W. et al[170]	Healthy young adults, n = 12, Mean Age (Range) = 29 (18 - 39) years	70 (54 - 72)	*0.07*	*P.O.*	30 min - 24 hrs	0 - 24 hrs	HPLC-Fluoroscence	LLOQ = 2 ng/ml	LLOQ = 100 ng/ml	NCA	Cumulative	-	-	2.9 (± 0.9)
			0.14											3.2 (± 1.0)
			0.21											3.2 (± 1.0)
Peck., W. et al[171]	Healthy subjects, n = 14, Age Range = 20 - 39 years	55 - 89	*0.14*	*P.O.*	30 min - 24 hrs	0 - 24 hrs	HPLC-Fluoroscence	LLOQ = 2 ng/ml	LLOQ = 100 ng/ml	NCA	Cumulative	-	-	3.5 (2.8 - 5.1)

Urinary Excretion Studies

1. Seaber. E., et al[168] calculated the CL_{ren} by using $CL_{ren} = A_e/AUC$ (Urine was collected in 3 free fractions up to 12 hrs) after I.V. administration and also after P.O. administration (but the urine was reported to be sampled up to 168 hrs)
2. Peck., W. et al[170,171] calculated the CL_{ren} by using $CL_{ren} = A_e/AUC$ (A_e is the amount excreted in urine for 24 hrs)

Plasma Protein Binding

Study	Subjects	Method	Concentration Range	Assay	f_u (%)
Rolan., PE et. al [172]	-	-	10 - 1000 ng/ml	-	75

Metabolism

In-vivo, three major metabolites have been identified, namely, N-desmethyl metabolite (which is 2- to 6-times more potent at 5-$HT_{1B/1D}$ receptors in animal models), N-oxide and indole acetic acid metabolite which is a major metabolite in plasma)[172–174]. Since indole acetic acid metabolite is also produced by sumatriptan via MAO-A mediated pathway, presumably, it plays a role in the disposition of zolmitriptan. Additionally, *in-vitro* studies[175] indicate the involvement of CYP450 enzymes (namely CYP1A2) in the metabolism of zolmitriptan and the schematic for the same is shown in Figure - 4.

Figure 4 - Schematic for *in-vitro* metabolism of Zolmitriptan[175]

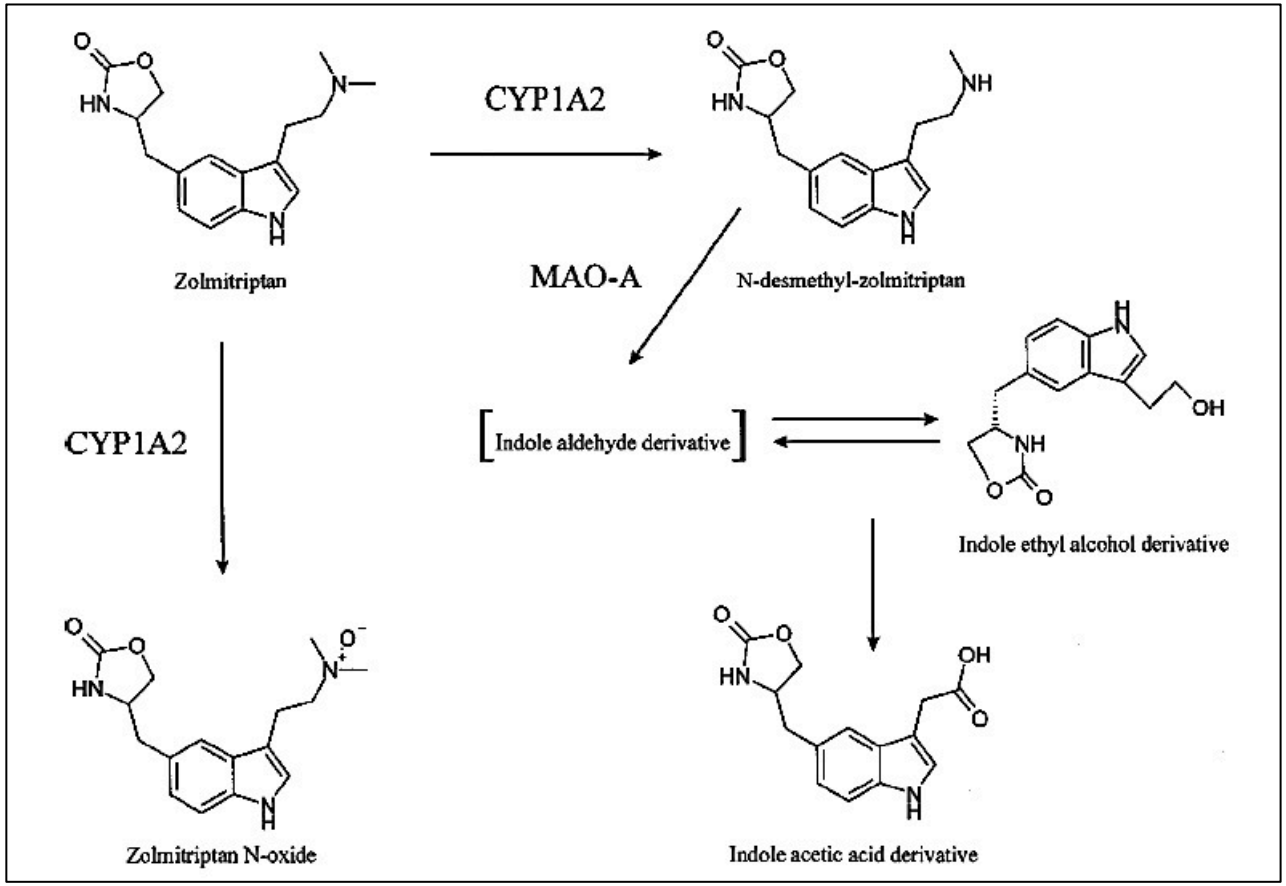

Eletriptan

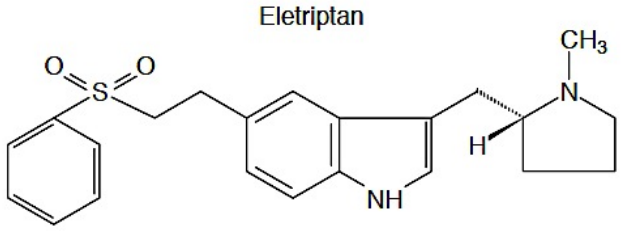

Study	Population	BW	Dose (IV/ *PO*)	Rate	PK Sampling Schedule		Assay Method	Analytical Method Parameters		PK Analysis	Urine Collection Method	Vd_{ss}	CL_{tot}	CL_{ren}
		(kg)	*(µg/ kg)**		Plasma	Urine		Plasma	Urine			(L/kg)	[ml/min/kg]	[ml/min/kg]
Milton. K., et al[176]	Healthy males, n = 8 - 11, Mean (Range) Age = 25 (18 - 38) years	76 (60 - 87)	5	15 min Infusion	7.5 min - 24 hrs	-	HPLC - UV	LLOQ = 0.5 ng/ml	-	NCA		1.9 (0.8 - 2.8)	6.3 (4.0 - 9.8)	-
			17									2.0 (1.5 - 2.4)	5.8 (4.4 - 6.7)	
			50			0 - 24 hrs			LLOQ = 0.5 ng/ml		Cumulative	2.0 (1.4 - 2.4)	5.6 (3.7 - 6.7)	0.5
	Healthy males, n = 8 - 9, Mean (Range) Age = 25 (19 - 33) years	75 (63 - 89)	50			-			-		-	3.0 (2.4 - 4)	7.0 (5.6 - 8.8)	
			75									2.6 (1.7	6.4 (4.7 -	

												- 3.4)	7.6)	
			100									2.6 (1.8 - 4.1)	6.7 (5.5 - 9.1)	

Please note that the doses were administered as ***µg/kg*

Urinary Excretion Studies

1. Milton. K., et al[176] calculated the CL_{ren} by using CL_{ren} by using $CL_{ren} = f_e * CL_{tot}$ (f_e is the percent of the dose excreted in urine to the administered dose, urine was collected up to 24 hrs)

Plasma Protein Binding

Study	Subjects	Method	Concentration Range	Assay	f_u (%)
Eletriptan FDA Label[177]	-	-	-	-	15

Metabolism

In-vivo, N-demethylated metabolite is the major metabolite found in the plasma (and also shows activity at 5-$HT_{1B/1D}$ receptors)[177]. *In-vitro* studies in human liver CYP450 microsomes suggest that it is metabolized primarily by CYP3A4[177,178].

Avitriptan

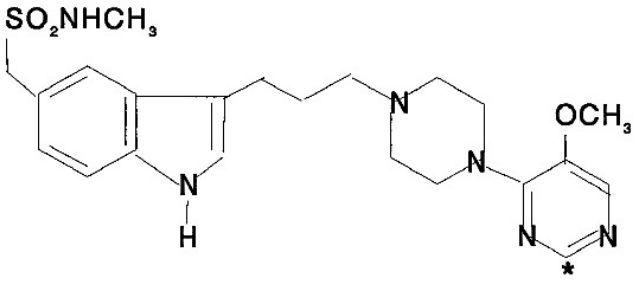

Study	Population	BW	Dose (IV/ *PO*)	Rate	PK Sampling Schedule		Assay Method	Analytical Method Parameters		PK Analysis	Urine Collection Method	Vd_{ss}	CL_{tot}	CL_{ren}
		(kg)	(mg/kg)		Plasma	Urine		Plasma	Urine			(L/kg)	[ml/min/kg]	[ml/min/kg]
Sharma. A., et al[179]	Healthy, n = 24, 6 (2 PL) in each dose group; Mean (Range) Age = 28 (21 - 43) years	74 (± 15)	0.17	30 min Infusion	5 min - 36 hrs	-	HPLC - Electrochemical detection	LLOQ = 1 ng/ml	-	Compartmental (3)	-	1.5 (± 0.9)	6.8 (± 0.4)	-
		72 (± 15)	0.35									1.1 (± 0.2)	7.6 (± 2.3)	
		76 (± 10)	0.50									0.8 (± 0.3)	7.7 (± 1.4)	

Appendix 3.2. TRP - MAO-mediated metabolic clearance

For TRP that are substrates of MAO, the contribution of MAO-mediated metabolic clearance towards CL_{tot}, i.e., $f_{pathway}$, can be assessed using exposure changes from human drug-drug interaction studies in the presence (and absence) of MAO-specific inhibitors such as moclobemide (see also Appendix Ib):

In the absence of inhibitor (Control):

$$CL_{tot}^{I.V.}(Control) / F_{oral}(Control) = Dose/AUC_{0-\infty}(Control)$$

$CL_{tot}^{I.V.}$ is the systemic total body clearance of TRP, which includes CL_{ren}, CL_{nonren} encompassing CL_{hep} (both MAO-mediated, CL_{hep}^{MAO} as well as non-MAO, i.e., by other DME, $CL_{hep}^{non\text{-}MAO}$) and also $CL_{extrahepatic}$ (primarily by MAO). F_{oral} information can be obtained from absolute bioavailability studies, but also requires information with respect to GI solubility, GI permeability and hepatic first-pass metabolism, ER_{hep}^{A} (encompassing both MAO-mediated and non-MAO-mediated pathways).

Furthermore, the amount of the parent drug appearing in the feces from radioactive mass balance studies, provides information about the fraction of the dose that is absorbed from the GI tract, F_{abs}, assuming that there are GI no solubility issues.

The hepatic first pass, ER_{hep}^{B} can also be estimated (independently) from systemic CL_{nonren} as the ratio of CL_{nonren} to LBF, assuming that there are no extrahepatic clearance pathways, i.e., $CL_{nonren} = CL_{hep}$. However, in case of MAO-substrate TRP, since there is evidence of MAO-mediated extrahepatic clearance pathways, and therefore ER_{hep}^{A} is expected to be lower than ER_{hep}^{B}, if the F_{abs} is accurately estimated.

$$CL_{tot}^{I.V.}(Control) = CL_{ren} + CL_{hep}^{MAO} + CL_{hep}^{non\text{-}MAO} + CL_{extrahepatic}^{MAO}$$

$$F_{oral}(Control) = F_{abs} * (1 - ER_{hep}^{A})$$

$$ER_{hep}^{B} = CL_{nonren}/LBF$$

In the presence of inhibitor (I):

$$CL_{tot}^{I.V.}(I)/F_{oral}(I) = Dose/AUC_{0-\infty}(I)$$

The MAO-specific inhibitor is assumed to completely shut off the MAO-mediated metabolic clearance, i.e., CL_{hep}^{MAO} and $CL_{extrahepatic}^{MAO}$ and therefore, $CL_{tot}^{I.V.}$ includes only CL_{ren} and $CL_{hep}^{non\text{-}MAO}$ (both of which are assumed to remain unchanged in the presence of the MAO inhibitor). The value for $F_{oral}(I)$ includes both F_{abs} and $ER_{hep}^{A'}$ which encompasses only non-MAO-mediated, i.e., non-inhibited presystemic metabolic pathways.

$$CL_{tot}^{I.V.}(I) = CL_{ren} + CL_{hep}^{non\text{-}MAO}$$

$$F_{oral} = F_{abs} * (1 - ER_{hep}^{A'})$$

Based on the available oral bioavailability studies in the absence of inhibitor, oral mass balance studies, the information on TRP that are MAO-substrates is compiled below:

TRP	**F_{oral} (%)**	**F_{abs} (%) 100 - %Dose excreted in the feces**	**ER_{hep}^{A} ($1- F_{oral}/F_{abs}$) (%)**	**ER_{hep}^{B} (CL_{nonren}/LBF) (%)**	**%Increase in AUC ($1 - AUC_{Control}/AUC(I)$)**
Almotriptan[135,137,142,143,146,180]	70	87	20	25	27
Zolmitriptan[168,169,173,174]	50	70	29	36	25
Rizatriptan[162,165–167]	43	89	51	54	55
Sumatriptan[131,132,134]	14	96	85	59	-

Interpretation:

1. Despite evidence of extrahepatic pathways for the four MAO-substrates, it can be observed that ER_{hep}^{A} is comparable to or greater than ER_{hep}^{B}, suggesting that the F_{abs} estimates may not be well estimated from the residual radioactivity in feces (which may have included not only radiolabeld parent drug, but also metabolites).
2. There, the contribution of the MAO-mediated metabolic clearance towards CL_{tot} could not be resolved for the four TRP, owing to the lack of information of ER_{hep}^{A} that is accounted for by non-MAO pathways and also because of the low confidence in F_{abs} estimates. As a result, the observed systemic exposure increase in presence of a MAO inhibitor could not be translated in $f_{pathway}$ as was the case for BZD (see Appendix 1.2).

Appendix 4 - Human PK Study Summaries of Class III Anti-Arrhythmics

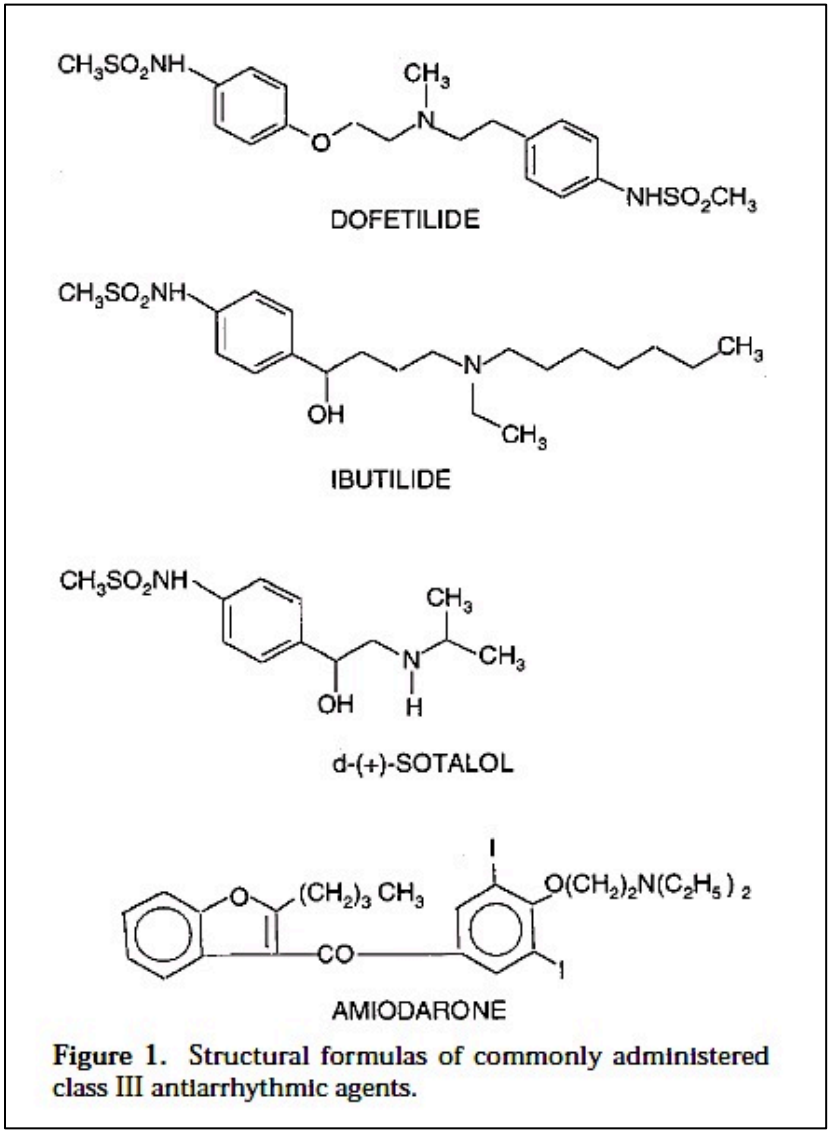

Figure 1. Structural formulas of commonly administered class III antiarrhythmic agents.

Azimilide

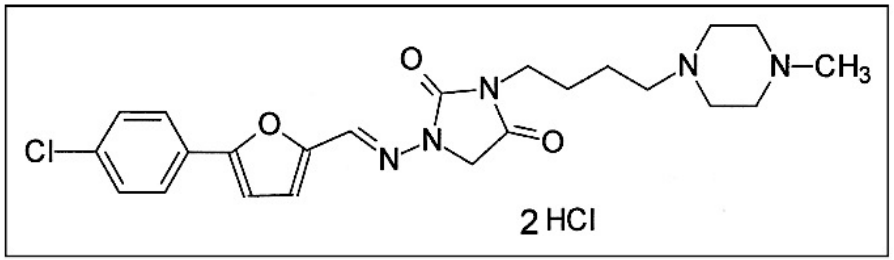

Study	Population	BW	Dose (IV/ *PO*)	Rate	PK Sampling Schedule		Assay Method	Analytical Method Parameters		PK Analysis	Urine Collection Method	Vd_{ss}	CL_{tot}	CL_{ren}
		(kg)	(mg/kg)		Plasma	Urine		Plasma	Urine			(L/kg)	[ml/min/kg]	[ml/min/kg]
Corey et al[181]	Healthy males, n = 25, Mean (SD) Age = 26 (1) years	74 (0.7)	1.0	18 min Infusion	8.5 min - 648 hrs	0 h - 48h, qd for 25 days	HPLC - UV	LLOQ = 5.2 ng/ml	LLOQ = 90 ng/ml	NCA	Fractionated	13.2 (± 3.1)	2.4 (± 0.9)	0.23 (± 0.08)
			2.0	*P.O.*								-	-	0.22 (± 0.07)
Corey et al[182]	Healthy males, n = 82, Mean (SD) Age = 27 (7) years	73 (10)	4.5 - 9.0	15 - 60 min	5 min - 336 hrs	Every 24 hrs for 96 hrs	Rp-HPLC-MS/MS	LLOQ = 5 ng/ml	LLOQ = 40 ng/ml	NCA	Fractionated	10	2.0	0.22

Corey et al[183]	Healthy males, n = 33, Mean Age = 49 years	80	*1.88*	*P.O.*	0.5 - 480 hrs	Every 24 hrs for 216 hrs	HPLC-UV	LLOQ = 10 ng/ml	LLOQ = 100 ng/ml	NCA	Fractionated	-	-	0.15 (± 0.04)
	Healthy females, n = 33, Mean Age = 53 years	66	*2.27*	*P.O.*										0.18 (± 0.05)
Corey et al[184]	Healthy males, n = 12, Mean (SD) Age = 52 (11) years	84 (13)	*1.79*	*P.O.*	0.5 hrs - 22 days	Every 24 hours for 10 days	HPLC-UV	LLOQ = 5 ng/ml	LLOQ = 50 ng/ml	NCA	Fractionated	-	-	0.23 (± 0.13)

rinary Excretion Studies

1. Corey et al[181] calculated the CL_{ren} by using CL_{ren} = Ae/AUC (Urine was collected in 2 hr fractions for first 12 hrs, 12-16, 16-24, 24-36, 36-48 hours, and then every 24 hr fraction for an additional 25 days)
2. Corey et al[182] calculated the CL_{ren} by using CL_{ren} = Ae/AUC (Urine was collected in 24 hr fractions up to 96 hours)
3. Corey et al[183] calculated the CL_{ren} by using CL_{ren} = Ae/AUC (Urine was collected in 24 hr fractions up to 216 hours)
4. Corey et al[184] calculated the CL_{ren} by using CL_{ren} = Ae/AUC (Urine was collected in 24 hr fractions up to 10 days)

Plasma Protein Binding Studies

Study	Subjects	Method	Concentration Range	Assay	f_u (%)
Corey et al[183]	Healthy males, n = 33	Equilibrium dialysis	-	Liquid Scintillation Counting	6
	Healthy females, n = 33		-		6
Corey et al[184]	Healthy males, n = 12	Equilibrium dialysis	Assessed at 7 h	Liquid Scintillation Counting	8
Mouelhi et al[185]	-	Equilibrium dialysis	13 - 173 ng/ml	Liquid Scintillation Counting	3

Metabolism

Azimilide metabolic clearance is claimed[184] to be mediated via (a) cleavage of the azomethine bond (up to 30%), (b) CYP1A1 (up to 25%) and (c) CYP3A4 (up to 25%). However, this was based on the internal report[184] and was inaccessible for further evaluation. It was also reported that azimilide did not form any active metabolites. The schematic of the metabolic routes for azimilide is shown in Figure - 1 below[184]. An *in-vivo* DDI study with ketoconazole, a selective and potent CYP3A inhibitor and (p.o. administration of) azimilide showed a 16% reduction in the apparent clearance - suggesting the reduction could have been due to either decrease in systemic clearance and/or increase in F_{oral}, although the latter is less likely to be clinically relevant, given the low ER_{hep} drug azimilide is[181].

Figure 5 - Schematic of Metabolism of Azimilide[185]

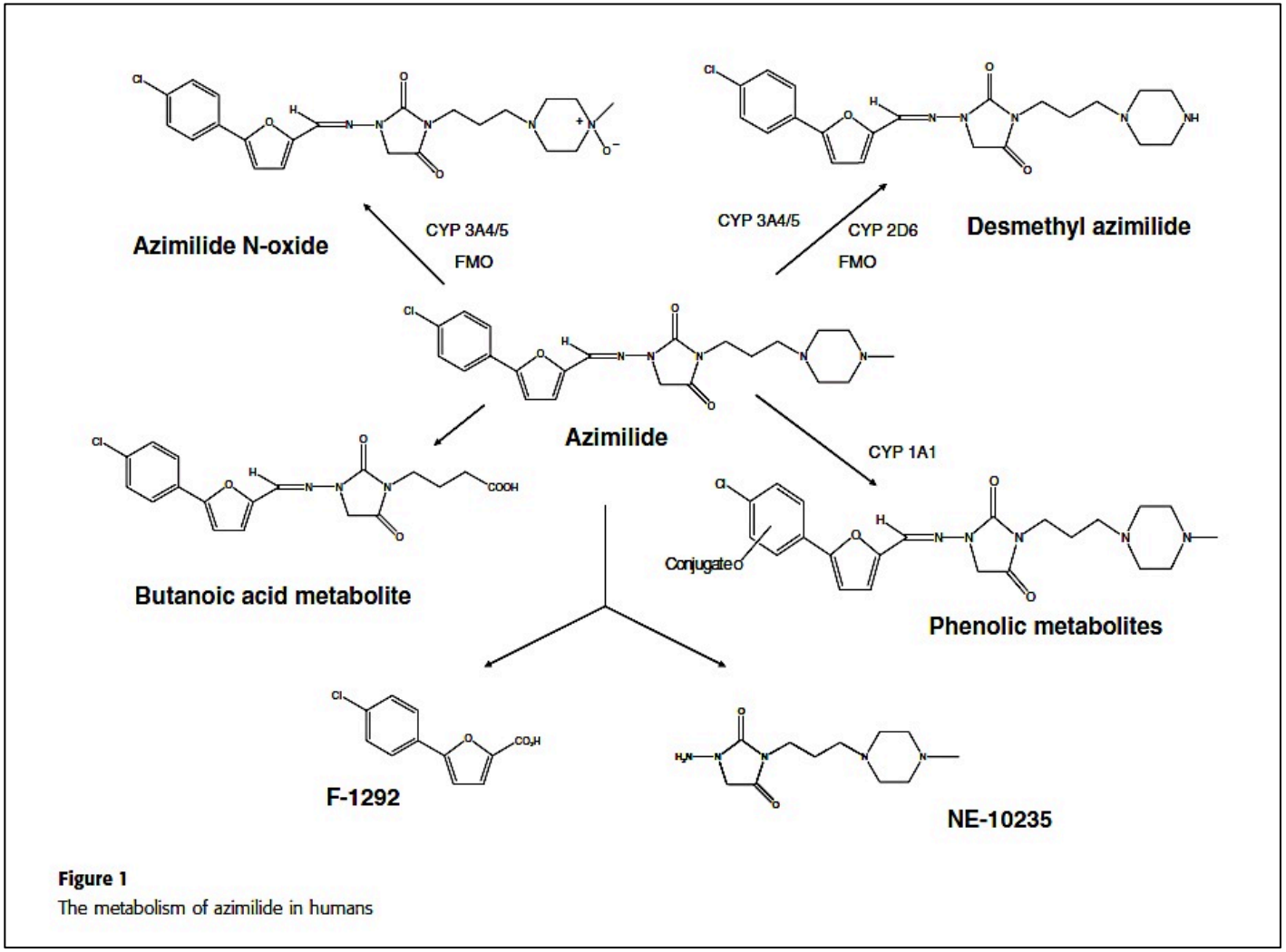

Figure 1
The metabolism of azimilide in humans

Amiodarone

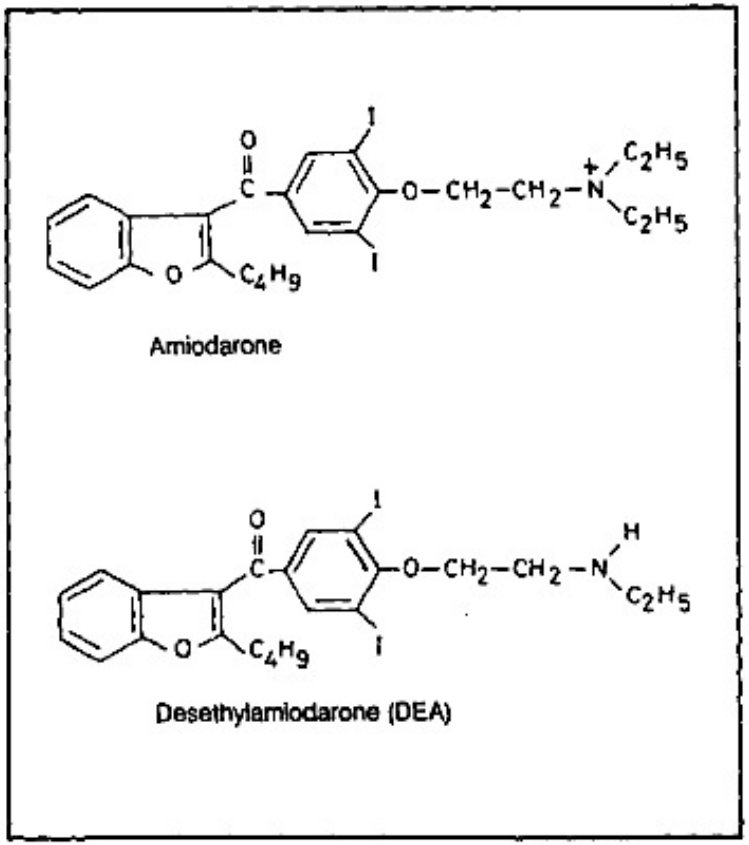

Study	Population	BW	Dose (IV/ *PO*)	Rate	PK Sampling Schedule		Assay Method	Analytical Method Parameters		PK Analysis	Urine Collection Method	Vd_{ss}	CL_{tot}	CL_{ren}
		(kg)	(mg/kg)		Plasma	Urine		Plasma	Urine			(L/kg)	[ml/min/kg]	[ml/min/kg]
Ujhelyi et al[186]	Healthy subjects, n = 11, Mean (SD) Age = 49 (14) years	79 (17)	5	15 min	15 min - 76 days	0 h - 34 h	HPLC - UV	LLOQ = 5 ng/ml	LLOQ = 5 ng/ml	NCA	Fractionated	60 (± 28)	1.88 (± 1.1)	-
Cushing et al[187]	Healthy subjects, n = 78, Mean (SD) Age = 37 (12) years	-	2	10 min	1 min - 72 hrs	-	LC-MS/MS	LLOQ = 5 ng/ml	-	NCA	-	-	3.72	-
Vadiei et al[188]	Healthy subjects, n = 11, Mean (SD) Age = 48 (10) years	77 (11)	5	15 min	15 min - 76 days	-	HPLC-UV	LLOQ = 5 ng/ml	-	NCA	-	59 (± 22)	1.7 (± 0.7)	-

Urinary Excretion Studies

1. Ujhelyi et al[186] calculated the CLren by using CLren = Ae/AUC (Urine was collected 0-2, 2-4, 4-8, 8-12, 12-24 and 24-34 hours)

Plasma Protein Binding Studies

Study	Subjects	Method	Concentration Range	Assay	f_u (%)
Ujhelyi et al[186]	Healthy subjects	Ultrafiltration	30 min Sample	HPLC-UV	3.2 (± 1.0)
Neyroz et al[189]	*In-vitro*	Ultracentrifugation	10 µg/ml	HPLC-UV	3.7

Metabolism

Amiodarone is known to show variable oral bioavailability (20 - 80%)[190,191] and it is primarily eliminated by metabolism with only less than 1% of excreted unchanged in the urine[186]. Biliary excretion may also play a role in the overall elimination of the drug[190]. The schematic of potential metabolic routes of amiodarone is shown in Figure below[191]. Desethylamiodarone (DEA) is the major active metabolite and the enzymes responsible for the metabolism of amiodarone are present in both liver and intestine[192].

Figure 6 - Potential Pathways of Metabolism of Amiodarone[191]

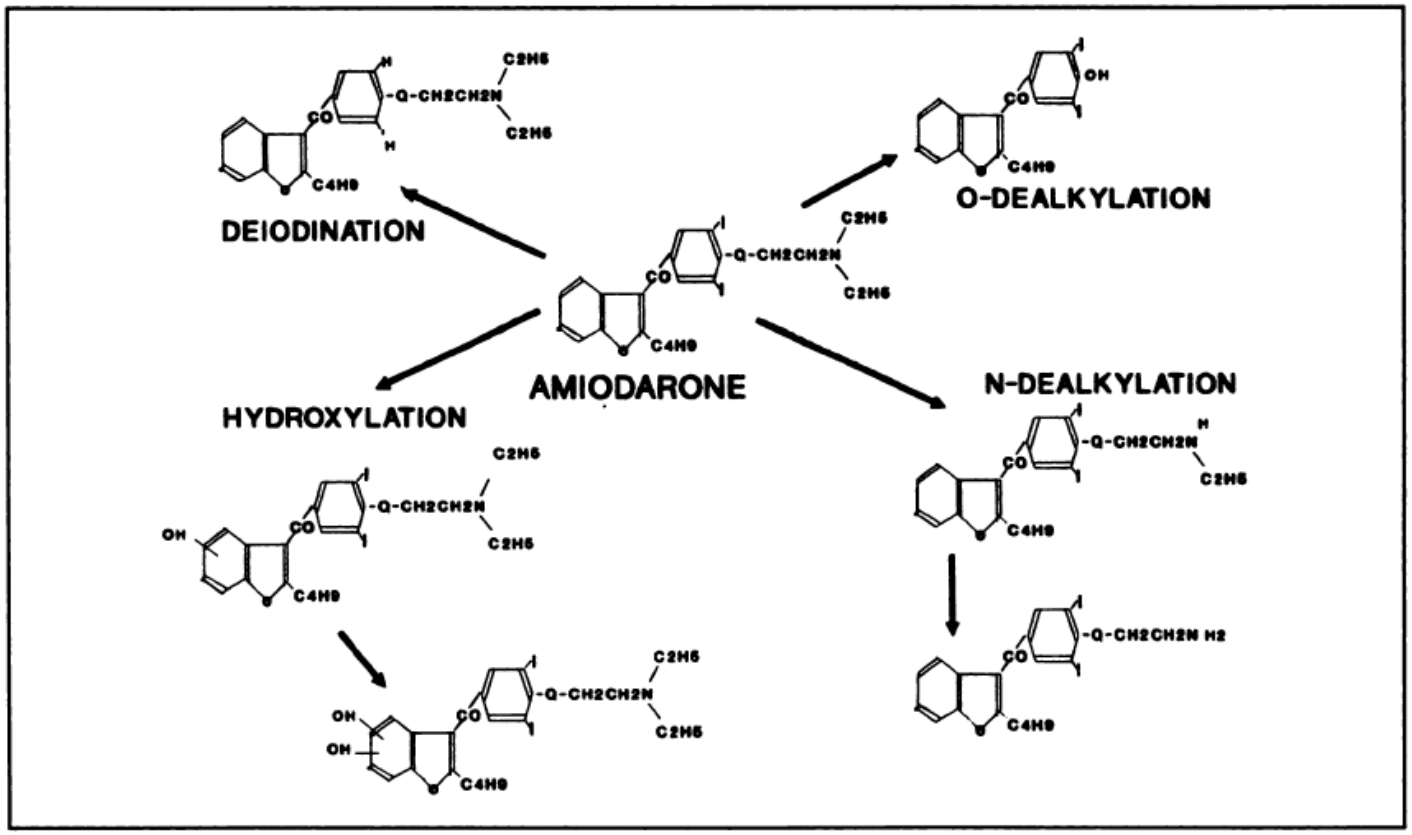

Blood-to-Plasma Ratio

Study	Subjects	Method	Concentration Range	Assay	B:P Ratio
Andreasen et al[193]	Healthy subjects	Centrifugation	-	HPLC	0.6

Dofetilide

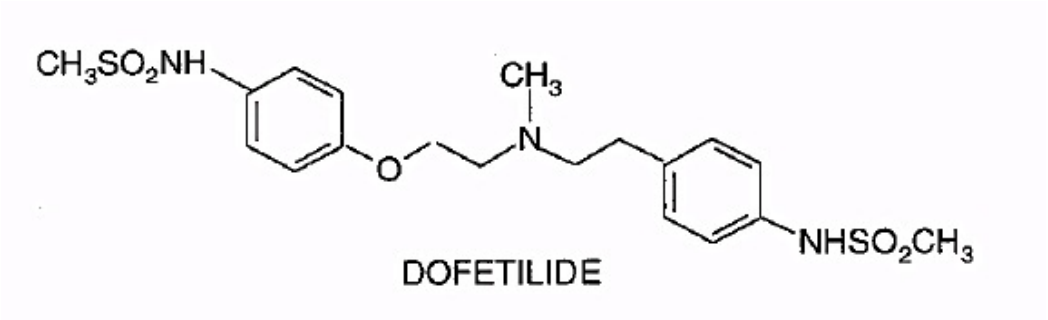

Study	Population	BW	Dose (IV/ *PO*)	Rate	PK Sampling Schedule		Assay Method	Analytical Method Parameters		PK Analysis	Urine Collection Method	Vd_{ss}	CL_{tot}	CL_{ren}
		(kg)	(mg/kg)		Plasma	Urine		Plasma	Urine			(L/kg)	[ml/min/kg]	[ml/min/kg]
Tham et. al[194]	Healthy subjects, n = 9, Mean (SD) Age = 23 (3) years	66 (6)	0.01	10 min	0.5 h - 96 h	0 h - 48 h	Radioimmunoassay for plasma and HPLC for urine	LLOQ = 0.05 ng/ml	LLOQ = 2.5 ng/ml	NCA	Fractionated	3.5 (± 0.3)	5.3 (± 0.3)	2.8
Sedgwick et al[195]	Subjects with suspected coronary artery disease, Mean (Range) Age = 55 (42-65)	-	0.001 - 0.006	15 min	0 h - 24 h	-	Radioimmunoassay	LLOQ = 0.05 ng/ml	-	NCA	-	-	4.7	-
Coz et al[196]	Healthy subjects, n = 10, Mean (Range) Age = 23.4 (19 - 30) years	68.4 (58 - 86)	0.5	30 min	10 min - 72 h	-	Radioimmunoassay	LLOQ = 0.05 ng/ml	-	NCA	-	3.3 (± 0.5)	5.8 (± 0.8)	-

Abel et al[197]	Healthy subjects, n = 20, Mean (Range) Age = 29 (19 - 42) years	79 (59 - 89)	*0.01*	-	0 h - 72 h	0 h - 48 h	Radioimmunoassay for plasma and HPLC for urine	LLOQ = 0.05 ng/ml	LLOQ = 5 ng/ml	NCA	Fractionated	-	-	3.5 (± 0.5)

Urinary Excretion Studies

1. Tham et al[194] calculated the CLren by using CLren = Ae/AUC (Urine was collected 0-12, 12-24 and 24-48 hours)
2. Abel et al[197] calculated the CLren by using CLren = Ae/AUC (Urine was collected 0-12, 12-24 and 24-48 hours)

Plasma Protein Binding Studies

Study	Subjects	Method	Concentration Range	Assay	f_u (%)
Smith et al[198]	*In-vitro*	Equilibrium Dialysis	10 - 100 ng/ml	Liquid Scintillation Counting	36

Metabolism

In humans, dofetilide was the only detectable component present in plasma extracts, as a discrete peak by radiochemical HPLC (i.e., no single metabolite accounted for > 5% of plasma radioactivity)[198]. The potential pathways of metabolism of dofetilide have also been shown in the figure below[198].

Figure 7 - Possible Metabolic Pathways of Dofetilide[198]

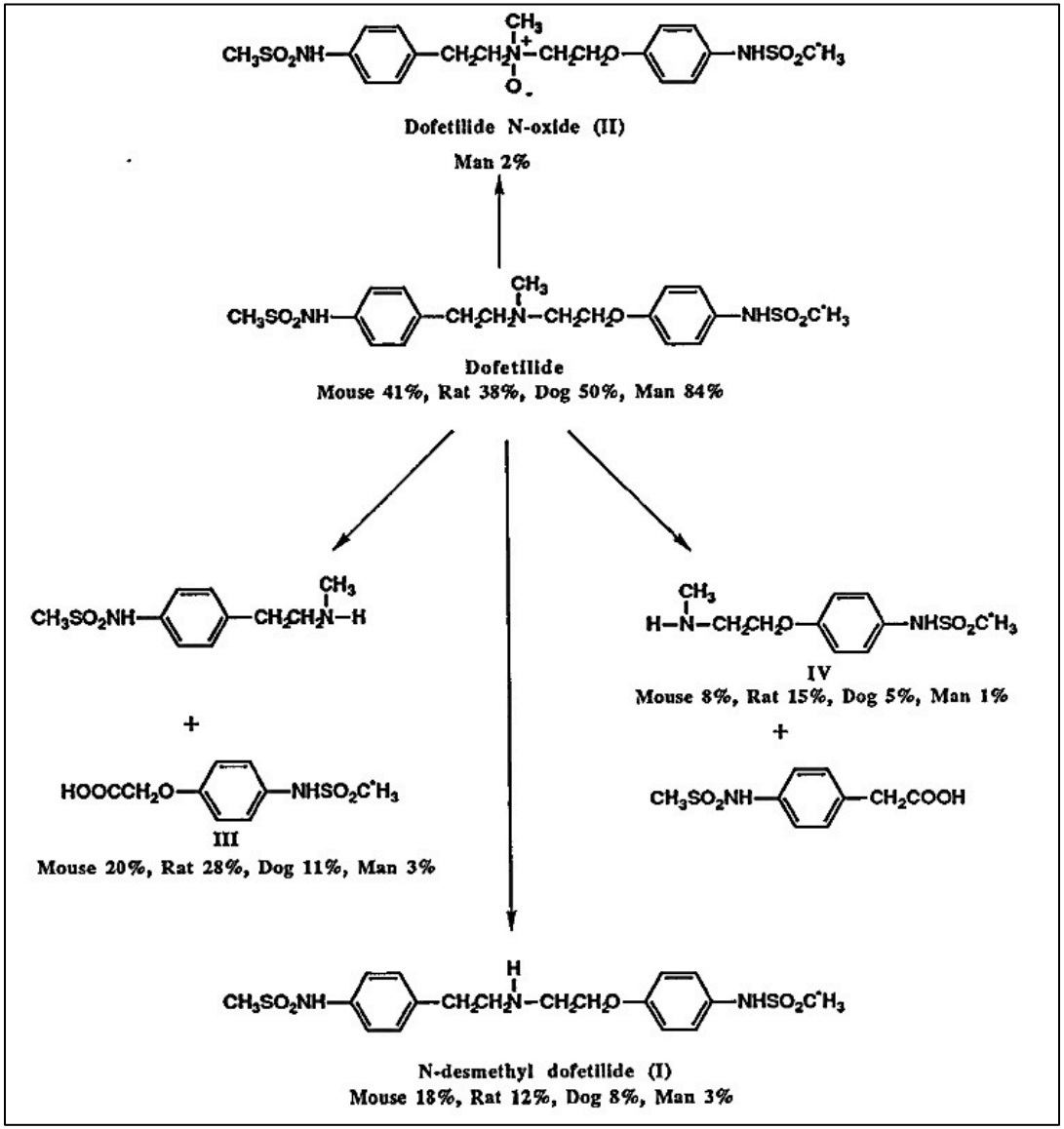

Ibutilide

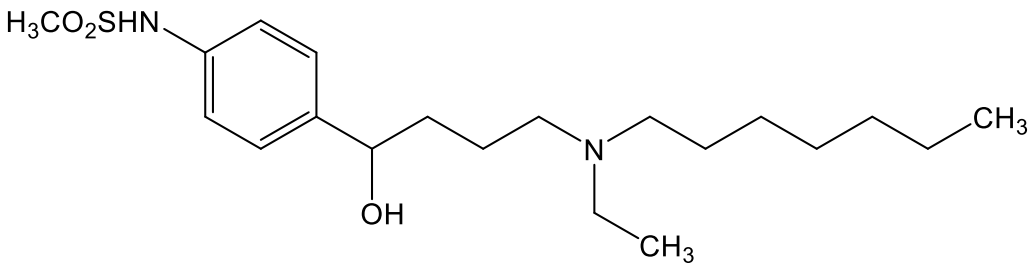

Study	Population	BW	Dose (IV/ *PO*)	Rate	PK Sampling Schedule		Assay Method	Analytical Method Parameters		PK Analysis	Urine Collection Method	Vd_{ss}	CL_{tot}	CL_{ren}
		(kg)	(mg/ kg)		Plasma	Urine		Plasma	Urine			(L/kg)	[ml/min/kg]	[ml/min/kg]
Jungbluth et al[199]	Healthy subjects, n = 6	-	0.01	10 min	-	-	HPLC - Chiral specific separation	-	-	-	Cumulative	12 (± 5)	26 (± 5)	2.6
Jungbluth et al[200]	Healthy volunteers, n = 44	-	0.01 - 0.1	10 min - 8 hrs	-	-	HPLC	-	-	-	Cumulative	13	27	-
FDA Label[201]	-	-	-	-	-	-	-	-	-	-	-	11	29	

Urinary Excretion Studies

1. Jungbluth et al[199] calculated the CLren by using CLren = fe*CLtot (fe = % of the dose excreted unchanged in the urine = 10±3)
2. Jungbluth et al[200] calculated the CLren by using CLren = fe*CLtot (fe = % of the dose excreted unchanged in the urine < 5%??)
3. FDA Label[201] - fe = 6%

Dronedarone

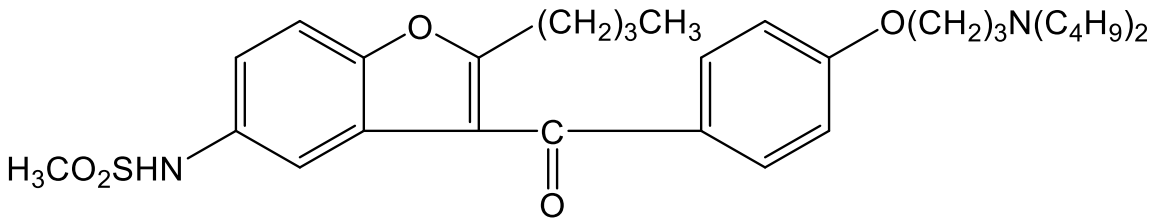

Study	Population	BW	Dose (IV/ *PO*)	Rate	PK Sampling Schedule		Assay Method	Analytical Method Parameters		PK Analysis	Urine Collection Method	Vd_{ss}	CL_{tot}	CL_{ren}
		(kg)	(mg/kg)		Plasma	Urine		Plasma	Urine			(L/kg)	[ml/min/kg]	[ml/min/kg]
FDA Label[202]	-	-	-	-	-	-	-	-	-	-	-	20	33.3	-
FDA Approval Package[203]	-	-	-	-	-	-	-	-	-	-	-	-	33.3	-

Urinary Excretion Study

It was reported[202] that a very negligible amount is excreted unchanged in the urine.

Plasma Protein Binding Studies

Study	Subjects	Method	Concentration Range	Assay	f_u (%)
FDA Label[202] and FDA Approval Package[203]	-	-	-	-	1%

Metabolism

In humans, dronedarone[203] is extensively metabolized and N-debutylation is reported to the major metabolic pathway. The other reported[203] pathways of metabolism include oxidative deamination and direct oxidation. It is also reported that over 30 metabolites are excreted in urine and feces.

Bretylium

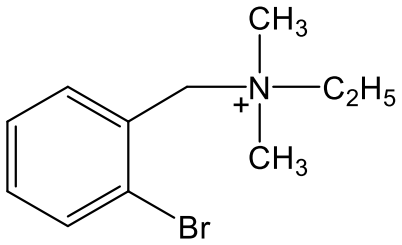

Study	Population	BW	Dose (IV/ *PO*)	Rate	PK Sampling Schedule		Assay Method	Analytical Method Parameters		PK Analysis	Urine Collection Method	Vd_{ss}	CL_{tot}	CL_{ren}
		(kg)	(mg/ kg)		Plasma	Urine		Plasma	Urine			(L/kg)	[ml/min/kg]	[ml/min/kg]
Narang et al[204]	Healthy subjects, n = 4; Mean (SD) Age = 26 (6) years	64 (3)	4.0	5 min	0 - 72 h	0 - 72 h	GC - Electron Capture	LLOQ = 5 ng/ml	LLOQ = 5 ng/ml	Compartmental (2)	Cumulative	6	12	2.6
Garrett et al[205]	Healthy volunteers, n = 9; Age range = 21 - 30 years	-	3 - 6	60 min	0 - 48 h	0 - 72 h	GC - Electron Capture	LLOQ = 5 ng/ml	-	Compartmental (3)	Fractionated	*8*	11	-

Urinary Excretion Studies

1. Narang et al[204]. calculated the CLren by using CLren = fe*CLtot (fe = % of the dose excreted unchanged in the urine = 77%)
2. Garett at al[205]. calculated the CLren by using CLren = Ae/AUC (Urine was collected at 2 hrs intervals up to 10 hrs, then at 10 -14, 14-18, 18-24, 24-30, 30-36, 36-48, 48-72 hours)

Plasma Protein Binding Study

Study	Subjects	Method	Concentration Range	Assay	f_u (%)
Garrett et al[205]	*In-vitro*	Ultrafiltration	10 - 10000 ng/ml	-	94%

Appendix References

1. Boxenbaum, H. G. *et al.* Pharmacokinetic and biopharmaceutic profile of chlordiazepoxide HC1 in healthy subjects: single-dose studies by the intravenous, intramuscular, and oral routes. *J. Pharmacokinet. Biopharm.* **5,** 3–23 (1977).

2. Sellers, E. M. *et al.* Chlordiazepoxide and oxazepam disposition in cirrhosis. *Clin. Pharmacol. Ther.* **26,** 240–6 (1979).

3. Greenblatt, D. J. *et al.* Kinetics of intravenous chlordiazepoxide: sex differences in drug distribution. *Clin. Pharmacol. Ther.* **22,** 893–903 (1977).

4. Moschitto, L. J. & Greenblatt, D. J. Concentration-independent plasma protein binding of benzodiazepines. *J. Pharm. Pharmacol.* **35,** 179–80 (1983).

5. Greenblatt, D. J., Shader, R. I., MacLeod, S. M. & Sellers, E. M. Clinical pharmacokinetics of chlordiazepoxide. *Clin. Pharmacokinet.* **3,** 381–94 (1978).

6. Berlin, a & Dahlström, H. Pharmacokinetics of the anticonvulsant drug clonazepam evaluated from single oral and intravenous doses and by repeated oral administration. *Eur. J. Clin. Pharmacol.* **9,** 155–9 (1975).

7. Crevoisier, C., Delisle, M. C., Joseph, I. & Foletti, G. Comparative single-dose pharmacokinetics of clonazepam following intravenous, intramuscular and oral administration to healthy volunteers. *Eur. Neurol.* **49,** 173–7 (2003).

8. Pacifici, G. M., Viani, A., Rizzo, G., Carrai, M. & Rane, A. Plasma protein binding of clonazepam in hepatic and renal insufficiency and after hemodialysis. *Ther. Drug Monit.* **9,** 369–73 (1987).

9. Lucek, R. W. & Countinho, C. B. The Role of Substituents in the Hydrophobic binding of 1, 4 Benzodiazepines by Human plasma proteins. *Mol. Pharmacol.* **12,** 612 (1976).

10. Bertler, Lindgren, S., Magnusson, J.-O. & Malmgren, H. Pharmacokinetics of chlorazepate after intravenous and intramuscular administration. *Psychopharmacology (Berl).* **80,** 236–239 (1983).

11. Klotz, U., Avant, G. R., Hoyumpa, a, Schenker, S. & Wilkinson, G. R. The effects of age and liver disease on the disposition and elimination of diazepam in adult man. *J. Clin. Invest.* **55,** 347–59 (1975).

12. Klotz, U., Antonin, K. H. & Bieck, P. R. Pharmacokinetics and plasma binding of diazepam in man, dog, rabbit, guinea pig and rat. *J. Pharmacol. Exp. Ther.* **199,** 67–73 (1976).

13. Cloyd, J. C., Lalonde, R. L., Beniak, T. E. & Novack, G. D. A single-blind, crossover comparison of the pharmacokinetics and cognitive effects of a new diazepam rectal gel with intravenous diazepam. *Epilepsia* **39,** 520–6 (1998).

14. Greenblatt, D. J. *et al.* Desmethyldiazepam pharmacokinetics: studies following intravenous and oral desmethyldiazepam, oral clorazepate, and intravenous diazepam. *J. Clin. Pharmacol.* **28,** 853–9 (1988).

15. Ochs, H. R. Kinetics of diazepam, midazolam, and lorazepam in cigarette smokers. *CHEST J.* **87,** 223 (1985).

16. Locniskar, A., Greenblatt, D. J., Zinny, M. A., Harmatz, J. S. & Shader, R. I. Absolute bioavailability and effect of food and antacid on diazepam absorption from a slow-release preparation. *J. Clin. Pharmacol.* **24,** 255–63 (1984).

17. Giles, H. G., Sellers, E. M., Naranjo, C. a, Frecker, R. C. & Greenblatt, D. J. Disposition of intravenous diazepam in young men and women. *Eur. J. Clin. Pharmacol.* **20,** 207–13 (1981).

18. Divoll, M., Greenblatt, D. J., Ochs, H. R. & Shader, R. I. Absolute bioavailability of oral and intramuscular diazepam: effects of age and sex. *Anesth. Analg.* **62,** 1–8 (1983).

19. Divoll, M. & Greenblatt, D. J. Binding of diazepam and desmethyldiazepam to plasma protein: Concentration-dependence and interactions. *Psychopharmacology (Berl).* **75,** 380–382 (1981).

20. Mandelli, M., Tognoni, G. & Garattini, S. Clinical Pharmacokinetics of Diazepam. *Clin. Pharmacokinet.* **3,** 72 (1978).

21. Sennesael, J., Verbeelen, D., Vanhaelst, L., Pirola, R. & Bareggi, S. R. Pharmacokinetics of intravenous and oral chlordesmethyldiazepam in patients on regular haemodialysis. *Eur. J. Clin. Pharmacol.* **41,** 65–8 (1991).

22. Bareggi, S. R., Pirola, R., Potvin, P. & Devis, G. Effects of liver disease on the pharmacokinetics of intravenous and oral chlordesmethyldiazepam. *Eur. J. Clin. Pharmacol.* **48,** 265–8 (1995).

23. Greenblatt, D. J. *et al.* Pharmacokinetics and bioavailability of intravenous, intramuscular, and oral lorazepam in humans. *J. Pharm. Sci.* **68,** 57–63 (1979).

24. Greenblatt, D. J. *et al.* Kinetic and dynamic study of intravenous lorazepam: comparison with intravenous diazepam. *J. Pharmacol. Exp. Ther.* **250,** 134–40 (1989).

25. Wermeling, D. P. H. & Miller, J. L. Bioavailability and Pharmacokinetics of Lorazepam after Intranasal, Intravenous, and Intramuscular Administration. *J. Clin. Endocrinol. Metab.* **96,** 1900–7 (2001).

26. Nielsen-Kudsk, F. *et al.* Pharmacokinetics and bioavailability of intravenous and intramuscular lorazepam with an adjunct test of the inattention effect in humans. *Acta Pharmacol. Toxicol. (Copenh).* **52,** 121–7 (1983).

27. Abernethy, D. R., Greenblatt, D. J., Divoll, M. & Shader, R. I. Enhanced glucuronide conjugation of drugs in obesity: studies of lorazepam, oxazepam, and acetaminophen. *J. Lab. Clin. Med.* **101,** 873–80 (1983).

28. Greenblatt, D. J., Allen, M. D., Locniskar, A., Harmatz, J. S. & Shader, R. I. Lorazepam kinetics in the elderly. *Clin. Pharmacol. Ther.* **26,** 103–13 (1979).

29. Jochemsen, R. *et al.* Pharmacokinetics and bioavailability of intravenous, oral, and rectal nitrazepam in humans. *J. Pharmacokinet. Biopharm.* **10,** 231–45 (1982).

30. Jochemsen, R., Van Beusekom, B. R., Spoelstra, P., Janssens, A. R. & Breimer, D. D. Effect of age and liver cirrhosis on the pharmacokinetics of nitrazepam. *Br. J. Clin. Pharmacol.* **15,** 295–302 (1983).

31. Kanto, J., Kangas, L., Aaltonen, L. & Hilke, H. Effect of age on the pharmacokinetics and sedative of flunitrazepam. *Int. J. Clin. Pharmacol. Ther. Toxicol.* **19,** 400–4 (1981).

32. Sonne, J. *et al.* Bioavailability and pharmacokinetics of oxazepam. *Eur. J. Clin. Pharmacol.* **35,** 385–9 (1988).

33. Shull, H. J., Wilkinson, G. R., Johnson, R. & Schenker, S. Normal disposition of oxazepam in acute viral hepatitis and cirrhosis. *Ann. Intern. Med.* **84,** 420–5 (1976).

34. Van Steveninck, a L. *et al.* Effects of intravenous temazepam. II. A study of the long-term reproducibility of pharmacokinetics, pharmacodynamics, and concentration-effect parameters. *Clin. Pharmacol. Ther.* **55,** 546–55 (1994).

35. Ghabrial, H. *et al.* The effects of age and chronic liver disease on the elimination of temazepam. *Eur. J. Clin. Pharmacol.* **30,** 93–7 (1986).

36. Venkatakrishnan, K. *et al.* Kinetics and dynamics of intravenous adinazolam, N-desmethyl adinazolam, and alprazolam in healthy volunteers. *J. Clin. Pharmacol.* **45,** 529–37 (2005).

37. Fleishaker, J. C., Friedman, H. & Pollock, S. R. Extent and variability of the first-pass elimination of adinazolam mesylate in healthy male volunteers. *Pharm. Res.* **8,** 162–167 (1991).

38. Ajir, K. *et al.* The pharmacokinetics and pharmacodynamics of adinazolam: multi-ethnic comparisons. *Psychopharmacology (Berl).* **129,** 265–70 (1997).

39. Fleishaker, J. C., Hulst, L. K., Ekernäs, S. A. & Grahnén, A. Pharmacokinetics and pharmacodynamics of adinazolam and N-desmethyladinazolam after oral and intravenous dosing in healthy young and elderly volunteers. *J. Clin. Psychopharmacol.* **12,** 403–14 (1992).

40. Fleishaker, J., Smith, T., Friedman, H. & Hulst, L. Separation of the pharmacokinetic/pharmacodynamic properties of oral and IV adinazolam mesylate and N-desmethyladinazolam mesylate in healthy volunteers. *Drug Investig.* **4,** 155–165 (1992).

41. Fleishaker, J. C., Friedman, H., Pollock, S. R. & Smith, T. C. Clinical pharmacology of adinazolam and N-desmethyladinazolam mesylate after single oral doses of each compound in healthy volunteers. *Clin. Pharmacol. Ther.* **48,** 652–664 (1990).

42. Smith, R. B., Kroboth, P. D., Vanderlugt, J. T., Phillips, J. P. & Juhl, R. P. Pharmacokinetics and pharmacodynamics of alprazolam after oral and IV administration. *Psychopharmacology (Berl).* **84,** 452–6 (1984).

43. Fleishaker, J. C., Phillips, J. P., Eller, M. G. & Smith, R. B. Pharmacokinetics and pharmacodynamics of alprazolam following single and multiple oral doses of a sustained-release formulation. *J. Clin. Pharmacol.* **29,** 543–9 (1989).

44. Greenblatt, D. J. *et al.* Pharmacokinetic and electroencephalographic study of intravenous diazepam, midazolam, and placebo. *Clin. Pharmacol. Ther.* **45,** 356–65 (1989).

45. Heizmann, P., Eckert, M. & Ziegler, W. H. Pharmacokinetics and bioavailability of midazolam in man. *Br. J. Clin. Pharmacol.* **16 Suppl 1,** 43S–49S (1983).

46. Smith, M. & Eadie, M. The pharmacokinetics of Midazolam in man. *Eur. J. Clin.* **278,** 271–278 (1981).

47. Thummel, K. E. *et al.* Oral first-pass elimination of midazolam involves both gastrointestinal and hepatic CYP3A-mediated metabolism. *Clin. Pharmacol. Ther.* **59,** 491–502 (1996).

48. Allonen, H., Ziegler, G. & Klotz, U. Midazolam kinetics. *Clin. Pharmacol. Ther.* **30,** 653–61 (1981).

49. Clausen, T. G. *et al.* Pharmacokinetics of midazolam and alpha-hydroxy-midazolam following rectal and intravenous administration. *Br. J. Clin. Pharmacol.* **25,** 457–63 (1988).

50. MacGilchrist, a J. *et al.* Pharmacokinetics and pharmacodynamics of intravenous midazolam in patients with severe alcoholic cirrhosis. *Gut* **27,** 190–5 (1986).

51. Kroboth, P. D., McAuley, J. W., Kroboth, F. J., Bertz, R. J. & Smith, R. B. Triazolam pharmacokinetics after intravenous, oral, and sublingual administration. *J. Clin. Psychopharmacol.* **15,** 259–62 (1995).

52. Vanderveen, R., Jirak, J., Peters, G., Cox, S. & Bombardt, P. Effect of ranitidine on the disposition of orally and intravenously administered triazolam. *Clin. Pharm.* **10,** 539 (1991).

53. Smith, R. B., Kroboth, P. D. & Varner, P. D. Pharmacodynamics of triazolam after intravenous administration. *J. Clin. Pharmacol.* **27,** 971–9 (1987).

54. Dingemanse, J. *et al.* Integrated pharmacokinetics and pharmacodynamics of Ro 48-6791, a new benzodiazepine, in comparison with midazolam during first administration to healthy male subjects. *Br. J. Clin. Pharmacol.* **44,** 477–86 (1997).

55. Van Gerven, J. M. *et al.* Integrated pharmacokinetics and pharmacodynamics of Ro 48-8684, a new benzodiazepine, in comparison with midazolam during first administration to healthy male subjects. *Br. J. Clin. Pharmacol.* **44,** 487–93 (1997).

56. Jochemsen, R., Wesselman, J. G., Hermans, J., van Boxtel, C. J. & Breimer, D. D. Pharmacokinetics of brotizolam in healthy subjects following intravenous and oral administration. *Br. J. Clin. Pharmacol.* **16 Suppl 2,** 285S–290S (1983).

57. D, B. W. Pharmacokinetics and metabolism of brotizolam in humans. *Br. J. Clin. Pharmacol.* **16 Suppl 2,** 279S–283S (1983).

58. Roncari, G., Ziegler, W. H. & Guentert, T. W. Pharmacokinetics of the new benzodiazepine antagonist Ro 15-1788 in man following intravenous and oral administration. *Br. J. Clin. Pharmacol.* **22,** 421–8 (1986).

59. Klotz, U., Ziegler, G. & Reimann, I. Pharmacokinetics of the Selective Benzodiazepine Antagonist Ro 15-1788 in Man. *Eur. J. Clin. Pharmacol.* **27,** 115–117 (1984).

60. Janssen, U., Walker, S., Maier, K., von Gaisberg, U. & Klotz, U. Flumazenil disposition and elimination in cirrhosis. *Clin. Pharmacol. Ther.* **46,** 317–23 (1989).

61. Pomier-Layrargues, G., Giguère, J. & others. Pharmacokinetics of Benzodiazepine Antagonist Ro 15-1788 in Cirrhotic Patients with Moderate or Severe Liver Dysfunction. *Hepatology* **10,** 969–972 (1989).

62. Klotz, U., Duka, T., Dorow, R. & Doenicke, a. Flunitrazepam and lormetazepam do not affect the pharmacokinetics of the benzodiazepine antagonist Ro 15-1788. *Br. J. Clin. Pharmacol.* **19,** 95–8 (1985).

63. Klotz, U. & Kanto, J. Pharmacokinetics and clinical use of flumazenil (Ro 15-1788). *Clin. Pharmacokinet.* **14,** 1–12 (1988).

64. Brown, M. W., Maldonado, a L., Meredith, C. G. & Speeg, K. V. Effect of ketoconazole on hepatic oxidative drug metabolism. *Clin. Pharmacol. Ther.* **37,** 290–7 (1985).

65. Lam, Y. W. F., Alfaro, C. L., Ereshefsky, L. & Miller, M. Pharmacokinetic and pharmacodynamic interactions of oral midazolam with ketoconazole, fluoxetine, fluvoxamine, and nefazodone. *J. Clin. Pharmacol.* **43,** 1274–82 (2003).

66. TSUNODA, S., VELEZ, R. & GREENBLATT, D. Ketoconazole (K) inhibition of intestinal and hepatic cytochrome P450 3A4 (CYP3A4) activity using midazolam (M) as an in vivo probe. *Clin. Pharmacol. Ther.* **65,** 172–172 (1999).

67. Tsunoda, S. M., Velez, R. L., von Moltke, L. L. & Greenblatt, D. J. Differentiation of intestinal and hepatic cytochrome P450 3A activity with use of midazolam as an in vivo probe: effect of ketoconazole. *Clin. Pharmacol. Ther.* **66,** 461–71 (1999).

68. Olkkola, K. T., Backman, J. T. & Neuvonen, P. J. Midazolam should be avoided in patients receiving the systemic antimycotics ketoconazole or itraconazole. *Clin. Pharmacol. Ther.* **55,** 481–5 (1994).

69. Greenblatt, D. J. *et al.* Ketoconazole inhibition of triazolam and alprazolam clearance: differential kinetic and dynamic consequences. *Clin. Pharmacol. Ther.* **64,** 237–47 (1998).

70. Von Moltke, L. L. *et al.* Triazolam biotransformation by human liver microsomes in vitro: effects of metabolic inhibitors and clinical confirmation of a predicted interaction with ketoconazole. *J. Pharmacol. Exp. Ther.* **276,** 370–9 (1996).

71. Varhe, A., Olkkola, K. T. & Neuvonen, P. J. Oral triazolam is potentially hazardous to patients receiving systemic antimycotics ketoconazole or itraconazole. *Clin. Pharmacol. Ther.* **56,** 601–7 (1994).

72. Schmider, J., Brockmöller, J., Arold, G., Bauer, S. & Roots, I. Simultaneous assessment of CYP3A4 and CYP1A2 activity in vivo with alprazolam and caffeine. *Pharmacogenetics* **9,** 725–34 (1999).

73. Osanai, T., Ohkubo, T., Yasui, N., Kondo, T. & Kaneko, S. Effect of itraconazole on the pharmacokinetics and pharmacodynamics of a single oral dose of brotizolam. *Br. J. Clin. Pharmacol.* **58,** 476–81 (2004).

74. Qin, X. P. *et al.* Effect of the gene dosage of CYP2C19 on diazepam metabolism in Chinese subjects. *Clin. Pharmacol. Ther.* **66,** 642–6 (1999).

75. Van Miert, M. M., Eastwood, N. B., Boyd, a H., Parker, C. J. & Hunter, J. M. The pharmacokinetics and pharmacodynamics of rocuronium in patients with hepatic cirrhosis. *Br. J. Clin. Pharmacol.* **44,** 139–44 (1997).

76. McCoy, E. P., Mirakhur, R. K., Maddineni, V. R., Wierda, J. M. & Proost, J. H. Pharmacokinetics of rocuronium after bolus and continuous infusion during halothane anaesthesia. *Br. J. Anaesth.* **76,** 29–33 (1996).

77. Wierda, J. M., Kleef, U. W., Lambalk, L. M., Kloppenburg, W. D. & Agoston, S. The pharmacodynamics and pharmacokinetics of Org 9426, a new non-depolarizing neuromuscular blocking agent, in patients anaesthetized with nitrous oxide, halothane and fentanyl. *Can. J. Anaesth.* **38,** 430–5 (1991).

78. Cooper, R. a, Mirakhur, R. K., Wierda, J. M. & Maddineni, V. R. Pharmacokinetics of rocuronium bromide in patients with and without renal failure. *Eur. J. Anaesthesiol. Suppl.* **12,** 43–4 (1995).

79. Van den Broek, L. *et al.* Clinical pharmacology of rocuronium (Org 9426): study of the time course of action, dose requirement, reversibility, and pharmacokinetics. *J. Clin. Anesth.* **6,** 288–96 (1994).

80. Khalil, M. *et al.* Pharmacokinetics and pharmacodynamics of rocuronium in patients with cirrhosis. *Anesthesiology* **80,** 1241–7 (1994).

81. Magorian, T. *et al.* The pharmacokinetics and neuromuscular effects of rocuronium bromide in patients with liver disease. *Anesth. Analg.* **80,** 754–9 (1995).

82. Proost, J. H., Roggeveld, J., Wierda, J. M. & Meijer, D. K. Relationship between chemical structure and physicochemical properties of series of bulky organic cations and their hepatic uptake and biliary excretion rates. *J. Pharmacol. Exp. Ther.* **282,** 715–26 (1997).

83. Roy, J. J. & Varin, F. Physicochemical properties of neuromuscular blocking agents and their impact on the pharmacokinetic-pharmacodynamic relationship. *Br. J. Anaesth.* **93,** 241–8 (2004).

84. Khuenl-Brady, K. S. & Sparr, H. Clinical pharmacokinetics of rocuronium bromide. *Clin. Pharmacokinet.* **31,** 174–83 (1996).

85. Cronnelly, R. *et al.* Pharmacokinetics and pharmacodynamics of vecuronium (ORG NC45) and pancuronium in anesthetized humans. *Anesthesiology* **58,** 405–8 (1983).

86. Caldwell, J. E. *et al.* The pharmacodynamics and pharmacokinetics of the metabolite 3-desacetylvecuronium (ORG 7268) and its parent compound, vecuronium, in human volunteers. *J. Pharmacol. Exp. Ther.* **270,** 1216–22 (1994).

87. Arden, J. R. *et al.* Vecuronium in alcoholic liver disease: a pharmacokinetic and pharmacodynamic analysis. *Anesthesiology* **68,** 771–6 (1988).

88. Rupp, S. M., Castagnoli, K. P., Fisher, D. M. & Miller, R. D. Pancuronium and vecuronium pharmacokinetics and pharmacodynamics in younger and elderly adults. *Anesthesiology* **67,** 45–9 (1987).

89. Van der Veen, F. & Bencini, A. Pharmacokinetics and pharmacodynamics of Org NC 45 in man. *Br. J. Anaesth.* **52 Suppl 1,** 37S–41S (1980).

90. Fahey, M. R., Morris, R. B., Miller, R. D., Nguyen, T. L. & Upton, R. a. Pharmacokinetics of Org NC45 (norcuron) in patients with and without renal failure. *Br. J. Anaesth.* **53,** 1049–53 (1981).

91. Cameron, M., Donati, F. & Varin, F. In vitro plasma protein binding of neuromuscular blocking agents in different subpopulations of patients. *Anesth. Analg.* **81,** 1019–25 (1995).

92. Duvaldestin, P. & Henzel, D. Binding of tubocurarine, fazadinium, pancuronium and Org NC 45 to serum proteins in normal man and in patients with cirrhosis. *Br. J. Anaesth.* **54,** 513–6 (1982).

93. Caldwell, J. E. *et al.* Pipecuronium and pancuronium: comparison of pharmacokinetics and duration of action. *Br. J. Anaesth.* **61,** 693–7 (1988).

94. Duvaldestin, P., Demetriou, M. & D'Hollander, a. Pharmacokinetics of pancuronium in man: a linear system. *Eur. J. Clin. Pharmacol.* **23,** 369–72 (1982).

95. Duvaldestin, P., Agoston, S., Henzel, D., Kersten, U. W. & Desmonts, J. M. Pancuronium pharmacokinetics in patients with liver cirrhosis. *Br. J. Anaesth.* **50,** 1131–6 (1978).

96. Duvaldestin, P., Saada, J., Berger, J. L., D'Hollander, a & Desmonts, J. M. Pharmacokinetics, pharmacodynamics, and dose-response relationships of pancuronium in control and elderly subjects. *Anesthesiology* **56,** 36–40 (1982).

97. D'Honneur, G. *et al.* Pharmacokinetics and pharmacodynamics of pipecuronium in patients with cirrhosis. *Anesth. Analg.* **77,** 1203–6 (1993).

98. Ornstein, E., Matteo, R. S., Schwartz, a E., Jamdar, S. C. & Diaz, J. Pharmacokinetics and pharmacodynamics of pipecuronium bromide (Arduan) in elderly surgical patients. *Anesth. Analg.* **74,** 841–4 (1992).

99. Wierda, J. M. *et al.* Pharmacokinetics and cardiovascular dynamics of pipecuronium bromide during coronary artery surgery. *Can. J. Anaesth.* **37,** 183–91 (1990).

100. Obach, R. S., Lombardo, F. & Waters, N. J. Trend Analysis of a Database of Intravenous Pharmacokinetic Parameters in Humans for 670 Drug Compounds. *Drug Metab. Dispos.* **36,** 1385 (2008).

101. Szenohradszky, J. *et al.* Influence of renal failure on the pharmacokinetics and neuromuscular effects of a single dose of rapacuronium bromide. *Anesthesiology* **90,** 24–35 (1999).

102. Van den Broek, L., Wierda, J. M., Smeulers, N. J. & Proost, J. H. Pharmacodynamics and pharmacokinetics of an infusion of Org 9487, a new short-acting steroidal neuromuscular blocking agent. *Br. J. Anaesth.* **73,** 331–5 (1994).

103. Schiere, S., Proost, J. H., Schuringa, M. & Wierda, J. M. Pharmacokinetics and pharmacokinetic-dynamic relationship between rapacuronium (Org 9487) and its 3-desacetyl metabolite (Org 9488). *Anesth. Analg.* **88,** 640–7 (1999).

104. Duvaldestin, P., Slavov, V. & Rebufat, Y. Pharmacokinetics and pharmacodynamics of rapacuronium in patients with cirrhosis. *Anesthesiology* **91,** 1305–10 (1999).

105. Wierda, J. M., Beaufort, A. M., Kleef, U. W., Smeulers, N. J. & Agoston, S. Preliminary investigations of the clinical pharmacology of three short-acting non-depolarizing neuromuscular blocking agents, Org 9453, Org 9489 and Org 9487. *Can. J. Anaesth.* **41,** 213–20 (1994).

106. Diefenbach, C., Künzer, T., Buzello, W. & Theisohn, M. Alcuronium: a pharmacodynamic and pharmacokinetic update. *Anesth. Analg.* **80,** 373–7 (1995).

107. Dresner, D. L. *et al.* Pharmacokinetics and pharmacodynamics of doxacurium in young and elderly patients during isoflurane anesthesia. *Anesth. Analg.* **71,** 498–502 (1990).

108. Gariepy, L. P., Varin, F., Donati, F., Salib, Y. & Bevan, D. R. Influence of aging on the pharmacokinetics and pharmacodynamics of doxacurium. *Clin. Pharmacol. Ther.* **53,** 340–7 (1993).

109. Cook, D. R. *et al.* Pharmacokinetics and pharmacodynamics of doxacurium in normal patients and in those with hepatic or renal failure. *Anesth. Analg.* **72,** 145–50 (1991).

110. Fahey, M. R. *et al.* The pharmacokinetics and pharmacodynamics of atracurium in patients with and without renal failure. *Anesthesiology* **61,** 699–702 (1984).

111. Parker, C. J. & Hunter, J. M. Pharmacokinetics of atracurium and laudanosine in patients with hepatic cirrhosis. *Br. J. Anaesth.* **62,** 177–83 (1989).

112. Fisher, D. M. *et al.* Elimination of atracurium in humans: contribution of Hofmann elimination and ester hydrolysis versus organ-based elimination. *Anesthesiology* **65,** 6–12 (1986).

113. Ward, S., Neill, E. a, Weatherley, B. C. & Corall, I. M. Pharmacokinetics of atracurium besylate in healthy patients (after a single i.v. bolus dose). *Br. J. Anaesth.* **55,** 113–8 (1983).

114. Ward, S., Boheimer, N., Weatherley, B. C., Simmonds, R. J. & Dopson, T. A. Pharmacokinetics of atracurium and its metabolites in patients with normal renal function, and in patients in renal failure. *Br. J. Anaesth.* **59,** 697–706 (1987).

115. Smith, C. E., van Miert, M. M., Parker, C. J. & Hunter, J. M. A comparison of the infusion pharmacokinetics and pharmacodynamics of cisatracurium, the 1R-cis 1'R-cis isomer of atracurium, with atracurium besylate in healthy patients. *Anaesthesia* **52,** 833–41 (1997).

116. Kent, A. P., Parker, C. J. & Hunter, J. M. Pharmacokinetics of atracurium and laudanosine in the elderly. *Br. J. Anaesth.* **63,** 661–6 (1989).

117. Lien, C. a *et al.* Pharmacokinetics of cisatracurium in patients receiving nitrous oxide/opioid/barbiturate anesthesia. *Anesthesiology* **84,** 300–8 (1996).

118. Ornstein, E. *et al.* Pharmacodynamics and pharmacokinetics of cisatracurium in geriatric surgical patients. *Anesthesiology* **84,** 520–5 (1996).

119. Tran, T. V, Fiset, P. & Varin, F. Pharmacokinetics and pharmacodynamics of cisatracurium after a short infusion in patients under propofol anesthesia. *Anesth. Analg.* **87,** 1158–63 (1998).

120. De Wolf, a M. *et al.* Pharmacokinetics and pharmacodynamics of cisatracurium in patients with end-stage liver disease undergoing liver transplantation. *Br. J. Anaesth.* **76,** 624–8 (1996).

121. Kisor, D. F. *et al.* Importance of the organ-independent elimination of cisatracurium. *Anesth. Analg.* **83,** 1065–71 (1996).

122. Kisor, D. F. & Schmith, V. D. Clinical pharmacokinetics of cisatracurium besilate. *Clin. Pharmacokinet.* **36,** 27–40 (1999).

123. Head-Rapson, a G., Devlin, J. C., Parker, C. J. & Hunter, J. M. Pharmacokinetics and pharmacodynamics of the three isomers of mivacurium in health, in end-stage renal failure and in patients with impaired renal function. *Br. J. Anaesth.* **75,** 31–6 (1995).

124. Cook, D. R. *et al.* Pharmacokinetics of mivacurium in normal patients and in those with hepatic or renal failure. *Br. J. Anaesth.* **69,** 580–5 (1992).

125. Head-Rapson, a G., Devlin, J. C., Parker, C. J. & Hunter, J. M. Pharmacokinetics of the three isomers of mivacurium and pharmacodynamics of the chiral mixture in hepatic cirrhosis. *Br. J. Anaesth.* **73,** 613–8 (1994).

126. Savarese, J. J. *et al.* The clinical neuromuscular pharmacology of mivacurium chloride (BW B1090U). A short-acting nondepolarizing ester neuromuscular blocking drug. *Anesthesiology* **68,** 723–32 (1988).

127. Duvaldestin, P., Henzel, D., Demetriou, M. & Desmonts, J. M. Pharmacokinetics of Fazadinium in Man. *Br. J. Anaesth.* **50,** 773–7 (1978).

128. d'Hollander, a a *et al.* Analytical model of some pharmacokinetic and pharmacodynamic properties of fazadinium in man. *Eur. J. Clin. Pharmacol.* **24,** 407–13 (1983).

129. Roy, J. J., Donati, F., Boismenu, D. & Varin, F. Concentration-effect relation of succinylcholine chloride during propofol anesthesia. *Anesthesiology* **97,** 1082–92 (2002).

130. Lacey, L., Hussey, E. & Fowler, P. Single dose pharmacokinetics of sumatriptan in healthy volunteers. *Eur. J. Clin. Pharmacol.* **47,** 543–548 (1995).

131. Dixon, C. M. *et al.* Disposition of sumatriptan in laboratory animals and humans. *Drug Metab. Dispos.* **21,** 761–9 (1993).

132. Fowler, P. *et al.* The Clinical Pharmacology, Pharmacokinetics and Metabolism of Sumatriptan. *Eur. Neurol.* **31,** 291–294 (1991).

133. Tfelt-Hansen, P. & Hougaard, A. Sumatriptan: a review of its pharmacokinetics, pharmacodynamics and efficacy in the acute treatment of migraine. *Expert Opin. Drug Metab. Toxicol.* **9,** 91–103 (2013).

134. Scott, A. K. Sumatriptan clinical pharmacokinetics. *Clin. Pharmacokinet.* **27,** 337–44 (1994).

135. Jansat, J. M., Costa, J., Salvà, P., Fernandez, F. J. & Martinez-Tobed, A. Absolute bioavailability, pharmacokinetics, and urinary excretion of the novel antimigraine agent almotriptan in healthy male volunteers. *J. Clin. Pharmacol.* **42,** 1303–10 (2002).

136. McEwen, J., Salva, M., Jansat, J. M. & Cabarrocas, X. Pharmacokinetics and safety of oral almotriptan in healthy male volunteers. *Biopharm. Drug Dispos.* **25,** 303–11 (2004).

137. Fleishaker, J. C. *et al.* Effect of MAO-A inhibition on the pharmacokinetics of almotriptan, an antimigraine agent in humans. *Br. J. Clin. Pharmacol.* **51,** 437–41 (2001).

138. Fleishaker, J. C., Ryan, K. K., Carel, B. J. & Azie, N. E. Evaluation of the potential pharmacokinetic interaction between almotriptan and fluoxetine in healthy volunteers. *J. Clin. Pharmacol.* **41,** 217–23 (2001).

139. Fleishaker, J. C., Sisson, T. a, Carel, B. J. & Azie, N. E. Pharmacokinetic interaction between verapamil and almotriptan in healthy volunteers. *Clin. Pharmacol. Ther.* **67,** 498–503 (2000).

140. Fleishaker, J. C., Herman, B. D., Carel, B. J. & Azie, N. E. Interaction between ketoconazole and almotriptan in healthy volunteers. *J. Clin. Pharmacol.* **43,** 423–7 (2003).

141. Baldwin, J. R., Fleishaker, J. C., Azie, N. E. & Carel, B. J. A comparison of the pharmacokinetics and tolerability of the anti-migraine compound almotriptan in healthy adolescents and adults. *Cephalalgia* **24,** 288–92 (2004).

142. Almotriptan FDA Label. at <http://www.accessdata.fda.gov/drugsatfda_docs/label/2009/021001s010s011lbl.pdf>

143. Almotriptan Drug Approval Package from Drugs@FDA. at <http://www.accessdata.fda.gov/drugsatfda_docs/nda/2001/21001_Axert.cfm>

144. Gras, J. *et al.* Almotriptan, a new anti-migraine agent: a review. *CNS Drug Rev.* **8,** 217–34 (2002).

145. Negro, A. *et al.* Pharmacokinetic evaluation of almotriptan for the treatment of migraines. *Expert Opin. Drug Metab. Toxicol.* **9,** 637–44 (2013).

146. McEnroe, J. D. & Fleishaker, J. C. Clinical pharmacokinetics of almotriptan, a serotonin 5-HT(1B/1D) receptor agonist for the treatment of migraine. *Clin. Pharmacokinet.* **44,** 237–46 (2005).

147. Fuseau, E., Baille, P. & Kempsford, R. A study to determine the absolute oral bioavailability of naratriptan. *Cephalalgia* **17,** 417 (1997).

148. Kempsford, R., Baille, P. & Fuseau, E. Oral naratriptan tablets (2.5 to 10 mg) exhibit dose-proportional pharmacokinetics. *Cephalalgia* **17,** 408 (1997).

149. Naratriptan FDA Approval Package. at <http://www.accessdata.fda.gov/drugsatfda_docs/nda/98/20763_Amerge_Bioeqr.pdf>

150. Naratriptan FDA Label. at <http://www.accessdata.fda.gov/drugsatfda_docs/label/2013/020763s001s002s010lbl.pdf>

151. Jhee, S. S., Shiovitz, T., Crawford, a W. & Cutler, N. R. Pharmacokinetics and pharmacodynamics of the triptan antimigraine agents: a comparative review. *Clin. Pharmacokinet.* **40,** 189–205 (2001).

152. Mathew, N. T. Naratriptan: a review. *Expert Opin. Investig. Drugs* **8,** 687–95 (1999).

153. Buchan, P., Keywood, C., Ward, C. The pharmacokinetics of Frovatriptan a potent selective 5-HT agonist following single dose administration by oral and intravenous routes to healthy male and female volunteers. *Headache* **38,** 410 (1998).

154. Buchan, P., Keywood, C., Wade, a & Ward, C. Clinical pharmacokinetics of frovatriptan. *Headache* **42 Suppl 2,** S54–62 (2002).

155. Frovatriptan Drug Approval Package from Drugs@FDA. at <http://www.accessdata.fda.gov/drugsatfda_docs/nda/2001/21-006_Frova_biopharmr.pdf>

156. Frovatriptan FDA Label. **1,**

157. Negro, A. *et al.* Pharmacokinetic evaluation of frovatriptan. *Expert Opin. Drug Metab. Toxicol.* **7,** 1449–58 (2011).

158. Balbisi, E. A. Frovatriptan succinate, a 5-HT1B/1D receptor agonist for migraine. *Int. J. Clin. Pract.* **58,** 695–705 (2004).

159. Sanford, M. Frovatriptan: a review of its use in the acute treatment of migraine. *CNS Drugs* **26,** 791–811 (2012).

160. Goldstein, J. Frovatriptan: A review. *Expert Opin. Pharmacother.* **4,** 83–93 (2003).

161. Markus, F. & Mikko, K. Frovatriptan review. *Expert Opin. Pharmacother.* **8,** 3029–33 (2007).

162. Lee, Y. *et al.* Pharmacokinetics and tolerability of intravenous rizatriptan in healthy females. *Biopharm. Drug Dispos.* **19,** 577–81 (1998).

163. Cheng, H. *et al.* Pharmacokinetics and food interaction of MK-462 in healthy males. *Biopharm. Drug Dispos.* **17,** 17–24 (1996).

164. Lee, Y. *et al.* Pharmacokinetics and tolerability of oral rizatriptan in healthy male and female volunteers. *Br. J. Clin. Pharmacol.* **47,** 373–8 (1999).

165. Vyas, K. P. *et al.* Disposition and pharmacokinetics of the antimigraine drug, rizatriptan, in humans. *Drug Metab. Dispos.* **28,** 89–95 (2000).

166. Rizatriptan FDA Approval Package. at <http://www.accessdata.fda.gov/drugsatfda_docs/nda/98/020864a-pharm-10.pdf>

167. Rizatriptan FDA Label. at <http://www.accessdata.fda.gov/drugsatfda_docs/label/2011/020864s011s016s017s018s019,020865s012s016s018s020s021lbl.pdf>

168. Seaber, E. *et al.* The absolute bioavailability and metabolic disposition of the novel antimigraine compound zolmitriptan (311C90). *Br. J. Clin. Pharmacol.* **43,** 579–87 (1997).

169. Seaber, E. J. *et al.* The absolute bioavailability and effect of food on the pharmacokinetics of zolmitriptan in healthy volunteers. *Br. J. Clin. Pharmacol.* **46,** 433–9 (1998).

170. Peck, R. W. *et al.* The pharmacodynamics and pharmacokinetics of the 5HT1B/1D-agonist zolmitriptan in healthy young and elderly men and women. *Clin. Pharmacol. Ther.* **63,** 342–53 (1998).

171. Peck, R. W. *et al.* The interaction between propranolol and the novel antimigraine agent zolmitriptan (311C90). *Br. J. Clin. Pharmacol.* **44,** 595–9 (1997).

172. Rolan, P. & Martin, G. Zolmitriptan: a new acute treatment for migraine. *Expert Opin. Investig. ...* **7,** 633–52 (1998).

173. Dixon, R. & Warrander, A. The clinical pharmacokinetics of zolmitriptan. *Cephalalgia* **17 Suppl 1,** 15–20 (1997).

174. Peterlin, B. L. & Rapoport, A. M. Clinical pharmacology of the serotonin receptor agonist, zolmitriptan. *Expert Opin. Drug Metab. Toxicol.* **3,** 899–911 (2007).

175. Wild, M. J., McKillop, D. & Butters, C. J. Determination of the human cytochrome P450 isoforms involved in the metabolism of zolmitriptan. *Xenobiotica.* **29,** 847–57 (1999).

176. Milton, K. A. *et al.* Pharmacokinetics, pharmacodynamics, and safety of the 5-HT(1B/1D) agonist eletriptan following intravenous and oral administration. *J. Clin. Pharmacol.* **42,** 528–39 (2002).

177. Eletriptan FDA Label. at <http://www.accessdata.fda.gov/drugsatfda_docs/label/2011/021016s018lbl.pdf>

178. Gawel, M. J. & Grujich, N. N. Eletriptan. *Expert Opin. Investig. Drugs* **10,** 1869–74 (2001).

179. Sharma, A. *et al.* Pharmacokinetics and pharmacodynamics of avitriptan during intravenous administration in healthy subjects. *J. Clin. Pharmacol.* **39,** 685–94 (1999).

180. Pascual, J., Vila, C. & McGown, C. C. Almotriptan: a review of 10 years' clinical experience. *Expert Rev. Neurother.* **10,** 1505–17 (2010).

181. Corey, a E. *et al.* Azimilide pharmacokinetics following intravenous and oral administration of a solution and capsule formulation. *J. Clin. Pharmacol.* **39,** 1272–6 (1999).

182. Corey, A. *et al.* Pharmacokinetics and pharmacodynamics following intravenous doses of azimilide dihydrochloride. *J. Clin. Pharmacol.* **39,** 1263–71 (1999).

183. Corey, a *et al.* Effect of age and gender on azimilide pharmacokinetics after a single oral dose of azimilide dihydrochloride. *J. Clin. Pharmacol.* **37,** 946–53 (1997).

184. Corey, A. E. *et al.* Effect of severe renal impairment on the pharmacokinetics of azimilide following single dose oral administration. *Br. J. Clin. Pharmacol.* **54,** 449–52 (2002).

185. El Mouelhi, M., Worley, D. J., Kuzmak, B., Destefano, A. J. & Thompson, G. a. Influence of ketoconazole on azimilide pharmacokinetics in healthy subjects. *Br. J. Clin. Pharmacol.* **58,** 641–7 (2004).

186. Ujhelyi, M. R. *et al.* Disposition of intravenous amiodarone in subjects with normal and impaired renal function. *J. Clin. Pharmacol.* **36,** 122–30 (1996).

187. Cushing, D. J., Adams, M. P., Cooper, W. D., Kowey, P. R. & Lipicky, R. J. Bioequivalence of 2 intravenous amiodarone formulations in healthy participants. *J. Clin. Pharmacol.* **49,** 407–15 (2009).

188. Vadiei, K. *et al.* Pharmacokinetics of intravenous amiodarone in patients with impaired left ventricular function. *J. Clin. Pharmacol.* **36,** 720–7 (1996).

189. Neyroz, P. & Bonati, M. In vitro amiodarone protein binding and its interaction with warfarin. *Experientia* **41,** 361–3 (1985).

190. Latini, R., Tognoni, G. & Kates, R. E. Clinical pharmacokinetics of amiodarone. *Clin. Pharmacokinet.* **9,** 136–56 (1984).

191. Freedman, M. D. & Somberg, J. C. Pharmacology and pharmacokinetics of amiodarone. *J. Clin. Pharmacol.* **31,** 1061–9 (1991).

192. Gonzalez, E. R., Kannewurf, B. S. & Ornato, J. P. Intravenous amiodarone for ventricular arrhythmias: overview and clinical use. *Resuscitation* **39,** 33–42 (1998).

193. Andreasen, F., Agerbaek, H., Bjerregaard, P. & Gøtzsche, H. Pharmacokinetics of amiodarone after intravenous and oral administration. *Eur. J. Clin. Pharmacol.* **19,** 293–9 (1981).

194. Tham, T. C., MacLennan, B. A., Burke, M. T. & Harron, D. W. Pharmacodynamics and pharmacokinetics of the class III antiarrhythmic agent dofetilide (UK-68,798) in humans. *J. Cardiovasc. Pharmacol.* **21,** 507–12 (1993).

195. Sedgwick, M., Rasmussen, H. S., Walker, D. & Cobbe, S. M. Pharmacokinetic and pharmacodynamic effects of UK-68,798, a new potential class III antiarrhythmic drug. *Br. J. Clin. Pharmacol.* **31,** 515–9 (1991).

196. Le Coz, F., Funck-Brentano, C., Morell, T., Ghadanfar, M. M. & Jaillon, P. Pharmacokinetic and pharmacodynamic modeling of the effects of oral and intravenous administrations of dofetilide on ventricular repolarization. *Clin. Pharmacol. Ther.* **57,** 533–42 (1995).

197. Abel, S., Nichols, D. J., Brearley, C. J. & Eve, M. D. Effect of cimetidine and ranitidine on pharmacokinetics and pharmacodynamics of a single dose of dofetilide. *Br. J. Clin. Pharmacol.* **49,** 64–71 (2000).

198. Smith, D. a, Rasmussen, H. S., Stopher, D. a & Walker, D. K. Pharmacokinetics and metabolism of dofetilide in mouse, rat, dog and man. *Xenobiotica.* **22,** 709–19 (1992).

199. Jungbluth, G., Della-Coletta, A. & VanderLugt, J. Evaluation of the Pharmacokineticsand Pharmacodynamics of Ibutilide Fumarate and its Enantiomers in Healthy Male Volunteers. *Pharm Res* **8,** S249 (1991).

200. Jungbluth, G., VanderLugt, J., Kabell, G. & Walters, R. The pharmacokinetics and pharmacodynamics of ibutilide fumarate after intravenous infusions in healthy volunteers. *Pharm Res* **7,** S211 (1990).

201. Ibutilide FDA Label. at <http://www.accessdata.fda.gov/drugsatfda_docs/nda/2001/20-491S003.pdf>

202. Dronedarone FDA Label. at <http://www.accessdata.fda.gov/drugsatfda_docs/label/2014/022425s023lbl.pdf>

203. Dronedarone FDA Approval Package. at <http://www.accessdata.fda.gov/drugsatfda_docs/nda/2009/022425s000_ClinPharm_P1.pdf>

204. Narang, P. K., Adir, J., Josselson, J., Yacobi, a & Sadler, J. Pharmacokinetics of bretylium in man after intravenous administration. *J. Pharmacokinet. Biopharm.* **8,** 363–72 (1980).

205. Garrett, E., Green, J. & Bialer, M. Bretylium Pharmacokinetics and Bioavailabilities in Man With Various Doses and Modes of Administration. *Biopharm. drug ...* **3,** 129–164 (1982).

VITA

Gopichand Gottipati was born on February 28, 1988 in Vijayawada, Andhra Pradesh, India and is an Indian citizen. He graduated from College of Pharmaceutical Sciences, Andhra University, Visakhapatnam, India, with a Bachelors degree in Pharmaceutical Sciences in 2010 before joining the PK-PD research group at Department of Pharmaceutics, Virginia Commonwealth University (VCU), Richmond, VA.

During his tenure as a graduate student at VCU, Gopichand has published six abstracts. He presented her research extramurally at American Society of Clinical Pharmacology and Therapeutics (ASCPT 2012, 2013 and 2014), in addition to intramural presentation both within the Department and School of Pharmacy. During the summer of 2013, he was selected as a 'Ph.D. summer intern' at the Center for Pharmacometrics and Systems Pharmacology (CPSP), University of Lake Nona, Orlando, FL, under the supervision of Dr. Larry Lesko and Dr. An Guohua. He received Presidential Trainee Award for the abstract based on his summer internship work at CPSP submitted to ASCPT Annual Meeting in Atlanta, 2014. He was selected to participate in the inaugural Personal and Professional Development Program (PPDP, now BEST program). In addition, he also received VCU Department of Pharmaceutics Pfizer Consumer Healthcare R & D Leading for Innovation Award, 2014 for his excellence in teaching, research and scholarly activities within the department, and VCU Graduate School Dissertation Award for Fall 2013 and Spring 2014.

Gopichand served as President for Graduate Student Association (GSA) within the Department from 2012-13 and GSA webmaster from 2010 - 2013. He also served as VCU - AAPS Student Chapter Chair-elect (2012-2013) and VCU - AAPS Student Chapter Chair (2013-14). He was a student advisor, University Honor Council and served as a student representative in Tompkins McCaw Library Graduate Advisory Committee (2011 - 13), Student Health Advisory committee (2012-13) and member of VCU School of Pharmacy Diversity Committee (2011-2014). He was awarded University Service and Leadership Award 2012-13 for his commitment towards leadership and service activities. She is a member of professional organizations: AAPS and ASCPT.

Abstracts:

- **Gottipati, G**., Trame, M. N., Lin, C. W., Venitz, J., Lesko, L.J., An, G., *Model-Based Meta-Analysis of Efficacy at End-of-Trial and Efficacy-Time Course for Drugs Evaluated for the Treatment of Fibromyalgia Pain* - presented at ASCPT Annual Meeting, Atlanta, GA, March 18-22, 2014.

  Clin Pharmacol Ther 95 (Suppl 1): S12, PT - 015 (2014)

  (Recipient of ASCPT Presidential Trainee Award 2014)

- **Gottipati, G**., Lin, C. W., Venitz, J., Lesko, L. J., An, G., *Model-Based Meta-Analysis of Adverse Events and Dropouts for Drugs Evaluated for the Treatment of Fibromyalgia Pain* - presented at ASCPT Annual Meeting, Atlanta, GA, March 18-22, 2014.

  Clin Pharmacol Ther 95 (Suppl 1): S22, P-I - 016 (2014)

- **Gottipati, G**., Venitz, J. *Quantitative Structure-Pharmacokinetic/Pharmacodynamic Properties-Relationships for Neuromuscular Blockers* - presented at ASCPT Annual Meeting, Atlanta, GA, March 18-22, 2014.

  Clin Pharmacol Ther 95 (Suppl 1): S22, P-I - 015 (2014)

- **Gottipati, G**., Venitz, J. *Interspecies Pharmacokinetic - Allometric Scaling for Benzodiazepines* - presented at ASCPT Annual Meeting, Indianapolis, IN, March 5-9, 2013.

  Clin Pharmacol Ther 93 (Suppl 1): S43, P-I 83 (2013)

- **Gottipati, G**., Venitz, J. *Quantitative Structure-Pharmacokinetic Property Relationship(s) for Benzodiazepines in Humans (significant update)* - presented at ASCPT Annual Meeting, Indianapolis, IN, March 5-9, 2013.

  Clin Pharmacol Ther 93 (Suppl 1): S43, P-I 82 (2013)

- **Gottipati, G**., Venitz, J. *Quantitative Structure-Pharmacokinetic Properties-Relationships for Benzodiazepines* - presented at ASCPT Annual Meeting, National Harbor, MD, March 12-17, 2012.

  Clin Pharmacol Ther 91 (Suppl 1): S70, P-II 50 (2012)